Development of green natural rubber composites : Effect of nitrile rubber, fiber surface treatment and carbon black on properties of pineapple leaf fiber reinforced natural rubber composites

Nuttapong Hariwongsanupab

CO-JOINT THESIS

To obtain the joint degrees of doctor (Material chemistry) at

UNIVERSITE DE HAUTE ALSACE, France

&

MAHIDOL UNIVERSITY, Thailand

By

Nuttapong HARIWONGSANUPAB

DEVELOPMENT OF GREEN NATURAL RUBBER COMPOSITES

Effect of nitrile rubber, fiber surface treatment and carbon black on properties of pineapple leaf fiber reinforced natural rubber composites

---

5th May 2017

Examination committee:

Dr. Costantino CRETON (President)

Prof. Christophe BALEY (Reporter)

Prof. Laurent CHAZEAU (Reporter)

Dr. Karine MOUGIN (Supervisor, Universite de Haute Alsace)

Assoc. Prof. Taweechai AMORNSAKCHAI (Supervisor, Mahidol University)

Dr. Marie-France VALLAT (Supervisor-invited, Universite de Haute Alsace)

ABSTRACT

The effects of nitrile rubber (NBR), fiber surface treatment and carbon black on properties of pineapple leaf fiber-reinforced natural rubber composites (NR/PALF) were studied. The incorporation of NBR and surface treatment of fiber were used to improve the mechanical properties of composites at low deformation, whereas carbon black was used to improve these properties at high deformation. The fiber content was fixed at 10 phr. The composites were prepared using two-roll mill and were cured using compression moulding with keeping the fiber orientation. These composites were characterized using moving die rheometer (MDR), dynamic mechanical thermal analysis (DMTA) and tensile testing. The morphology after cryogenic fracture was observed using scanning electron microscopy (SEM). The effect of NBR from 0 to 20 phr of total rubber content was investigated. NBR is proposed to encase PALF leading to higher stress transfer between matrix and PALF. The method of mixing was also studied. For the fiber surface treatment, propylsilane, allylsilane and silane-69 were treated on the alkali-treated fiber. Treated fibers were characterized using Fourier-Transform infrared spectroscopy (FTIR), x-ray photoelectron spectroscopy (XPS) and SEM. Silane-69 treatment of fiber increased the modulus at low deformation more than the incorporation of NBR of NR/PALF composites due to the chemical crosslinking between rubber and fiber from silane-69 treatment rather than the physical interaction of NR, NBR and fiber. However, reinforcement by fiber reduced the deformation at break. Hence, carbon black was also incorporated into NR/NBR/PALF and NR/surface-treated PALF composites to improve the ultimate properties. By incorporation of carbon black 30 phr in both composites, the mechanical properties of composites were improved and can be controlled at both low and high deformations.

KEY WORDS: PINEAPPLE LEAF FIBER / NATURAL RUBBER / REINFORCEMENT / INTERFACIAL STRESS TRANSFER

ACKNOWLEDGEMENTS

I started my role as Ph.D. student under the double degree between Université de Haute Alsace in France and Mahidol University in Thailand. First, my appreciation goes to the Franco-Thai scholarship for financial supports along my study.

I would like to express my sincere gratitude and appreciation to Assoc. Prof. Taweechai AMORNSAKCHAI, Dr. Karine MOUGIN, Dr. Marie-France VALLAT my advisors, for their excellent supervision, encouragement, and helpful discussion throughout this research. Moreover, the collaboration between Mahidol University and Université de Haute Alsace would be not occurred without them. I also extend my appreciation to Assoc. Prof. Sombat THANAWAN and Assoc. Prof. Pranee PHINYOCHEEP, my co-advisor, for their valuable advice and suggestion for completion this research. My appreciation also goes to Prof. Christophe BALEY, Prof. Laurent CHAZEAU and Dr. Costantino CRETON for being my thesis committee.

I am deeply grateful to all technicians and staffs in Rubber Technology Research Centre (RTEC) at Mahidol University and Institut de Science des Matériaux de Mulhouse (IS2M) in France for their helpful and convenient corporation.

Furthermore, my sincere thanks go to all teachers, laboratory members, polymer graduated students, my nice friends in France and Thailand, and others, whose names are not mentioned here, for their kindnesses, encouragement, and helping in various ways. Finally, I would like to grateful thank for my family for their love, care, understanding, and encouragement in every ways through this study.

Nuttapong Hariwongsanupab

LIST OF ABBREVIATIONS

NR	Natural rubber
NBR	Nitrile rubber
PALF	Pineapple leaf fiber
UPALF	Untreated pineapple leaf fiber
APALF	Alkali-treated pineapple leaf fiber
SiPALF	Silane-treated pineapple leaf fiber
CBS	(N-Cyclohexyl-2-benzothaiazolesulfenamide)
Silane-69	Bis-(triethoxysilylpropyl)tetrasulfide
ZnO	Zinc oxide
ASTM	American society of testing materials
phr	part per hundred of rubber
MDR	Moving die rheometer
DMTA	Dynamic mechanical thermal analysis
DSC	Differential scanning calorimetry
SEM	Scanning electron microscope
XPS	X-ray photoelectron spectroscopy
ATR-FTIR	Attenuated total reflection-Fourier Transform Infrared spectroscopy
NMR	Nuclear magnetic resonance
t_{s2}	scorch time
t_{c90}	Cure time
M_L	Minimum torque
M_H	Maximum torque
E′	Storage modulus
Tan δ	Tan delta
T_d	Dynamic transition temperature
T_g	Glass transition temperature

E_{10}	Modulus at 10% strain
E_{100}	Modulus at 100% strain
E_{300}	Modulus at 300% strain
σ_y	Yield stress

CONTENTS

CHAPTER I
INTRODUCTION

Recently, the development of green composites has been gaining more interest and attention due to the depleting petroleum reserves and environmental awareness. Natural fibers are the one of green fillers with high strength that can be used to reinforce polymer materials.

Short and fine pineapple leaf fibers (PALF) have been successfully developed by Amornsakchai's research group at Mahidol University, and has been used to reinforce polypropylene (PP), polyamide (nylon), vulcanizable thermoplastics (Santoprene^{TM}) and also nitrile rubber (NBR) effectively. Natural rubber (NR), one of Thailand's top exports, was chosen as the matrix for fiber reinforcement in this study. The major component of NR is high molecular weight *cis*-1,4-polyisoprene polymeric movable chains. Due to the difference in polarities between NR and PALF, the interfacial strength and hence stress transfer between them are low. If interfacial adhesion of NR and PALF is improved, better properties of composite should be obtained.

In this study, the stress transfer between NR and PALF was first improved. Two different methods were used which are, on the one hand, the incorporation of small amount of NBR and, on the other hand, silane treatment of the fibers. In first method, NBR surrounded PALF from the polar-polar interactions. NBR-encased fibers enhanced the stress transfer by increasing interfacial strength between rubber and fibers. Although NR and NBR are not compatible, the mechanical properties improvement of composite could be obtained from the frictional stress transfer between rubbers. In the second method, PALFs were treated with silane to provide the chemical bonding between rubber and fibers during vulcanization of NR.

Reinforcement by fibers always reduce the deformation at break of composites. Thus, carbon black was incorporated into NR/PALF composites in both previous approaches to improve mechanical properties at high deformation. Thus, mechanical properties of composites were improved and could be controlled at both low and high deformation

CHAPTER II
OBJECTIVES

The objective of this work has been divided into two main parts. The improvement of the interfacial adhesion between NR and PALF was first studied. By increasing the interfacial adhesion, modulus at low deformation was improved. Then, the improvement of strength at high deformation of composites by incorporation of carbon black was studied.

1. Two different approaches to improve the mechanical reinforcement of NR at low deformation reinforced with PALF were performed:

1.1) Small amount of NBR was incorporated into NR/PALF composite. NBR is a polar elastomer that will show higher compatibility with cellulose surface that is also polar. Therefore, it is expected that PALF will be surrounded by NBR *via* non dispersive interactions such as dipole-dipole or hydrogen interactions. Although this method provided only physical interactions between rubber and PALF, it is a convenient method due to its possible *in situ* mixing. To study the compatibility between rubbers and the effect of NBR on mechanical properties, amount of NBR and mixing method were varied. To get deeper understanding of the mechanism of NBR/PALF reinforcement, curatives migration in the blends were also studied.

1.2) PALFs were modified in a first step with chemical reagents before mixing with NR. Alkali-treatment of PALF was used as a pre-treatment to clean the surface of the fibers. Then, PALF were further treated with three types of silanes. Propyltrimethoxysilane is considered as reference for a non-reactive treatment during vulcanization of the rubber. Allyltrimethoxysilane is used as a reactive site that contains allyl group. This bond is proposed to lead to co-crosslinking with NR via sulfidic bonds at the allylic hydrogen atoms. Silane-69 is a silane containing sulfur that provides free sulfur for co-crosslinking with rubber during the vulcanization at high temperature. The amount of silane, solvent effect of silane treatment, and the method of treatment have been investigated.

2. After the enhancement of the stress transfer between NR matrix and fiber, mechanical properties at high deformation were further improved. Carbon black was incorporated into NR/NBR/PALF and NR/silane-treated PALF composites. On the one hand, PALF and the enhancement of the interfacial strength improved tensile properties at low deformation. On the other hand, carbon black improved tensile properties at high deformation. In case of hybrid composites containing NBR, the mixing method was also studied to optimize the mechanical properties of composite and understand the influence of the fillers distribution in rubber blends. Thus, the tensile properties of composites will be controllable, which could open new end-used applications.

Plan of the work

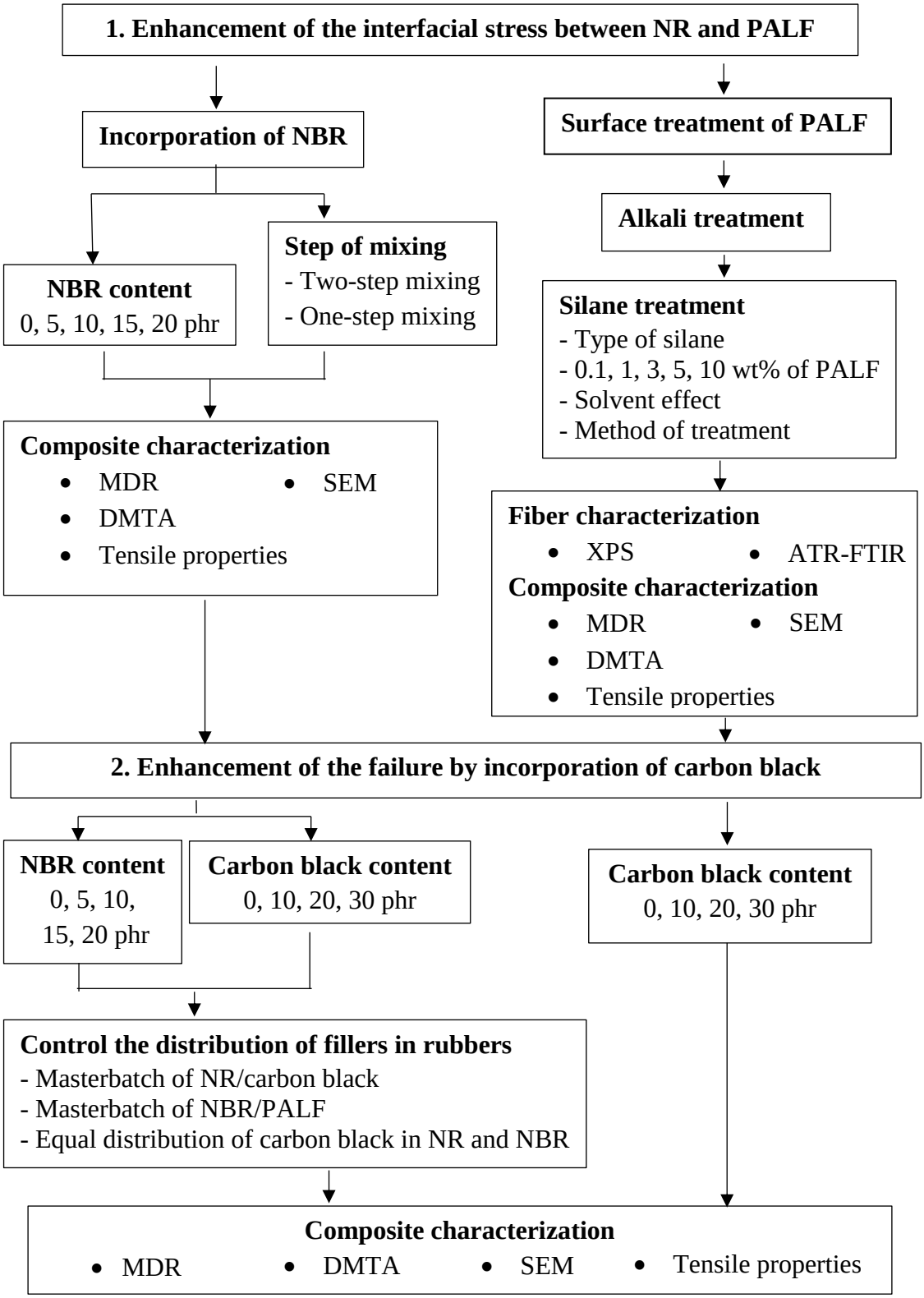

CHAPTER III
LITERATURE REVIEW

3.1 Elastomer

Elastomer is a polymeric material, which the usual working domain is in the rubbery plateau, whereas other polymers are in the glassy plateau. Thus, the outstanding properties of elastomer is the failure resistance at high deformation, compared to thermoplastics or thermosets, metals or alloys. Rubber is the technological word used for elastomer. Rubber is often crosslinked with sulfur by vulcanization process. The ambient temperature of those rubbers is above the glass transition temperature, hence polymeric chains are able to move. Rubbers are generally divided into two types which are natural rubber and synthetic rubber.

3.1.1 Natural rubber

Natural rubber (NR) is the one of the most useful in elastomer applications such as parts of tire, especially for aircraft applications, trucks and heavy loaded trucks [1,2], footwear [3,4] and conveyor belts [5–7]. It is considered as a bio and green raw materials. Although NR could be obtained from many species, *Hevea brasiliensis* specie is mostly used to produce commercial rubber products [8]. The evolution, and particularly the increase of the production and consumption of NR is shown in Figure 3.1.

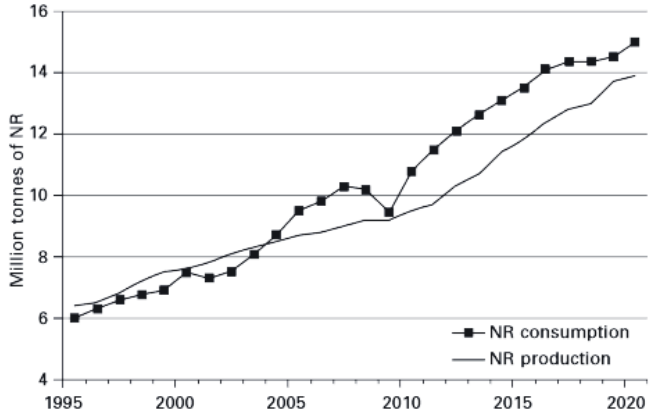

Figure 3.1 Annual global production and consumption of natural rubber from 1995 to 2012 with projections to 2020. [Data from the International Rubber Study Group]

NR is harvested from Hevea brasiliensis tree in a form of latex. It is a colloidal suspension in water. NR is a polymer with cis-1,4 isoprene as repeating units as a major component, which is produced by biosynthesis process. The chemical structure of NR is displayed in Figure 3.2. Apart from hydrocarbon polymeric chain component, NR latex also contains proteins, lipids and other ingredients. A typical composition of NR latex is shown in Table 3.1. Proteins in natural rubber are hypothesized to promote the storage hardening behavior of dry rubber due to the spontaneous crosslinking reactions during storage [9]. Lipids are the plasticizers of natural rubber, while fatty acids nucleate the strain-induced crystallization [10-11].

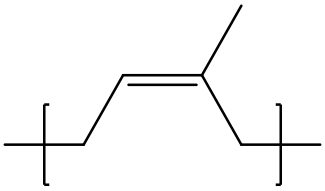

Figure 3.2 Chemical structure of NR

Table 3.1 Composition of fresh NR latex [12]

Component	Percentage (w/w)
Rubber hydrocarbon	36.0
Proteins, amino acids, nitrogenous compounds	1.7
Lipids	1.6
Ashes	0.5
Carbohydrates	1.6
Water	58.6

NR latex has been mostly processed into dry rubber due to the transportation cost and ease to processing. Dry rubber is used in many applications, which depends on the classification of rubber. The standard Thai specific rubber is named as STR such as STR5L, STR10L and STR20L. The number indicates the impurities ratio in bulk rubber. Lower number on the name indicates higher purity, whereas higher number indicates lower purity. The letter "L", which is on the end of the name, specifies a light color of dry rubber.

NR is a flexible polymeric chain with molecular weight (MW) higher than 10^6 Da [13]. Thus, it has high elasticity that can be used in various applications. Unvulcanized NR is soft and sticky, thus the vulcanization process is required to link polymer chains together [14–16]. Vulcanized NR exhibits high tensile strength, hardness and also abrasion resistance. However, NR has low chemical, aromatic oil and atmosphere resistance due to its unsaturated double bond on the main polymeric chain.

3.1.2 Nitrile rubber

Nitrile rubber (NBR) is a synthetic rubber. The chemical structure of NBR, which is a copolymer of acrylonitrile (ACN) and butadiene, is displayed in Figure 3.3. It is produced from radical polymerization in emulsion processing at 5-30 °C [17]. The applications of NBR depend on acrylonitrile content. NBR with high acrylonitrile content is generally used for oil-resistant products such as O-rings, gloves.

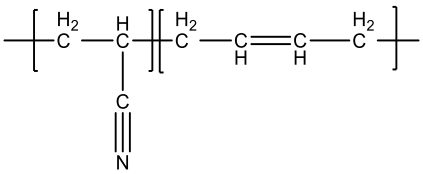

Figure 3.3 Chemical structure of NBR

Similar to NR, vulcanization of NBR is required in order to increase the mechanical properties of rubber. Mechanical properties of NBR and other synthetic rubber vulcanizates are shown in Figure 3.4 [18]. The disadvantage of NBR and also other synthetic rubbers such as butadiene rubber (BR) and styrene-butadiene rubber (SBR) is the low failure stress at high deformation due to the absence of nucleating agent (*e.g.* fatty acids in NR) for strain-induced crystallization [18]. Thus, these rubbers are limited to use in static applications. Fillers can be incorporated to enhance the mechanical properties to overcome this limitation, which will be shown in sections 3.4 to 3.6.

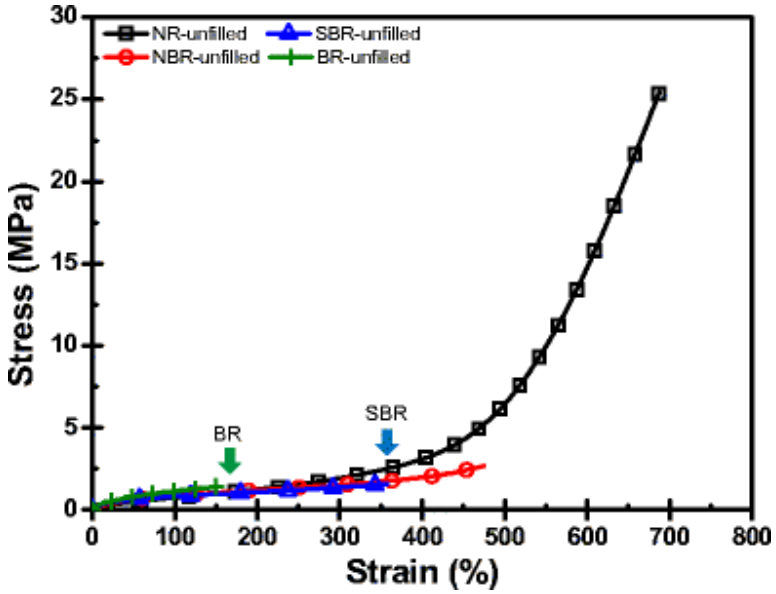

Figure 3.4 Stress-strain curves of unfilled NR, NBR, BR and SBR [18]

3.2 Vulcanization

Vulcanization is a chemical process to crosslink unsaturated polymeric chains of rubber using sulfur. This process has played an important role to achieve the elasticity of rubber. Vulcanization was first discovered by Goodyear and has been developing since the past century [19–21]. Nowadays, accelerator and activator have been used in the process to control the kinetics of vulcanization and the elasticity of rubber.

3.2.1 Sulfur vulcanization mechanism

The mechanism of accelerated sulfur vulcanization, which was proposed by Morrison and Porter [22], is shown in Figure 3.5. In general, curing additives are added directly during rubber mixing in order to disperse and distribute all ingredients. After rubber and fillers are mixed together, ZnO (a typical activator) and stearic acid are incorporated. When mixed with accelerator, they form the accelerator complex. After sulfur is incorporated, accelerator complex further activates cyclic S_8. Then, this complex is used to crosslink the rubber chains. The reactive sites of rubber are allylic hydrogens (hydrogen atoms next to carbon lying adjacent to carbon double bonds) [23].

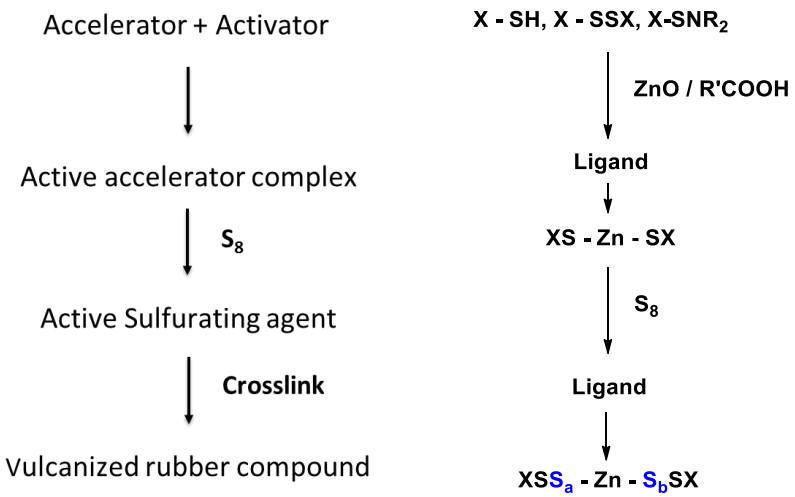

Figure 3.5 General mechanism of sulfur vulcanization [22]

The simple and effective characterization of vulcanization is to follow the evolution of crosslinks, which is determined by oscillating disc rheometer (ODR) or moving die rheometer (MDR). Compound of rubber with curing additives is pressed and then sheared at the curing temperature. The measured torque is plotted as a function of time. A general cure curve is shown in Figure 3.6.

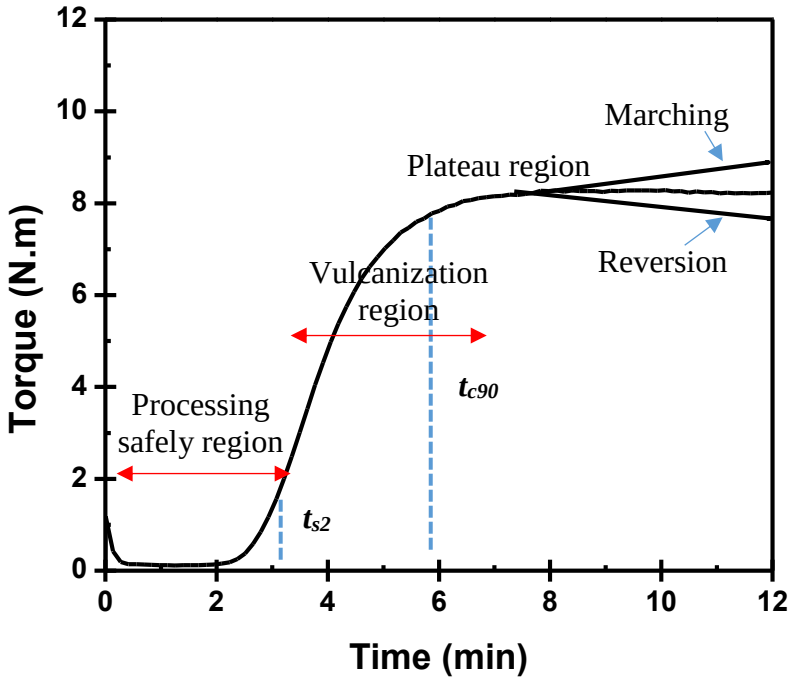

Figure 3.6 Typical cure curves of rubber compounds [24]

The first region of curing behavior of rubber compound is the safe processing region during which the rubber can still flow into a cavity in a mold. This region is related to the time that torque raises to 2 N.m, which is called scorch time, t_{s2}. After t_{s2}, rubber compound starts to vulcanize. Torque raises rapidly due to the increase of crosslink density. Finally, compound is in the plateau region during which the vulcanization is going to reach an equilibrium state. Cure time t_{c90} is the time that 90% of vulcanization is taking place, which is generally used to cure compound in a mold. If compound is further cured after torque rises to the maximum, marching or reversion process might occur depending on the stability of polysulfidic bonds. Marching is a process during which torque rises continuously. It may occur in all rubbers, however, the mechanism of this process is still unclarified. Reversion process is the decrease of

torque after it raises to the maximum value. This process occurs because of the thermal instability of polysulfidic bonds, which can be shorten into mono- or di-sulfidic bonds or be devulcanized by cleaving these bonds into non-crosslinked sulfurs [23]. The possibilities of side reactions are displayed in Figure 3.7.

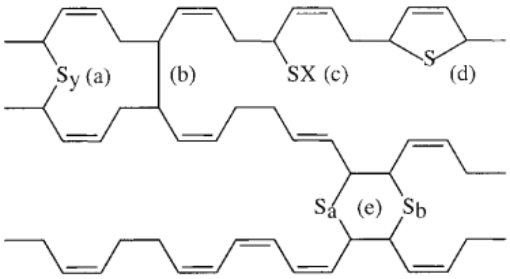

Figure 3.7 Various chemical structures of vulcanization (a) and side reactions: carbon-carbon crosslink (b), pendant accelerator sulfide (c), cyclic sulfide (d) and vicinal crosslinks (e) [23]

3.2.2 Important factors of vulcanization

Curing temperature, type of accelerator and the ratio of sulfur and accelerator are important factors in order to control the kinetics of vulcanization. In addition, crosslink density and crosslink length strongly depend on vulcanization process. Thus, unlike thermoplastics, vulcanization is correlated directly to mechanical properties.

3.2.2.1 Curing temperature

Curing temperature is one important factor for the length of sulfidic crosslinks. The original rheometer curves of NR is shown in Figure 3.8. Loo reported that high curing temperature leads to shorter sulfidic bonds (mono-, di-sulfidic bond), whereas low curing temperature leads to longer sulfidic bonds (polysulfidic bond) those are less stable [25]. Moreover, devulcanization might occur when using high curing temperature [26].

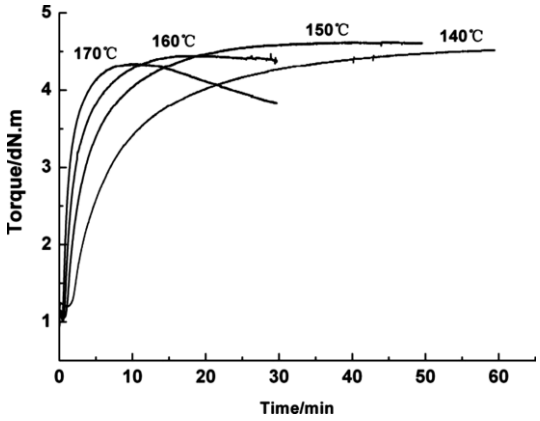

Figure 3.8 Cure curves of NR with various curing temperatures [27]

3.2.2.2 Type of accelerators

Accelerator also plays an important role on curing kinetics. They can be classified by chemical groups and are displayed in Table 3.2.

Table 3.2 Classification of accelerator types [according to ASTM D4818]

Chemical group	**Accelerator**	**Vulcanization rate**
Guadinine	• Diphenyl guanidine (DPG) • N,N'-Diorthotolyl guanidine (DOPG)	Slow
Thiazole	• 2- Mercaptobenzothiazole (MBT) • 2-2'-Dithiobis(benzothiazole) (MBTS)	Fast
Sulfenamide	• N-Cyclohexyl-2-benzothiazole sulfenamide (CBS) • N-tert-butyl-2-benzothiazole sulfenamide (TBBS) • 2-(4-Morpholinothio)- benzothiazole (MBS)	Fast-delayed action
Thiuram	• Tetramethylthiuram Monosulfide (TMTM) • Tetramethylthiuram Disulfide (TMTD)	Ultra fast
Dithiocarbamate	• Zinc dimethyldithiocarbamate (ZDMC) • Zinc diethyldithiocarbamate (ZDEC)	Ultra fast

Sulfenamide and thiazole are commonly used as primary accelerators due to the preventability of scorching. In case of inappropriate behavior of curing (slow or fast cure), secondary accelerator such as guadinine, thiuram and

dithiocarbamate can be added to adjust the cure rate. The selection of accelerators depends on the rubber solubility and cure rate requirement.

3.2.2.3 Ratio of sulfur and accelerators

The ratio of sulfur and accelerator indicates the sulfidic bond formation, which also affects directly mechanical properties of end-used rubber products [15,26]. The three curing systems are conventional (CV), efficient (EV) and semi-EV vulcanization systems depending on the ratio of sulfur/accelerator are shown in Table 3.3. Relative rubber characteristics are given in the same table.

Table 3.3 Vulcanizate structures and properties [26]

	CV	**Semi-EV**	**EV**
Sulfur / Accelerator ratio	0.1 - 0.6	0.8 - 1.2	2.5 - 12
Polysulfidic crosslinks (%)	95	50	10
Mono- and Di-sulfidic crosslinks (%)	5	50	90
Mechanical strength	High	Medium	Low
Flexibility	High	Medium	Low
Modulus	Low	Medium	High
Heat resistance	Low	Medium	High

Bateman reported that using CV and EV systems for vulcanization of ribbed smoked sheets NR (RSS1), NR resulted in different degrees of crosslinking and sulfidic bond length [28]. The relation between chemical crosslinks and cure time using CV and EV systems are plotted in Figure 3.9.

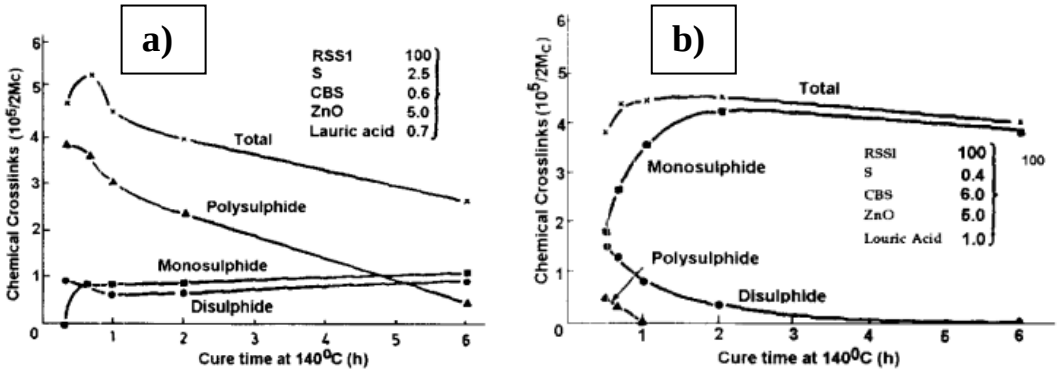

Figure 3.9 Feature of NR vulcanizates produced by conventional (a) and efficient (b) crosslinking systems [28]

Using high ratio of sulfur/accelerator results in high amount of polysulfidic linkages. It should be noted that polysulfidic length corresponds to initial sulfur that is incorporated in the rubber, which is generally in the length of S_8. However, polysulfide content decreases corresponding to longer cure time due to the thermal instability of the linkages. Low amounts of mono- and di-sulfidic bonds are obtained and slightly increases with cure time. Hence, cure time has to be fixed so that thermal decomposition does not occur. On the other hand, using low ratio of sulfur/accelerator results in high amount of monosulfidic linkages. These linkages increase initially and decrease with longer cure time. At the same time, polysulfidic and disulfidic linkages decreased with cure time. From these results, it can be concluded that the crosslink length using CV system is mainly polysulfidic linkages, whereas EV system is mainly monosulfidic bonds. Thus, the appropriate curing system should match the end-used rubber products thermal stability.

3.3 Rubber blends

To overcome the limitation of single rubber properties, two or more rubbers can be blended together. For example, NR has outstanding elastic properties, but it has low chemical and oil resistance. Thus, NBR can be incorporated to improve these properties [29]. Generally, rubber blend technique does not provide a homogeneous blend due to a large difference between high molecular weight of chemical polymeric

structures. Because of the blends of two or more different polymeric structures with high molecular weight, a phase separation can occur. Rubber blends can be separated into co-continuous phases and dispersed phase in rubber matrix depending on the ratio of rubber content, viscosity of the rubbers, as shown in Figure 3.10.

Figure 3.10 Increase of polymer B (blue) content in polymer A (yellow)

The final properties of rubber blends are not proportional to the rule of mixture [29]. Rubber ratio, phase morphology, interfacial tension and crosslink distribution in rubbers represent important factors that influence the final properties. Moreover, when a filler is incorporated, the filler distribution between two rubbers has a strong impact on the final properties.

3.3.1 Rubber ratio and phase morphology

Rubber ratio is a factor that is taking part into the properties of end-used products. Rubber with higher content dominates the major properties of the blend, whereas rubber with lower content is used to improve the properties of matrix. Phase morphology should be controlled in order to achieve the designed blend properties [30]. Thus, rubber ratio is the one factor that can be adjusted. The goal of the blending is to achieve the small size of droplets of the dispersed phase, which will result in the improvement of properties [31]. Hence, the method of mixing represents a critical parameter to control in order to optimize the final properties of the product.

Sirisinha, Limcharoen and Thunyarittikorn studied the effect of viscosity of NR and NBR on the morphology of its blends [30]. The ratio of NR/NBR was 20/80 wt% in order to ensure that NR is dispersed in NBR matrix. The viscosity ratio of NR/NBR were varied at 0.5, 1.0 and 2.0 by mastication of rubbers, incorporation of liquid NR (LNR) in NR and epoxidized liquid NR (ELNR) in NBR. The blending process of viscosity-modified rubbers was carried out using internal mixer. The

morphologies of the blends are displayed in Figure 3.11. At high viscosity ratio (viscosity of NR is higher than that of NBR matrix), the size of NR dispersed phase was larger than that at low viscosity ratio. Thus, shear force during mixing could be transferred from NBR matrix to NR dispersed phase and disrupt the morphology of the blends.

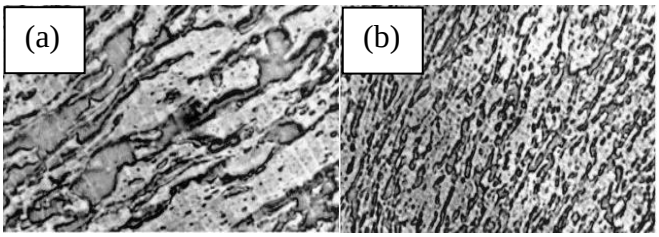

Figure 3.11 Morphologies of the NR/NBR blends (20/80 wt%) with viscosity ratio of 2.0 (a) and 0.5 (b)

3.3.2 Interfacial tension

Although the method of mixing represent a key parameter to adjust the phase morphology of rubbers, interfacial tension between the rubbers is also important to designate phase size of rubber blends. The lower the interfacial tension is, the smaller the droplet size of dispersed phase is obtained. For example, natural rubber and butadiene rubber were successfully blended to achieve small phase size due to their non-polar chemical structures [32]. The blending of natural rubber and nitrile rubber is difficult due to their large different of polarities [33-34]. The immiscibility of the blend can be briefly explained using thermodynamic (equation 1).

$$\Delta G_m = \Delta H_m - T\Delta S_m \qquad \text{equation 1}$$

Where ΔG_m is the free energy of mixing, ΔH_m is the enthalpy of mixing and ΔS_m is the entropy of mixing. The blend is miscible when ΔG_m is smaller than 0. In polymeric blends, the term of $T\Delta S_m$ can be neglected due to the constraints on the segmental mobility of polymer chains. Thus, the energy of mixing is directly proportional to ΔH_m. The equation was further developed by Cruz and co-workers [35] (equation 2)

$$\Delta G_m \approx \Delta H_m = \chi_{12} RT \left(\frac{V}{V_1}\right) \phi_1 \phi_2 \qquad \text{equation 2}$$

Where V is the total volume of the mixture and V_1 is the molar volume of polymer 1. ϕ_1 and ϕ_2 are the volume fractions of polymer 1 and 2. ΔH_m is proportional to the interaction parameter (χ_{12}) of the polymers. The equation was further developed to find the relationship between χ_{12} and the solubility parameter defined by Hildebrand and Scott [36]. The relationship of $\Delta G_m, \Delta H_m$ and solubility parameter (δ) is shown on equation 3:

$$\Delta H_m = V(\delta_1 - \delta_2)^2 \phi_1 \phi_2 \qquad \text{equation 3}$$

where V is the volume of the mixture. The difference between δ of the two rubbers is related to the interfacial tension between rubbers. Less difference between δ indicates low interfacial tension whereas large difference indicates high interfacial tension. The solubility parameters of rubbers are shown in Table 3.4. The solubility parameter can be used to explain that NR is compatible with butyl rubber or polyisopren, but incompatible with nitrile rubber. The incompatibility increases with acrylonitrile content increase [37].

Table 3.4 Solubility parameters of rubbers [37]

Rubber	**δ (MPa)$^{0.5}$**
Natural rubber	18.1
Butyl rubber	17.9
Polyisoprene	18.0
Nitrile rubber (18% ACN)	19.2
Nitrile rubber (26% ACN)	19.6
Nitrile rubber (40% ACN)	20.2

3.3.3 Degree of crosslinking in each rubber phase in blends

Due to the heterogeneous blending of rubbers, the solubility of the additives in each rubber phase is also an important parameter in blending. Solubility and saturation can be very different. The curatives distribution depends on the chemical structure and the compatibility of each ingredient of the vulcanization recipe. Tinker and co-workers studied the unequal curatives distribution in NR and NBR [29], which resulted in an unequal crosslink density in each rubber. By using osmium staining, the

phase contrast between NR and NBR can be detected [38]. Blending NR and NBR (41% ACN content) 1:1 ratio resulted in NR as matrix phase and NBR as dispersed phase, which is shown in Figure 3.12 (a). The network visualization of the blends was developed from Shiibashi [39] and carried out by swelling vulcanizates in styrene then it was polymerized to freeze the structure. TEM micrograph of the blends is illustrated in Figure 3.12 (b). It can be observed that rubbers are separately cured in each phase.

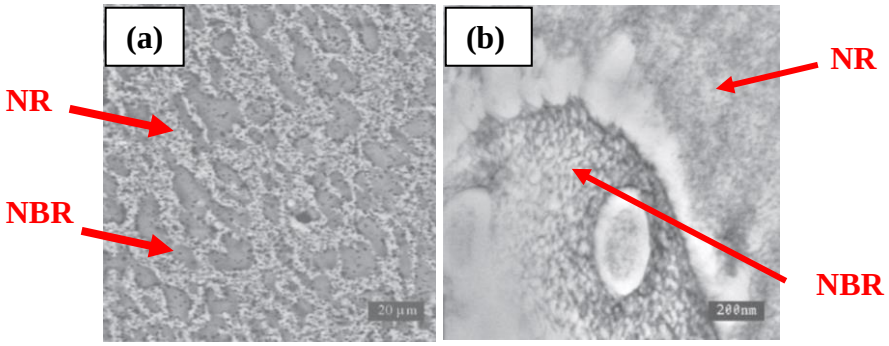

Figure 3.12 Phase contrast micrograph (a) and TEM micrograph (b) of NR/NBR blends swollen in styrene that is polymerized after equilibrium swelling [29]

The unequal crosslink distribution using CBS as primary accelerator and varying secondary accelerators in NR and NBR is shown in Figure 3.13 [29]. The crosslink distribution in each phase was characterized using swollen ^{1}H NMR [40]. The authors varied the amount of sulfur and accelerator content (fixing the ratio at 5:2) of NR and NBR separately then plotted the calibration between crosslink densities and sulfur content. By using the different signals of H% of NR and NBR, crosslink densities in each phase in the blends could be estimated using the calibration curves. The result shows that accelerator type, curing temperature and acrylonitrile (ACN) content of NBR directly affect the crosslink density of each phase in the blends. It can be seen that most of sulphenamide cure systems give a maldistribution in NR phase rather than NBR (ACN 41%) phase when curing at 150 °C. Addition of small amounts of secondary accelerators affects the distribution of crosslink density. TMTM is a polar molecule, thus, it causes maldistribution in NBR. ODIP has larger alkyl substituents than TMTM, thus, it causes more crosslink in NR. Addition of DPG, MBTS or TBTD does not affect crosslink distribution of the blends. Crosslink distribution favors in NBR phase when curing at 180 °C. Thus, curing temperature also affects crosslink distribution. However,

the authors did not mention on the effect temperature on the migration rates and also the length of sulfidic bonds.

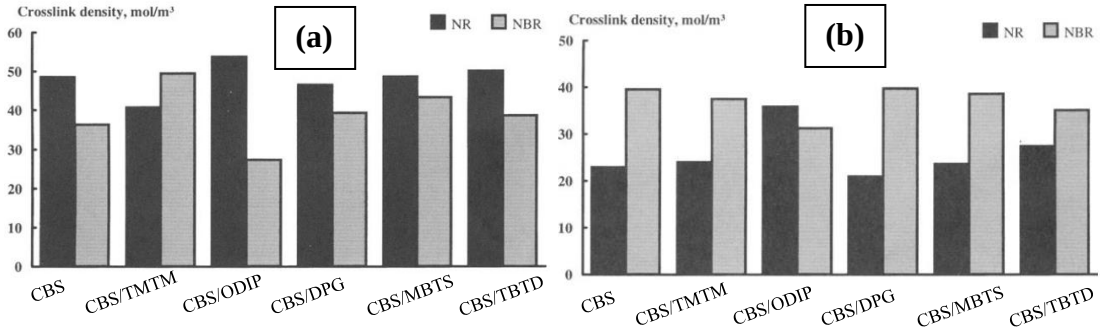

Figure 3.13 Crosslink density distributions in NR/NBR (41% ACN content) blends curing at 150 C (a) and 180 °C (b) [29]

Changing NBR from 41% to 34% ACN content also affects the crosslink distribution. It can be seen in Figure 3.14 that using most of accelerators gives a maldistribution in NBR phase rather than NR phase. Again, the authors did not mention on the length of sulfidic bonds.

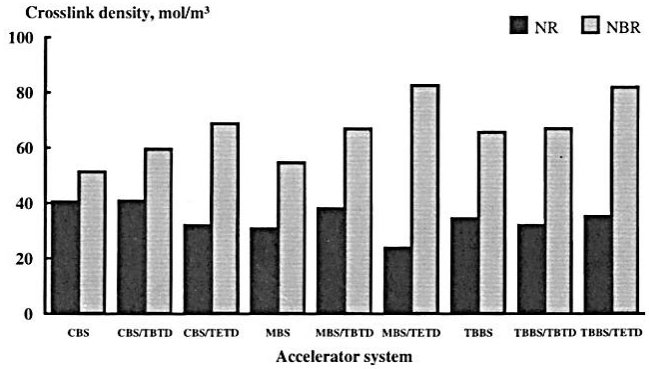

Figure 3.14 Crosslink density distributions in NR:NBR (34% ACN content) blends curing at 150 °C [29]

The type of accelerators as displayed in Figure 3.15 modifies the tensile strength of the blends. Using CBS as main accelerator provides higher tensile strength than using TBBS or MBS. By the way, the relationship between tensile strength and ratio of crosslink distribution is not clear in this case. It is difficult to clarify due to the crosslink distribution is skewed towards in NBR which is the dispersed phase.

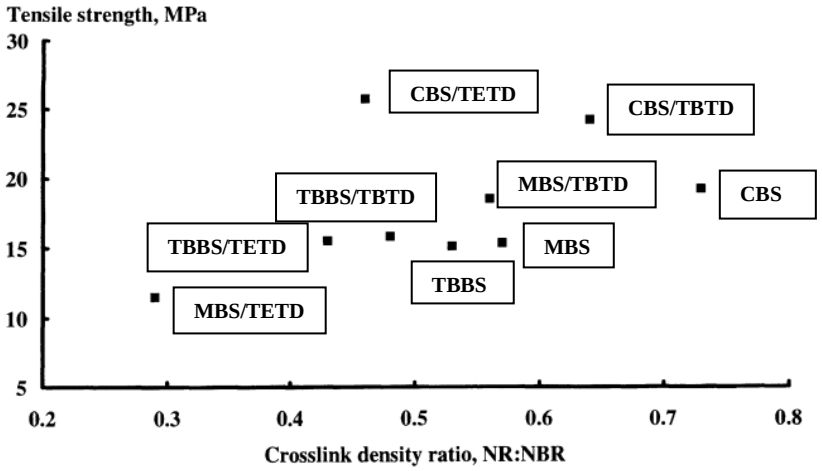

Figure 3.15 Dependence of tensile strength on NR:NBR crosslink density ratio for 1:1 ratio of NR:NBR with 34% acrylonitrile content [29]

In the blends with different ratios of rubbers, the relationship between crosslink density and mechanical properties may not be proportioned. In order to enhance the mechanical properties of rubber blends, curing additives can be incorporated in the major rubber component. Thus, the continuous phase is crosslinked to enhance the final properties. The masterbatch of major rubber component and curing additives could be mixed first to control the curative distribution in blends, although the curative migration can occur.

Wootthikanokkhan and Tongrubbai blended various ratios of NR and acrylic rubber using two different mixing methods [41]. In method A, NR and acrylic rubber were masticated together, then curing additives were added directly to the blends. In method B, curing additives were added to NR, then acrylic rubber was further incorporated. The relationship between rubber ratio and stress at break is displayed in Figure 3.16. Mechanical properties of the blends using method B are higher than those using method A when the NR content is high enough for co-continuous morphology. Thus, mechanical properties of the blend can be improved in some cases by mixing curing additives with continuous phase of NR, even if the crosslink densities are not equal in each rubber.

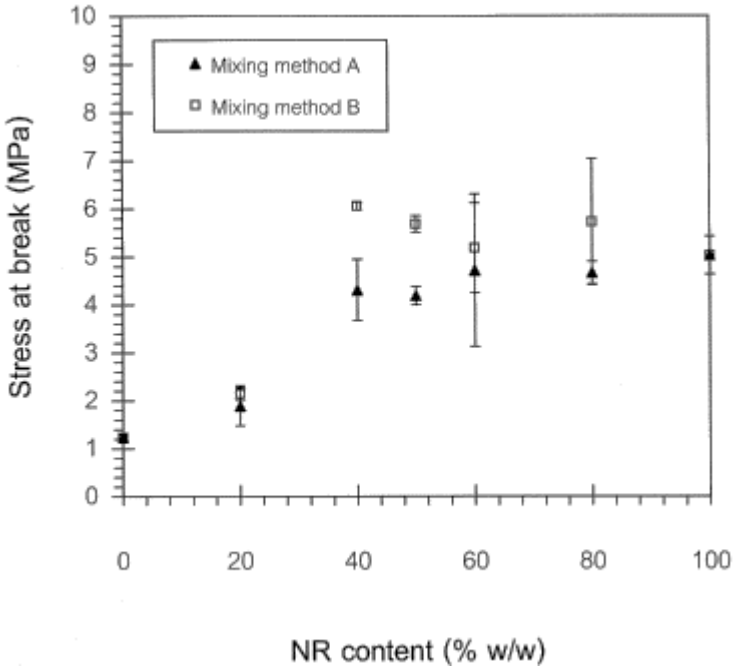

Figure 3.16 Tensile stress of NR and acrylic rubber blends as a function of NR content and mixing method [41]

3.3.4 Filler distribution

Not only distribution of curing additives can affect the properties of the rubber blends, filler distribution is also one important factor to control the final properties. Similar to curing additives, filler distribution depends on chemical structure of filler and the compatibility with each rubber. Carbon black is the most common filler that has been studied.

The distribution of carbon black (N550 grade) in the blends of NR and BR was first studied [42]. Due to the compatibility with these rubbers, carbon black was distributed homogeneously in both rubbers. By the way, the content of carbon black in each rubber phase could be controlled by the mixing method. Once carbon black was incorporated into rubber, the migration of carbon black to another rubber does rarely occur. The mechanism of the carbon black reinforcement will be discussed in the section 3.4.

The distribution of carbon black in the immiscible blends of NR and polar synthetic rubber was also studied. Wootthikanokkhan and Rattanathamwat incorporated carbon black (N330 grade) into NR and acrylic rubber blends [43]. Due

to non-polarity of carbon black used, carbon black was incorporated into NR phase rather than to acrylic rubber. To control the carbon black distribution in immiscible blends, the mixing method should be considered.

Edirisinghe and Freakley incorporated carbon black in NR and NBR blends [44]. The incorporation of carbon black (N660 grade) in each rubber before blending can be used to control the filler distribution in NR/NBR blends (45% ACN content) in a ratio of 40/60 wt%. The masterbatches of NR/carbon black and NBR/carbon black were prepared by varying the amounts of carbon black in NR phase at 10, 50, 90 wt%. In this study, NBR is the matrix and NR is dispersed phase due to the higher amount of NBR. The migration of carbon black was rarely observed in the blend, which is consistent to the other works i e. the blends of SBR and cis-polybutadiene [45–47]. The blend containing carbon black 90% in NBR phase exhibited higher modulus at 100% strain, hardness and tear strength. This enhancement is originated from the reinforcement effect of carbon black in NBR matrix.

To summarize, the control of the filler distribution in rubber depends also on the interactions between the rubber and the carbon black. The properties of carbon black depend also on the process used to produce them or the surface treatment that was used.

3.4 Carbon black reinforcement

Carbon black is a particulated porous substance, which can be obtained from the incomplete combustion of petroleum products. The structure of carbon black is illustrated in Figure 3.17. Not only carbon black is used as a diluent for decreasing the cost of rubber product, but it also reinforces the material [48]. Carbon black can be divided into many grades, which depends on the specific area and its structure. Carbon black grades are shown in Table 3.5. Primary particle size of carbon black is proportional to grade number. The primary particle size indicated the reinforcement effect in composites. Carbon black with smaller particle size reinforces the composite more effectively than larger particle size. However, the mixing process of carbon black with small particle size is more difficult than larger particle size.

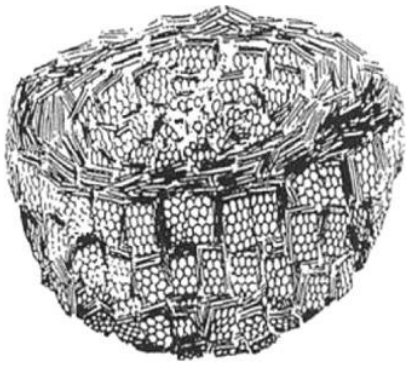

Figure 3.17 Sketch of carbon black primary particle [49]

Table 3.5 Grades of carbon black [according to ASTM D24]

Grade	Surface area (m^2/g)	Primary particle size (nm)
1	121-150	11-19
2	100-120	20-25
3	70-99	26-30
4	50-69	31-39
5	40-49	40-48
6	33-39	49-60
7	21-32	61-100

The principles of carbon black-reinforced elastomer has been proposed by Kraus [50] and Leblanc [51], which are Van der Waals interactions between carbon black and rubber, chemical crosslinks or chemisorption of rubber on the surface of carbon black from the free radical reaction and mechanical interlocking of rubber chains on the surface of carbon black. The general model was described using bound rubber, which was reported by Dannenberg [48]. The reinforcement of carbon black is shown in Figure 3.18.

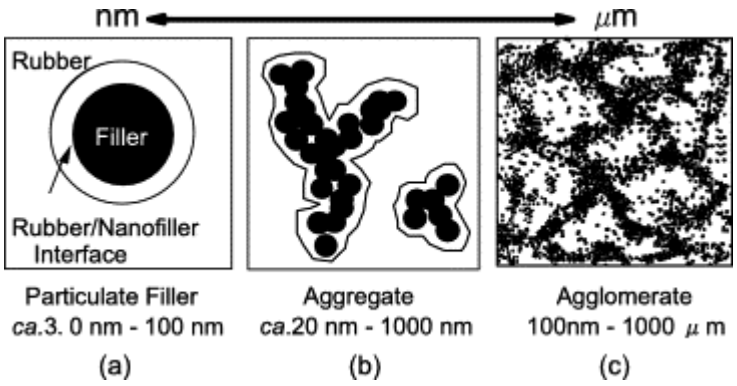

Figure 3.18 Schematic representation of carbon black-reinforced rubber [52]

The close layer of rubber attached on the surface of carbon black is called bound rubber, which is insoluble in good solvent of elastomer. Kaufman further reported that bound rubber can be divided into immobilized layer and outer mobile layer (or occluded rubber) [53]. It was hypothesized that the immobilized layer occurs only at 5% of total bound rubber. Thus, Fukahori proposed the new model on the interface of carbon black for elastomer reinforcement [54] as displayed in Figure 3.19. The glassy layer or inner polymer layer (GH-phase) is the inner rubber layer that rubber is immobilized on the surface of carbon black, whereas the sticky hard layer (SH-phase) is the layer that rubber has less mobility, compared to the bulk.

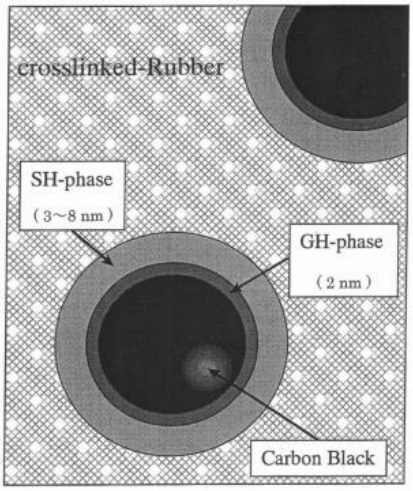

Figure 3.19 The interface model of carbon black-reinforced rubber [54]

Dannenberg [48], Kraus [50] and Wolff et al. [55] studied the effect of particle size of carbon black on SBR compounds. It was found that the smaller carbon black particle size is, lower bound rubber per unit surface is obtained. The aggregation of small particles of carbon black is likely occurring due to the strong filler-filler interactions. The effect of carbon black size on SBR is displayed in Figure 3.20 [50]. It can be seen that the higher specific surface area is, the higher tensile strength and elongation at break are obtained.

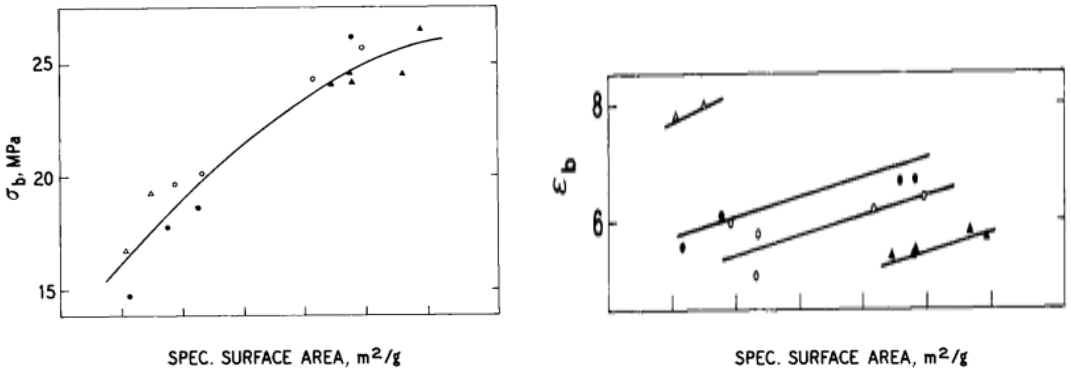

Figure 3.20 Tensile strength and elongation at break of SBR reinforced with various surface areas of carbon black 50 phr [50]

3.5 Natural fiber reinforcement

It is well-known that natural fibers is one of the fillers that can be incorporated into many composites due to its high specific strength properties, eco-friendly and abundancy in many countries. Classification of natural fibers is shown in Figure 3.21. Natural fibers can be divided, based on their sources, into many types such as wood, straw fibers, bast, leaf, seed, and grass.

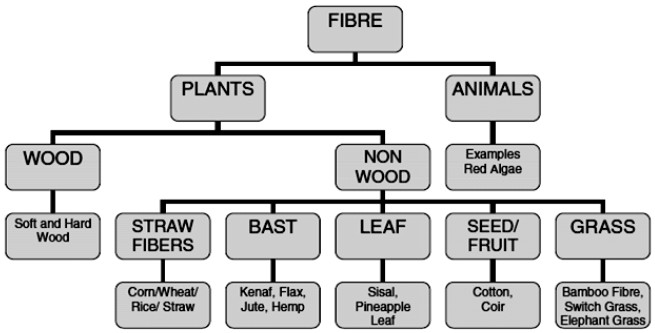

Figure 3.21 Classification of natural fiber [56]

3.5.1 Structure of natural fiber

The general structure of natural fibers is represented in Figure 3.22. The major component is cellulose, which has a crystalline structure, connectied with each other by hemicellulose and lignin [57]. Natural fiber is formed by cell wall and lumen as a transportation vessel. Cell wall of cellulose can be divided into primary cell wall and secondary cell wall. Secondary cell wall can be further divided into external secondary (S1), middle secondary (S2) and internal secondary cell walls (S3). The primary cell wall is indicated by the growth of the cell. Non-cellulosic substances such as wax, lignin and hemicellulose are presented at this cell wall area. Secondary cell wall indicates the arrangement of microfibrils in a helix structure of long chain cellulose. Microfibrillar angle, which represents the angle between the direction of cellulose helix structure and the fiber axis, has been used to predict the mechanical properties of fiber. Microfibrillar angle at the middle secondary cell wall has been measured by X-ray diffraction [58]. Lower microfibrillar angle is, higher mechanical properties of fiber is obtained. Thus, the mechanical properties of fibers depend on the cellulosic content and its microfibrillar angle.

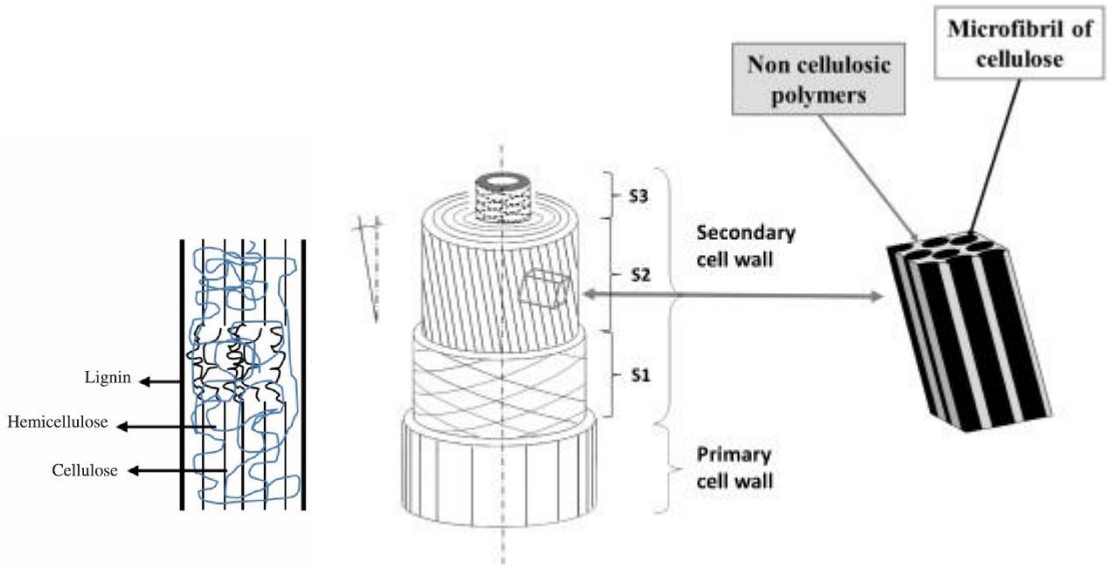

Figure 3.22 Schematic representation of flax fiber [59]

3.5.2 Pineapple leaf fiber

Thailand is the largest producer of pineapple in the world. While fresh and juice of pineapple are widely used in cuisines, pineapple leaf fibers (PALF) represent an agricultural waste. After farmers harvest the fruit, a large amount of pineapple leaf remains in the land and causes problems to farmers. Nowadays, PALF are used in a very limited way in leather and handcraft paper [60–62]. To use PALF in engineering applications, the deep understanding of PALF characteristics is required.

PALF consists of high cellulosic content, as can be seen in Table 3.6. Hence, the mechanical properties of PALF are very attractive, compared to other natural fibers as shown in Table 3.7. Moreover, modulus of PALF is comparable with glass fibers. Mechanical properties of PALF is also depended on the extraction method. Amornsakchai's research group at Mahidol University has invented mechanical milling to extract PALF with high yield and fine of pure PALF [63]. The extraction of PALF is shown in Figure 3.23. The fibers are in the bundle shape with 6 mm in length and 3-15 μm of elementary fibers diameter after processing. Using PALF as a reinforcing agent in polymer gives many advantages due to its high aspect ratio and its high strength. Major component of PALF is cellulose, which chemical structure is shown in Figure 3.24. Cellulose consists of three hydroxyl groups per one repeat unit, hence it is a high polar substance. Thus, the incorporation of PALF into non-polar polymer will not result

in the optimum mechanical properties. Thus, the improvement of the interfacial adhesion between rubber and PALF is required to improve the stress transfer between them.

Table 3.6 Chemical composition and structural parameters of various natural fibers [64]

Fibers	**Cellulose (%wt)**	**Lignin (%wt)**	**Hemi-cellulose (%wt)**	**Pectin (%wt)**	**Wax (%wt)**	**Microfibrillar angle (Deg.)**
Ramie	68.6-76.2	0.6-0.7	13.1-16.7	1.9	0.3	7.5
PALF	**70-82**	**5-12**	**9**	**-**	**-**	**14.0**
Flax	71	2.2	18.6-20.6	2.3	1.7	10.0
Jute	61-71.5	12-13	13.6-20.4	0.2	0.5	8.0
Sisal	67-78	8-11	10.0-14.2	10.0	2.0	20.0
Cotton	82.7	-	5.7	-	0.6	-

Table 3.7 Comparatives properties of fibers [64]

Fibers	**Density (g/cm^3)**	**Tensile strength (MPa)**	**Young's modulus (GPa)**	**Elongation at break (%)**
Ramie	1.5	400-938	61.4-128	1.2-3.8
PALF	**1.44**	**413-1627**	**34.5-82.5**	**1.6**
Flax	1.5-3	450-1100	27.6	2.7-3.2
Jute	1.3-1.45	393-773	13-26.5	7-8
Sisal	1.45	468-640	9.4-22	3-7
Cotton	1.5-1.6	287-800	5.5-12.6	7-8
E-glass	2.5	2000-3500	70	2.5
S-glass	2.5	4570	86	2.8
Carbon	1.7	4000	230-240	1.4-1.8

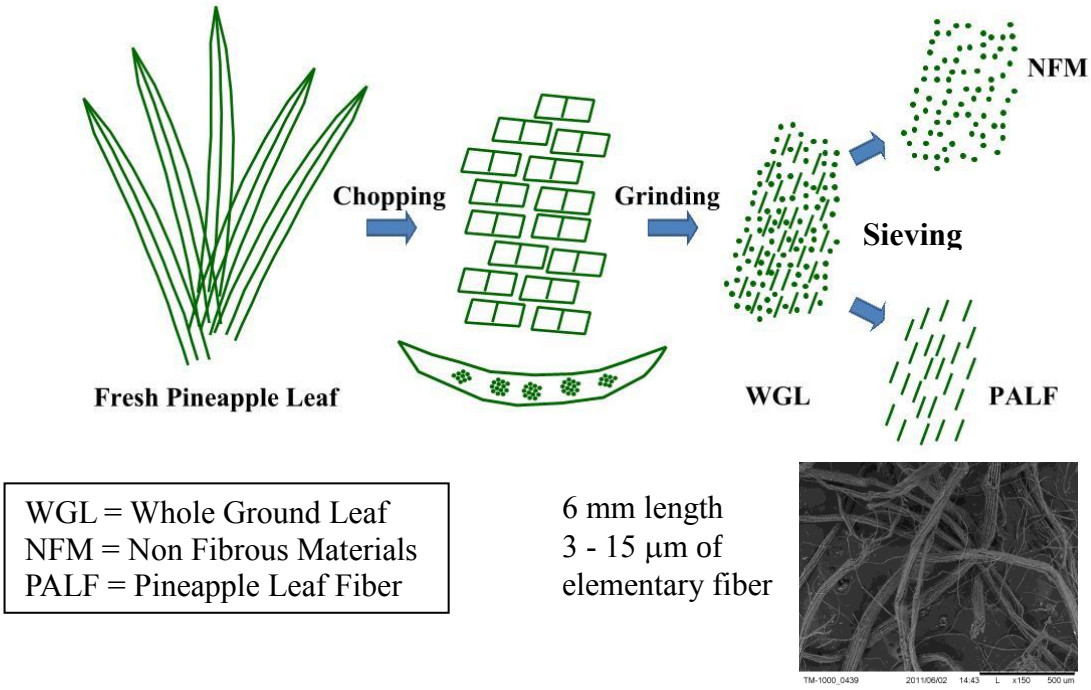

Figure 3.23 Extraction of PALF at Mahidol University [63]

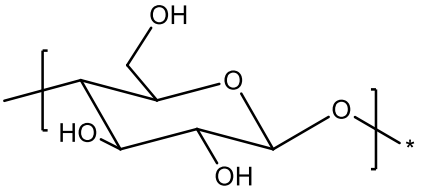

Figure 3.24 Chemical structure of cellulose

3.5.3 The using of short fibers as reinforcing fillers for natural rubber

Although long fibers have high aspect ratio, high elastic modulus and high strength, the incorporation of them is difficult due to fibers entanglement and alignment [65]. Thus, nowadays, short fibers have been extensively studied instead of long fibers. The advantage of short fibers-reinforced composites is the processability (fiber orientation), which results in high mechanical properties.

The effect of short fiber orientation has been published by Jacob, Thomas and Varughese [66]. The authors incorporated short coir/oil palm hybrid fibers in NR composites. The average lengths of sisal fibers are at 10 mm and oil palm fiber are at 6 mm, whereas average diameters are 120 µm and 150-500 µm respectively. The short

fibers orientation was determined by measurement of the green strength of composites in longitudinal and transversal directions [67]. The relationship between fiber orientation and fiber loading is displayed in Figure 3.25. At low loading, fibers were suggested to move in the matrix. By increasing fibers content, the orientation was obtained. At excessive fiber loading, the fibers orientation was lower due to the entanglement. By the way, it should be mentioned that the fiber orientation is depended on aspect ratio of fibers.

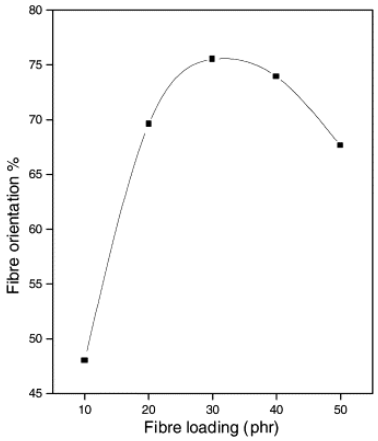

Figure 3.25 Effect of fiber loading on percentage orientation [66]

The typical stress strain curve for short fibers-reinforced rubber has been published by O'connor [68] and is shown in Figure 3.26 (a). Young's modulus is significantly improved by short fibers due to the fiber orientation. Yield point might occur depending on elastomer, fibers and their interactions. O'Connor introduced various types of short fibers into NBR and the stress-strain curves are shown in Figure 3.26 (b). It can be observed that Young's modulus significantly increases by incorporation of short fibers. This improvement is unique for short fiber reinforcement. By the way, the level of improvement was affected by the fiber types. The author suggested that it depends on many factors i e. aspect ratio of fibers, moduli of fibers and matrix and the interactions between them.

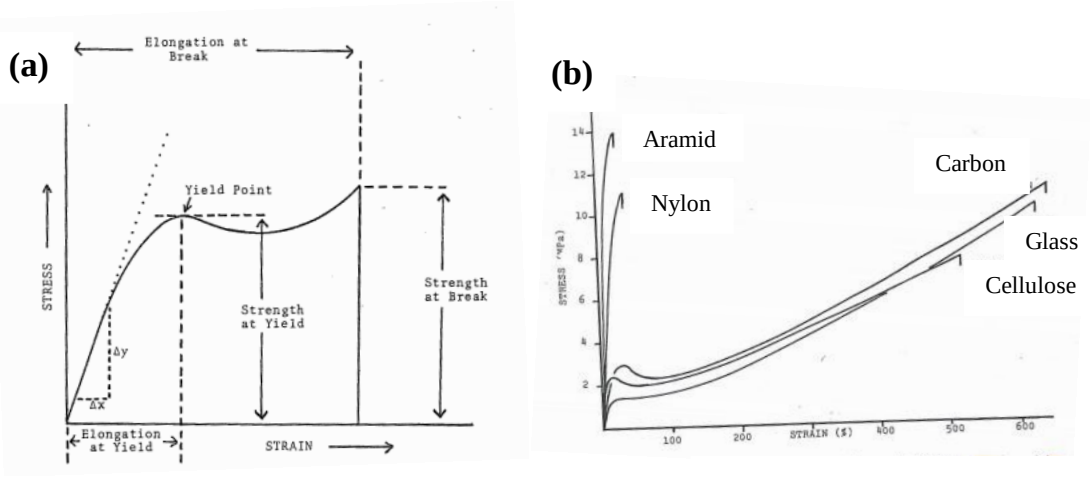

Figure 3.26 Typical stress-strain curve of short fibers-reinforced composites (a) and stress-strain curves of short fibers-reinforced NBR in a longitudinal direction (b) [68]

3.5.4 Proposed mechanism of short fiber reinforced composites

The elastic properties of short-fiber-reinforced polymer have been predicted from mathematical models. Rule of mixture [69], shear lag model [70] and Halpin-Tsai equation [71] have been reported to predict the modulus of composites. However, it has been reported that Halpin-Tsai equation can produce the minimum total error from the experiments for short-fiber-reinforced composites [72].

Halpin-Tsai equation has been widely used for predicting the elastic modulus of short-fiber reinforced composites (equation 4).

$$E = E_m \frac{1+\xi\eta V_f}{1-\eta V_f}, \quad while \quad \eta = \frac{\left(\frac{E_f}{E_m}\right)-1}{\left(\frac{E_f}{E_m}\right)+\xi} \qquad \text{equation 4}$$

Where E is the elastic modulus of composites, E_m is the elastic modulus of matrix, E_f is the elastic modulus of filler, ξ is a geometric factor, V_f is the volume fraction of filler.

The geometric factor plays the important role to describe the influence of geometry of reinforcing fillers. For modulus in tensile testing of short fiber-reinforced composite, ξ depends on the direction and aspect ratio of fibers (equation 5).

$$\xi_L = 2\frac{L}{D}, \xi_T = 2 \qquad \text{equation 5}$$

Where L is the fiber length and D is the fiber diameter.

It can be seen that the geometry of the fibers, moduli of fiber and matrix are taken into account to increase the modulus of composite. However, there are still limitations of this equation. The various approaches assume that matrix and fibers is perfectly bonded and fibers are perfectly aligned in one direction. Moreover, they assumed that the slippage between the interface of fibers and matrix or pullout fibers are not occurring during measurement.

3.5.5 Natural fiber-reinforced elastomer and improvement of stress transfer between them

The effect of the incorporation of natural fibers into NR on mechanical properties such as Young's modulus, tear strength, tensile strength, hardness has been studied [66,73–75]. Most of the goals of NR/natural fiber composites are to improve the interfacial strength between them. If the interfacial strength between NR and fibers is improved, the stress-transfer between them will also improve.

Natural rubber is incompatible with natural fiber due to the large difference between their polarities. Thus, the stress transfer between them is low, which results in low mechanical properties. To improve the stress transfer between them, two different approaches are proposed. First approach is to enhance the physical interactions between rubber and fibers by using compatibilizer as an intermediate substance. Incorporation of dry bonding agent and incompatible rubber will be reviewed. Second approach is to generate chemical bonding between rubber and fiber by surface treatment of fiber i e. alkali treatment and silane treatment. However, it is difficult to compare the results of various studies. Most of the parameters such as nature of fibers, fiber length, L/D ratio, amount of fibers in composite, composite production method and curing system are not fixed.

3.5.5.1 Incorporation of dry bonding agent

Dry bonding agent represents as one of the compatibilizers that can enhance the interfacial adhesion between rubber and fiber or silica. Dry bonding agent consists of resorcinol, hexamethylene tetramine and hydrated silica, which are crosslinked together during the mixing process [76]. Mechanism of the interfacial adhesion improvement was previously described by Dressler [77]. Hydrogen bonding and Chroman ring formation between NR/bonding agent and hydrogen bonding between bonding agent/silica are able to improve the interfacial adhesion between them. Nowadays, bonding agent has been also utilized using fiber as filler. The presence of hydroxyl group is the opportunity to enhance the interfacial adhesion between fiber and rubber by bonding agent. The adapted mechanism of dry bonding agent on fiber and rubber is shown in Figure 3.27.

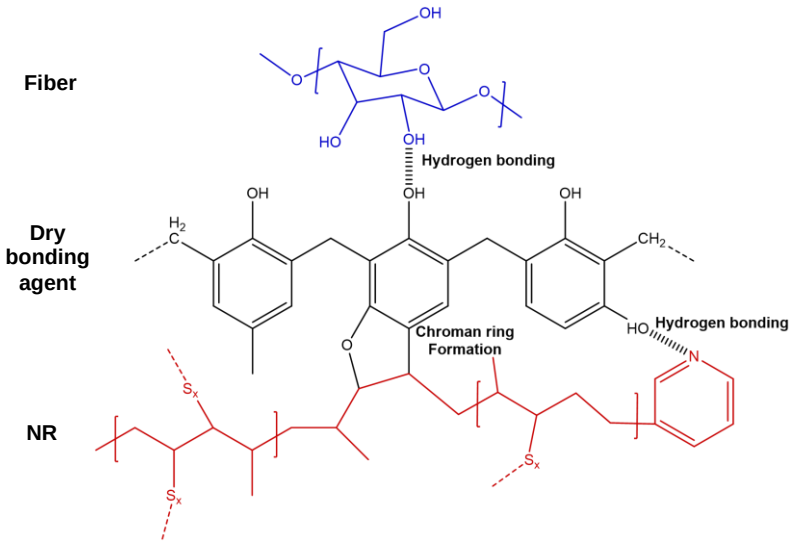

Figure 3.27 Adapted Resorcinol chemistry mechanism of NR and fiber using RFL additives

The incorporation of dry bonding agent in rayon fiber and polymer matrix was first investigated by Derringer [78]. Dry bonding agent was incorporated into polyester resin containing rayon fiber. Their stress-strain curves are represented in Figure 3.28. Modulus at low strain, yield stress, and also stress at moderate strain were significantly improved in the presence of dry bonding agent due to the enhancement of the interfacial adhesion between polyester and rayon fiber.

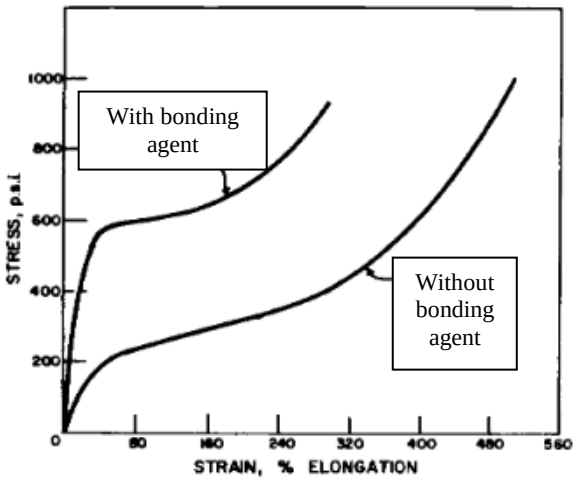

Figure 3.28 Stress-strain curves of polyester/fiber composites [78]

Ismail and co-workers studied the effect of dry bonding agent on mechanical properties of fiber-reinforced rubber composites [79]. Various types of bonding agents were incorporated into NR containing oil palm fiber. Phenol formaldehyde (PF) and resorcinol formaldehyde (RF) containing silica and hexamethylene tetramine were investigated. By incorporation of RF:silica:hexamethylene tetramine in a ratio of 5:2:5 (in part per hundred of rubber), the highest mechanical properties was observed due to the strongest binding between rubber and oil palm fiber. The improvement of mechanical properties using dry bonding agent was also reported by Mathew, Ulahannan and Joseph [80]. RF, silica and hexamethylene tetramine in a ratio of 5:2:1.6 (in part per hundred of rubber) were added to isora fiber-reinforced NR composite. The swelling ratio of NR/fiber composites decreased by incorporation of bonding agent due to stronger interfacial strength.

Dry bonding agents, nowadays, has been investigated due to its ease to process and less energy consumption. However, the incorporation of a large amount of three components containing RF, silica and hexamethylene tetramine causes complex mechanism in composite during mixing and shaping. Moreover, the actual mechanism is still unclear. Moreover, the mixing is limited to only high shear force mixing in order to disperse all components of bonding agent into matrix.

3.5.5.2 Incorporation of incompatible rubber

There are only few reports on the incorporation of incompatible rubber as a compatibilizer in natural rubber/natural fiber composites. Although the incorporation of this rubber enhances only physical interactions between rubber and fiber, it is more convenient to process. Since compatibilizer can be incorporated directly into the mixing process, this method is simple and consumes less energy. It also allows a simple transfer to rubber technology and industry.

Epoxidized natural rubber (ENR), maleated NR (MNR) and NBR have been used as compatibilizers to improve the interfacial adhesion between NR and fiber. The chemical structures of ENR and MNR are shown in Figure 3.29.

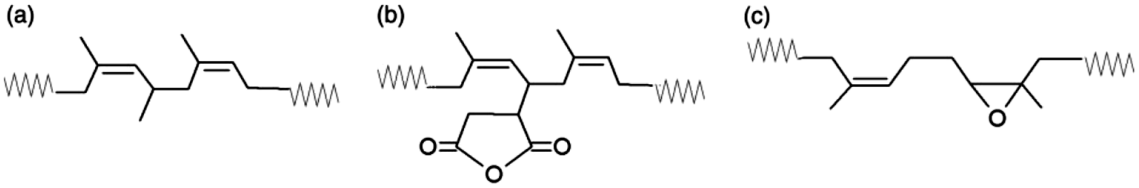

Figure 3.29 Chemical structures of NR (a), MNR (b) and ENR (c)

ENR has been modified from NR latex using peracid solution [81]. After modification, it is coagulated using methanol then the solution is evaporated to produce ENR. The amount of epoxide groups can be adjusted by varying the peracid concentration. The degree of epoxidation varies generally between 25 and 50%. Although the elasticity of ENR is lower than that of NR, oil and chemical resistance is higher [82]. In addition, ENR can be used as compatibilizer for filled NR due to its higher polarity than NR with a similar backbone chain structure.

Ismail and co-workers incorporated paper sludge into NR and compared with that of ENR having 50% degree of epoxidation composites [83]. Dynamic properties i e., maximum torque, elastic modulus and tensile modulus increased by loading fillers in both rubbers. For composites with the same amount of fillers, ENR composite exhibited higher modulus at 100% and 300% strains and also tensile strength. The authors concluded the stress transfer improvement from the stronger rubber-filler interactions between hydroxyl groups of cellulose and epoxy groups of ENR.

MNR has been modified from NR using maleic anhydride (MA). This modification can be done during mixing in internal mixer [84,85]. The concentration of MA on NR indicates the increase of glass transition temperature of NR [84]. Generally, MNR has been utilized as the compatibilizer of immiscible rubber blends [84,86-87] and also used to enhance the interactions between rubber and filler [85,88].

Zeng and co-workers grafted MA on NR using internal mixer and incorporated the various amounts of MNR from 0 to 20 phr (of total rubber content) in cotton-filled NR composites [85]. By increasing MA content in MNR up to 20 phr, modulus at 100% strain increased up to 21% and tensile strength increased 6%. Higher interfacial adhesion between NR and fiber has been indicated by the incorporation of MNR, which is compatible with cotton fiber due to its high polarity. The authors proposed the effect of hydrogen bonding between fiber and MNR in Figure 3.30.

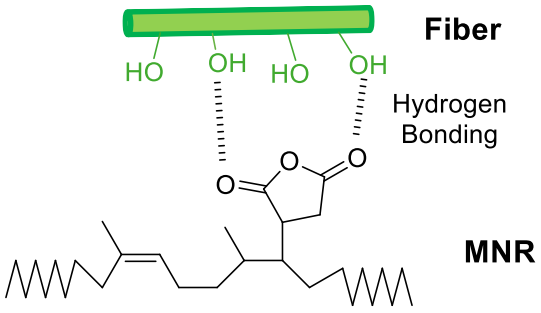

Figure 3.30 Hydrogen bond formation between fibers and MNR [85]

Wongsorat, Suppakarn and Jarukumjorn compared the effect of MNR and ENR on NR/sisal fiber composites [89]. Purchased ENR was 50% epoxy content, whereas MNR was prepared by grafting MA. Grafted MA content was quantified as 1.38 wt% by titrating the anhydride functional groups. ENR or MNR was further incorporated into NR/sisal fiber composites at 5 phr in a presence of sisal fiber 10 phr. MNR provides higher improvement of mechanical properties rather than ENR. Using MNR increased moduli at 100% and 300% strains for uncompatibilized NR/sisal fiber composite by 44 and 53% respectively. However, the authors did not discuss in details the comparison of the effects of MNR and ENR.

Although ENR and MNR are effectively used to improve interfacial adhesion between NR and fiber, there is one more preparation step to modify and control functional groups of NR as compatibilizer.

There is only one study on the incorporation of NBR in order to improve the mechanical properties of filler-reinforced NR composite. Yan and co-workers incorporated NBR into NR/silica composite in order to improve the dispersion of silica [90]. It was observed by SEM and is shown in Figure 3.31. It was suggested that NBR prevents the curatives adsorption on the surface of silica. The compatibility of NBR and silica was the driving force to improve the mechanical properties of composite due to their close polarities.

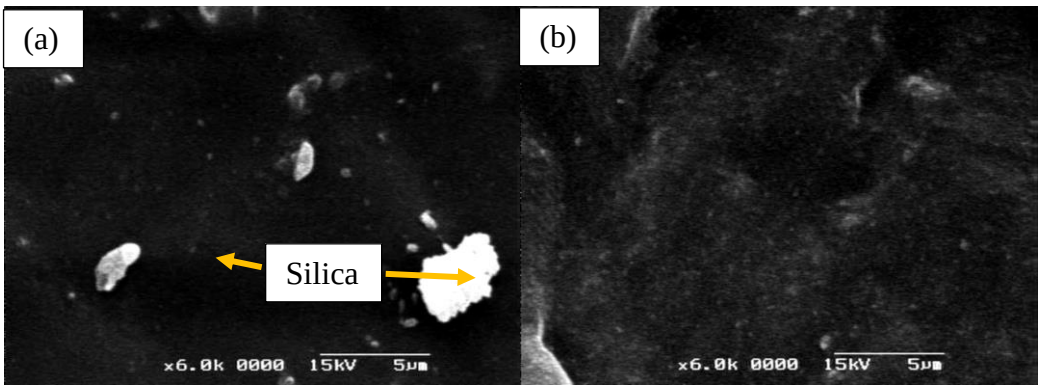

Figure 3.31 SEM images of NR/silica composite without NBR (a) and with NBR 16 phr (b) [90]

By replacing NR by NBR from 0 to 16 phr of total rubber content, modulus at 100% strain increased proportionally to NBR content up to 15%. Modulus at 300% strain did not further increase. Tensile strength and elongation at break reached the maximum value when 4 phr of NBR was added to the composite. In conclusion, although NBR is not compatible with NR, NBR can be used to improve the mechanical properties of filler-reinforced NR composites. However, the authors did not discuss anything on the distribution of curatives and fillers in the two rubbers. Moreover the mechanical properties did not significantly improve.

3.5.5.3 Alkali treatment of fibers

Unlike synthetic or glass fibers, natural fibers are gathered from natural substances. It still contains contaminations on the surface such as hemicellulose, waxes and lignin. Thus, the surface treatment can be required to clean non-cellulosic substances. Fibers are soaked in sodium hydroxide (NaOH) solution at room temperature then washed for several times. Excessive NaOH concentration and soaking time will result in weakening mechanical properties of fibers due to excessive delignification [91-92]. Alkali treatment is commonly used to clean the fiber to remove waxes and also hemicellulose [93-94]. Moreover, the surface is rough after treatment. SEM images of untreated and alkali-treated fibers are shown in Figure 3.32.

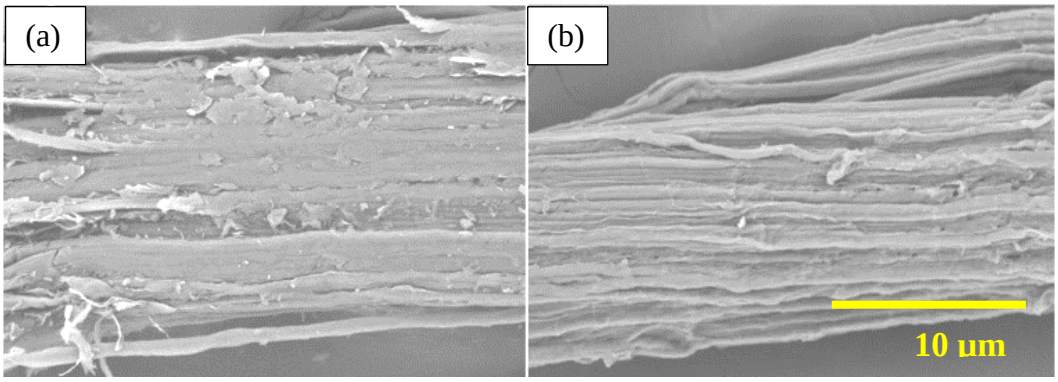

Figure 3.32 SEM images of untreated PALF (a) and alkali-treated PALF (b) [94]

Thus, alkali treatment of fibers results in an increase of surface roughness and an increase of amount of cellulosic content [93]. Moreover, chemical treatment can be further used to reduce polarity of cellulose or generate the designated functional groups in a specific way.

Sreekala et al. treated oil palm fibers with 5 wt% NaOH solution for 24 h [95]. It was observed that tensile strength and elongation at break of fibers decreased after treatment. By incorporation of alkali-treated fibers into phenol formaldehyde resin, tensile modulus at 2% strain and flexural strength increased, compared to untreated fibers. It was reported that the interfacial strength between natural fibers and polymer was improved due to the increase the surface roughness of the fibers.

Bay et al. treated jute fibers with 5 wt% NaOH solution for 0, 2, 4, 6 and 8 h before incorporation into vinylester resin [96]. Fibers were incorporated at 35 wt% of composite. The optimum condition for reinforcement is treatment for 4 h leading to flexural strength, modulus and laminar shear strength improved by 20%.

Mwaikambo, Tucker and Clark treated hemp fibers with 0.16 wt% NaOH solution for 48 h before incorporation into euphoria resin [97]. Fibers were incorporated at 20 wt% of composite. Modulus and tensile strength of composites were improved. It was suggested that the mechanical locking was obtained from resin and the rough surface of the fibers.

In Mahidol University, the effect of alkali treatment of PALF has also been studied. Nopparut and Amornsakchai treated PALF with 10 wt% NaOH solution for 30 min then incorporated in nylon 6 composite [94]. Tensile and flexural strengths increased by 12% and 11% with the incorporation of alkali-treated PALF 20 wt%, compared to untreated PALF. In addition, tensile and flexural moduli also increased by 33% and 14%.

Although many researchers have been working on alkali treatment of natural fibers, only a few researchers have worked on effect of alkali treatment of fibers in natural rubber composites. Geethamma, Joseph and Thomas treated short coir fibers with 5 wt% NaOH for 4, 24, 48, 72 h then incorporated into NR [73,98]. Modulus, tensile strength and tear strength increased by incorporation of alkali-treated fibers, which are treated for 24 h. It was also hypothesized that the improvement of tensile properties was obtained from the mechanical interlocking between rough surface of fibers and NR.

Wongsorat, Suppakarn and Jarukumjorn treated sisal fibers with NaOH solution and incorporated in NR composites [99]. It was found that modulus at 10, 100 and 300% strain increased. Similar to previous research works, the better interfacial strength was obtained from the mechanical interlocking between fibers and NR.

3.5.5.4 Silane treatment of fibers

Silane treatment is used for surface modification in inorganic filler reinforced polymer composites and mineral filled polymer composites [100–103]. This method has been widely utilized due to its cost, compared to other treatments such as phosphorus treatment or benzoyl treatments. Generally, the interactions between natural fibers and silane coupling agents is carried out through following steps, which are shown in Figure 3.33.

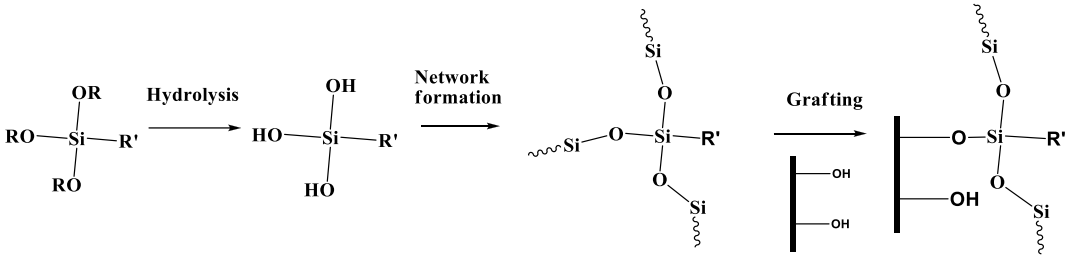

Figure 3.33 Reaction scheme of silane treatment [102]

1. *Hydrolysis* : Silane coupling agent is hydrolyzed in presence of water and catalyst.
2. *Network formation* : Silane network is formed by self-condensation.
3. *Grafting* : After fiber is added into the mixture, hydrogen bonds between silanes and hydroxyl groups at the surface of fiber react with each other

From all above, the structure of silane is the most important variable for coupling with fiber and polymer. The structure of silane is divided into two parts: (1.) a tail made of an alkoxy (OR), which affects the hydrolysis and network formation processes for coupling with fiber surface ; (2.) an alkyl group for the corpse and an end-group which represents a reactive site for coupling with the polymer.

Silane coupling agent has been widely used to enhance the interactions between fillers and polymer matrix. Bi-functional molecular structure of silane is the key to enhance the interactions. Thus, silanes with various type of functional groups have been studied in order to improve the interfacial adhesion between fillers and polymer. Silane coupling agent can be used in most polymer composites such as thermoplastic [93,104] and resin [105-106].

Recently, silane coupling agents have also been used in rubber composites. Generally, Bis(3-triethoxysilylpropyl tetrasulfide) (Silane-69 or TESPT) has been used to couple silica with NR [107]. Silane is not only used to reduce the polarity of silica, it also provides free sulfur to form chemical bonding between them via crosslinking process of rubber. Thus, the interactions between rubber and silica are significantly increased from the lower difference of polarities and chemical bonding formation between them. The improvement of mechanical properties is achieved by increasing the interactions between NR and silica. Brinke proposed the reactions of bonding silane-69 to the silica surface and bonding of silane-69-treated silica to NR, which are shown in Figure 3.34 [108]. The reaction is first occurring by hydrolysis and condensation of silane-69 on the surface of silica. After that, the reactive sites (cyclic sulfur and free sulfur for silane-69) are crosslinked to NR during vulcanization.

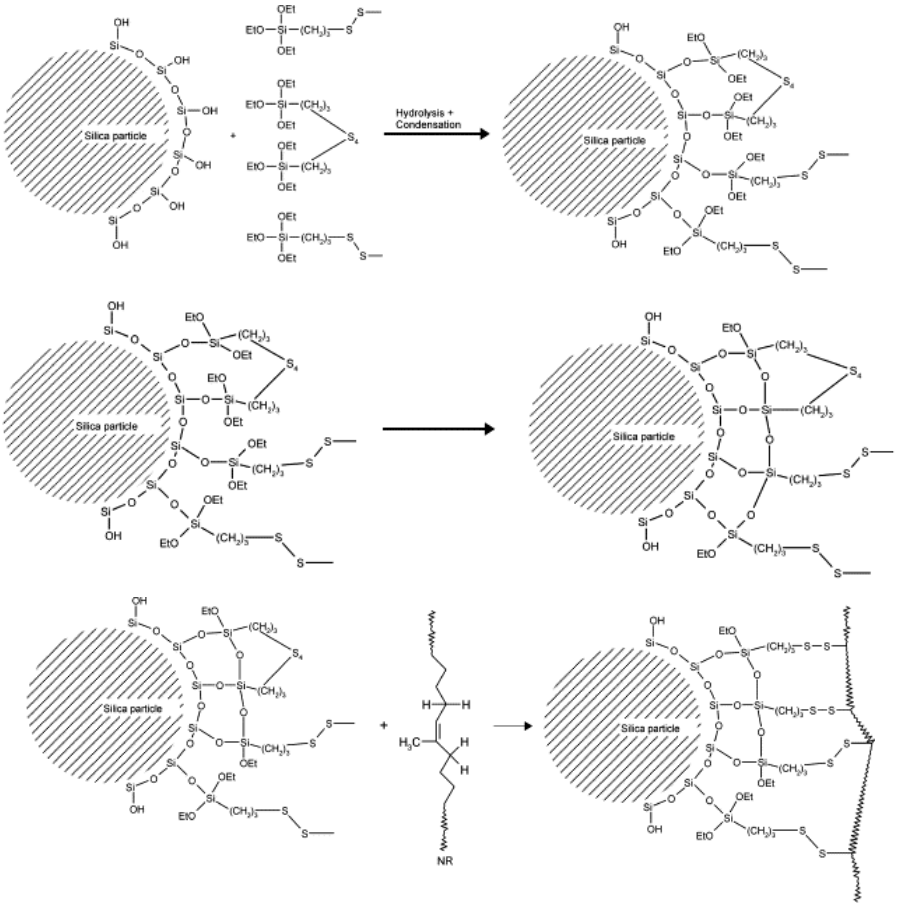

Figure 3.34 Reaction schemes of silane-69 on silica particles and NR [108]

There are two methods to utilize silane to improve the mechanical properties of composite. On the one hand, silane has been incorporated directly during mixing. This method is easy to process, however, only parts of silane can act as compatibilizer. On the other hand, silane has been used to treat the filler's surface before mixing with the rubber. Although this method requires one more step to process, silane is strongly bonded to the surface of the filler, which results in higher mechanical properties. Generally, silane has been directly incorporated to NR/silica composites due to high surface area of silica.

Ten-Brinke et. al. have studied the incorporation of various types of silanes into SBR/BR and silica tire tread compounds to improve the interfacial adhesion between rubbers and silica [108]. The chemical structures of silane coupling agents are shown in Table 3.8. It was reported that silane-69 increased the interfacial adhesion between rubbers and silica, which led to increase the modulus of composites as shown in Figure 3.35.

Table 3.8 Silane coupling agents and their chemical structures

Coupling agents	Name	Chemical structure
Bis(triethoxysilylpropyl)-tetrasulphide	TESPT	$(C_2H_5\text{-}O)_3\text{-}Si\text{-}CH_2)_3\text{-}S_4\text{-}(CH_2)_3\text{-}Si\text{-}(O\text{-}C_2H_5)_3$
Bis(triethoxysilylpropyl)-disulphide	TESPD	$(C_2H_5\text{-}O)_3\text{-}Si\text{-}(CH_2)_3\text{-}S_2\text{-}(CH_2)_3\text{-}Si\text{-}(O\text{-}C_2H_5)_3$
Bis(triethoxysilylpropyl)monosulphide	TESPM	$(C_2H_5\text{-}O)_3\text{-}Si\text{-}(CH_2)_3\text{-}S\text{-}(CH_2)_3\text{-}Si\text{-}(O\text{-}C_2H_5)_3$
Bis(triethoxysilyl) ethane	ETES	$(C_2H_5\text{-}O)_3\text{-}Si\text{-}(CH_2)_2\text{-}Si\text{-}(O\text{-}C_2H_5)_3$
Bis(triethoxysilyl)hexane	HTES	$(C_2H_5\text{-}O)_3\text{-}Si\text{-}(CH_2)_6\text{-}Si\text{-}(O\text{-}C_2H_5)_3$
Bis(triethoxysilyl) decane	DTES	$(C_2H_5\text{-}O)_3\text{-}Si\text{-}(CH_2)_{10}\text{-}Si\text{-}(O\text{-}C_2H_5)_3$
γ-Mercaptopropyl-triethoxysilane	MPTES	$(C_2H_5\text{—}O)_3\text{—}Si\text{—}(CH_2)_3\text{—}SH$

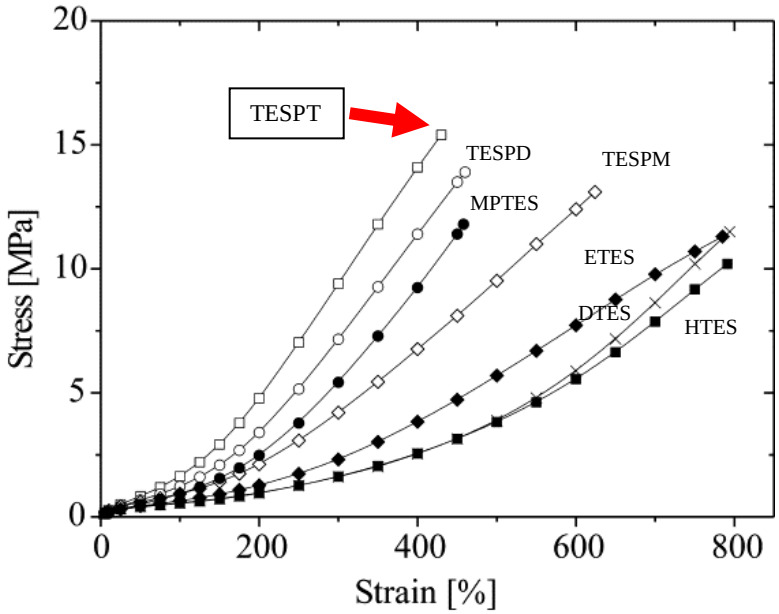

Figure 3.35 Stress-strain curves of SBR/BR/silica composites with various types of silanes with silica content 80 phr [108]

Dohi and Horiuchi studied the effect of mixing temperature for coupling silane-69 with silica and NR [109]. This system has been characterized by Energy-Filtering Transmission Electron Microscopy (EFTEM). Silane could be coupled to NR and silica by mixing at 110 °C. Furthermore, when mixing at 150 °C, bound rubber content was increased from 9.8 to 18.3%. The authors suggested that a larger number of silanol groups on the silica surface reacted with TESPT, resulting in a thick coupling layer at the interface.

Choi, Kim and Woo studied the effect of silane-69 content on silica-filled NR [110]. Silane-69 content was varied from 0 to 4.8 phr, which was incorporated in NR with silica during mixing. Crosslink-density as a function of silane content in NR/silica composites is plotted in Figure 3.36. Higher amount of silane-69 increased the total crosslink density of the composites. The increasing ratio of polysulfidic crosslinks is higher than mono and disulfides. It was suggested that polysulfide (from accelerated sulfur vulcanization system) can dissociate and form with silane-69.

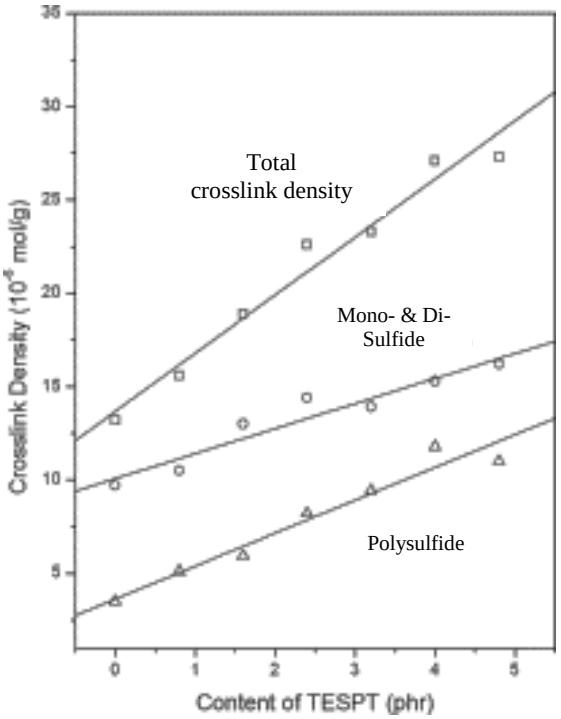

Figure 3.36 Crosslink density of the NR/silica vulcanizates with silane-69 [110]

It can be seen that silane-69 is an effective coupling agent for elastomers and silica. However, there are only few researchers who reported the effect of silane coupling agent on natural fibers. Silane coupling agent of natural fibers is more difficult than on silica due to its lower surface area and contamination on the surface of fiber. Surface treatment has been studied instead of directly incorporation during mixing to achieve the optimum conditions.

Valadez-Gonzalez et.al. have studied the effect of alkali and silane treatments of natural fibers on HDPE composites [93]. Natural fibers were pre-treated with alkali treatment and silane treatment before incorporation into HDPE during mixing process. It was reported that vinylsilane was successfully attached on alkali-treated fibers. HDPE composites containing fibers, which was treated by alkali treatment followed by silane treatment fiber exhibited the highest tensile strength, as can be seen in Figure 3.37.

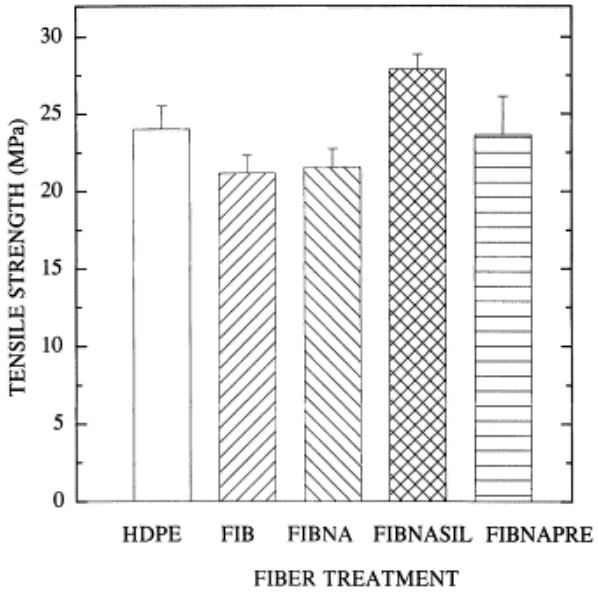

Figure 3.37 Tensile strengths of HDPE, HDPE with untreated fiber (FIB), HDPE with alkali-treated fiber (FIBNA), HDPE with alkali-silane-treated fiber (FIBNASIL) and HDPE with alkali-treated fiber followed by immersion in PE dilute solution (FIBNAPRE) [93]

Zeng and co-workers incorporated silane-69 into NR and cotton fibers composites during mixing [111]. The initial temperature of mixing was set at 80 °C in order to hydrolyze and condense Silane-69 during mixing. After that, silane-grafted fibers were coupled with NR during vulcanization. Crosslink density of composites containing 10 phr of cotton fibers slightly increased from 0.18 to 0.23 by addition of silane-69. Initial modulus of composites was increased from 2.25 to 2.92 MPa. Modulus at 100% strain slightly increased from 2.2 to 2.4 MPa and modulus at 300% strain also slightly increased from 2.9 to 3.4 MPa. It can be concluded that the mechanical properties of NR/cotton fibers composites were improved by silane-69. However, the magnitude of improvement is low due to the low surface area of fibers, compared to silica. Moreover, silane-69 was less reactive during mixing, compared to the surface treatment before mixing.

In conclusion, silane treatment has successfully improved the mechanical properties of rubber/filler composites. The treatment of fibers in the silane solution before mixing with polymer does not give the similar result as for silane

treatment during mixing process. The treatment of fibers is more able to control and no non-reacted silane is incorporated into the mixing. However, silane treatment of fibers still requires more experiments to improve the mechanical properties of rubber/fiber composites effectively. The deep understanding of the silane treatment on fibers such as the silane concentration, solvent effect and washing method is still unclear.

3.6 Natural fiber and particulated filler reinforced NR

Nowadays, the reinforcement of hybrid composites based on two or more fillers has been studied. The goal of these studies are to maximize the fillers efficiency and combining the reinforcement effects. Hybrid fillers have been recently used in thermoplastics [112–114]. However, only few researchers have been studied hybrid rubber composites.

Jacob, Thomas and Varughese studied on the sisal/oil palm hybrid fibers for reinforcing NR [66]. While sisal fibers exhibit high tensile strength, oil palm fibers exhibit toughness. The average lengths of sisal and oil palm fibers are respectively equal to 10 mm and 6 mm whereas average diameters are 120 µm and 150-500 µm respectively. The effects of fiber loading was studied. By increasing the fibers content from 10 phr (5/5 phr of sisal/oil palm fibers) to 50 phr, modulus at 100% strain increases two-fold. Tensile strength reaches the maximum value when total fiber content is 30 phr. It was suggested that the low amounts of fibers do not produce the orientation of fibers, resulting in lower tensile strength. Excessive amounts of fibers more than 30 phr cause the agglomeration of fibers as bundles. These bundles act as a barrier for stress transfer as the interfacial surface is lower. They only discussed on the combined reinforcing effects. Moreover, the fibers have low aspect ratio. Thus, the effect of reinforcement by the orientation of fibers is low.

Loppattanon, Jitkalong and Seadan treated silica and cellulose using silane-69 before incorporation into NR [115]. The average length and diameter of fibers are 120 µm and 20 µm respectively. The successful treatments of silica and cellulose were characterized by FTIR. However, the amount of silane was not reported. Tensile properties of hybrid composites are shown in Figure 3.38. Modulus and tensile strength

of composited slightly increased by silane treatment. It was suggested that the interfacial crosslinking between NR and fillers enhanced tensile properties of composites. The authors did not mention on the role of each fillers in the composites. The reinforcement effect from fiber orientation might not occur due to the low aspect ratio of fibers.

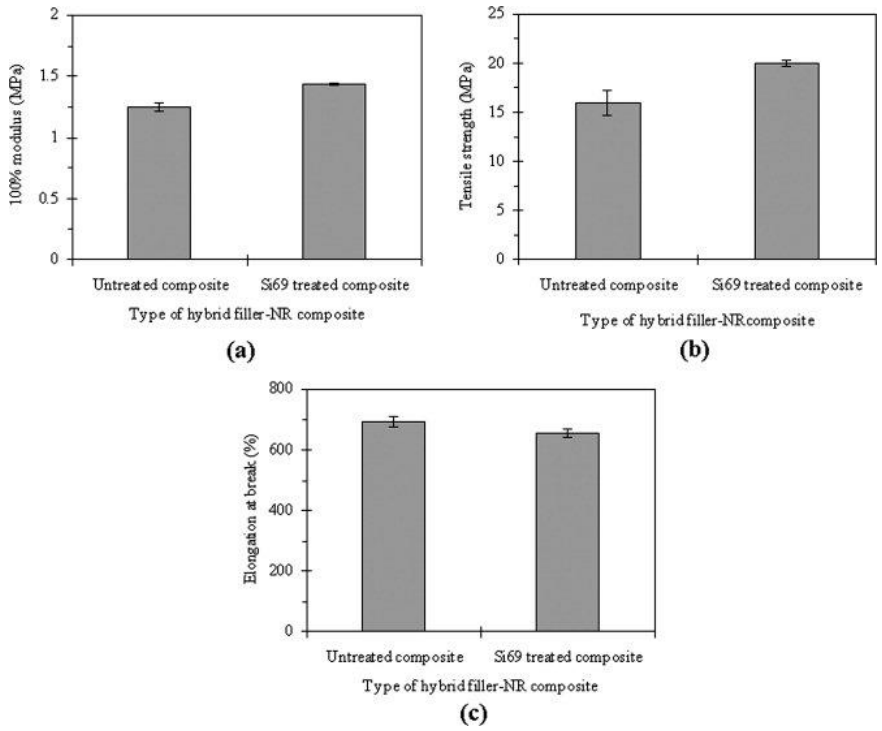

Figure 3.38 Tensile properties of NR with untreated and silane-treated silica/cellulose (10/10 phr) [115]

In research group at Mahidol University, PALF and silica or carbon black were successfully incorporated into NBR [116-117]. The average length of short PALF is 6 mm, whereas the bundle and elementary diameters are 18 μm and 3 μm respectively [63]. Thus, the aspect ratio of fibers is high, compared to the previous researches. This results in the high reinforcing effect at low deformation. Stress-strain curves of NBR/silica/PALF and NBR/carbon black/PALF composites are shown in Figure 3.39 and Figure 3.40, respectively. It can be seen that Young's modulus of composites containing fibers in longitudinal direction is significantly higher than those in transversal direction. By incorporation of silica, the stress at high deformation of PALF-

filled composites increased to a constant value and elongation at break increased. Young's modulus still increased as a consequence of fiber reinforcement. By incorporation of carbon black, mechanical properties improve. Moreover, Young's modulus is still high due to fiber reinforcement.

It can be concluded that PALF was successfully used to reinforce NBR at low deformation whereas particulate fillers improved tensile properties at high deformation.

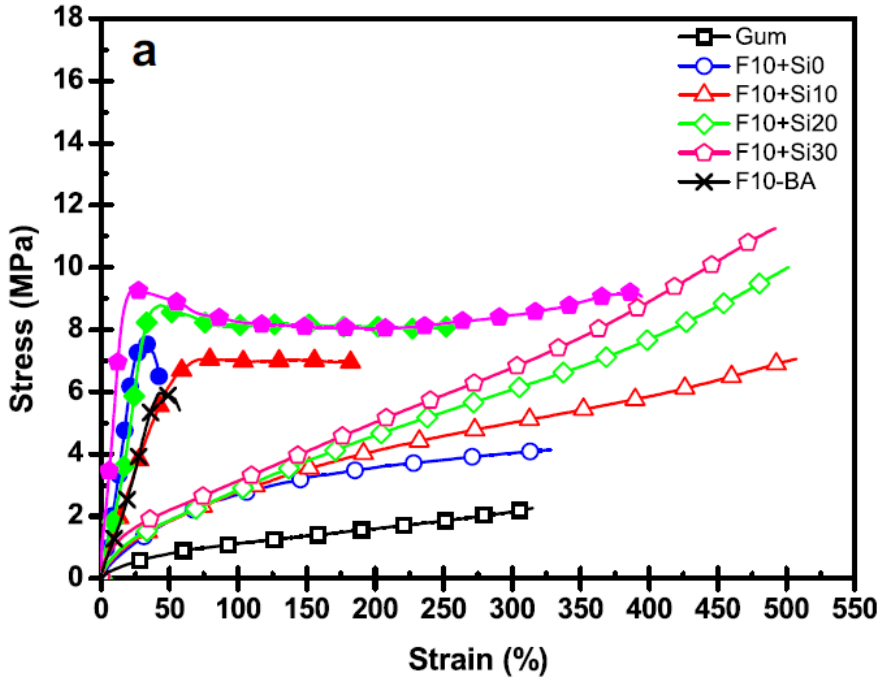

Figure 3.39 Stress-strain curves of NBR composites with hybrid fillers (PALF and silica). Closed symbols represent property measured in the longitudinal direction and open symbols in the transverse direction. [116]

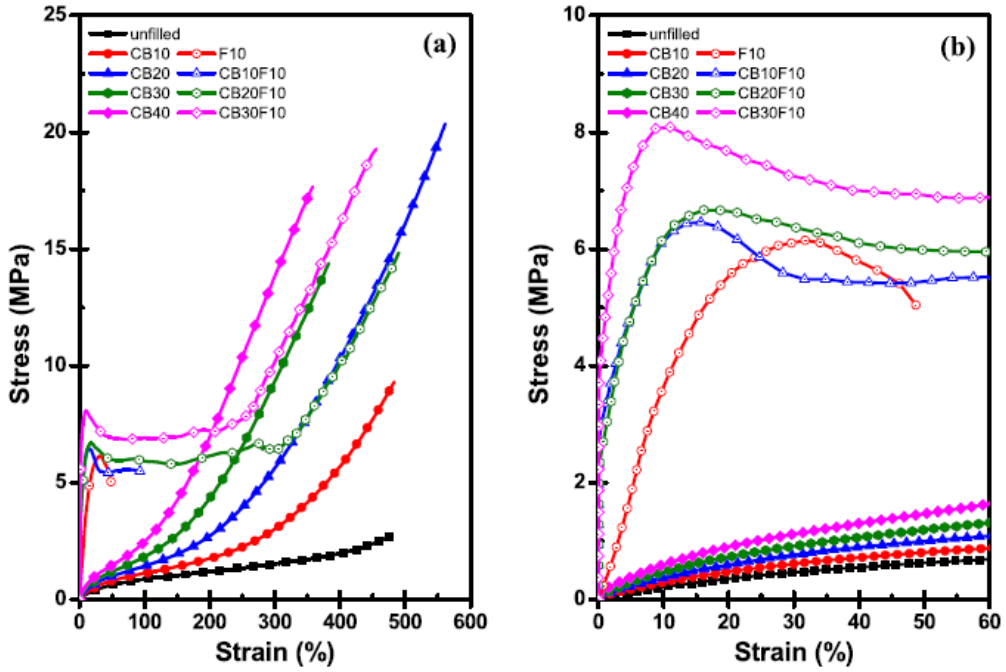

Figure 3.40 Stress–strain curves of PALF/CB-NBR and controlled CB-NBR composites, in the longitudinal direction (a) and the expanded low strain region (b). The number in the legend indicates the amount in phr of the carbon black filler and letter F means PALF which is fixed at 10 phr [117]

The successful incorporation of PALF and carbon black into NR in Amornsakchai's research group has been recently published [118]. The stress-strain curves of NR hybrid composites are shown in Figure 3.41. It can be seen that by increasing the amount of carbon black in composites, strength at high deformation increased. The stress upturned earlier when carbon black content increased. When PALF and carbon black were incorporated, the combination reinforcement effects occurred. The incorporation of PALF has significantly increased modulus at low deformation, whereas carbon black increased strength at high deformation. Thus, the combination of PALF and particulate filler is an effective method to adjust the suitable mechanical properties for end-use products.

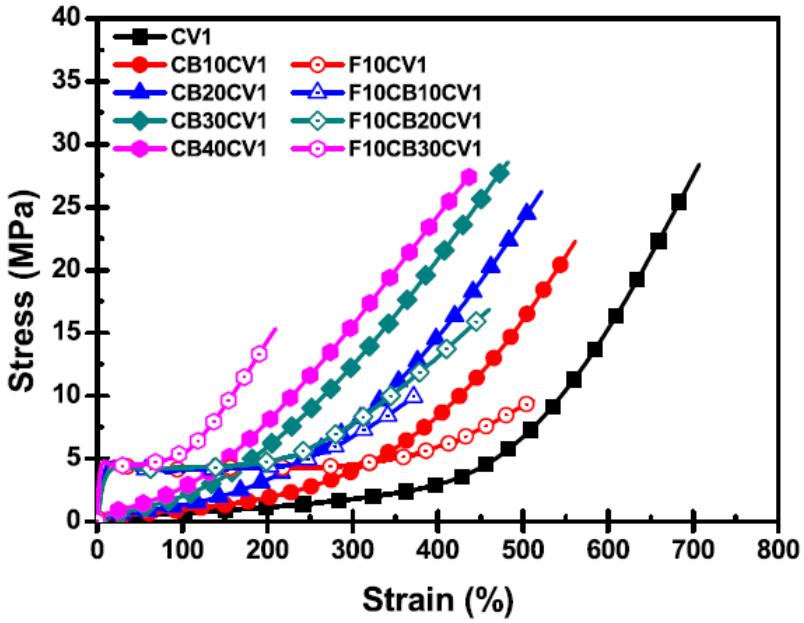

Figure 3.41 Stress–strain curves of PALF/CB-NR and controlled CB-NR composites, in the longitudinal direction. The number in the legend indicates the amount in phr of the fillers (carbon black (CB) and PALF (F). The CB content varies whereas the PALF content is fixed at 10 phr [118]

However, the reinforcement effects by the incorporation of carbon black and PALF in NR are lower than those of NBR composites. Modulus at both low and high deformation of NBR/PALF/carbon black hybrid composites, which can be observed in Figure 3.40, with the same components were higher than those of NR/PALF/carbon black hybrid composites, as shown in Figure 3.41. This is due to the difference in polarities between rubber and fibers. NBR is a polar rubber and is more compatible with PALF fibers than NR.

In conclusion, the reinforcement of particulated filler and fibers in NR is still required the development due to the incompatible between rubber and fiber. The improvement of the interfacial stress between rubber and fiber has to be improved. Thus, the combination effects of particulated filler and fibers reinforcements will be optimized.

CHAPTER IV
MATERIALS AND METHODS

4.1 Materials and instruments

4.1.1 Rubbers, carbon black and curing additives

NR was STR5L grade purchased from M.B.J. Enterprise Co., Ltd. NBR was JSL N230 SL grade manufactured by JSR Corporation, Japan with 35% acrylonitrile content and Mooney Viscosity (ML1+4(100 °C)) of 42. Carbon black was N330 grade. Curing agents and chemicals e.g. zinc oxide, stearic acid, sulfur and CBS (N-Cyclohexyl-2-benzothaiazolesulfenamide) were commercial grade.

4.1.2 Pineapple leaf fibers (PALF)

Pineapple leaves were harvested in Bang Yang District, Phitsanulok Province, Thailand. These pineapple leaves were cleaned, cut into small pieces to fix the length at 6 mm and fed into a milling machine. After drying, the fibers were separated by sieving. The processed PALF shows an 18 μm average bundles diameter with 3 μm average elementary fibers [63]. The average fiber length is approximately 6 mm.

4.1.3 Chemical reagents for surface treatment of PALF

Sodium hydroxide (NaOH) was commercial grade reagent (ACI labscan). Propyltrimethoxylsilane and allyltrimethoxylsilane were purchased from ABCR. Bis-[γ-(triethoxysilyl)-propyl]-tetrasulfide (silane-69) was purchased from Sigma-Aldrich. Distilled water and analytical grade of ethanol were used as solvent.

4.1.4 Instruments

All instruments, manufacturers, models and places are listed in Table 4.1.

Table 4.1 Instruments, manufacturers and models

Instrument	Manufacturer	Model	Place
X-ray photoelectron spectroscopy (XPS)	Omicron	EA 125 HIR U7/7	IS2M[b]
Attenuated total reflection FTIR (ATR- FTIR)	Bruker	IFS66/S	IS2M[b]
Moving die rheometer (MDR)	Alpha technologies	Rheo TECH MD+	MU[a]
Two roll mill	Nishimura	-	MU[a]
Internal mixer	Melchers Co.	Brabender	MU[a]
Press	Mach Group (1992) Co., Ltd	Mach Group	MU[a]
Tensile tester	Instron	5566	MU[a]
Scanning electron microscope (SEM)	FEI microscope	Quanta 400	IS2M[b]
Differential scanning calorimetry (DSC)	Toledo	DSC 1	IS2M[b]
Dynamic thermal mechanical analyzer (DMTA)	Metravib	VA 4000	IS2M[b]

MU[a]: Mahidol University, Thailand

IS2M[b]: Institut de Science des Matériaux de Mulhouse, France

4.2 Surface treatment of PALF

Two types of treatment were proposed. The first one is alkali treatment, which is a pretreatment method to clean the surface of the fibers. After that, alkali-treated PALFs were further treated by silane treatment.

4.2.1 Alkali treatment

After drying PALF at 80 °C for 24 h, 100 g of untreated PALF (UPALF) were put into a reactor containing 10% NaOH solution in distilled water 2.5 L. The reaction was kept at room temperature for 30 min. Then, fibers were washed with distilled water until pH of water reached 7.0. These fibers are called APALF (Alkaline-treated PALF). APALF were dried at 80 °C for 24 h to remove all residual water.

4.2.2 Silane treatment

Three different types of silane treatment were performed. Treated fibers were named as shown in Table 4.2. Silane solution was first prepared by addition of silane in ethanol/water 200 mL with the ratio of 80/20 v/v. The silane concentrations were varied at 0.1, 1, 3, 5, 10 wt% of PALF. The solvent effect was also studied using pure ethanol as a solvent instead of ethanol/water solution. Silane was first hydrolyzed by stirring the aqueous solution for 1 h and then, APALF fibers were added. The reaction was kept at room temperature for 72 h and fibers were washed with solvent several times before drying at 80 °C for 24 h to remove all residual solvent. These fibers will be called SiPALF (Silane-treated PALF).

Table 4.2 Name of fiber with different silane treatments

Fiber	PALF treatment
pSiPALF	Propyltrimethoxylsilane-treated PALF
aSiPALF	Allyltrimethoxylsilane-treated PALF
sSiPALF	Silane-69-treated PALF

4.3 Composite preparation

The mixing of composites was carried out using a laboratory two-roll mill. Total ingredients were fixed at 40 g. Rotor speed and nip gap were fixed at 50 rpm and approximately 0.25 mm respectively. The initial mixing temperature was around 40 °C. After rubber and all ingredients were mixed, pre-preg was sheeted out to keep the fiber orientation. Then, pre-preg was shaped and cured by compression moulding with keep also the fiber orientation to obtain 1 mm thickness sheet. Molding temperature and hydraulic pressure of press were set at 150 °C and 10.3 MPa respectively. Curing time (t_{c90}) for each composite was obtained from MDR measurement. No degradation of fibers at this temperature is observed, which is shown in appendix E.

4.3.1 Two-step mixing of NR/NBR/PALF composites

NR, NBR and PALF were first prepared as compound A. Various ratio of NR and NBR with fixed amount of PALF were prepared (Table 4.3). All rubber components in the first step mixing were masticated together for 2 min then PALF was incorporated and further mixed for 6 min. Compound A was sheeted out and kept for 1 day before use in the second step mixing.

Table 4.3 Formulation of 1st step mixing (in phr* of total rubber contents)

Ingredients	**A1**	**A2**	**A3**	**A4**	**A5**
NR	100	75	50	25	0
NBR	0	25	50	75	100
PALF	50	50	50	50	50
Using for	**0NBR**	**5NBR**	**10NBR**	**15NBR**	**20NBR**

*phr: part per hundred of rubber

The formulation and the sequence of second step mixing are shown in Table 4.4 and Table 4.5 respectively. After mixing all components, the mixture was sheeted out carefully to induce the fiber orientation. The compound was vulcanized at 150 °C for optimum cure time with compression machine into 1 mm thickness sheet.

Table 4.4 Formulation of rubber mixing (in phr of total rubber content)

Ingredients	**NR**	**5NBR**	**10NBR**	**15NBR**	**20NBR**	**NBR**
Rubbe ratio	NR:NBR 100:0	NR:NBR 95:5	NR:NBR 90:10	NR:NBR 85:15	NR:NBR 80:20	NR:NBR 0:100
NR	80	80	80	80	80	-
Compound A	(A1) 30	(A2) 30	(A3) 30	(A4) 30	(A5) 30	-
*Content in compound A	NR 20 NBR 0 PALF 10	NR 15 NBR 5 PALF 10	NR 10 NBR 10 PALF 10	NR 5 NBR 15 PALF 10	NR 0 NBR 20 PALF 10	-
NBR	0	0	0	0	0	100
PALF	-	-	-	-	-	10
ZnO	5	5	5	5	5	5
Stearic acid	2	2	2	2	2	2
CBS	1	1	1	1	1	1
Sulfur	2	2	2	2	2	2

4.3.2 Single-step mixing of unfilled rubbers, NR/NBR/PALF and NR/surface-treated PALF composites

The sequence of the single-step mixing of unfilled rubbers, NR/NBR/PALF and NR/surface-treated PALF composites were similar to the 2nd step mixing in previous part (Table 4.5). NR and NBR were masticated together then PALF were incorporated. Curing additives were further added before sheeting out. The formulations of unfilled rubbers, NR/NBR/PALF, and NR/surface-treated PALF composites are shown in Table 4.6. Single-step-mixed NR/NBR/PALF composites were named as *x*NBR-SM, where *x* is NBR content. NR/surface-treated PALF composites were named as *y*PALF, where *y* is the type of treatment.

Table 4.5 Sequence of rubber mixing

Step	Ingredients	Time (min)
1	NR (and NBR for single step mixing)	0-2
2	• Compound A for two-step-mixing • PALF for single-step-mixing	2-8
3	ZnO and stearic acid	8-10
4	Sulfur and CBS	10-13
Total time		**13**

Table 4.6 Formulation of non-reinforced rubbers, NR/NBR/PALF and NR/surface-treated PALF composites

Ingredients	Non-reinforced *x*NBR[a]	*x*NBR-SM[a]	*y*PALF[b]
Rubbers	100	100	100
PALF	-	10	10
ZnO	5	5	5
Stearic acid	2	2	2
CBS	1	1	1
Sulfur	2	2	2

x: NBR amount in a total rubbers content, which are 0, 5, 10, 15, 20 wt% of total rubbers

y: A for alkali treatment, Si for silane treatment

4.3.3 Mixing of NBR/PALF composite

NBR/PALF composite is a control sample for comparison. The formulation of 100NBR is shown in Table 4.4. Since it is more difficult to incorporate the curatives into NBR, the sequence of mixing was changed slightly as reported previously [119]. The sequence of mixing is shown in Table 4.7. NBR was first masticated then sulfur was added and followed by PALF. Then, ZnO and stearic acid were added to mixture, followed with CBS. The compound was then sheeted out in the manner described above to produce the fiber orientation.

Table 4.7 Mixing scheme of NBR/PALF composite

Step	Ingredients	Content	Time (min)
1	NBR	100	0-1
2	Sulfur	2	1-2
3	PALF	10	2-11
3	ZnO and stearic acid	7	11-17
4	CBS	1	17-20
Total time			**20**

4.3.4 Mixing of NR/NBR/carbon black/PALF hybrid composites

All NR/NBR/carbon black/PALF hybrid composites were named as *x*NBR*y*UP*z*CB. *x* is the amount of NBR, *y* is the amount of untreated PALF and *z* is the amount of carbon black in composite. The formulation of NR/carbon black/PALF,with and without NBR 20 phr, and varying carbon black content from 0 to 30 phr are shown in Table 4.9 and Table 4.10 respectively. NR/NBR/carbon black/PALF with varying NBR content are shown in Table 4.11. The sequence of mixing, which is as mixing scheme A, is shown in Table 4.8. Mixing scheme A was used to study the filler effect, carbon black content and NBR content. NR and carbon black were first mixed as masterbatch in internal mixer in the ratio of NR:carbon black as 60/40 wt%. Initial mixing temperature was set at 50 °C and rotor speed was 40 rpm. Fill factor was 0.75. NR was first masticated for 1 min then carbon black was gradually incorporated for the period of 6 min. Mixing was continued for another 3 min. NR, NBR and masterbatch were first masticated together using two-roll mill then PALF was further added at 2 min. Curing additives were further added then the compound was sheeted out on the two-roll mill.

Table 4.8 Mixing order for the three mixing schemes

Mixing order	**Mixing scheme A**	**Mixing scheme B**	**Mixing scheme C**	**Time (min)**
1	Prepare masterbatch of NR and carbon black (MB[NR-CB])	1.) Prepare MB[NR-CB] 2.) Prepare masterbatch of NBR, carbon black and PALF (MB[NBR-CB-PALF])	1.) Prepare MB[NR-CB] 2.) Prepare masterbatch of NBR and PALF (MB[NBR-PALF])	-
2	Mix NR, MB[NR-CB] and NBR	Mix NR and MB[NR-CB]	Mix NR and MB[NR-CB]	0-2
3	Add PALF	Add MB[NBR-CB-PALF]	Add MB[NBR-PALF]	2-8
4	Add ZnO and stearic acid			8-10
5	Add sulfur and CBS			10-13
Total time				**13**

Table 4.9 Formulation of NR/carbon black/PALF composites with varying carbon black content (in phr of total rubber content)

Ingredients	**0NBR10UP 0CB**	**0NBR10UP 10CB**	**0NBR10UP 20CB**	**0NBR10UP 30CB**
NR	100	85	70	55
Masterbatch of NR/CB	-	25	50	75
*Content in masterbatch	-	NR 15 CB 10	NR 30 CB 20	NR 45 CB 30
PALF	10	10	10	10
ZnO	5	5	5	5
Stearic acid	2	2	2	2
CBS	1	1	1	1
Sulfur	2	2	2	2

Table 4.10 Formulation of NR/carbon black/PALF composites with NBR 20 phr and varying carbon black content (in phr of total rubber content)

Ingredients	**20NBR10UP 0CB**	**20NBR10UP 10CB**	**20NBR10UP 20CB**	**20NBR10UP 30CB**
NR	80	65	50	35
NBR	20	20	20	20
MB of NR/CB	-	25	50	75
*Content in MB	-	NR 15 CB 10	NR 30 CB 20	NR 45 CB 30
PALF	10	10	10	10
ZnO	5	5	5	5
Stearic acid	2	2	2	2
CBS	1	1	1	1
Sulfur	2	2	2	2

Table 4.11 Formulation of NR/NBR/carbon black/PALF composites with varying NBR content (in phr of total rubber content)

Ingredients	**0NBR 10UP 30CB**	**5NBR 10UP 30CB**	**10NBR 10UP 30CB**	**15NBR 10UP 30CB**	**20NBR 10UP 30CB**
NR	55	50	45	40	35
NBR	0	5	10	15	20
MB of NR/CB*	75	75	75	75	75
*Content in MB	NR 45 CB 30	NR 45 CB 30	NR 45 CB 30	NR 45 CB 30	NR 45 CB 30
PALF	10	10	10	10	10
ZnO	5	5	5	5	5
Stearic acid	2	2	2	2	2
CBS	1	1	1	1	1
Sulfur	2	2	2	2	2

4.3.5 Mixing of 20NBR10UP30CB-B and C composites

In order to enhance rigidity of NBR phase, carbon black and PALF were first mixed with NBR. The content of carbon black in NR and NBR phases was distributed equally to the ratio of rubber:carbon black in composite. The formulation of 20NBR10UP30CB-B is shown in Table 4.12. 20NBR10UP30CB-B was prepared by mixing of NR, masterbatch of NR/carbon black and masterbatch of NBR/PALF/carbon black together. Then curing additives were incorporated, as seen in Table 4.8.

To produce the composite with incorporation carbon black into NR phase and incorporation PALF into NBR phase, 20NBR10UP30CB-C was prepared. The formulation of 20NBR10UP30CB-C is shown in Table 4.12. NR was first masticated to produce the masterbatch of NR/carbon black. Then, masterbatch of NBR/PALF was added followed by curing additives, as described in Table 4.8.

Table 4.12 Formulation of 20NBR10U30CB composites with changing the method of mixing (in phr of total rubber content)

Ingredients	**20NBR10UP 30CB-B**		**20NBR10UP 30CB-C**	
	phr	**Wt%**	**phr**	**Wt%**
NR	44	29.3	35	23.3
MB1 (NR/CB)	60	40.0	75	50.0
*Content in MB1	NR 36 CB 24	NR 24.0 CB 16.0	NR 45 CB 30	NR 45.0 CB 30.0
MB2 (NBR/CB/PALF)	36	24.0	30	20.0
*Content in MB2	NBR 20 CB 6 PALF 10	NBR 13.3 CB 4.0 PALF 6.6	NBR 20 PALF 10	NBR 13.3 PALF 6.6
ZnO	5	3.3	5	3.3
Stearic acid	2	1.3	2	1.3
CBS	1	0.7	1	0.7
Sulfur	2	1.3	2	1.3

4.3.6 Mixing of NR/carbon black/surface treated PALF hybrid composites

NR/carbon black/surface-treated PALF hybrid composites were named as NR*x*YP*z*CB. *x* is the amount of PALF, *Y* is the method of treatment and *z* is the amount of carbon black. The method of treatment was named as U: untreat, A: alkali treatment and Si: silane treatment. The formulation of NR/carbon black/PALF was listed in Table 4.13.

Table 4.13 Formulation of NR/carbon black/surface-treated PALF with varying carbon black content (in phr)

Ingredients	**NR10*Y*P0CB**	**NR10*Y*P10CB**	**NR10*Y*P20CB**	**NR10*Y*P30CB**
NR	100	85	70	55
Masterbatch of NR/CB*	-	25	50	75
*Content in masterbatch	-	NR 15 CB 10	NR 30 CB 20	NR 45 CB 30
PALF**	10	10	10	10
ZnO	5	5	5	5
Stearic acid	2	2	2	2
CBS	1	1	1	1
Sulfur	2	2	2	2

***UP: Untreated PALF, AP: Alkali-treated PALF, SiP: Silane69-treated PALF*

4.4 Characterizations

For the surface treatment of PALF, ATR-FTIR and X-ray photoelectron spectroscopy (XPS) were used to characterize the functionalization. After that, NR/PALF composites were prepared. Rubber compounds after mixing by two roll mill were first characterized by MDR. The cured sheets were cured and characterized by tensile testing, dynamic mechanical thermal analysis (DMTA), differential scanning calorimetry (DSC), and scanning electron microscopy (SEM).

4.4.1 ATR-FTIR spectroscopy

ATR-FTIR spectroscopy was used to characterize fiber surface after treatment and also NBR content in NR/NBR/PALF composite. An infrared beam is directed onto an optically dense Ge crystal with high refractive index at a certain angle. The signal is detected after the beam come to contact with sample. Diameter of the crystal is 2 mm. The fundamental of ATR-FTIR is illustrated in Figure 4.1. A Ge crystal was used in this study. The measurement was operated with 128 scans at resolution 4 cm^{-1} over the range of 4000 to 600 cm^{-1}.

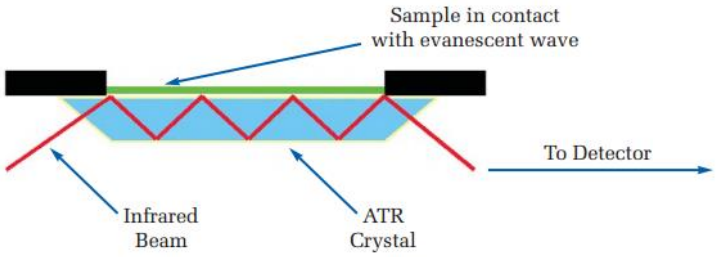

Figure 4.1 ATR-FTIR [120]

Fiber samples were prepared by compression of a small amount of fibers. For NR/NBR/PALF composite, sample was cut at the cross-section area by microtoming at temperature of -70 °C into 2×1×150 mm sheet. Then it was analyzed with ATR-FTIR at three places along the measured area, as can be seen in Figure 4.2.

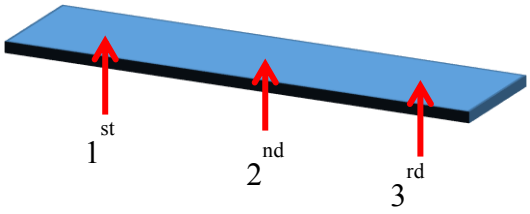

Figure 4.2 ATR-FTIR analysis of NR/NBR/PALF composite

4.4.2 X-ray photoelectron spectroscopy (XPS)

XPS spectra were carried out using double anode (Al Kα = 1486.6 eV and Mg Kα = 1253.6 eV) and hemispherical analyzer. The measurement was operated under high vacuum. The survey spectrum and high resolution scan of C1s and O1s were examined. The thickness of the surface of specimen around 10 nm was characterized.

4.4.3 Moving die rheometer (MDR)

Curing behaviors of composites were studied with a moving die rheometer (MDR), (Rheo TECH MD+), according to ISO 6502. 5 g of unvulcanized rubber was placed between the dies. The disc is biconical in shape with the cone angle of ± 1.3%. The applied force was 11 kN ± 0.5 kN to press the sample. The dynamic frequency after force was applied is 1.7 Hz ± 0.1 Hz. The curing temperature was fixed at 150 °C. Maximum torque (M_H), minimum torque (M_L), scorch time (t_{s2}) and optimum cure time (t_{c90}) were reported. Cure rate index was determined with the following equation.

$$cure\ rate\ index = \frac{100}{t_{c90} - t_{s2}} \qquad \text{Equation 4.1}$$

4.4.4 Tensile tester

Tensile properties of composites were determined at room temperature by using universal tensile testing machine (Instron 5566) with a long travel contacted style extensometer, according to ISO 37 but with thinner specimen. A crosshead speed was set at 500 mm/min and load cell was fixed at 1 kN. Composite sheets were punched into a dumbbell shape using type C die such that the fiber align along the specimen long axis. At least five specimens were measured for each sample. The average values of moduli at 10% strain (E_{10}), 100% strain (E_{100}), 300% strain (E_{300}), yield stress (σ_y), onset strain upturn, tensile strength and elongation at break were reported.

4.4.5 Differential scanning calorimetry (DSC)

Calorimetery measurements were performed on a DSC (Toledo, DSC1). The specimen was cut into cylindrical flat shape in the weight of 8 mg. Two cycles were performed to erase the thermal history. The first cycle was carried out by cooling to -90 °C then heating to 90 °C at scan rate of 10 °C/min. The specimen was hold at this temperature for 5 min. After that, the second cycle was carried out by cooling to -90 °C then heating to 90 °C using the same scan rate. The relationship between heat flow and temperature was plotted from the second cycle.

4.4.6 Dynamic mechanical thermal analyzer (DMTA)

DMTA was performed on a viscoanalyzer (METRAVIB VA 4000). A specimen with a dimension of 30 x 10 x 1 mm^3 was used for the measurement. The gauge length was fixed at 20 mm. The measurement was carried out in tension mode. First, the temperature of the closed chamber was reduced from room temperature to -90 °C at scan rate of 10 °C/min using liquid nitrogen. Then, the measurement was scanned from -90 °C to 50 °C with the same scan rate of 10 °C/min. The specimen was pre-strained at 1% and the dynamic strain was 0.5% with a frequency of 10 Hz.

4.4.7 Scanning electron microscope (SEM)

The morphology of fibers and composites was studied by using a SEM. For fibers, the individual fibers were placed on the carbon film and coated with gold layer before measurement. Tensile-fractured sample was observed at the fractured cross-section and also was coated with thin gold layer before measurement. The magnification was set at 250x, 1000x, 2500x and 5000x.

CHAPTER V
RESULTS AND DISCUSSION

The results and discussion of this study can be divided into two main parts. The first one is the introduction of PALF in NR that can be subdivided into three parts: incorporation of NBR, surface treatment of PALF by silane, and the comparison of reinforcing effect via these two solutions.

The second main part of chapter V concerns the reinforcement effect by hybrid fillers, PALF and carbon black, in order to increase the mechanical properties at low strain without drastic decrease of ultimate properties. Again, the improvement of reinforcement with hybrid fillers is divided into three sub parts: the effect of NBR, surface treatment by silane of PALF with incorporation of carbon black and the comparison of reinforcing effect of both solutions.

5.1 Effect of NBR on NR/PALF composites

Small amounts (5 to 20 parts of total rubber content) of NBR were incorporated into NR/PALF composites in order to improve the stress transfer between rubber and fibers. NBR is expected to encase PALF in order to enhance the matrix and fiber interfacial strength. First, the properties of NR, NBR and their blends without fiber were investigated as control samples. Then, the effect of NBR on NR/PALF composites was studied.

5.1.1 Non-reinforced rubber blends

Non-reinforced NR, NBR and their blends were investigated in order to analyze their cure behavior, the compatibility between rubbers, the tensile properties and the morphology of the blends. For the blends, the amount of NBR was varied at 0, 5, 10, 15, 20 wt% of total rubber content. NR and NBR were masticated together before the addition of curing additives as described in chapter IV.

5.1.1.1 Cure characteristics

Rheographs displaying cure characteristics of compounds containing different amounts of NBR are shown in Figure 5.1 and their numerical values i e. M_L, M_H, t_{s2} and t_{c90} are listed in Table 5.1.

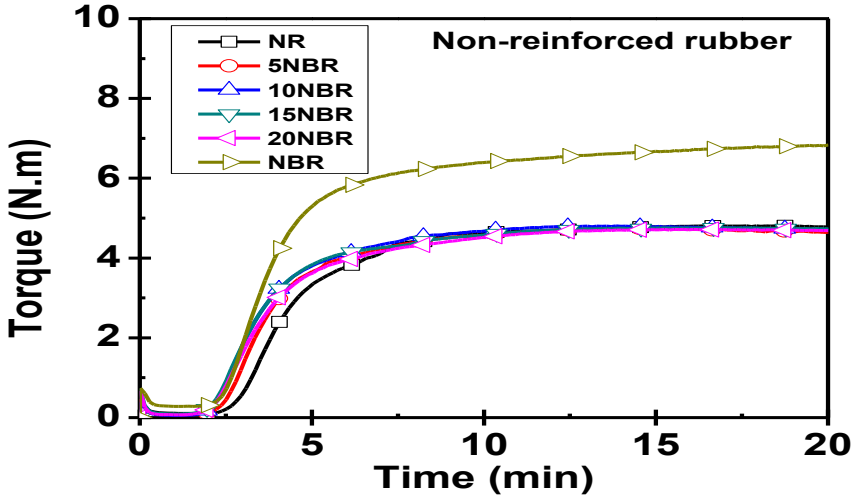

Figure 5.1 Cure curves of non-reinforced NR, NBR and its blends with NBR at 5, 10, 15, 20 wt% of total rubber content

Table 5.1 Cure characteristics of non-reinforced NR, NBR and its blends with NBR at 5, 10, 15, 20 wt% of total rubber content

	M_L (N.m)	M_H (N.m)	t_{s2} (min)	t_{c90} (min)
NR	0.1	4.8	3.9	7.4
5NBR	0.1	4.7	3.4	7.2
10NBR	0.1	4.8	3.1	7.0
15NBR	0.1	4.8	3.2	7.5
20NBR	0.1	4.7	3.3	7.6
NBR	0.3	6.8	3.1	7.7

The curing behavior of NR reaches the plateau region with constant M_H, while NBR is marching, in which M_H slightly increases corresponding to the time. t_{s2} of NBR (3.1 min) is shorter than for NR (3.9 min), whereas M_H of NBR (6.8 MPa) is significantly higher than NR (4.8 MPa). By blending NBR and NR, t_{s2} is slightly

higher than for pure NR, whereas M_H remains unchanged. The shortened cure time for composites containing NBR can be hypothesized by the activation of a zinc complex on the nitrile group of NBR [121]. By the way, the migration of curatives in the blends could not be observed by MDR. To study the migration of the curatives, swelling measurement is further studied.

5.1.1.2 Curatives migration in the blends

The curatives migration in the incompatible rubber blends has been studied by Clythong [122], Sahakaro [123] and Tinker [33,40,124]. To understand the migration of curing additives between rubber blends, pre-sheets of NR and NBR those mixed with curing additives separately were attached together and cured under different temperatures.

After NR and NBR sheets were cured and separated from each other, the contacted sheets were cut and studied by the swelling behavior, compared with those of non-contacted sheets. Swelling results of NR and NBR are shown in Figure 5.2. Swelling ratio (Q) of NR increases after contacted with NBR at all curing temperatures. The increase of Q indicates lower degree of crosslinking. Moreover, Q of NBR does not change after contacts with NR for curing temperature 150 and 170 °C. It decreases for the lowest curing temperature at 130 °C.

This means that the migration of the additives loss from NR has a significant effect on the degree of crosslinking. When the curing rate is lower at lower temperature (130 °C), the curing rate of NBR decreases and the curing additives from NR can participate to vulcanization reactions.

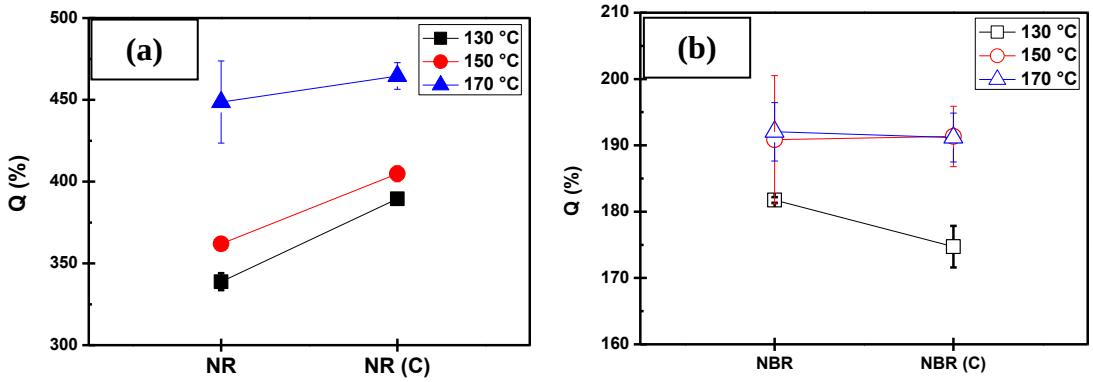

Figure 5.2 Swelling results of (a) NR and contacted NR sheets and (b) NBR and contacted NBR sheets with different curing temperatures

Moreover, the swollen contacted sheets of NR and NBR are curled as shown on Figure 5.3. The curvature indicates that an effect of varying degree of crosslinking exists in the depth of rubber sheets.

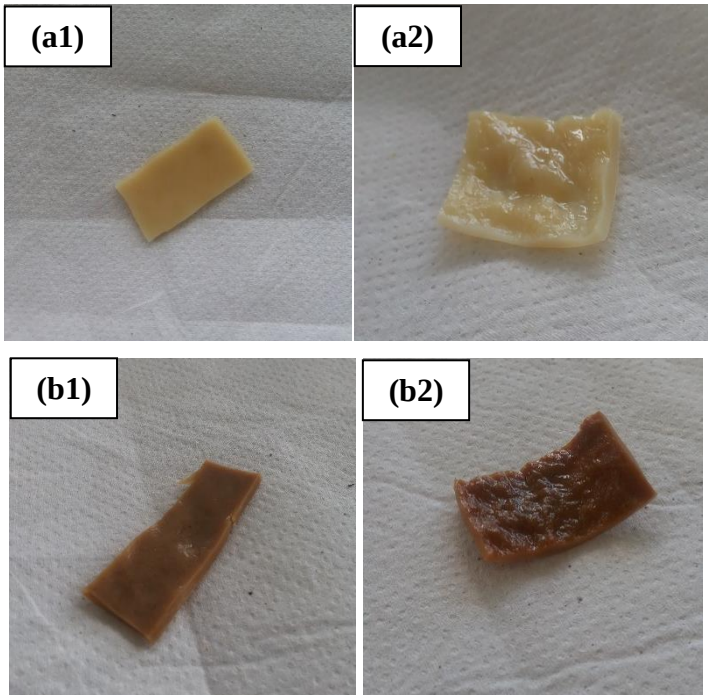

Figure 5.3 NR sheet (a1), contacted NR sheet (a2), NBR sheet (b1) and contacted NBR sheet (b2) after swelling in toluene

The migration of curing additives was also studied by NMR spectroscopy, which is shown in appendix A. Although the curatives could migrate from NR to NBR, the amounts of curatives migration and actual degree of crosslinking at the interface between rubbers in the blends are still unclarified.

5.1.1.3 Determination of glass transition domain of non-reinforced rubber blends

To gain better insight into the compatible of rubber blends, dynamic mechanical testing (DMTA) and thermal analysis (DSC) of all samples were carried out. On one hand, DMTA is used to determine the dynamic transition temperature (T_d) of rubbers by applying the dynamic force in the tension mode and increase the temperature from -90°C to 50 °C at scan rate 10 °C/min. On the other hand, DSC is used to determine the glass transition temperature (T_g) of the rubbers by detection the changing of heat flow while the temperature is increased from -90°C to 90 °C at scan rate 10 °C/min. The DMTA curves and tan δ of rubbers are shown in Figure 5.4 and in Table 5.2. T_d of pure NR is -47 °C whereas T_d of NBR is around -10 °C. These two peaks do not overlap. In the blend, T_d of NR is not shifted and a shoulder appears at the expected position for NBR. This clearly indicates that NR and NBR are not compatible. These results of T_ds are in agreement with Kader and coworkers [125] who reported that T_ds of pure NR and pure NBR (34% ACN content) are -49.3 °C and 13.8 °C. In the blends with 1:1 weight ratio, T_ds of both NR and NBR do not shift, which indicates the immiscibility of NR and NBR.

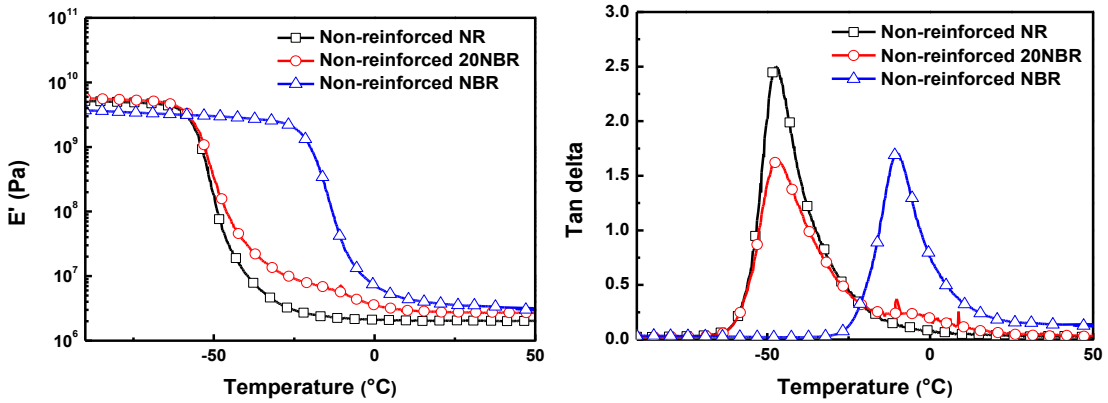

Figure 5.4 Temperature dependences of E´ and tan delta of non-reinforced NR, NBR and their blend with NBR 20 wt% of total rubber content

Table 5.2 DMTA results of non-reinforced NR, NBR and their blend with NBR 20 wt% of total rubber content

	Tan δ_{NR}		**Tan δ_{NBR}**	
	Magnitude	**T (°C)**	**Magnitude**	**T (°C)**
Non-reinforced NR	2.5	-47	-	-
Non-reinforced 20NBR	1.6	-47	0.2	-9
Non-reinforced NBR	-	-	1.7	-10

The DSC curves and T_g of each rubber are displayed in Figure 5.5 and Table 5.3 respectively. T_g is defined by determining the highest slope of the curve. T_gs of NR and NBR in the blends are not shifted which results are in good agreement with DMTA results.

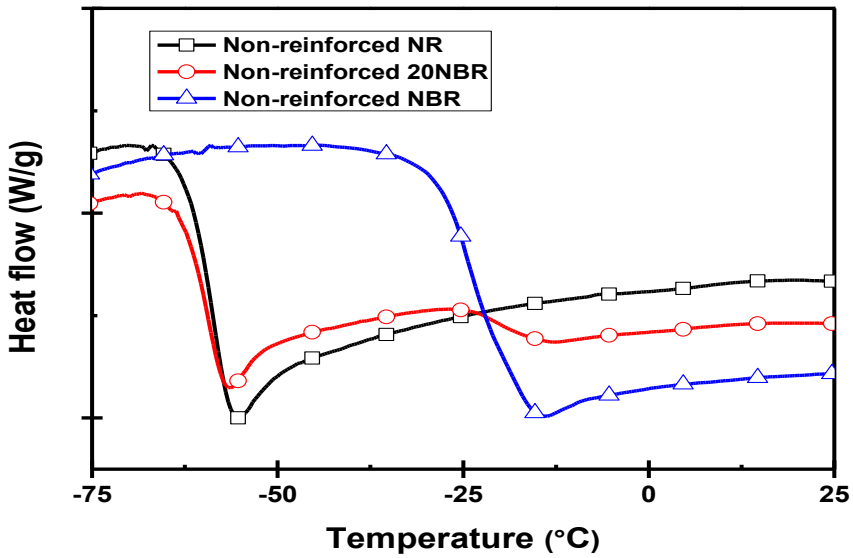

Figure 5.5 DSC curves of non-reinforced NR, NBR and their blend with NBR 20 wt% of total rubber content

Table 5.3 T_gs of non-reinforced NR, NBR and their blend with NBR 20 wt% of total rubber content

	T_g NR (°C)	**T_g NBR (°C)**
Non-reinforced NR	-60	-
Non-reinforced 20NBR	-60	-21
Non-reinforced NBR	-	-19

5.1.1.4 Mechanical properties

Tensile properties of NR, NBR and their blends (0, 5, 10, 15, 20 wt% of total rubber content) were studied. The stress strain curves are shown in Figure 5.6. Modulus at low deformation of NBR is slightly higher than NR. However, only NR has the upturn which corresponds to the strain induced crystallization phenomena. In the incompatible blends, stress-strain curves are similar to NR and do not depend on the amount of NBR.

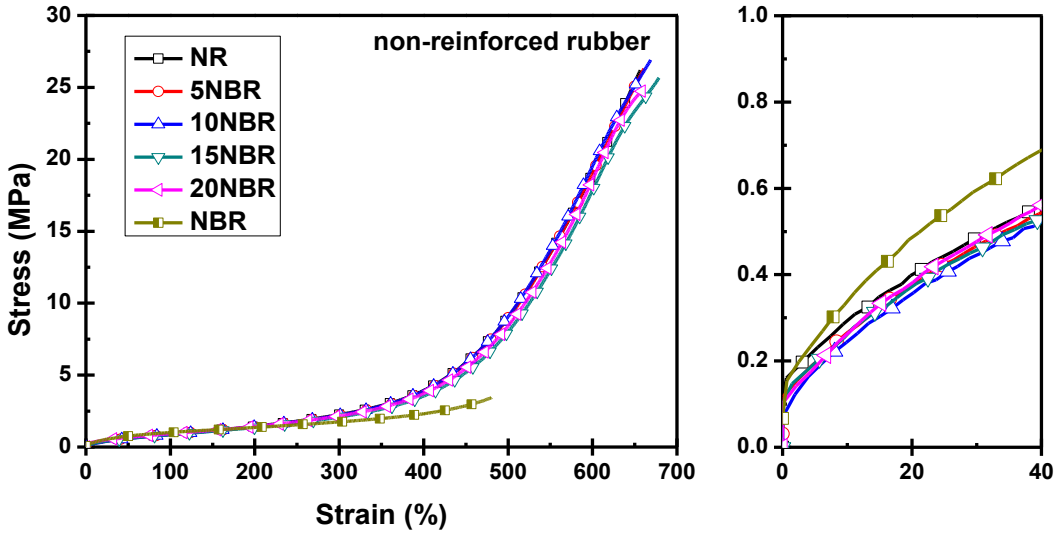

Figure 5.6 Stress strain curves of non-reinforced NR, NBR and its blends with NBR at 5, 10, 15, 20 wt% of total rubber content

5.1.1.5 Morphology of the blends

The morphology of incompatible rubber blends was studied using SEM. Blade-cut at room temperature and tensile-fractured specimens were carried out. SEM images of cross-sectioned specimens are displayed in Figure 5.7. The

presence of dispersed nodules with size less than 1 µm were observed in all rubbers. Nor and coworkers [126] and Helaly and coworkers [127] reported that the dispersed nodules are attributed to zinc stearate. Blade-cut specimens were first studied. SEM images of blade-cut 20NBR show 2.5 µm diameter of spherical particles in matrix, which cannot be observed in blade-cut NR or NBR. The presence of NBR is clearly seen in tensile-fractured 20NBR, which is shown in Figure 5.7 (B2). The particles or nodules with approximate diameter of 2.5 µm, are dispersed in NR matrix. It is unclear that the dispersed phase is NBR. Lewan studied on the morphologies of NR/NBR blend vulcanizates using osmium tetroxide to stain the unsaturated hydrocarbon on the main chain of rubber and observed by scanning transmission electron microscopy (STEM) [29]. In our case, however, no changes could be observed after staining procedure.

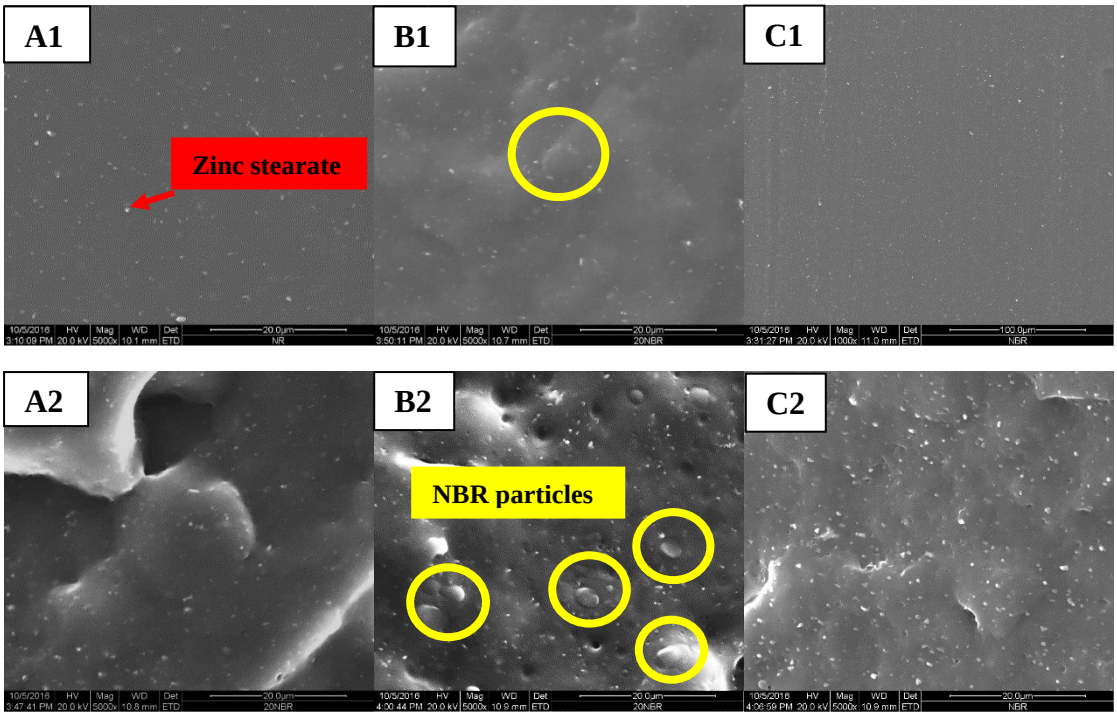

Figure 5.7 SEM images of blade-cut NR (A1), 20NBR (A2), NBR (A3) and tensile-fractured NR (A2), 20NBR (B2) and NBR (C2)

In conclusion, NR and NBR are incompatible. Small particles of NBR are dispersed in NR matrix. Curatives migration cannot be detected by MDR. Moreover, it does not affect significantly the mechanical properties of rubber. The next step of our work is the study of the effect of NBR on NR/PALF composites.

5.1.2 Incorporation of NBR into NR/PALF composites

Small amount of NBR was incorporated into NR/PALF composites in order to improve the stress transfer between rubber and fiber. Only one amount of PALF, 10 phr, was considered. Two-step-mixed NR/NBR/PALF composites were prepared. Compound A consists of various amount of NR/NBR and PALF, were prepared as first step mixing, then they were incorporated into NR in the second step. After that, the mixed compound was cured. The model of composite is displayed in Figure 5.8. Cure characteristics of compounds were first studied to understand overall curing behavior. The incorporation of NBR into NR was characterized using ATR-FTIR, which is shown in Appendix B. As unfilled blends, the glass transition temperatures of composites were measured by using DMTA and DSC. Tensile properties were measured and used to study the reinforcement of the rubber by the fibers. The cross-section area of tensile-fractured specimen was also observed using SEM to get more information on the interface between matrix and fiber. Single-step-mixed composites with the same ingredients of two-step-mixed composites were also prepared in order to compare the effect of mixing.

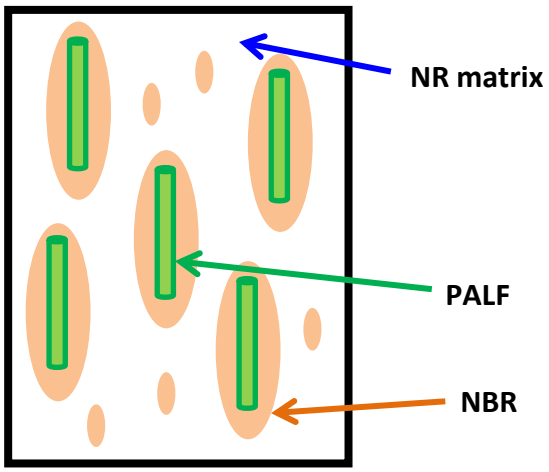

Figure 5.8 Model of NR/NBR/PALF composites

5.1.2.1 Cure characteristics

Rheograms displaying cure characteristics of NR/PALF compounds containing different amounts of NBR are shown in Figure 5.9. Numerical values for different cure characteristics of these compounds are tabulated in Table 5.4.

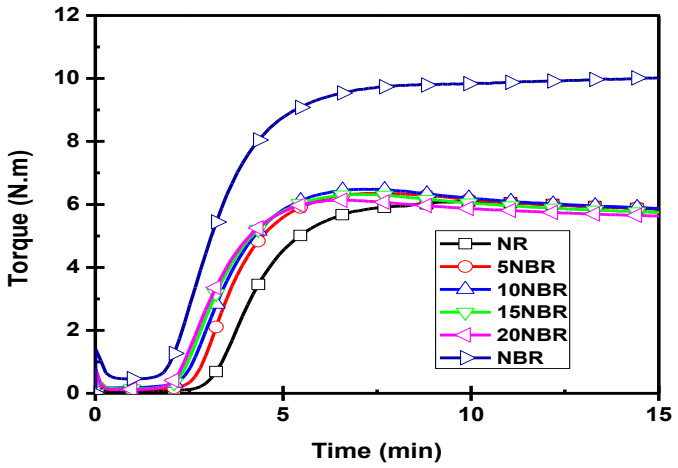

Figure 5.9 Cure curves of NR/NBR/PALF composites with NBR content of 0, 5, 10, 15, 20 and 100 % of total rubber content

Table 5.4 Cure characteristics of NR/NBR/PALF composites with NBR content of 0, 5, 10, 15, 20 and 100 % of total rubber matrix

	M_L (N.m)	M_H (N.m)	t_{s2} (min)	t_{c90} (min)	Cure rate index (min $^{-1}$)
NR	0.1	6.1	3.8	6.2	41.5
5NBR	0.1	6.4	3.2	5.2	51.0
10NBR	0.2	6.5	3.0	5.0	49.3
15NBR	0.1	6.4	2.9	5.0	47.4
20NBR	0.1	6.1	2.8	4.7	52.6
NBR	0.5	10.3	2.4	5.8	29.4

Replacing part of NR with NBR clearly affects the cure characteristics of NR/PALF composite compounds. The curing behavior of NR/PALF and NBR/PALF compounds reaches the plateau region with constant M_H, while NR/NBR/PALF is going through a maximum indicating a reversion process. t_{s2} of NR/PALF is significantly lower than NBR/PALF from 3.8 to 2.4 min. M_L of NBR/PALF composites are three times higher than those NR/PALF and NR/NBR/PALF composites, whereas M_H is higher from 6.1 to 10.3 MPa.

For NR/NBR/PALF compounds, t_{s2} and t_{c90} decrease by incorporation of NBR from 3.8 to 3.0 min and 6.2 to 5.0 min respectively, however, they appear not to depend on the amount of NBR. Cure rate indexes increase with the incorporation of NBR, although it is more important for NBR, but do not depend significantly on the amount of NBR. M_H slightly increases by increasing the amount of NBR in NR/PALF compounds from 6.10 to 6.38 N.m, except for 20NBR compound.

5.1.2.2 Determination of glass transition domain of composites

To gain better insight into the mechanical behavior of the rubber blend composites, DMTA of NR/NBR/PALF composites with different NBR contents and of NBR/PALF composite were carried out. The specimen are measured in tension mode in the same condition as previously indicated. The temperature dependence of elastic modulus (E´) and tan delta of the composites are shown in Figure 5.10. At low temperatures in the glassy state region, the NBR/PALF composite has the lowest storage modulus while the NR/PALF composites all have similar higher moduli. As the temperature increases, the moduli remain roughly constant up to the glass to rubber transition temperatures. The transitions start at about -62 and -25 °C for the NR pure or blended and NBR systems respectively. Above the transition, the NBR system has the lowest value.

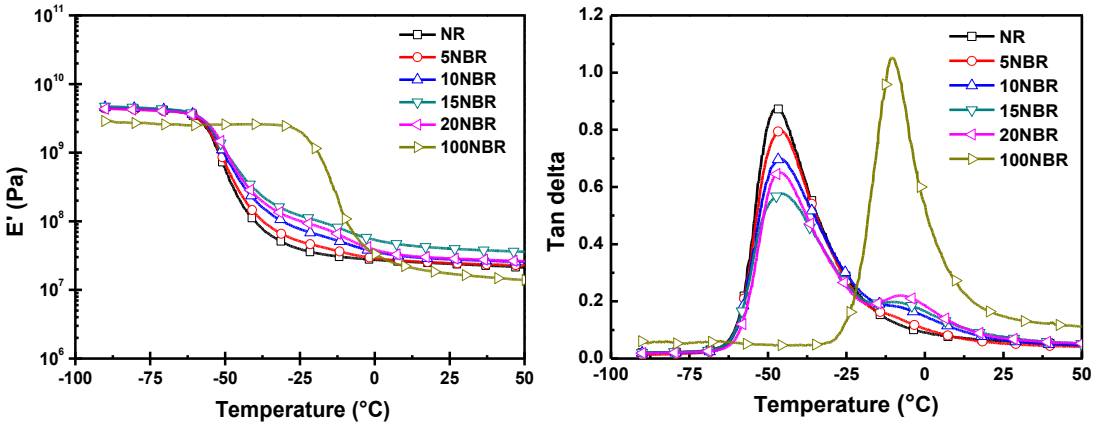

Figure 5.10 Temperature dependences of Elastic modulus E´ and tan delta of NR/PALF with NBR 0, 5, 10, 15, 20 wt% and NBR/PALF composites

The dynamic transition temperatures (T_d) are more clearly seen in the tan δ curves. The control composites NR/PALF and NBR/PALF exhibit the difference of T_d around -44 and -4 °C respectively. In NR/NBR/PALF composites, the

intensity of the NR tan δ peak decreases with increasing NBR content. In the blends, the NBR tan δ peak appears only for NBR content above 5 % first as a shoulder and then more clearly as a peak. The numerical values of E´ at 25 °C and tan δ are listed in Table 5.5.

Table 5.5 Viscoelastic properties of NR/NBR/PALF composites with NBR content of 0, 5, 10, 15 20 wt% of total rubber matrix and NBR/PALF composites

	E´ at 25 °C (MPa)	**Tan δ of NR**		**Tan δ of NBR**	
		Intensity	**T (°C)**	**Intensity**	**T (°C)**
NR	25.0	0.9	-47	-	-
5NBR	24.6	0.8	-46	-	-
10NBR	27.9	0.7	-46	-	-
15NBR	40.0	0.6	-45	-	-
20NBR	28.8	0.7	-46	0.2	-8
NBR	17.3	-	-	1.1	-10

E´ at room temperature of NR/PALF composites increases from 25.0 MPa up to 40.0 MPa by incorporation of NBR up to 15 wt%. However, E´ decreases to 28.8 MPa by incorporation of NBR 20 wt%. The relationship between tan δ of NR and NBR content is plotted in Figure 5.11. Tan δ of NR consequently decreases by increasing an amount of NBR up to 15 wt% and again, tan δ of NR increases by incorporation of NBR 20 wt%. This is due to the difficulty of dispersion of compound A5 in 20NBR composite (compound A5 contains only NBR/PALF, whereas other compounds A contain NR/NBR/PALF).

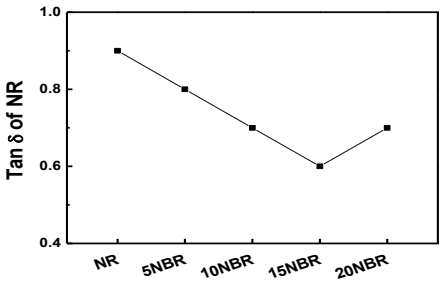

Figure 5.11 Relationship between tan δ_{NR} and NBR content

Thermal analysis results are displayed in Figure 5.12 and Table 5.6. T_gs of NR in the blends are not shifted whereas T_gs of NBR in the blends are not significantly shifted compared to the T_g of NBR/PALF composite.

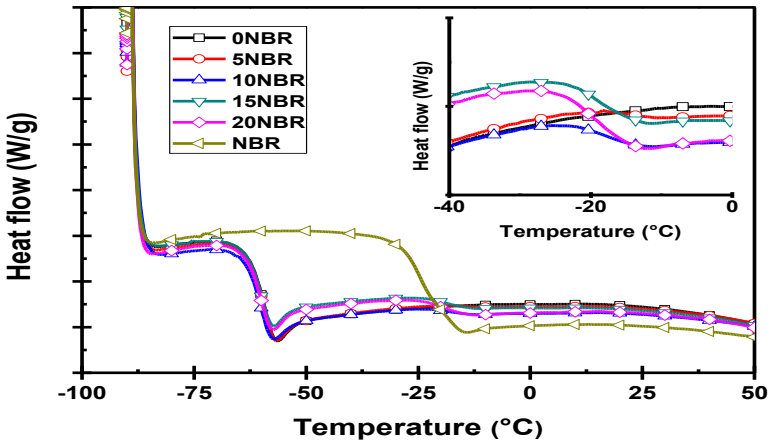

Figure 5.12 DSC curves of NR/PALF with NBR 0, 5, 10, 15, 20 wt% and NBR/PALF composites same remarks as previously

Table 5.6 T_gs of NR/PALF with NBR 0, 5, 10, 15, 20 wt% and NBR/PALF composites

	T_g NR (°C)	**T_g NBR (°C)**
NR	-61	-
5NBR	-61	-
10NBR	-61	-19
15NBR	-61	-20
20NBR	-61	-17
NBR	-	-24

5.1.2.3 Mechanical properties of NR/NBR/PALF composites

The tensile properties are the most important properties in this study of the strengths and weaknesses of composite rubber blends. Two-step-mixing of NR/NBR/PALF composites were first studied. Compound A was prepared by incorporation of PALF in NBR and small parts of NR before mixing with NR in the second step. Modulus at 10% strain (E_{10}) and yield stress (σ_y) are reported. Moduli at 100% (E_{100}) and 300% strain (E_{300}) and onset upturn strain are reported according to the stress after yield point. Tensile strength and elongation at break correspond to the ultimate properties of the composites.

Room temperature stress-strain curves of two-step-mixed NR/NBR/PALF composites are displayed in Figure 5.13. In the low strain region, all the composites strongly resist the applied stress and the apparent moduli are very high. The stresses then reach a maximum value being a yield point for each composition. NBR/PALF composite fails at this point while the others continue to deform. The stress slightly decreases at the yield point and then remains roughly constant before rising with a greater slope at high deformations.

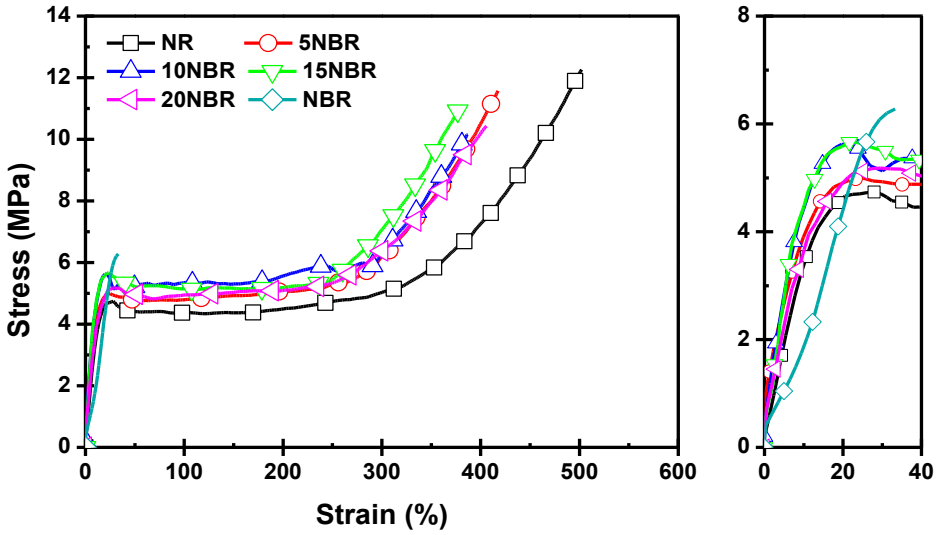

Figure 5.13 Stress-strain curves of two-step-mixed NR/NBR/PALF composites with NBR content of 0, 5, 10, 15 and 20 wt% of total rubber and NBR/PALF composite

These trends can be qualified using E_{10} and σ_y as shown in Figure 5.14. The tensile strength at break of NBR/PALF composite is included for comparison. E_{10} of NBR/PALF is lower than that of the composite blends. It should be

noticed that the failure of the NBR/PALF composite occurring at low strain (30%) is in marked contrast with that of unblend NR/PALF (500%). By replacing at least 10% of NR with NBR, σ_y increases from 4.8 MPa to 5.5 MPa, which are the same level as that at the break of NBR/PALF. However, incorporation of NBR at 20 wt% decreases E_{10} from 15NBR from 4.5 to 3.8 MPa. This might be caused to the difficulty of dispersion compound A5 in NR matrix (compounds A1 – A4 consist of NR, which is accessible to mix with NR matrix).

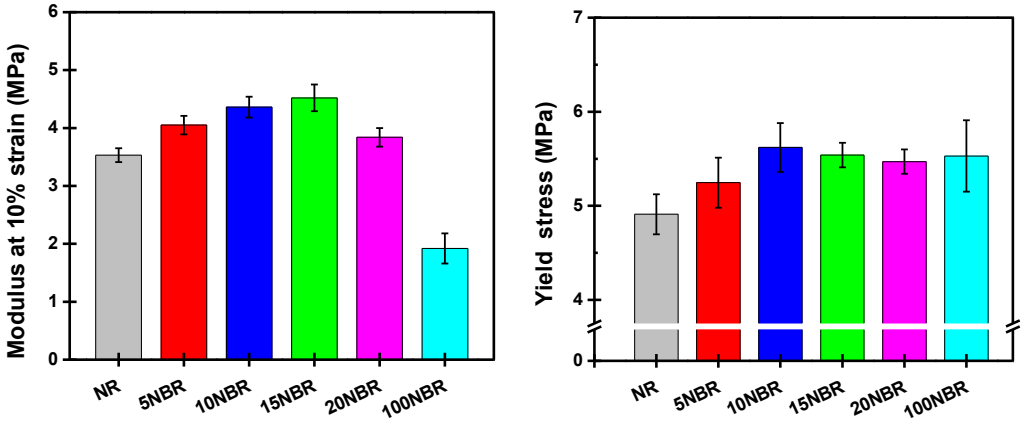

Figure 5.14 E_{10} and σ_y of two-step-mixed NR/NBR/PALF composites with NBR content of 0, 5, 10, 15 and 20 wt% of total rubber and 100 wt% NBR

Similar behavior is also observed for the E_{100}, which is after the yield point and E_{300} as shown in Figure 5.15. E_{100} and E_{300} are higher when NBR is blended into NR/PALF composite. By incorporation of NBR into composites, onset upturn strain is appearing significantly for lower strains (360 %strain to approximate 275 %strain).

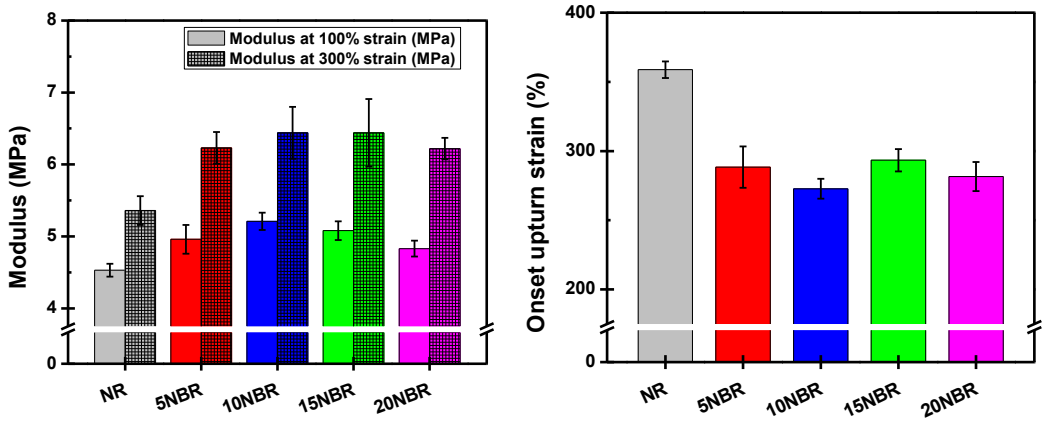

Figure 5.15 E_{100}, E_{300} and onset upturn strain of two-step-mixed NR/NBR/PALF composites with NBR content of 0, 5, 10, 15 and 20% of total rubber

Ultimate properties of these composites are given in Figure 5.16. Tensile strength of NR/PALF composites decreases when NBR is blended at least 10% wt of total rubber. Elongation at break dramatically decreases from 500 to 380% when the amount of NBR is increased and remains constant when NBR is incorporated up to 10 wt%.

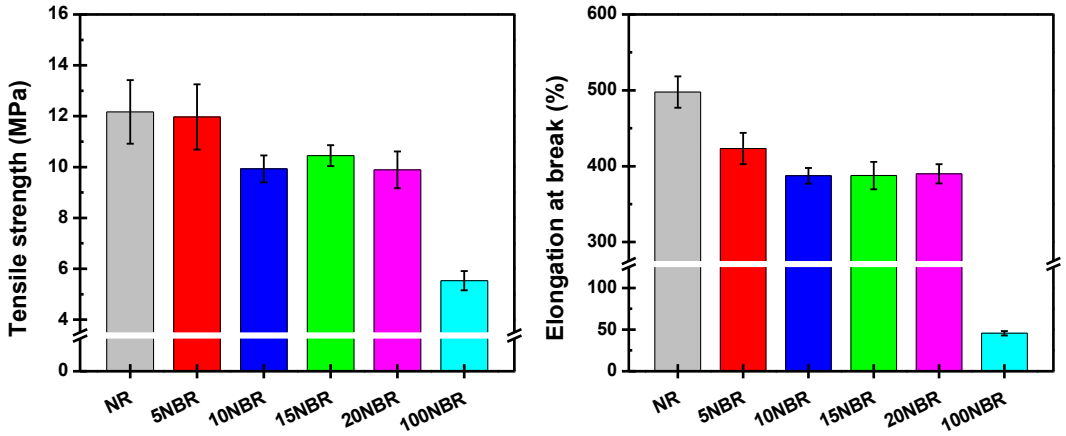

Figure 5.16 Tensile strength and Elongation at break of two-step-mixed NR/NBR/PALF composites with NBR content of 0, 5, 10, 15 and 20 wt% of total rubber and 100 wt% NBR

The results show that the deformation behavior at low strain of NR/PALF composite can be improved by incorporation of NBR. Cross-sectioned areas of tensile-fractured composites were further observed by SEM.

5.1.2.4 Morphology of tensile-fractured composites

In order to gain better understanding of the mechanical behavior of NR/PALF composites, the morphology of tensile-fractured composites was examined with a scanning electron microscope (Figure 5.17). On one hand, the NR/PALF composite without NBR shows rather clean pull-out of fibers without any remaining rubber on the fiber surface. On the other hand, the two-step-mixing NR/PALF composite blended with NBR, despite showing pulled-out fibers, show some material remaining on their surfaces. It is postulated that this material is NBR which had encased the fibers, held by "polar" interactions that can be dipole-dipole interaction or hydrogen bonding. Although NR and NBR are incompatible, the improvement of mechanical properties of composites blended with NBR is occurred. It is difficult to identify those encased materials on the fibers. First, AFM was used to study the fiber surface. However, the specimen cannot be analyzed due to the large difference of modulus of fiber and rubber. Second, osmium staining was used to stain the tensile-fractured samples in order to enhance the contrast of rubbers. No changes after staining could be observed.

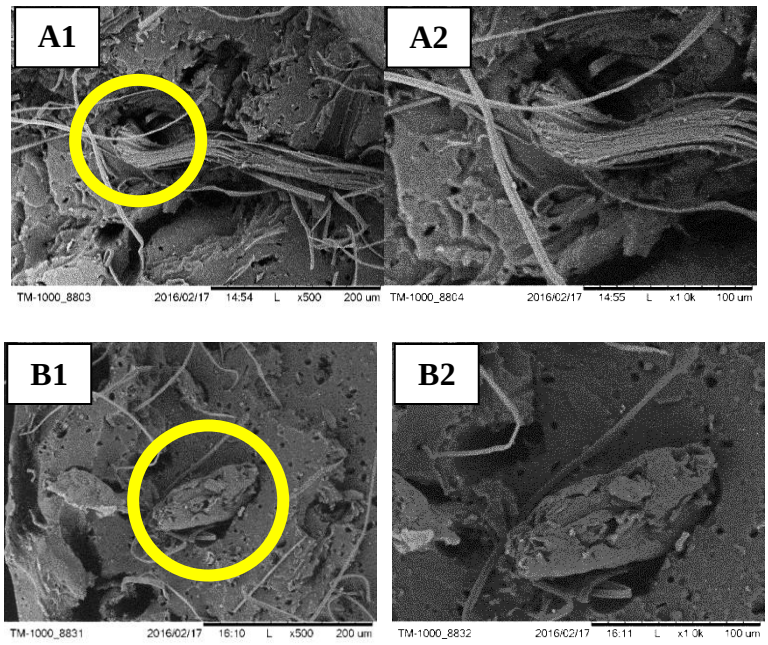

Figure 5.17 SEM micrographs of NR/PALF (A1, A2) and two-step-mixed NR/NBR/PALF with NBR content of 15 wt% of total rubber (B1, B2)

5.1.3 Discussion

Effect of NBR on the non-reinforced rubber blends will first be discussed in order to explain the curing behaviors, their mechanical properties and morphology of the blends. The results of the DMTA and DSC analysis of indicate that NR and NBR are immiscible as expected and well known [125]. By incorporation of small amounts of NBR into NR, small nodules of NBR are dispersed in NR. Due to the immiscibility of the rubbers, the curatives distribution is not identical in each phase. It was reported by Tinker and co-workers that crosslink distribution in immiscible blends of NR and NBR is not equal [124]. For NR/NBR blends, Chapman and Tinker suggest that the primary influence on crosslink distribution is the difference in polarity of the two rubbers. This difference has an effect on the distribution of curatives and vulcanization intermediates because of differences in solubility. For example, sulfur will rather migrate to NBR due to its higher solubility parameter (29.8 $MPa^{1/2}$). The one for NBR ranges between 17.8 and 21.3 $MPa^{1/2}$ depending on the nitrile content whereas NR solubility parameter is equal to 16.7 $MPa^{1/2}$. When using CBS as an accelerator in the same concentration (1,3 phr), the authors show that the crosslink density of NR is lower than that of NBR when the ACN content is equal to 34% whereas the reverse is observed for higher ACN content (41%). It depends on the type of accelerator, curing temperature, the difference between polarities of rubbers. From the swelling and NMR results, in our case, it can be concluded that curing additives can migrate from NR to NBR phase. A small effect can be observed on the kinetics of vulcanization that is accelerated by the presence of NBR. But M_H reached the plateau region of NR and does not depend on NBR content. In addition, tensile properties of the blends are similar to NR. It is suggested that the size of the NBR nodules (about 2.5 µm in diameter) is not big enough to modify significantly the mechanical properties of the matrix. Thus, the diffusion of curing distribution in the bulk can be neglected in our NR/NBR blends that contain 20 phr of NBR at the maximum.

It is observed from two T_gs and T_ds that NR and NBR are still immiscible in NR/NBR/PALF composites. The observation of two T_ds of NR/NBR immiscible blend was also reported by Kader and coworkers [125]. The authors blended NR and NBR (34%ACN content) at 50/50 (w/w) using trans-polyoctylene as compatibilizer, however, T_ds of NR and NBR still remained at the same position. Although trans-

polyoctylene was used to reduce the size of NBR dispersed phase, the authors suggested that NR and NBR are still immiscible.

Incorporation of NBR into NR containing PALF using two-step-mixing modify significantly both curing behavior and mechanical properties. NBR is suggested to encase the fibers due to their close polarities, thus, the distribution of the curatives in the NR matrix is modified in presence of PALF. The composition of the vulcanization system corresponds to a conventional one with the level of sulfur (2 phr) equal to twice the level of accelerator. This system should lead to a preponderance of polysulfidic crosslinks at optimum cure. These crosslinks are less stable than mono- or disulfidic crosslinks. However, results obtained on NR/NBR blends do not show a reversion process in the same conditions of testing.

The curing behaviors of single-step-mixed NR/NBR/PALF composites are different from two-step-mixed composites, which are displayed in Figure 5.18. The single-step-mixed composites were produced by mastication of NR and NBR together followed by the incorporation of PALF and finally the curatives. Hence, NBR is suggested to disperse in NR rather than encased PALF. While two-step-mixed NR/NBR/PALF composites all exhibit the reversion process, single-step-mixed composites reaches a plateau region that is higher than that for pure filled NR without a reversion. However, it was reported by Chapman and Tinker [124] that curing behaviors of the immiscible blends are depended on many parameters i.e. ratio of the rubbers, type of the accelerator, amount and ratio of the accelerator and sulfur and mixing process. Thus, it is difficult to clarify the curing behaviors of the blends. The effect of the incorporation of NBR into NR/PALF composites on mechanical properties will be further discussed.

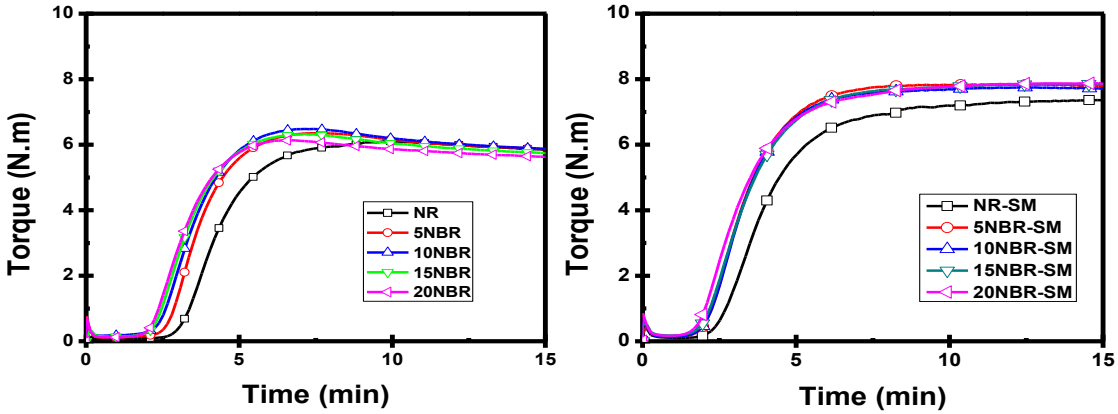

Figure 5.18 Cure curves of two-step-mixed and single-step-mixed NR/PALF composites containing NBR 0, 5, 10, 15, 20 wt% of total rubber matrix

Modulus and strength are modified in both the low and high strain regions. The following explanation is presented. Interactions between the rubber NR matrix and the fibers in NBR-PALF are greater than that in NR-PALF due to the more closely matching polarities of the two phases. This can be seen first by comparing the M_H (Figure 5.9) of NR/PALF and NBR/PALF composites. By replacing parts of NR by NBR, it is suggested that the NBR will encase the fibers. NR and NBR are not miscible and thus remain phase-separated. However, stress can still be transferred from the NR matrix to the NBR encased fiber via frictional forces at the rubber/rubber interface. This, in effect, improves the stress transfer between the rubber matrix and the fibers during tensile testing. Thus, both E_{10} and σ_y should increase, as is observed. When the stress is greater than the friction at the NR-NBR interface, pull-out of the coated fiber occurs. This is manifested as a drop in stress similar to that seen in plastic yielding. Turning to the 20% NBR, the E_{10} and σ_y are lower than those of 15% NBR. This is because the high content of NBR makes the pre-mixed compound A difficult to disperse during mixing (other compounds A consist of NR, which is accessible to mix with NR matrix). When the single-step mixing method is used for this high NBR content, the dispersion problem can be overcome and better low strain properties are then obtained, which are shown in Figure 5.19. By the way, the onset upturn strain is occurring earlier in two-step-mixed composites. It seems that it is rather the embedding of the fibers by NBR that will lead to higher stress transfer between fibers and NR matrix and higher friction between NR and NBR that would improve mechanical properties.

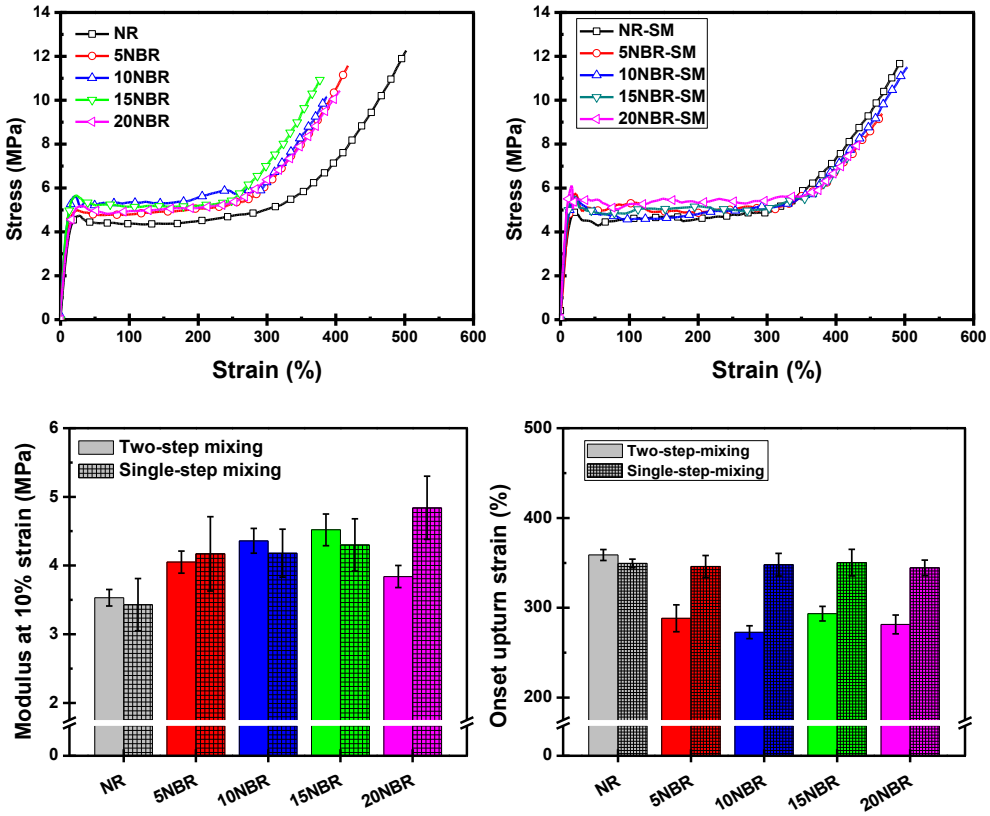

Figure 5.19 Stress-strain curves and tensile characteristics of two-step- and single-step-mixed NR/PALF composites containing NBR 0, 5, 10, 15, 20 wt% of total rubber matrix

5.1.4 Summary

The mechanical properties of NR/PALF can be improved by replacing a certain amount of the NR matrix with NBR. The level of improvement depends on how the NBR is introduced into the system. To optimize the effect, the PALF should be first dispersed in NBR before being added to a NR matrix. It is postulated that NBR encases the fibers and so improves the stress transfer from the matrix to the fiber. This improves the moduli at both low as well as at high strains (10% and 300%). Mixing of the same composition in one step, however, does not provide the same level of improvement unless there is a very high NBR content.

5.2 Effect of surface treatment of PALF on NR/PALF composites

The silane treatment of PALF was used to improve interfacial strength between NR and PALF. Three types of silane containing non-reactive group, double bonds and sulfidic bonds, were studied in this work. They are named according to their treatment (Table 5.7). It should be noted that alkali treatment was first treated before silane treatment. Then, the effect of silane concentration, solvent effect and the washing method for surface treatment were investigated.

Table 5.7 Name of fibers with different surface treatments

Name	PALF Treatment	Silane structure
UPALF	Untreated PALF	-
APALF	Alkali-treated PALF	-
pSiPALF	Propyltriethoxylsilane-treated PALF	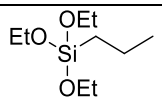
aSiPALF	Allyltriethoxylsilane-treated PALF	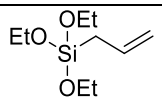
sSiPALF	Silane-69-treated PALF	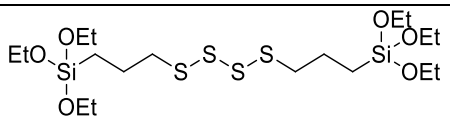

Alkali treatment is a pretreatment to remove non-cellulosic substances at the surface of PALF. Propyltriethoxysilane is considered as reference for a non-reactive treatment during vulcanization of the rubber. However the surface is becoming hydrophobic and better compatibility should be observed with hydrophobic NR. Allyltriethoxysilane is used as a reactive site that contains allyl group. This bond is proposed to react during co-crosslinking with NR via sulfidic bonds at the allylic hydrogen atoms. Silane-69 is a silane containing sulfur that provides free sulfur for co-crosslinking with rubber during the vulcanization at high temperature. The reaction schemes of silane treatment are proposed in Figure 5.20.

For the treatment, the concentration of silane was fixed at 3 wt% of APALF. Ethanol/water at the ratio of 80/20 v/v was used as a solvent. After silane treatment, fibers were washed using solvent at least three times then dried in the oven at 80 °C.

For non-washing method, which is used as optimized silane amount, solvent was evaporated using rotary evaporator and the fibers were dried.

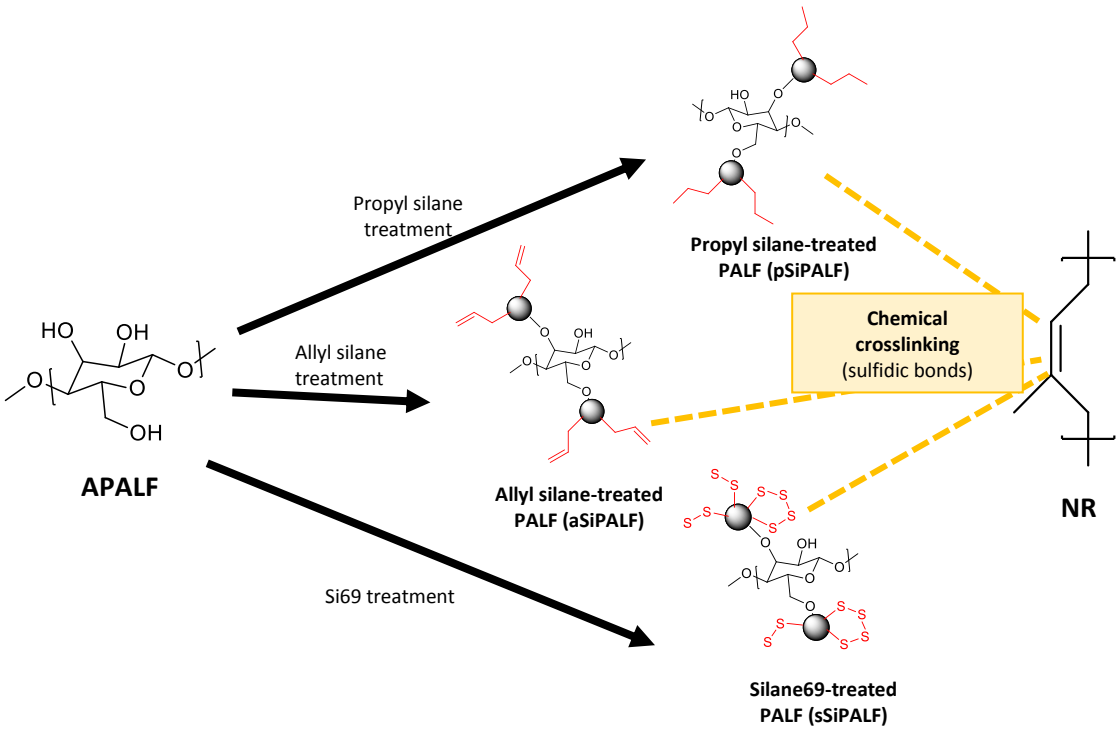

Figure 5.20 The reaction schemes of silane treatments

5.2.1 Characterization of fibers

Alkali and silane treatments of fibers were characterized using XPS to investigate the modified functional groups on the surface of fibers. Silane treatment using washing method and non-washing method were studied to compare the amount of silane on the surface of fibers. Weight loss after alkali treatment was 25-30 %, whereas no weight loss was observed after silane treatment. The morphology of fibers was also characterized using SEM.

5.2.1.1 XPS analysis

In this work, three types of silane were used to treat on the surface of APALF. X-ray photoelectron spectroscopy (XPS) were further used to characterize the elements present at the surface of the fibers. Silane-69 treatment was used as a representative of other silanes for fiber characterizations due to the presence of sulfur, which can be identified apart from the cellulose structure. Silane-69

treatments using washing and non-washing method were analyzed and compared to each other to quantify the amount of silane on the fiber. Treatment by washing method was done by washing with ethanol several times after finishing the reaction, while treatment by non-washing method was done by evaporation of solvent. After these processes, fibers were dried to remove all residual solvent.

Chemical structure of cellulose and silane-69, which is used as reference, are displayed in Figure 5.21 and Figure 5.22 respectively. The XPS analysis is carried out in term of %atomic content, O/C ratio and the binding energies of carbon, oxygen, silicon and sulfur.

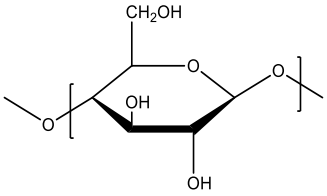

Figure 5.21 Chemical structure of cellulose

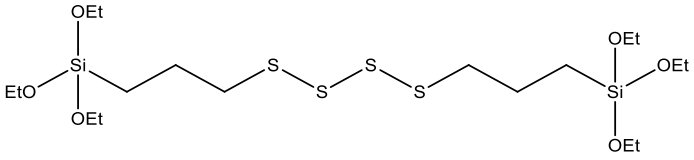

Figure 5.22 Chemical structure of silane-69

The experimental result of untreated fiber was first studied. Wide scan spectra of UPALF is displayed in Figure 5.23, which indicates the relation between binding energy in electron volt and intensity of the signal. The spectra of PALF contain 1s electrons of carbon and oxygen. The atomic composition of various surface treatment fibers and silane-69 are shown in Table 5.8. The theoretical value of O/C ratio of cellulose from the molecular structure is 0.83. O/C ratio of UPALF is 0.30, which is lower than that of pure cellulose [128]. This result shows that the surface of UPALF might be covered by a large aromatic structure of lignin, which the O/C ratio is around 0.30-0.36 [129]. The large aromatic structure of lignin is generated from the condensation of small aromatic molecules, which are shown in Figure 5.24. However, no π-π^* satellite signal of lignin around binding energy 290-292 eV is observed. Thus, it is still unclear that the surface of fibers is covered by lignin.

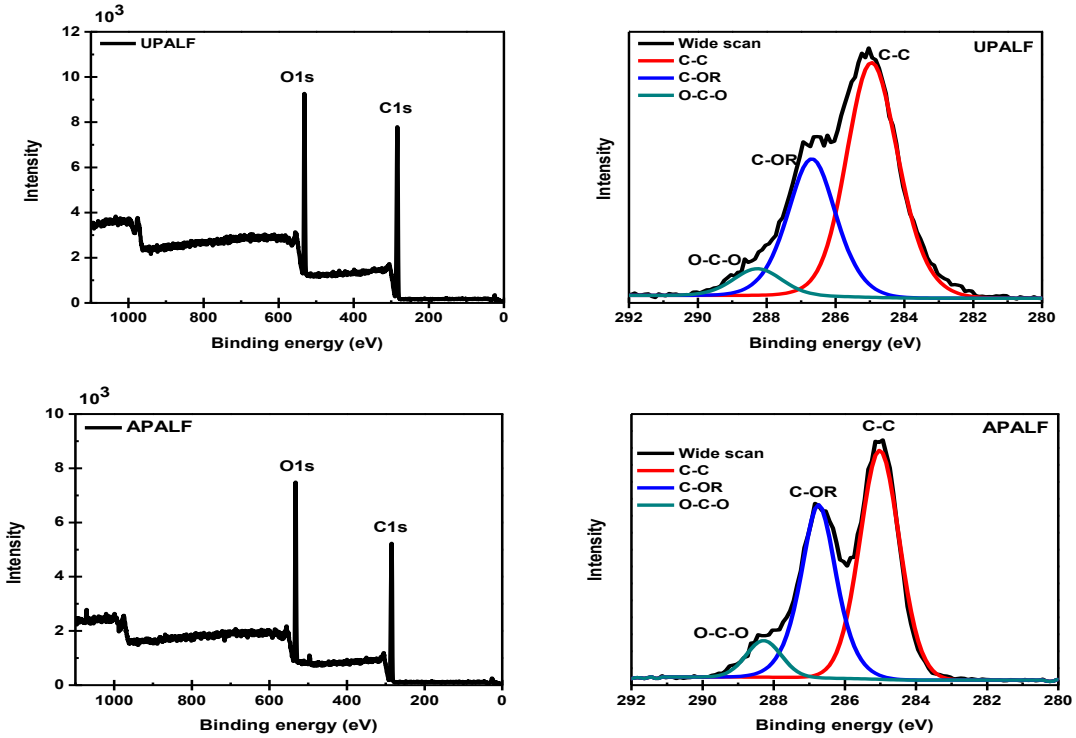

Figure 5.23 XPS wide scan and high resolution spectra of C1s of UPALF and APALF

Table 5.8 Extracted elemental compositions of UPALF and APALF

Element (%atomic content)	C (%)	O (%)	O/C ratio	C1s		
				C-C	C-OR	C-O-C
UPALF	77.2	22.8	0.30	66.0	24.5	5.7
APALF	75.0	25.0	0.33	60.4	33.3	6.3

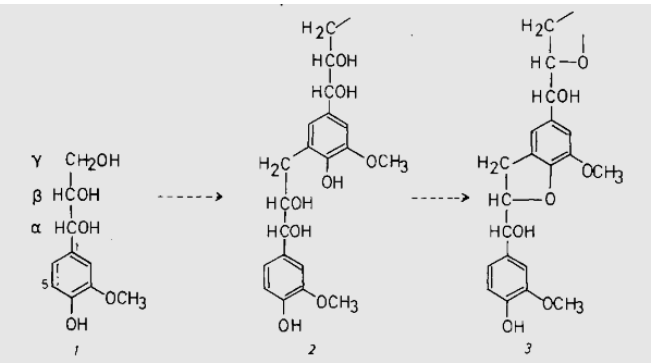

Figure 5.24 Basic chemical structure of lignin [130]

XPS spectra of APALF are analyzed and shown in Figure 5.23 and their experimented values are listed in Table 5.8. The wide scan spectra, carbon and oxygen atomic contents, and O/C ratio are similar to untreated fiber. **C**-OR slightly increases from 24.5 to 33.3% and **C**-C slightly decreases from 66.0 to 60.4% compared to UPALF, whereas **C**-O-C does not significantly changed. It was reported by Islam [131] that hemicellulose and waxes can be removed by alkali treatment. Waxes removal results in lower C-C signal, however, XPS analysis cannot be used to distinguish between hemicellulose and cellulose. This is due to the structure of hemicellulose is almost similar to cellulose, except for the different sugar units and the degree of polymerization is lower than cellulose (100 times) [132]. The evidence of hemicellulose removal can be seen in FTIR analysis, which is shown in appendix C.

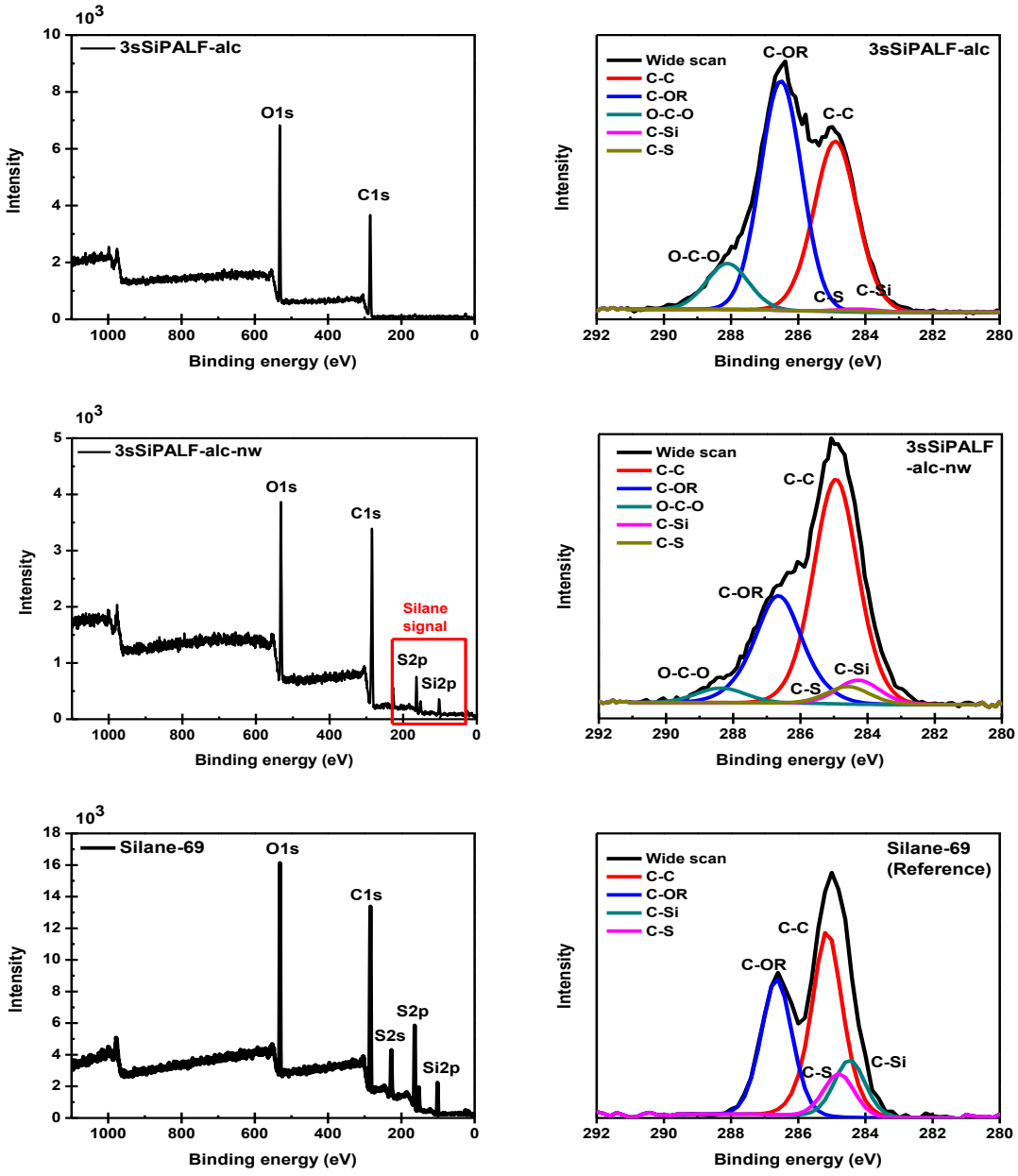

Figure 5.25 XPS Wide scan spectra and high resolution spectra of C1s of fibers with silane treatments and silane-69 as reference

Table 5.9 Extracted elemental compositions of PALF with surface treatments. Silane-69 is used as reference.

Element (%atomic content)	C (%)	O (%)	O/C ratio	Si (%)	S (%)	C1s (%)		
						C-C	C-OR	C-O-C
APALF	75.0	25.0	0.33	-	-	60.4	33.3	6.3
sSiPALF-alc-nw	68.0	22.0	0.33	4.0	5.7	56.3	29.8	3.9
sSiPALF-alc	67.8	31.2	0.46	0.5	0.5	45.8	44.1	8.3
Silane-69	61.7	18.4	0.30	8.0	13.0	45.0	31.6	-

The effect of silane treatment on fiber by non-washing method (sSiPALF-alc-nw) was first analyzed. By using this method, silane still remains on the fiber that could be continued to form network during drying. The wide scan spectrum of sSiPALF-alc-nw, which is displayed in Figure 5.25, shows the signal of silicon and sulfur atoms. By the way, O/C ratio is not increased by silane treatment, as shown in Table 5.9. It can be seen that O/C ratio of sSiPALF-alc-nw is closed to silane-69 and also APALF. Thus, it is unable to analyze by using O/C ratio. The C1s analysis confirmed the appearance of **C**-Si and **C**-S after treatment. Moreoever, the evidence that the analyzed area is not only silane-69 is the appearance of O-**C**-O signal, which is the signal of cellulose. The relative amount of silane by atomic content of PALF is calculated. It should be noted that the analyzed surface of fiber is approximately 10 nm. Thus, the atomic contents include silane on the surface of fiber and parts of cellulose. The relative amount of silane on the surface of the fibers was 47.4% atomic content (appendix D).

XPS spectra of silane treatment of fiber using washing method (3sSiPALF-alc) was analyzed. The elemental compositions of 3sSiPALF-alc and references including O/C ratio are shown in Table 5.9. O/C ratio increases from 0.34 to 0.46 after silane treatment. Moreover, signals of silicon and sulfur appear, although their atomic contents are low. The successful treatment is further investigated by studying the high resolution spectra of C1s. The decreasing of **C**-C from 60.4 to 45.8% with the increasing of **C**-OR from 33.3 to 44.1%, while O-**C**-O remains the same as

before treatment, indicates the presence of grafted silane on the fiber. The amount of **C**-OR, which increases after treatment, is attributed to residual ethoxyl groups from silane-69. The signals of **C**-S and **C**-Si appear, although the intensities are low. The amount of silane on the surface of fiber was estimated to 3.8% by atomic content (appendix D).

5.2.1.2 Fiber morphology by SEM

The effect of treatments on the morphology of fiber was investigated using SEM. Morphologies of UPALF, APALF and SiPALF are displayed in Figure 5.26. The hemicellulose removal is confirmed by the partial absence of binding between elementary fibers. The morphology of fiber after silane treatment is not changed compared to APALF.

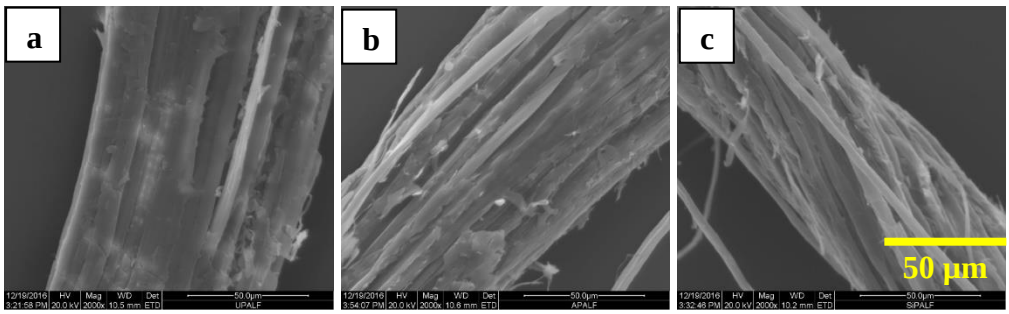

Figure 5.26 SEM micrographs of UPALF (a), APALF (b) and sSiPALF (c)

5.2.2 Effect of type of fiber surface treatment on composite properties

The effect of type of silanes was first studied. For the study of type of silanes, the treatment condition is 3 wt% concentration of silane. Ethanol/water at the ratio of 80/20 v/v was used as a solvent. After treatment as previously described, fibers were mixed with NR and curatives using two-roll mill. Curing behavior of compounds after mixing was first studied by moving die rheometer (MDR). Then, the study of reinforcement of NR by PALF was performed by tensile testing and their morphologies of tensile-fractured specimens was observed by SEM.

5.2.2.1 Cure characteristics

The cure characteristics of NR with different surface-treated fibers were first investigated. The rheograms of composites are displayed in Figure 5.27 and their cure characteristics are shown in Table 5.10.

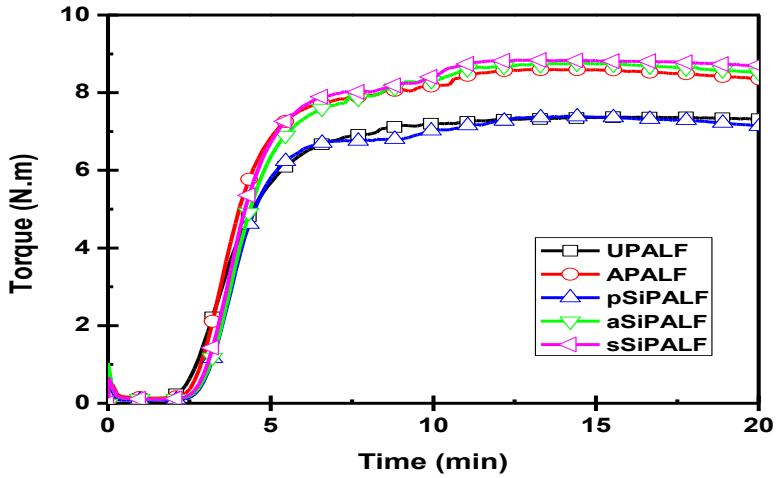

Figure 5.27 Cure curves of NR/PALF composites with different surface treatments of PALF

Table 5.10 Cure characteristics of NR/PALF composites with different surface treatments of PALF

	M_L (N.m)	M_H (N.m)	t_{s2} (min)	t_{c90} (min)
UPALF	0.1	7.4	3.2	7.3
APALF	0.1	8.6	3.2	6.5
pSiPALF	0.1	7.4	3.5	6.4
aSiPALF	0.1	8.8	3.5	7.9
sSiPALF	0.1	8.8	3.6	6.9

Alkali treatment of fiber improves M_H of composites from 7.4 to 8.6 MPa, while silane treatments of fiber has no effect on cure behavior of composites, except for pSiPALF: UPALF and pSiPALF behave the same curing behavior. Thus, propylsilane treatment erases the effect of alkali treatment.

5.2.2.2 Mechanical properties

Tensile properties of composites with different surface treatments of PALF were studied. The stress-strain curves of composites are displayed in Figure 5.28. In the low strain region, composites strongly resist to the applied force and reach the yield point. The effect of interfacial strength between rubber and fiber, which is the main factor to enhance tensile properties, is observed in this region. After composites reach the yield point, the applied force slightly decreases to a constant value. By the way, the failure of NR/surface-treated PALF composites are more rapidly than UPALF. Ultimate properties are lower by fiber surface treatment.

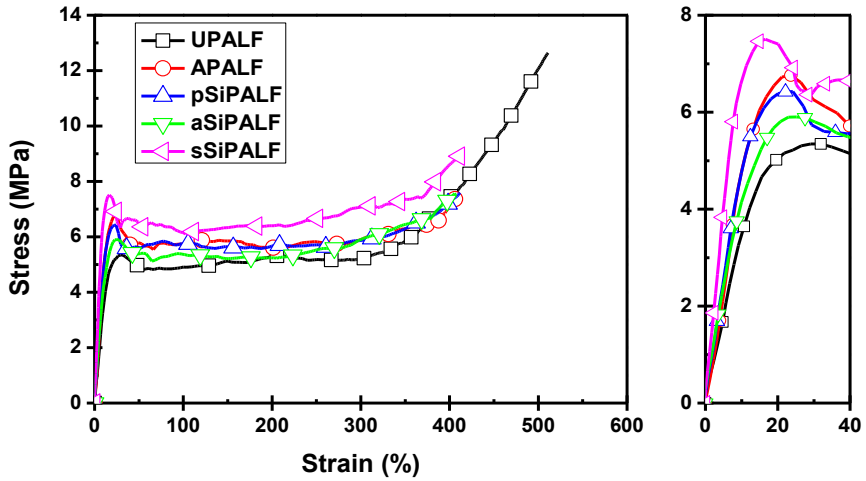

Figure 5.28 Stress-strain curves of NR/PALF composites with different surface treatments of PALF

Tensile characteristics of composites are displayed in Figure 5.29. Alkali treatment increases E_{10} and σ_y by 49% and 26% respectively compared to UPALF. However, these values are not further improved by propyl and allyl silane treatments. Silane-69 treatment is the only one type of silane that can be used to increase further E_{10} and σ_y by 21% and 7% respectively. E_{100} and E_{300} slightly increase by alkali treatment, but there is no significant difference after silane treatments. Tensile strength and elongation at break significantly decrease by alkali treatment, whereas silane treatments do not cause significant differences compared to alkali treatment.

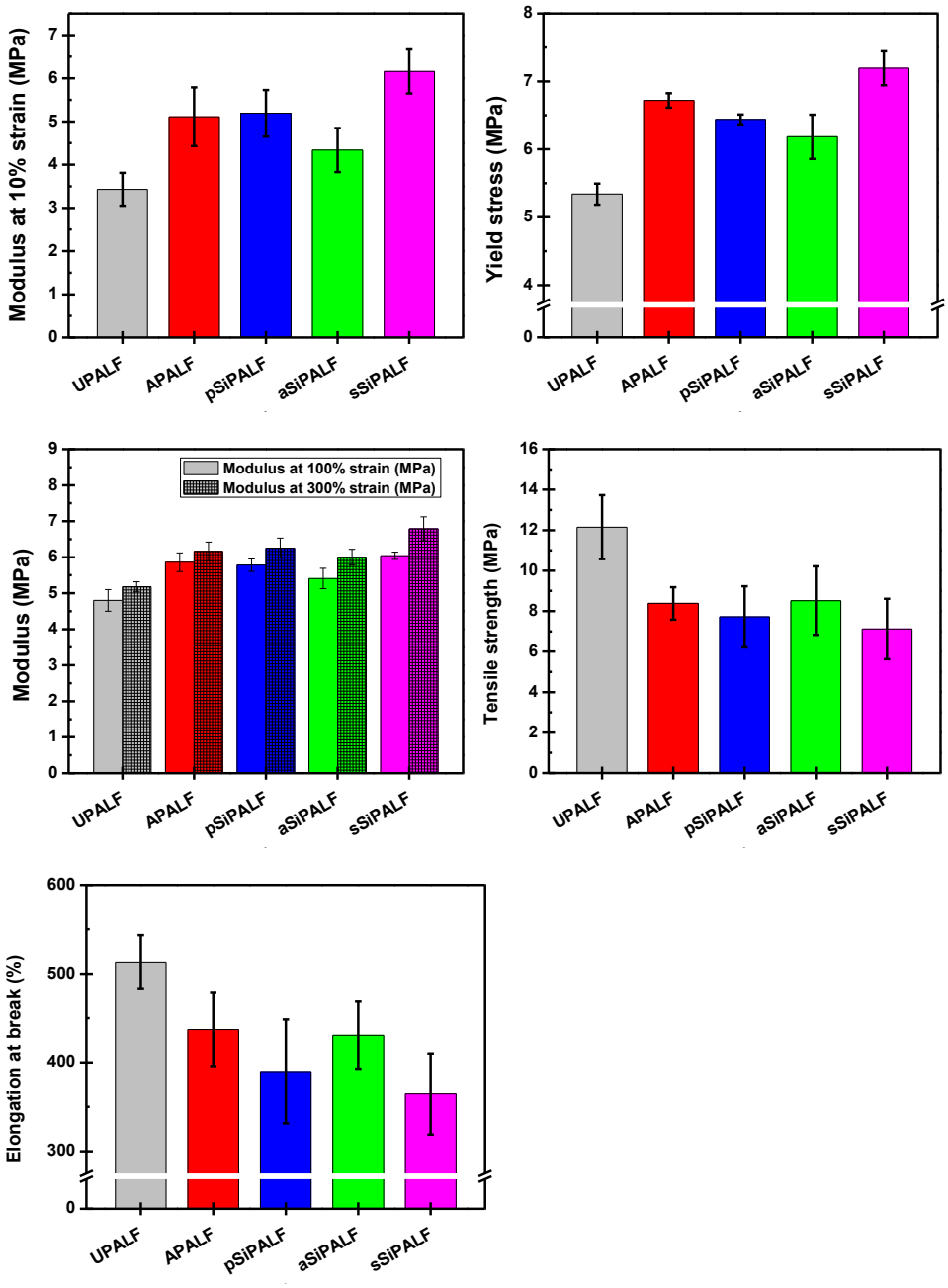

Figure 5.29 Tensile strength and elongation at break of NR/PALF composites with different surface treatments of PALF

5.2.2.3 Morphology of tensile-fractured composites

The morphology of tensile fractured composites was further examined by SEM. The images of composites containing untreated, alkali-treated and silane-69-treated fibers are displayed in Figure 5.30. It can be observed that less pull-out fibers and voids between NR and fiber occur after alkali and silane treatments. This observation is consistent with the improvement of mechanical properties of composites after treatment.

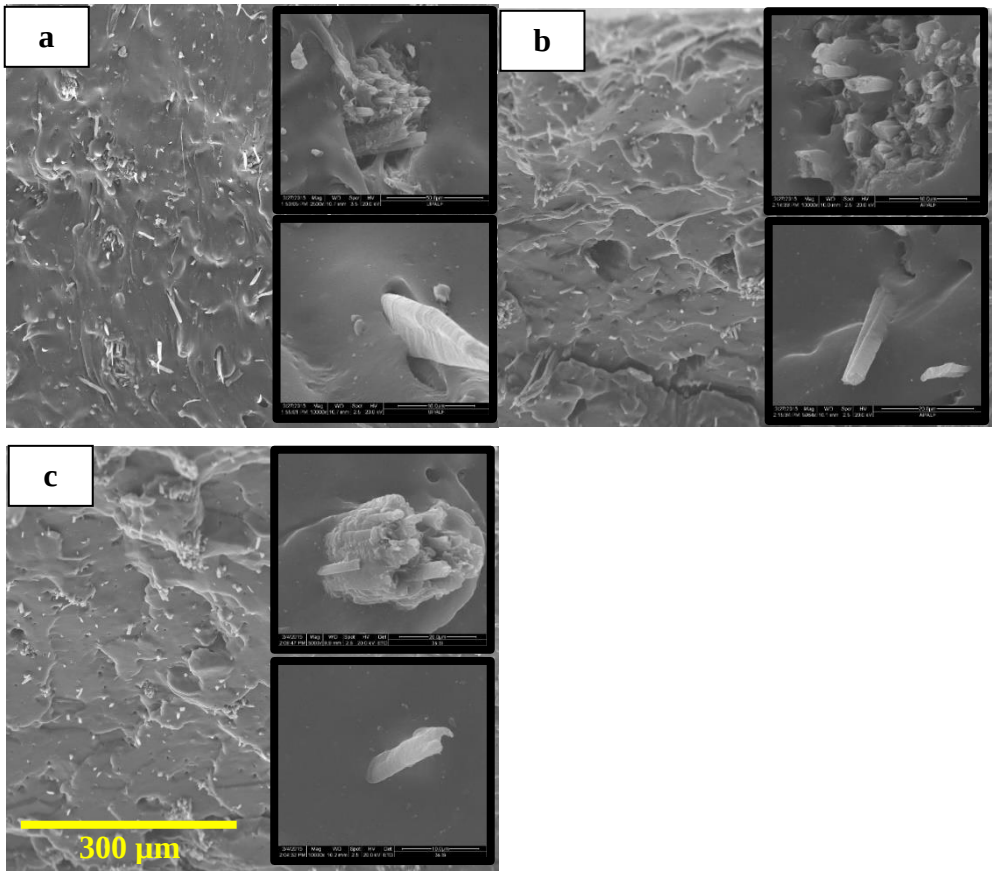

Figure 5.30 SEM micrographs of overall tensile-fractured composites containing untreated (a), alkali-treated (b) and silane-69-treated (c) fibers and zoom-in of fiber bundle and elementary fiber

We have clearly shown that alkali treatment followed by silane-69 treatment of fibers can be used to improve the mechanical properties of composites. Next, we will attempt to study the effect of silane concentration on fiber treatment.

5.2.3 Effect of silane concentration

Silane concentration is one of the important factor that should be controlled to improve the mechanical properties of composites. On the one hand, low amount of silane causes less reinforcement effect on composites due to low amount of reactive sites. On the other hand, excessive amount of silane causes a thick layer, which cannot ensure efficient stress transfer from the rubber to the fibers. Thus, the appropriate amount of silane should be considered. Silane-69 was chosen to study the concentration of silane due to the improvement of mechanical properties. The concentrations of silane were varied at 0, 0.1, 1, 3, 5, 10 wt% of PALF. After the treatment, fibers were washed with mixed solvent for several times to remove residual unattached silane. Treated fibers were incorporated into NR. Cure characteristics and mechanical properties of composites were studied. Composites were named as *x*sSiPALF, where *x* is silane concentration.

5.2.3.1 Cure characteristics

The effect of silane concentrations on cure characteristic of composites was first studied. The rheograms of composites are displayed in Figure 5.31 and their cure characteristics are reported in Table 5.11. It can be observed that silane concentration does not affect significantly cure characteristics of composites.

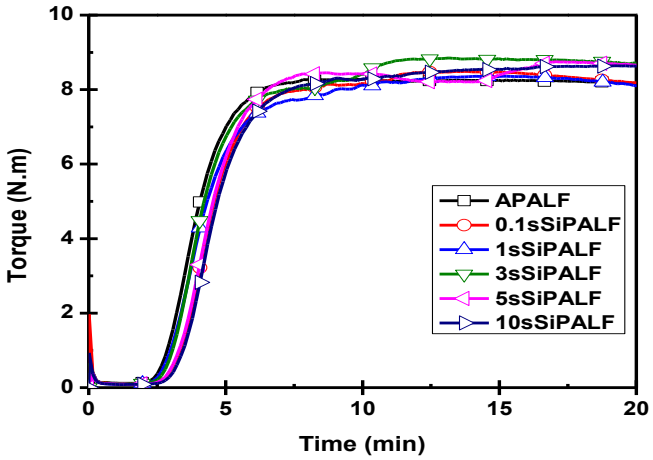

Figure 5.31 Cure curves of NR/silane-treated PALF composites with different silane concentrations

Table 5.11 Cure characteristics of NR/silane-treated PALF composites with different silane concentrations

	M_L (N.m)	M_H (N.m)	t_{s2} (min)	t_{c90} (min)
APALF	0.1	8.3	3.2	6.8
0.1sSiPALF	0.1	8.5	3.8	6.4
1sSiPALF	0.1	8.4	3.4	6.6
3sSiPALF	0.1	8.8	3.6	6.9
5sSiPALF	0.1	8.5	3.7	7.4
10sSiPALF	0.1	8.6	3.9	6.7

5.2.3.2 Mechanical properties

The effect of silane-69 concentration on tensile properties of NR/PALF composites was studied (Figure 5.32). To clarify the uncertainty of tensile properties, the average values of 5 specimens were reported. The slope at low strain region is not modified by using silane 0.1 and 1 wt%, while it increases by using silane 3 wt%. The slope is dropped again by using silane 5 wt%, however, it is increased by using silane 10 wt%. Yield stresses of composites increase only when using silane concentration at 3%. However, silane concentration does not affect significantly the ultimate properties.

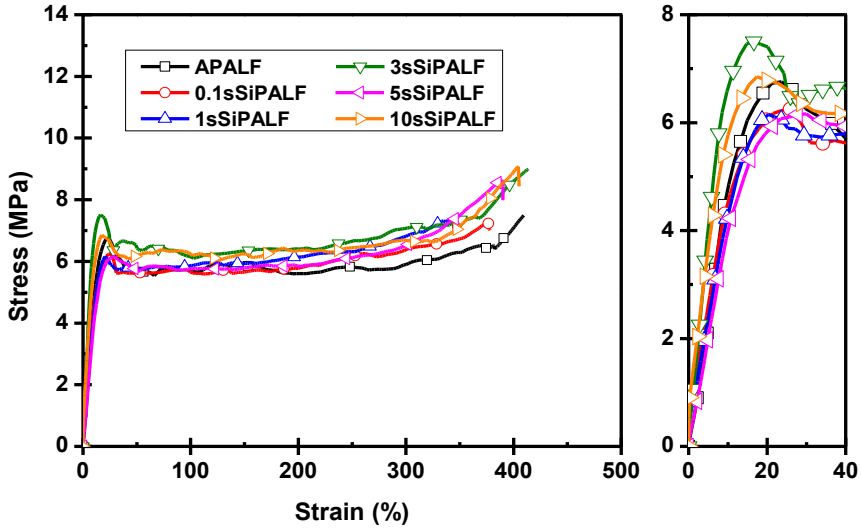

Figure 5.32 Stress-strain curves of NR/silane-treated PALF composites with different silane concentrations

E_{10}, σ_y, E_{100}, E_{300}, tensile strength and elongation at break are displayed in Figure 5.33. Silane treatment at low concentration does not affected on the low strain characteristics of composites. E_{10} and σ_y increase to 6.1 and 7.2 MPa respectively by incorporation of sSiPALF, which were treated using 3 wt% silane concentration. By the way, the incorporation of sSiPALF, which was treated using 5 wt% of silane, does not improve the tensile properties at low strain region. Using 10 wt% of silane increases E_{10} and σ_y again to 5.5 and 6.6 MPa. To clarify this result, the experiment was repeated. However, these values of 5sSiPALF are still lower than 3sSiPALF and 10sSiPALF composites. E_{100}, which is indicated to the moderate deformation region, slightly increases when increasing silane concentration. However, by incorporation of 5sSiPALF, E_{100} does not improve. E_{300}, increases when the concentration of silane reaches to 1 wt% of PALF. The increasing of silane concentration more than 1 wt% does not further induce an increase of E_{300}. Tensile strength and elongation at break of composites are not affected by silane treatment. It cannot be distinguished the changing of values due to the high standard deviation.

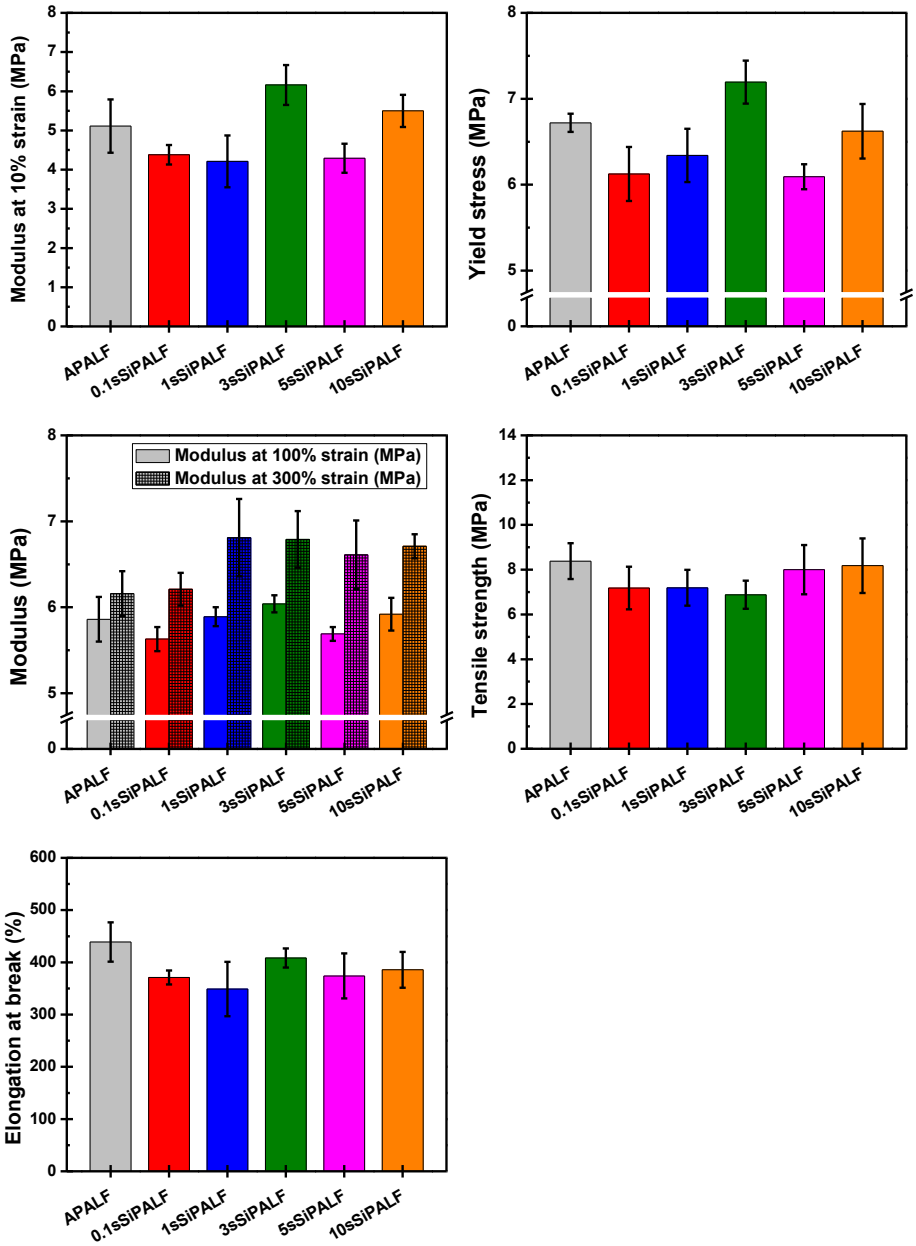

Figure 5.33 Tensile properties of NR/silane-treated PALF composites with different silane concentrations

Low amounts of silane do not improve the tensile properties until it reaches an appropriate amount. By the way, abundant amount of silane does not further improve tensile properties. Hence, 3 wt% silane-69 concentration is chosen due to the highest enhancement of tensile properties. Next, silane-69, which is treated using 3 wt% of silane concentration will be used to study the effect of solvent on the silane treatment. 5wt% of silane with the changing of solvent for treatment will also be studied to clarify the unexpected decrease of E_{10} and σ_y.

5.2.4 Solvent influence on silane treatment

Solvent influence on the treatment is also the one of parameters that can be adjusted to control the treatment. The mixture of ethanol/water or pure ethanol have been generally used as a solvent for silane-69 treatment [133]. Ethanol is chosen as main or pure solvent due to the release of ethoxy groups of silane from a hydrolysis process, which is considered as the similar functionality as ethanol. A minor component of water can be used as a catalyst for hydrolysis. Thus, the mixture of ethanol/water at the ratio of 80/20 v/v and pure ethanol were used to study the solvent influence on silane treatment. The contents of silane-69 were fixed as 3 and 5 wt% of fiber. Composites were named as *x*sSiPALF for treated fibers using ethanol/water as a solvent and *x*sSiPALF-alc for treated fibers using pure ethanol as a solvent.

5.2.4.1 Cure characteristics

The solvent influence of silane treatment on cure characteristics are displayed in Figure 5.34 and Table 5.12 respectively. Treated fibers using pure ethanol as a solvent increase t_{c90} and M_H of composites from 6.5 to 9.2 min and 8.6 to 9.0 MPa respectively compared to those fibers using ethanol/water as a mixed solvent.

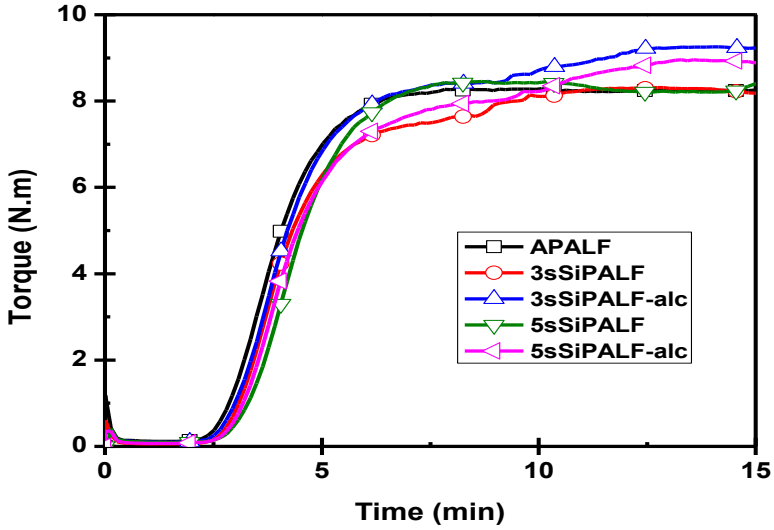

Figure 5.34 Cure curves of NR/silane-treated PALF composites with different solvents for silane treatment of PALF

Table 5.12 Cure characteristics of NR/silane-treated PALF composites with different solvents for silane treatment of PALF

	M_L (N.m)	M_H (N.m)	t_{s2} (min)	t_{c90} (min)
APALF	0.1	8.6	3.2	6.5
3sSiPALF	0.1	8.5	3.6	6.9
3sSiPALF-alc	0.1	9.4	3.4	9.2
5sSiPALF	0.1	8.5	3.7	7.4
5sSiPALF-alc	0.1	9.0	3.6	9.3

5.2.4.2 Mechanical properties

The solvent influence of silane treatment on tensile properties was studied. The stress strain curves and expanded low strain region are displayed in Figure 5.35. At low strain region, using pure ethanol as a solvent causes higher slope, modulus at low strain and also yield stress of composites. Treated fiber using silane 5 wt% results in the same tensile behavior as treated fiber using silane 3 wt% when pure

ethanol is used as solvent. The results are overcome the lower of tensile properties of 5sSiPALF when ethanol/water is used a mixed solvent.

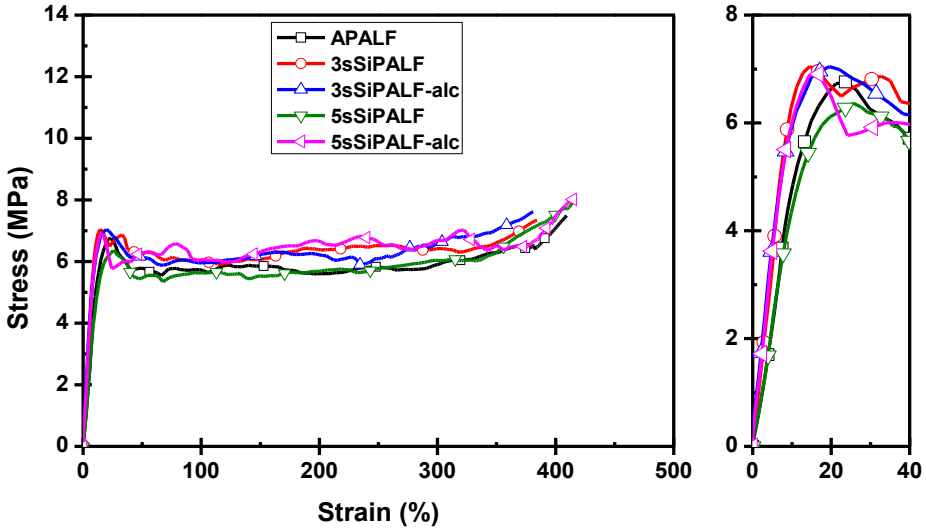

Figure 5.35 Stress-strain curves of NR/silane-treated PALF composites using different solvents for silane treatment of PALF

E_{10}, σ_y, E_{100}, E_{300}, tensile strength and elongation at break are displayed in Figure 5.36. An increase in E_{10} is observed in all cases except for 5sSiPALF for which a significant decrease is observed. Moreover, σ_y for this last composite is lower than composite containing APALF. Other silane treatments increase σ_y. E_{100} and E_{300} of 5sSiPALF composite, which drop after treatment using mixed solvent, are increased to the same values as 3sSiPALF composite by using pure ethanol as a solvent. Using either mixed solvent or ethanol as a solvent for the treatment does not changed ultimate properties.

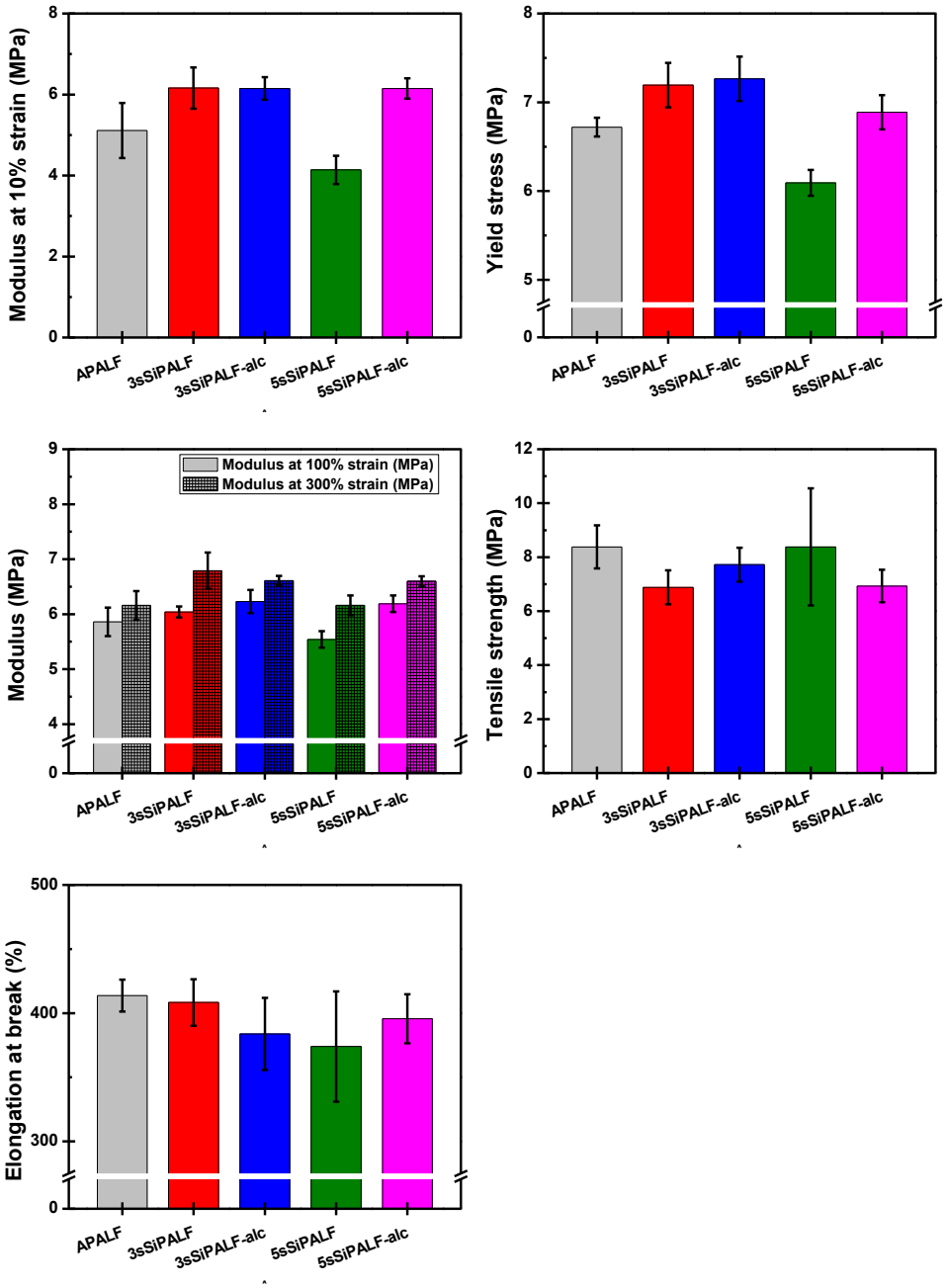

Figure 5.36 Tensile strength and elongation at break of NR/silane-treated PALF composites with different solvents for silane treatment of PALF

Tensile properties of NR/silane-treated PALF composites are improved by changing the solvent from the treatment process. Pure ethanol can be used as a solvent, which is more effective for treatment using silane concentration 5 wt%. The effect of treatment method will be further studied in order to reach the optimum tensile properties.

5.2.5 Method of treatment

The termination of silane treatment was studied to understand the effect of excessive amount of silane on the surface of fiber. In this study, Silane-69 3 wt% of fibers was treated using pure ethanol as a solvent. Two termination methods of treatment were proposed, which are washing method and non-washing method. After fibers have reacted with silane solution, fibers were washed with solvent for at least three times to remove all residual unattached ingredients then dried. For non-washing method, after the reaction was finished, solvent was evaporated slowly in order to get a large amount of silane on the fibers. Fibers were further fried at 80 °C to achieve silane-grafted fiber. Composites containing Si-69-treated PALF with non-washing method was named as 3sSiPALF-alc-nw. From the results of XPS in section 5.2.1.2, using non-washing method provides higher amount of silane rather than washing method.

5.2.5.1 Cure characteristics

Cure behavior of NR/sSiPALF composites with different treatment methods were studied. The rheograms of composites are shown in Figure 5.37 and their cure characteristics are illustrated in Table 5.13. Cure behavior of silane treatment using non-washing method shows a reversion process, which is different from treatment using washing method. t_{s2} and t_{c90} are significantly lower than those of washing method, whereas M_H is slightly lower.

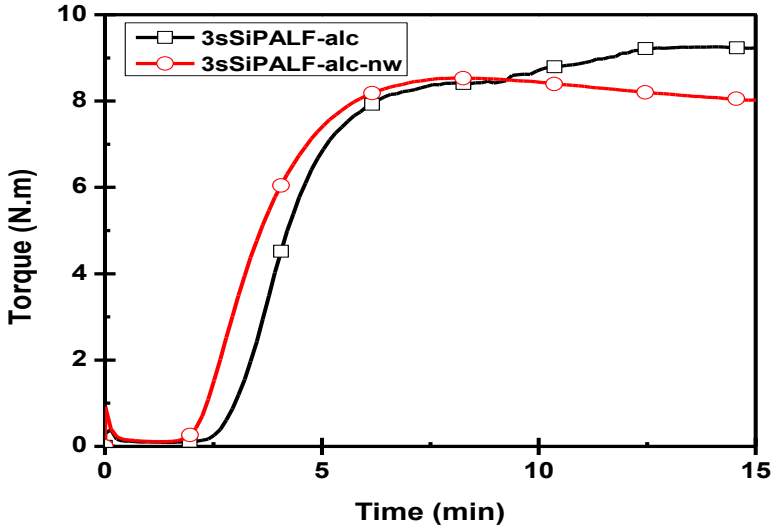

Figure 5.37 Cure curves of NR/silane-treated PALF composites with different treatment methods

Table 5.13 Cure characteristics of NR/silane-treated PALF composites with different treatment methods

	M_L (N.m)	M_H (N.m)	t_{s2} (min)	t_{c90} (min)
3sSiPALF-alc	0.10	9.39	3.4	9.2
3sSiPALF-alc-nw	0.11	8.53	2.7	5.3

5.2.5.2 Mechanical properties

Stress-strain curves of NR/3sSiPALF composites with different treatment methods are displayed in Figure 5.38. Method of treatment affects the tensile properties at high deformation of composites. Young's modulus of 3sSiPALF-alc-nw is slightly higher than 3sSiPALF-alc. However, after the yield point, the curve is not smooth and ultimate properties are significantly lower, compared to composite containing fibers that was washed. No upturn in the stress strain curve is obtained in both composites.

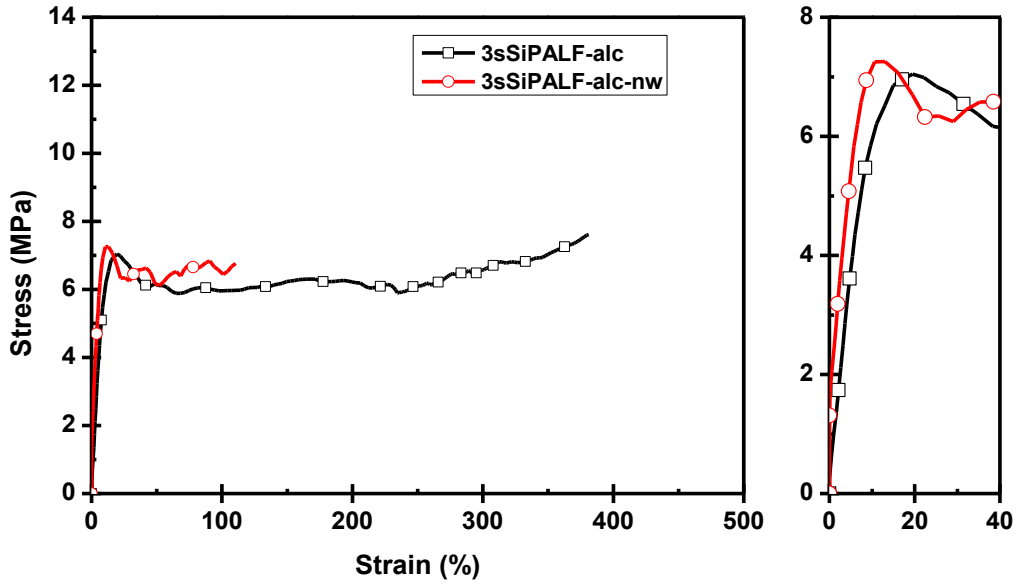

Figure 5.38 Stress strain curves of NR/silane-treated PALF composites with different treatment methods

E_{10}, σ_y, E_{100}, E_{300}, tensile strength and elongation at break are shown in Figure 5.39. E_{10} of composites containing fiber with non-washing treatment is slightly higher than that of washing treatment. σ_y remains a constant value. E_{100} of 3sSiPALF-alc-nw is slightly higher than 3sSiPALF-alc. Both tensile strength and elongation at break are significantly lower than composite containing fiber with washing treatment.

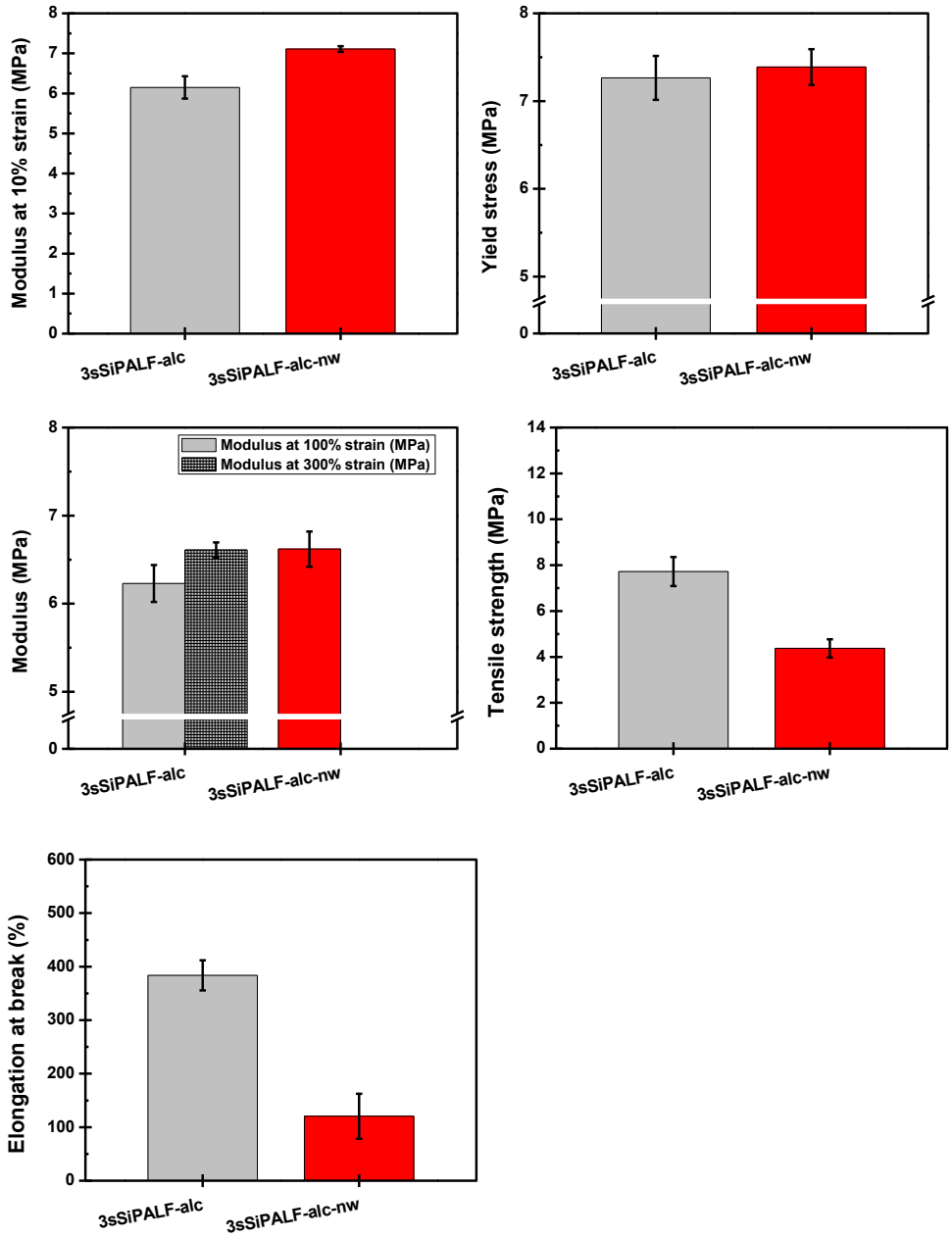

Figure 5.39 Tensile properties of NR/silane-treated PALF composites with different treatment methods

5.2.6 Discussion

The surface treatments of fibers including alkali and silane treatments were studied. These fibers can be used to improve the mechanical properties of composites in low strain region. We will now attempt to explain, first, the successful treatment of fiber. After that, the discussion of the effect of fiber surface treatment on the mechanical properties of composites will be presented.

The surface of untreated PALF is not an exact cellulose structure, which can be observed from XPS analysis on O/C ratio. O/C ratio of UPALF is 0.30, while cellulose is 0.83. A similar result was reported by Tran [129] that the O/C ratio of untreated coir fiber is 0.29. It is suggested that the surface of fiber might be covered by lignin, which O/C ratio is around 0.30 – 0.36 [129]. Lignin is a binding substance between cell fibers and vessel, thus, it can be used to partially reinforce the fiber. The mechanical properties of fibers decrease by delignification [129], [134]. Thus, it is not mandatory to remove lignin from the fiber for reinforcing composite. However, no π-π^* satellite signal of aromatic rings of lignin is observed. Thus, the chemical structure of the surface of PALF is still unclarified.

It is clearly observed that alkali treatment can be used to remove hemicellulose. With the appropriate condition i e. NaOH concentration or soaking time, hemicellulose can be removed without damaging fibers [92]. The atomic compositions of fibers with alkali treatment are not significantly modified from untreated fibers. This is due to the structure of hemicellulose, which is almost similar to cellulose, except for the different sugar units and the degree of polymerization is lower than cellulose (100 times) [132]. Weight loss after alkali treatment is 25-30 %, thus, the volume fraction of the fibers is higher when incorporate the same weight of fibers into composites. The surface of fibers is cleaned and seems to be smoother after the treatment, which can be further used for another specific treatment.

Silane was grafted on the surface of alkali-treated fibers using both washing and non-washing methods. Silane treatment using washing method provides a thin layer of silane on the surface, which cannot be observed by SEM. The similar result was reported by Zhou and coworkers that sisal fibers were treated by silane [135]. The appearance of sulfur and silane signals and the increasing of O/C ratio by XPS analysis indicate the successful silane-69 treatment. Huda reported the similar result of the

increasing of O/C ratio after silane treatment on poultry feather [136]. It was suggested that the increasing of oxygen atoms refers to high hydroxyl group content, which was grafted silane on the surface of fiber. The relative amount of silane to fiber, which is calculated from XPS analysis, is equal to 3.8% by atomic content. The difference after silane treatment with non-washing method still cannot be detected by FTIR and observed by SEM. The appearance of sulfur and silane signals in wide scan XPS spectrum indicates the successful treatment with high silane amount on the surface. O/C ratio is closed to silane-69. The relative amount of silane is higher than washing method, which is 47.4% by atomic content.

These fibers were used to reinforce rubber. The improvement of mechanical properties of composites with different fiber surface treatment will be explained. Type of silane, silane concentration and solvent effects using silane washing method on the mechanical properties of composites will be first presented. Then, the effect of an additional step of washing will be discussed.

Alkali treatment improves curing behavior of composites in term of M_H. The rise of M_H of NR/isora fiber composite by alkali treatment was also reported by Matthew and coworkers [80]. In addition, alkali treatment has the efficient reinforcing effect to improve tensile properties of composites in the low strain region. This is due to higher volume fraction of cellulose after treatment and higher mechanical interaction between rubber and fiber. Weight loss after alkali treatment is 25-30 %, thus, the volume fraction of fibers in composites is higher. Moreover, it was reported that polymer can penetrate into bundles of fibers, which results in a better mechanical interlocking between matrix and fiber [95,97,137].

The effect of silane containing propyl as functional group is first discussed. The treatment is expected to decrease the different of surface energies between fibers and rubber. pSiPALF causes slightly decrease of M_H on curing behavior of composite, whereas it does not modify the mechanical properties of composites. The similar result was reported by Abdelmouleh and co-workers [138]. The authors treated hexadecyltrimethoxysilane (HDS) on natural fibers and then incorporated into NR matrix, however, no evolution of E´ is observed. It is suggested that the improvement of hydrophobicity of fiber is not enough to affect the mechanical properties of composites.

Chough reported that the vulcanization of rubber occurred between the allylic hydrogen atoms of rubber chains [139]. Allyl group on fiber after treatment represents a reactive site for coupling with polymer between allylic hydrogen atoms of NR and fiber. There is no report on the use of allyl silane in NR containing fibers or silica. Allyl silane treatment still does not modify the curing behavior or mechanical properties of composites. It is suggested that the crosslinking reaction between allyl-silane-treated fiber and NR might not occur, as the result is similar to propyl silane treatment. Thus, only the reduction of surface energies between fiber and NR might be not high enough to affect the composites.

Only silane-69 treatment can be used to enhance the mechanical properties of composites. Silane-69 is not only used to reduce the polarity of filler, it also provides free sulfur, which can co-crosslink with rubber [107]. Hence, the enhancement of stress transfer can be achieved by this covalent bonds between them. In a previous work, silane-69 can be directly incorporated during mixing with silica [110]. By the way, the surface area of short macro fiber is lower than silica. Thus, the surface treatment of fiber has been used to optimize the mechanical properties of composites. Loppattanon et al. reported that the silane-69 treatments of silica and cellulose improved E_{100} by 8% of hybrid NR composites [115]. However, no yield point was observed on their composites due to its low uniaxial stress-strain response. Their fibers are in the length of 120 μm and diameter of 20 μm, whereas PALFs in our research are in the length of 6 mm and diameter of elementary fiber of 3 μm (the bundle diameter is 18 μm). E_{10} and σ_y of composites are significantly improved by 21% and 8% respectively using silane-69 treatment. The mechanical properties of composites can be improved due to better stress transfer between rubber and filler. Thus, silane-69 was chosen to optimize the mechanical properties of composites. Next, the effect of silane-69 concentration will be discussed.

The appropriate amount of silane on the surface of fiber was studied by varying amount of silane during treatment from 0 to 10 wt% of fiber. Small amounts of silane at 0.1 and 1 wt% of fibers do not modify the mechanical properties of composites. This is due to low chemical crosslinking between fiber and rubber because the amount of silane is not high enough. When the silane concentrations reach 3 and 10 wt%, mechanical properties at low strain region are significantly increased to the same value.

The co-crosslinking between rubber and fiber can occur, leading to the enhancement of mechanical properties. It was reported that the first mono layer of silane has a strong chemical interaction with substrate [140]. The next layers near the interface are adsorbed layers. The outer layers are loosely bound with other layers, which are able to be removed by solvent extraction. Thus, it is suggested that the excessive amounts of silane at the outer layers are removed when using high concentration. Surprisingly, 5 wt% of silane treatment does not increased the properties of composites, as expect to be in the same level of 3wt% or 10 wt%. Silane treatment using silane 5 wt% had been reproduced several times, however, no improvement in mechanical properties was observed. This might be due to a solvent influence on the treatment. Thus, the solvent effect on silane treatment will be further discussed.

The solvent effect on silane-69 treatment using 3 wt%, which enhances the mechanical properties, and 5 wt%, which reproduces to understand the unexpected properties of composites, are investigated. Ethanol/water with a ratio of 80/20 v/v and pure ethanol are investigated. Using ethanol as a solvent for silane 3 wt% treatment causes the similar mechanical properties as using mixed solvent. E_{10} and σ_y of composites using 5 wt% silane treatment are increased by using pure ethanol as a pure solvent. These values are consistent with the previous study on the silane concentration, which the amount of silane is excess at 3 wt% of treatment. Thus, pure ethanol represents an effective solvent to treat the fibers as a lower standard deviation on mechanical properties results is observed. Now, it can be summarized that the appropriate condition is using silane-69 for 3 wt% of fiber and pure ethanol as a solvent for the treatment. Next, the effect of different termination methods of treatment will be explained.

The termination method of treatment also affected curing behaviors and mechanical properties of composites. Washing and non-washing methods were studied. From the result of XPS analysis, the relative atoms of silane molecule on the washing method is 3.8% and non-washing method is 47.4% by atomic content. Using non-washing method causes shorter cure time than washing method due to a large amount of silane, which has more active sites to react with rubber. Non-washing method causes the reversion process due to the excess sulfur from silane, which polysulfidic bonds can be broken [118]. Non-washing treatment causes higher mechanical

properties at low strain region, however, ultimate properties are significantly decreased. It can be explained that a high amount of silane can crosslink with rubber, however, polysulfidic bonds might be broken into mono- or di- sulfidic bonds. These shorten sulfidic bonds enhance the stiffness of composites, however, they can reduce the ultimate properties.

5.2.7 Summary

Alkali treatment can be used as a pretreatment on fiber and silane is successfully treated on alkali-treated fiber. The mechanical properties of NR/PALF are improved by silane treatment. Silane-69 treatment enhances the interfacial stress between rubber and fiber by chemical crosslinking between them. The optimum condition is using silane-69 for treatment at concentration of 3 wt% of PALF using washing method. Pure ethanol is used as a solvent. This treatment condition will be further used to study the effect of silane treatment on NR/PALF/carbon black hybrid composites.

5.3 Comparison between the effect of NBR and silane treatment on the mechanical properties of NR/PALF composites

The reinforcing effects of the incorporation of NBR into NR/PALF composites and the incorporation of surface-treated PALF are compared. Composites with highest mechanical properties, which were studied in the previous parts, are chosen to compare with each other. 15NBR content corresponds to the highest improvement of tensile properties for the incorporation of NBR in the composite. No treatment of the fibers is performed. The properties of these composites are compared to those containing alkali-treated PALF (APALF) and silane-treated PALF (3sSiPALF-alc). Tensile results of NR (with untreated PALF), 15NBR (with untreated PALF), APALF and sSiPALF composites are shown in Figure 5.40. It should be noted that NR/PALF prepared by two-step mixing is similar to single-step mixing. Both incorporation of NBR and surface treatment of PALF lead to the increase of the initial modulus at low strain region and also to the stress at yield point. This result shows the successful improvement of the stress transfer between matrix and PALF.

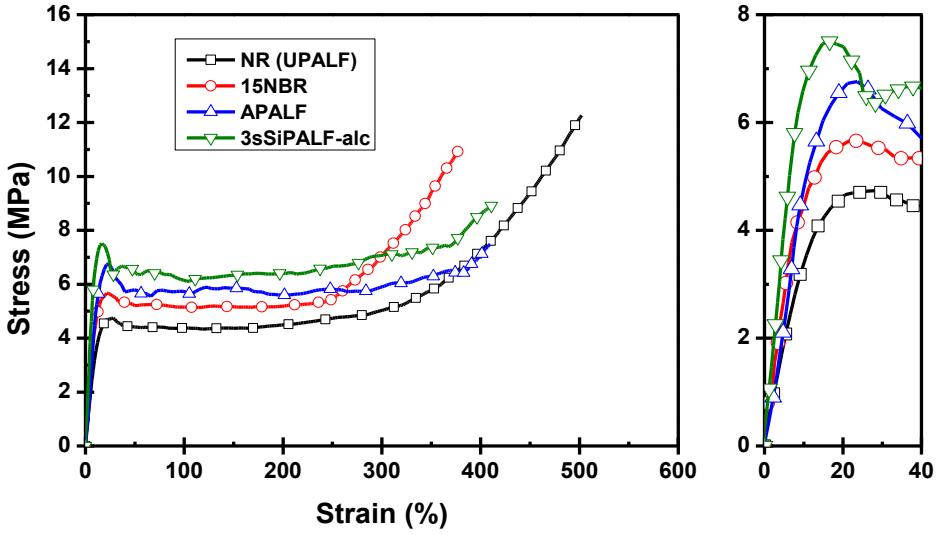

Figure 5.40 Stress-strain curves of NR, 15NBR, APALF and 3sSiPALF-alc composites. UPALF was incorporated into NR and 15 NBR. All composites contain PALF 10 phr.

Tensile characteristics of these composites are shown in Figure 5.41. By silane treatment of PALF, the improvement of E_{10} is about 80% higher than UPALF, whereas APALF does 45% of the improvement. The incorporation of NBR improves E_{10} by about 30%. This improvement of E_{10} is similar to σ_y, which silane treatment causes highest σ_y. Thus, NR/silane-treated PALF composites show higher modulus and σ_y than that of NR/NBR/PALF composite. This important result indicates that the stress transfer between NR and PALF is more improved by chemical crosslinking between NR and Silane-69-treated PALF than by incorporation of NBR in the blend. Earlier upturn stress is obtained only by incorporation of NBR, whereas surface treatment causes no upturn stress of composites. NBR encases the fiber, leading to the enhancement of stress transfer and high deformation by friction and physical interaction at the interface between matrix NR and NBR covering the fibers.

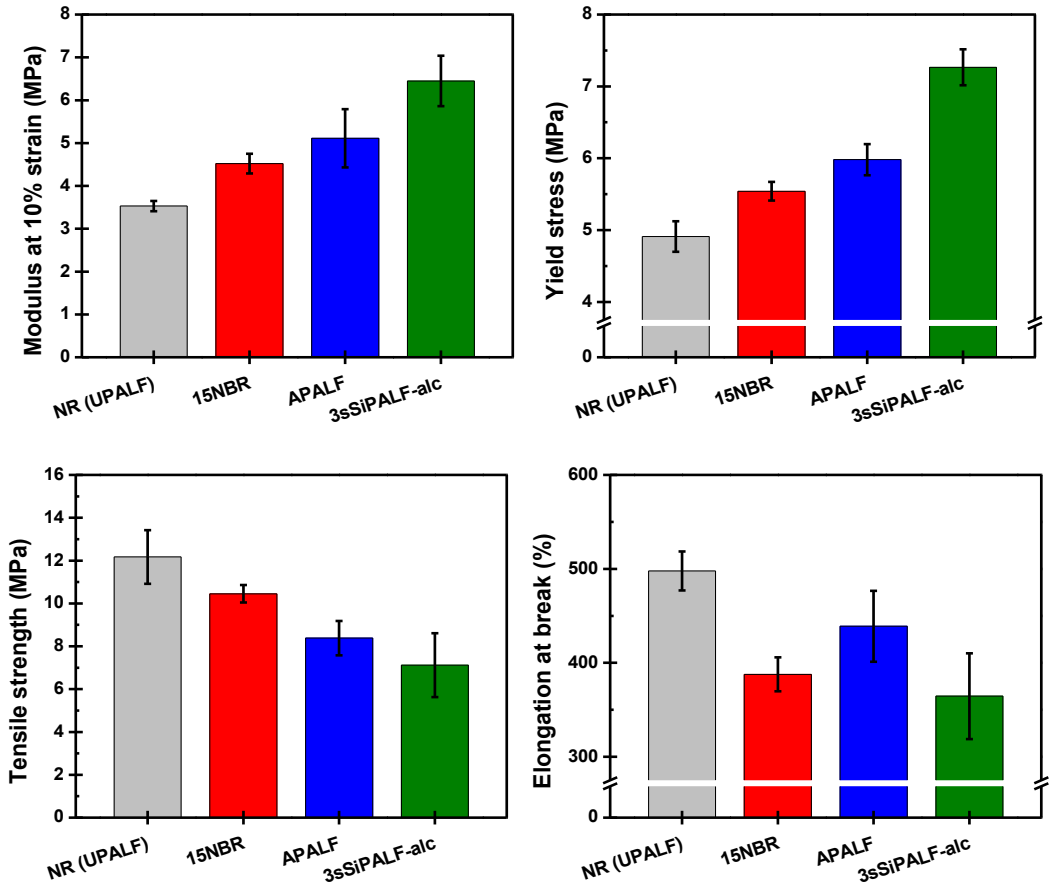

Figure 5.41 Tensile properties of NR, 15NBR, APALF and sSiPALF-alc composites

However, in all composites, the ultimate properties, *e.g.* tensile strength and elongation at break, decrease by both incorporation of NBR and fiber surface treatment. Hence, in the next sections, the incorporation of carbon black combining either NBR or surface-treated PALF in order to improve mechanical properties at high deformation will be further studied.

5.4 Effect of NBR on NR/PALF/carbon black hybrid composites

From the previous results, tensile properties at low strain region of NR/PALF composites were successfully improved by incorporation of NBR. However, the ultimate properties such as tensile strength and elongation at break of the composites were still lower. In order to improve tensile properties at high deformation, carbon black was further incorporated into NR/NBR/PALF composites. Thus, tensile properties of

NR/PALF could be improved at both low and high strain regions. The effects of filler, carbon black, NBR contents have been investigated. The proper sequence of mixing was also studied to optimize the properties of the composites. Composites were named as *x*NBR*y*UP*z*CB, where UP is untreated PALF, *x* is NBR content, *y* is PALF content and *z* is carbon black content. Composites without NBR were named as NR*y*UP*z*CB.

5.4.1 Filler effect

Shape of fillers can affect the properties of composites [141]. Thus, the effect of fillers on the properties of NR and 20NBR was first studied. PALF, carbon black and hybrid PALF/carbon black were chosen as the fillers. The effect of NBR on the properties of NR with different fillers has been investigated. In this study, PALF and carbon black were fixed at 10 and 30 phr, respectively. First, NR/carbon black masterbatch was dispersed in NR. Amount of NBR was added in this step. After rubbers and masterbatch of NR and carbon black were mixed homogenously, PALF was incorporated into the mixture, followed by curing additives. Cure characteristics were first studied to understand the curing behaviors. Then, T_ds of rubbers with fillers were determined using DMTA. Tensile properties of composites were measured and used to study the role of fillers and also effect of NBR in composites.

5.4.1.1 Cure characteristics

Cure characteristics of NR and NR/NBR blend with the weight ratio of 80:20 (20NBR) were first studied. Rheographs of NR and 20NBR with different types of fillers are shown in Figure 5.42 and their numerical values of cure characteristics are reported in Table 5.14. The incorporation of NBR in NR change only slightly the cure behavior of NR. When fillers are added, the effect becomes more drastic on both vulcanization kinetics and cure characteristics. Moreover, incorporation of hybrid fillers leads to reversion process whereas the incorporation of carbon black or PALF leads to an equilibrium process.

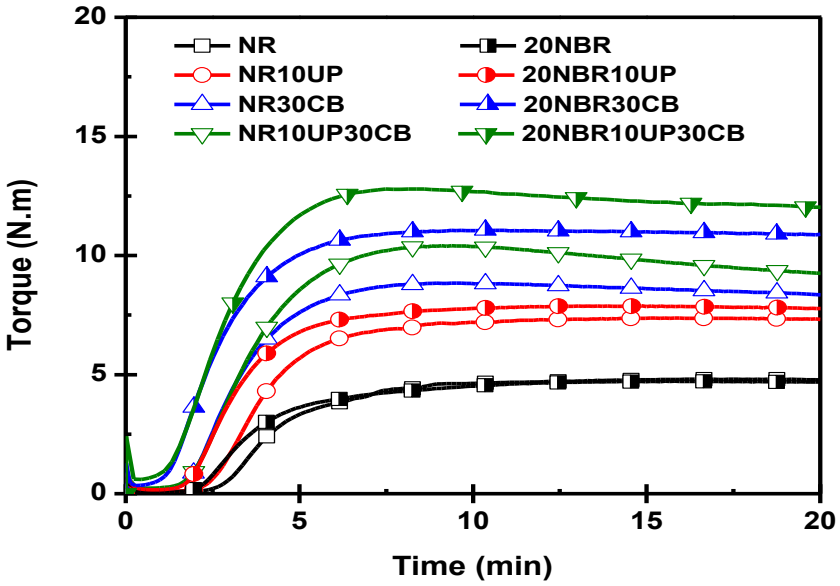

Figure 5.42 Cure curves of unfilled rubbers, composites with PALF, carbon black and PALF/carbon black. Open symbols represent NR and half-open symbols represent 20NBR as matrices

Table 5.14 Cure characteristics of unfilled rubbers, composites with PALF, carbon black and PALF/carbon black

	M_L	M_H	t_{s2} (min)	t_{c90} (min)
NR	0.1	4.8	3.9	7.4
NR10UP	0.1	7.4	3.2	6.5
NR30CB	0.1	8.8	2.4	5.5
NR10UP30CB	0.2	10.4	2.4	5.8
20NBR	0.1	4.7	3.3	7.6
20NBR10UP	0.2	7.9	2.4	5.6
20NBR30CB	0.4	10.7	1.7	5.0
20NBR10UP30CB	0.6	12.8	1.7	5.4

The presence of NBR in the compounds affects the cure characteristics. M_H, M_L and t_{c90} remain roughly unchanged for unfilled blend while t_{s2} slightly decreases. The effect depends on the type of fillers. NBR causes a higher increase in M_L and M_H for carbon black filled compound than PALF filled compound. NBR also causes the reduction in both t_{s2} and t_{c90} for carbon black filled and PALF filled compounds. The incorporation of NBR in NR/PALF/carbon black hybrid compound further increases both M_H and M_L, reduces t_{s2} while it does not affect t_{c90}.

5.4.1.2 Dynamic mechanical thermal analysis

In order to understand the effect of filler on composites and also their distributions in the immiscible NR/NBR blend, dynamic mechanical-thermal analysis (DMTA) of composites was carried out. Graphs of elastic modulus (E´) and tan δ vs temperature are illustrated in Figure 5.43 and their numerical values at specific temperatures are shown in Table 5.15. At low temperature, $T < T_g$, composites are in the glassy state. As the temperature increases, E´ of all materials sharply drop at approximately -60 °C which in the glass transition behavior of NR. The drop of E´ at this temperature depends on the filler. The curves of E´ and tan δ of unfilled rubbers (NR and 20NBR) after T_g of NBR are not smooth due to the slippage of rubbers during testing. For composites containing NBR, the shoulder at the temperature around -20 °C is observed. Unfilled rubbers have the lowest E´ when the temperature is higher than T_g, whereas rubbers containing hybrid PALF/carbon black fillers have the highest E´. Incorporation of PALF increases E´ more than carbon black does. E´ of PALF-filled NR increases from 2.04 to 19.8 MPa, whereas carbon black is 8.97 MPa. T_d can be observed from tan δ against temperature. The peak position of the tan δ does not greatly depend on the fillers. The intensity of tan δ is mainly affected by fillers. By incorporation of fillers, tan δ decreases corresponding to the sharp drop of E´. The intensities of T_d of rubbers containing hybrid fillers are the lowest, whereas those of unfilled rubbers are the highest. PALF causes a higher decrease in tan δ than does carbon black.

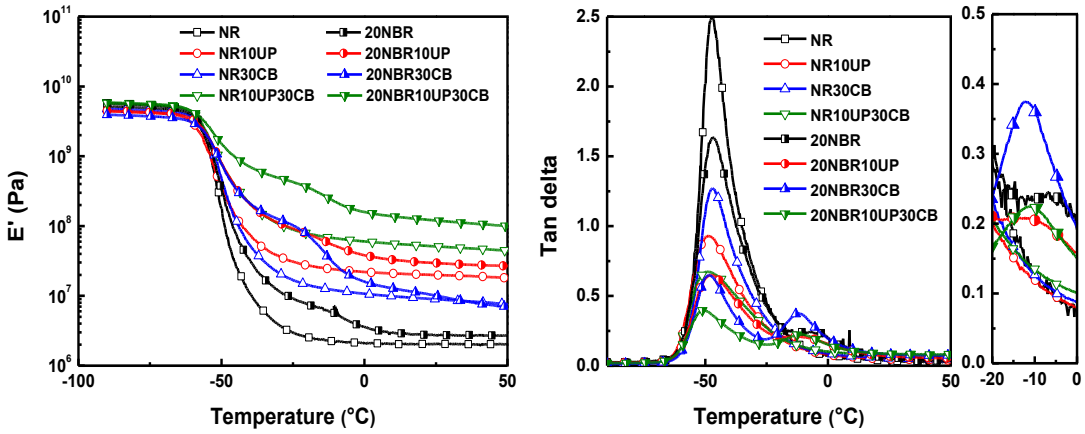

Figure 5.43 Temperature dependences of Elastic modulus (E´) and tan delta of unfilled rubbers, composites with PALF, carbon black and PALF/carbon black

Table 5.15 Viscoelastic properties of unfilled rubber, composites with PALF, carbon black and PALF/carbon black

	E´ at 25 °C (MPa)	Tan δ_{NR}		Tan δ_{NBR}	
		Magnitude	T (°C)	Magnitude	T (°C)
NR	2.0	2.5	-47	-	-
NR10UP	19.8	0.9	-48	-	-
NR30CB	9.0	1.3	-47	-	-
NR10UP30CB	51.0	0.7	-48	-	-
20NBR	2.7	1.7	-49	0.2	-11
20NBR10UP	29.4	0.7	-48	0.2	-11
20NBR30CB	10.1	0.7	-48	0.4	-11
20NBR10UP30CB	120.8	0.4	-50	0.2	-11

The incorporation of NBR has affected E´ and tan δ of composites. The second drop of E´ is observed when the temperature reaches around -10 °C, which corresponds to the dynamic transition temperature of NBR. E´ at room temperature of those rubbers containing NBR is higher than NR for all types of filler. The increasing of E´ by NBR is significantly increased in PALF-filled composite

by about 50% and PALF/carbon black-filled composites by 140%. The magnitude of tan δ relates with the amount of filler in the corresponding matrix phase. Thus filler distribution in each phase of immiscible rubber blends can be deduced. Two tan δ peaks are observed corresponding to the T_gs of NR and NBR at around -44°C and -10°C, respectively. Tan δ_{NR} magnitudes of composites significantly decrease with the addition of either carbon black or PALF and further decrease to the lowest value when both carbon black and PALF with NBR are incorporated. The magnitude of tan δ_{NBR} of 20NBR30CB is higher than other samples. By the way, the incorporation of carbon black into NR/NBR/PALF composites does not modify this value. This indicates that in presence of fibers, the effect of carbon black in NBR is neglectable. Moreover, once carbon black is incorporated into NR, the migration is rarely occurring [42]. Thus, by mixing scheme A, carbon black is mainly distributed in NR phase. This phenomenon will be confirmed in section 5.4.2.2.

5.4.1.3 Mechanical properties

The effect of fillers on tensile properties was studied. Stress-strain curves of NR and 20NBR with different types of fillers are displayed in Figure 5.44. It should be noted that NBR has a secondary effect on the stress-strain behavior. Unfilled rubbers and carbon black-filled rubbers exhibit low modulus at low strain region, while PALF-filled rubbers and hybrid-filled rubbers exhibit greater resistance to the applied strain and moduli are much higher. Those composites exhibit yield-like behavior, then the stress slightly decreases and remains roughly on a constant level. At high strain region, unfilled rubbers and carbon black-filled rubbers exhibited greater slope, while PALF-filled composites exhibited lower slope. It can be summarized that PALF increases modulus at low deformation, whereas carbon black increases stress at high deformation. In hybrid composites in which both PALF and carbon black are present, the applied stress over the whole strain region increased.

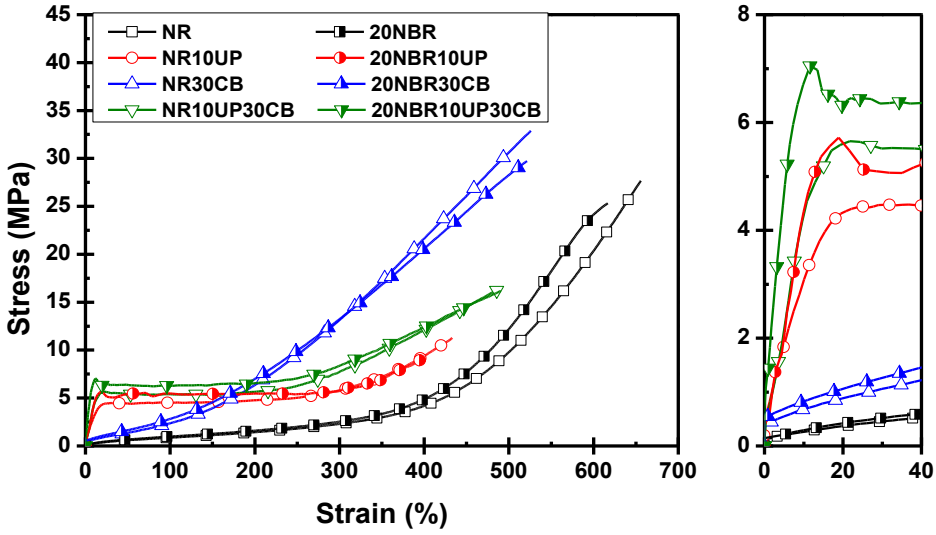

Figure 5.44 Stress-strain curves of unfilled rubbers, composites with PALF, carbon black and PALF/carbon black. Open symbols represent NR and half-open symbols represent 20NBR as matrices

Average values of tensile characteristics are shown in Figure 5.45 and Figure 5.46. Effect of NBR can be clearly seen by considering these graphs. The effects are more pronounced in E_{10} and σ_y. E_{300}, onset upturn strain, tensile strength and elongation at break are not much affected.

The effect of replacing parts of NR with NBR on E_{10} and σ_y will now be considered. For unfilled and carbon black-filled NR, NBR causes no change in these values. For PALF-filled composites, E_{10} and σ_y of NR composites significantly increase by replacing some parts of NR with NBR. E_{10} of PALF-filled increased 25%, whereas σ_y increases by 10%. The improvement is higher for hybrid-filled composites, as E_{10} increases by 35%, whereas σ_y increases by 25%.

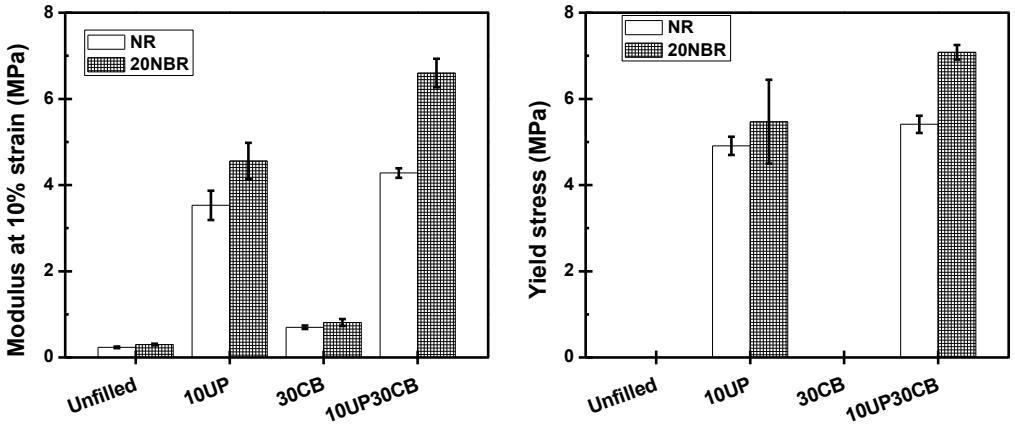

Figure 5.45 E_{10} and σ_y of unfilled rubbers, composites with PALF, carbon black and PALF/carbon black

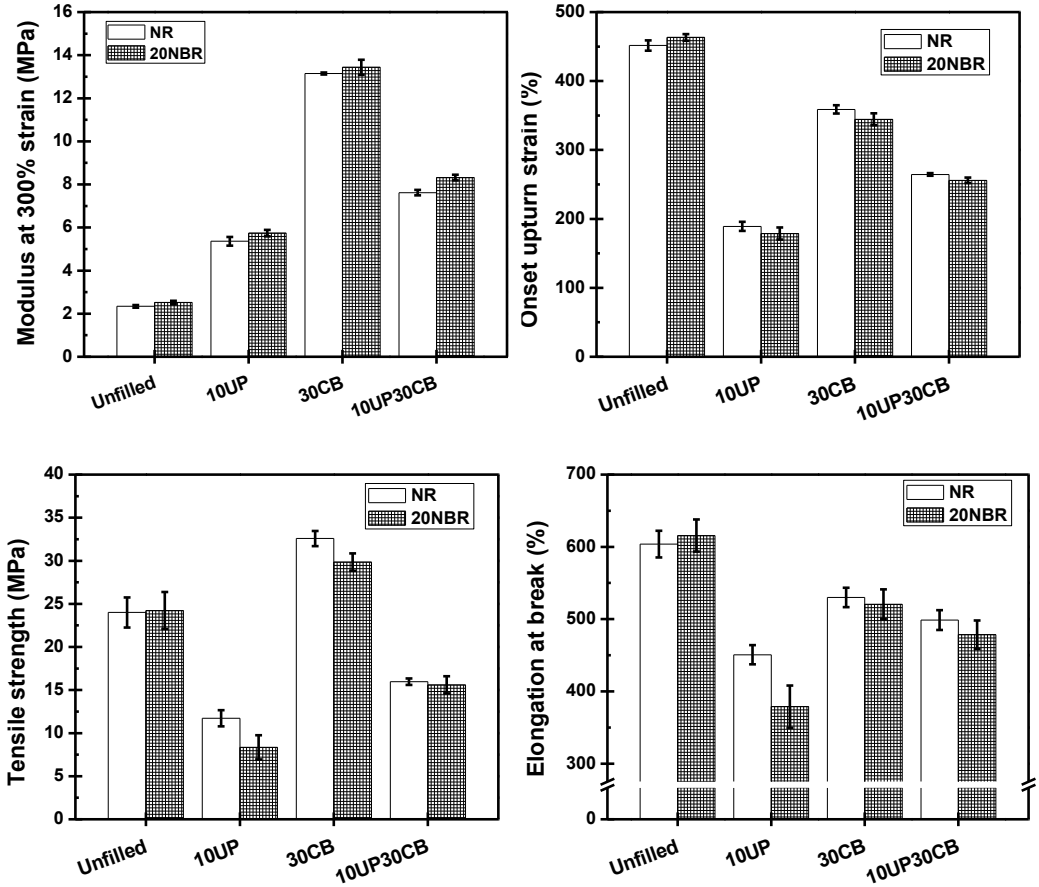

Figure 5.46 E_{300}, onset upturn strain, tensile strength and elongation at break of unfilled rubbers, composites with PALF, carbon black and PALF/carbon black

It is clear that tensile properties of NR can be improved by the incorporation of PALF and carbon black. PALF improves tensile properties at low deformation, while carbon black improves tensile properties at very high deformation. The incorporation of NBR improves tensile properties of PALF-filled and hybrid-filled composites at low strain due to the better stress transfer, which was discussed in the previous section 5.1. The magnitude of tensile properties improvement i e. E_{10} and σ_y of hybrid-filled composite is higher than PALF-filled composite. To understand the role of carbon black and NBR in more details, we will attempt to study the effects of carbon black content and also NBR content based on NR/PALF composites.

5.4.2 Effect of carbon black content

Carbon black has been generally used to reinforce rubbers due to strong interactions between them [48,142-143]. In last decade, carbon black has been also used as a hybrid filler with fibers to reinforce rubber at both low and high deformation regions [117,118]. The effect of carbon black content of NR/PALF and NR/NBR/PALF composites on cure characteristics was studied. Carbon black contents were varied at 0, 10, 20, 30 phr, while PALF content was fixed at 10 phr. After that, the distribution of carbon black in the blends containing PALF was investigated. Finally, tensile properties were characterized to study the improvement of composites by the incorporation of carbon black.

5.4.2.1 Cure characteristics

The rheograms and cure characteristics of NR and 20NBR composites with different amounts of carbon black are illustrated in Figure 5.47 and Table 5.16. Carbon black content affects directly the cure characteristics of composites in term of reversion process and M_H. The reversion process occurs and is clearly seen when carbon black content increases.

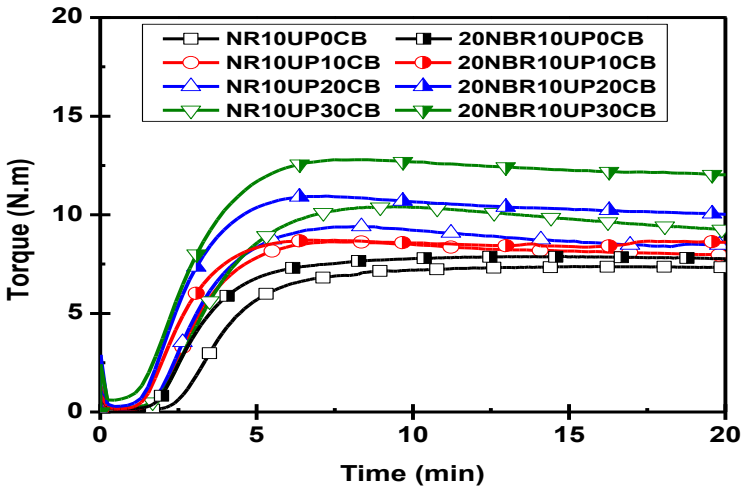

Figure 5.47 Cure curves of composites containing different amounts of carbon black. Open symbols represent composites without NBR and half-open symbols represent composites with NBR

t_{s2} and t_{c90} decrease by incorporation of carbon black by 30% and 23% respectively and do not depend on carbon black content. M_H increases by increasing the amount of carbon black.

Replacing part of NR with 20 wt% of NBR does not change the reversion process, while it reduces t_{s2} and t_{c90} comparing to NR composites with the same carbon black content. NBR does not significantly affect M_H of composites when carbon black content is low (0 and 10 phr), whereas it increases M_H when carbon black is incorporated at 20 and 30 phr. The difference between M_H of composites containing NBR is higher when carbon black content increases, which increases by 15% for carbon black 20 phr and 20% for carbon black 30 phr. The improvement of M_H by carbon black and NBR in NR/PALF composites indicates the combined reinforcing effects of carbon black and NBR.

Table 5.16 Cure characteristics of NR and 20NBR composites containing different amounts of carbon black

Composites		M_L	M_H	t_{s2} **(min)**	t_{c90} **(min)**
NR	0CB	0.1	7.4	3.2	6.5
20NBR		0.2	7.9	2.4	5.6
NR	10CB	0.1	8.6	2.3	5.0
20NBR		0.2	8.7	1.9	4.3
NR	20CB	0.2	9.4	2.3	5.1
20NBR		0.3	11.0	1.8	4.5
NR	30CB	0.2	10.4	2.4	5.8
20NBR		0.6	12.8	1.7	5.4

5.4.2.2 Dynamic mechanical thermal analysis

To understand the role of carbon black on the enhancement of modulus in NR/PALF and NR/NBR/PALF composites and its distribution in immiscible rubber blends, DMTA was carried out. The temperature dependence of E´ is shown in Figure 5.48. From the plotted between E´ vs carbon black content in Figure 5.48, E´ of NR composites increases linearly when carbon black content increases up to 20 phr and remains the same when carbon black is incorporated to 30 phr. When NBR is incorporated, the linear relationship between E´ vs carbon black content is observed. E´ at room temperature of those NR composites increases up to 180% by increasing carbon black content up to 20 phr, whereas E´ at room temperature of 20NBR composites further increases up to 310% by incorporation of carbon black 30 phr. Thus, E´ of composites containing NBR is higher than those composites without NBR and the difference of E´ is higher when carbon black content increases.

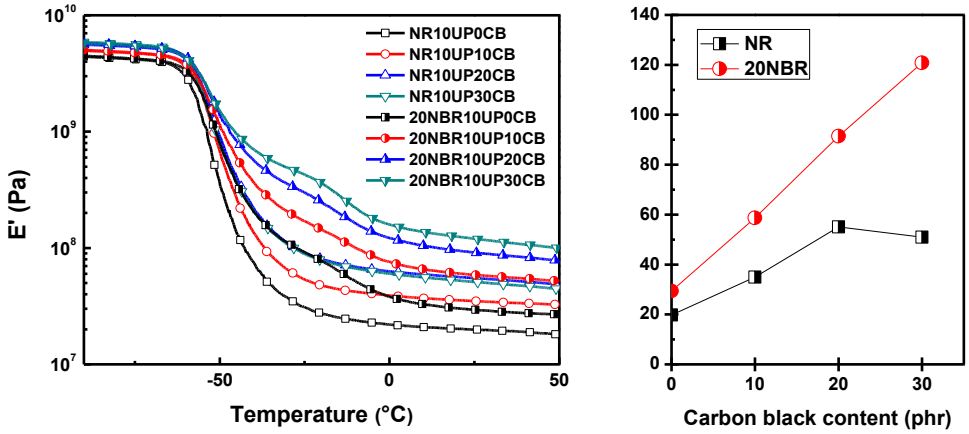

Figure 5.48 Temperature dependences of elastic modulus (E´) of NR/PALF and NR/NBR/PALF composites containing different amounts of carbon black

E´ at room temperature of composites without carbon black increases 50% by incorporation of NBR, whereas E´ composites with carbon black 30 phr increases 140%. The enhancement of E´ is consistent with the increasing of M_H, thus, it indicates the combined reinforcement effects of carbon black and NBR in NR/PALF composites.

T_ds are more clearly seen in the tan delta curves, displayed in Figure 5.49. T_ds are not shifted by incorporation of carbon black. The intensity of T_d of NR, which is observed at lower temperature, decreases about 40% by increasing carbon black content to 20 phr. This T_d does not further decrease by adding 30 phr of carbon black. Unlike NR/PALF composites, T_d of NR decreases continuously 60% by incorporation of carbon black up to 30 phr in NR/NBR/PALF composites. The unchanged T_d of NBR when carbon black content increases in the composites indicates that carbon black was incorporated mainly in NR phase.

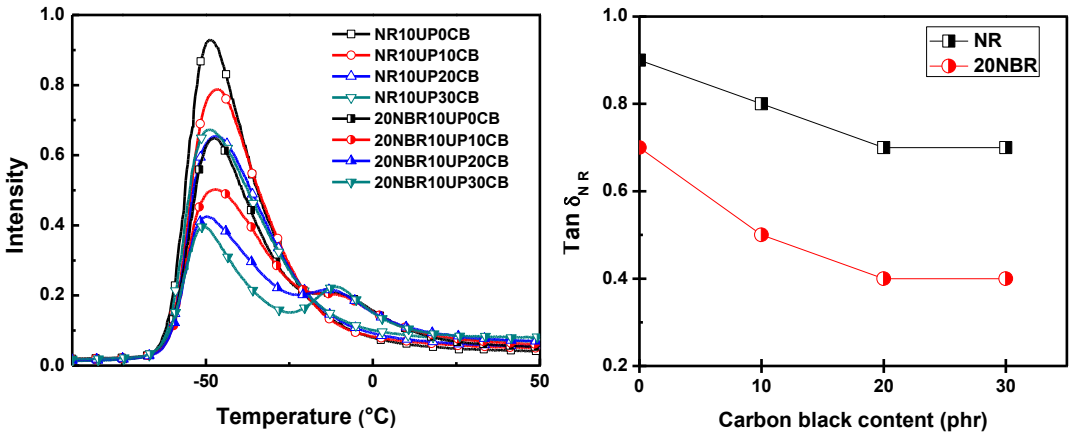

Figure 5.49 Temperature dependences of tan delta of NR/PALF and NR/NBR/PALF composites containing different amounts of carbon black

5.4.2.3 Mechanical properties

The effect of carbon black on tensile properties of the same samples was studied. Stress-strain curves of composites without NBR are displayed in Figure 5.50, while those composites with NBR are displayed in Figure 5.51. It can be seen that the curves are rough when carbon black is incorporated at 10 and 20 phr in NR composites and clearly seen in 20NBR composites. This might be due to the low reinforcing effect of carbon black.

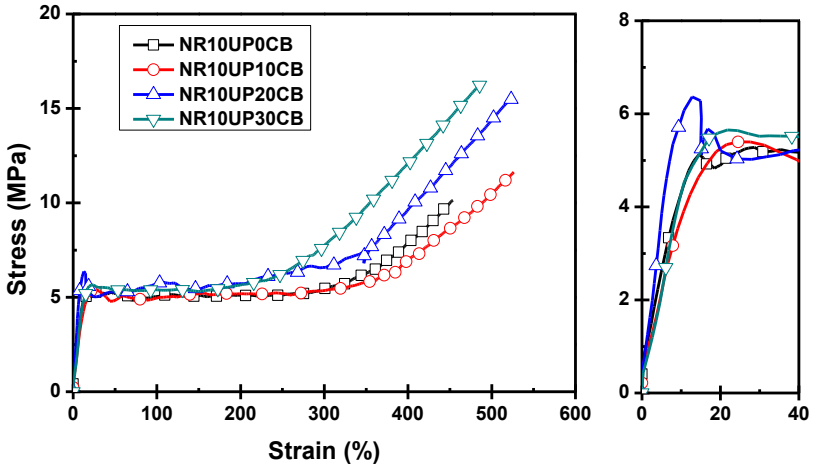

Figure 5.50 Stress-strain curves of NR/PALF composites containing different amounts of carbon black

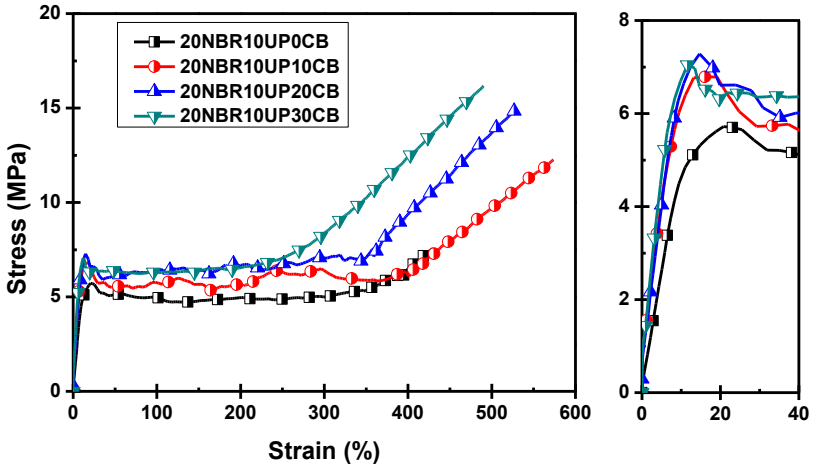

Figure 5.51 Stress-strain curves of NR/NBR/PALF composites containing different amounts of carbon black

E_{10} and σ_y are shown in Figure 5.52. Carbon black does not increase E_{10} and σ_y of composites without NBR, except for composite containing carbon black 20 phr. Higher values of E_{10} and σ_y can be achieved in composites with NBR. E_{10} increases from 4.8 to 6.3 MPa and σ_y increases from 5.5 to 7.0 MPa by incorporation of 10 phr of carbon black. These values do not further increase by increasing carbon black content.

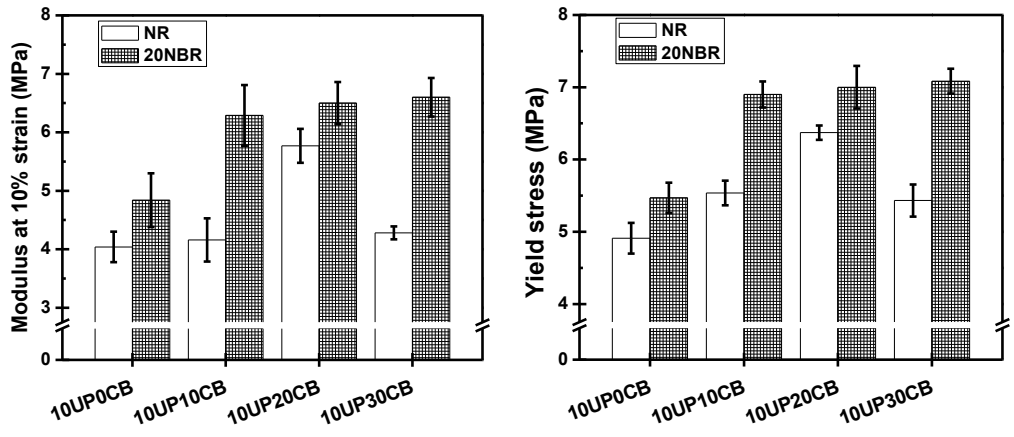

Figure 5.52 E_{10} and σ_y of NR/PALF and 20NBR/PALF composites containing different amounts of carbon black

The reinforcement of NR/PALF composites by carbon black is clearly seen at high deformation region. Onset upturn strain, E_{300}, tensile strength and elongation at break are displayed in Figure 5.53. Onset upturn strain decreases from 350 to 250 % strain by increasing carbon black content up to 30 phr. E_{300} and tensile strength increase too. By the way, the incorporation of NBR into the hybrid composites does not significantly improve tensile properties at high deformation. Onset upturn strain and elongation at break are similar to composites without NBR, whereas E_{300} slightly increases. It can be seen that the decreasing of tensile strength by the incorporation of NBR into NR/PALF composites can be solved by carbon black, which improves tensile strength to reach the same value as composites without NBR for all carbon black content.

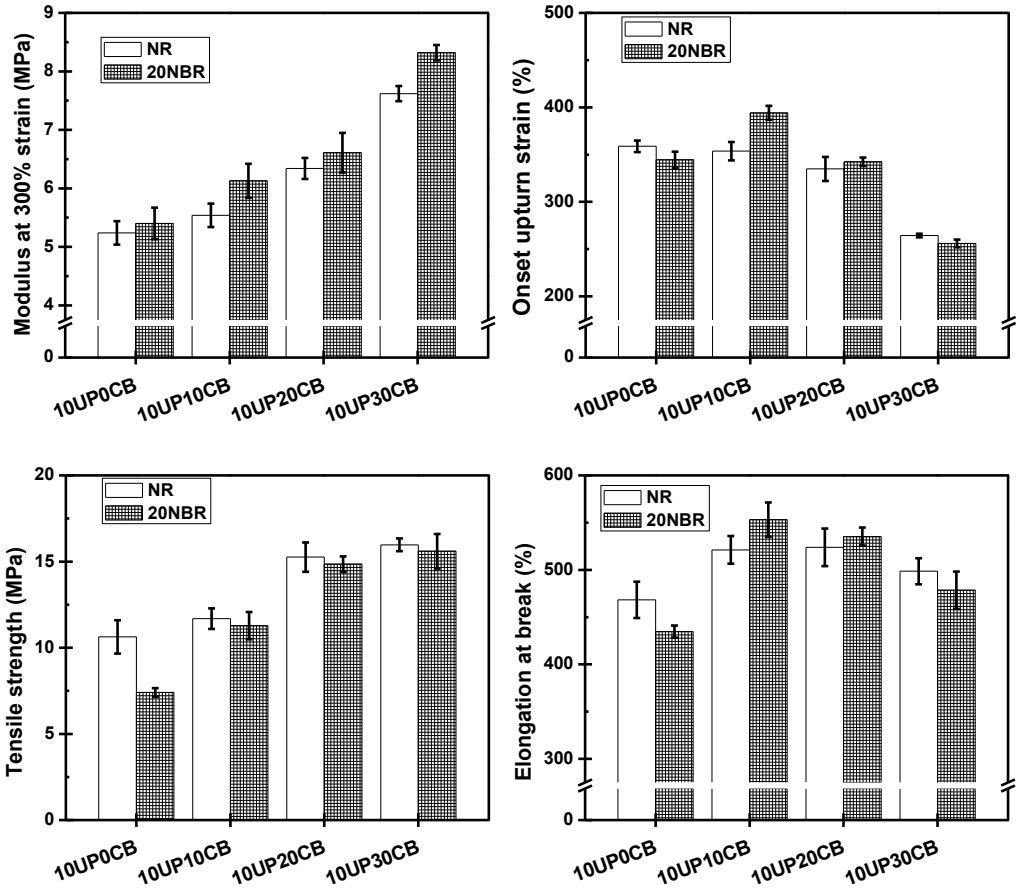

Figure 5.53 E_{300}, onset upturn strain, tensile strength and elongation at break of NR/PALF and 20NBR/PALF composites containing different amounts of carbon black

The incorporation of carbon black improves tensile properties of composites, especially at high deformation region. These properties could further enhance NR/PALF composites in presence of NBR. As a result of the distribution of carbon black in mainly NR phase (From DMTA result in section 5.4.2.2), NBR can be used to enhance the stress transfer between carbon black-filled matrix and PALF, which leads to higher E_{10} and σ_y. Thus, the effects of rigidity of NR by carbon black and the enhancement of stress transfer between NR and PALF by NBR lead to the improvement of tensile properties of composite. Next, the effect of NBR content will be further studied to understand the role of NBR on hybrid composites.

5.4.3 Effect of NBR content

The results of the incorporation of NBR into NR/PALF composites from a previous part (5.1) show that NBR can be used to improve the stress transfer between NR matrix and PALF. In this study, the effect of NBR on the NR/PALF/carbon black hybrid composites was investigated. The amounts of NBR were varied as 0, 5, 10, 15, 20 wt% of total amount of rubbers. The amount of carbon black and PALF were fixed at 30 phr and 10 phr respectively. The mixing scheme A was used, which NR, masterbatch of NR/carbon black and NBR were mixed together, then PALF were incorporated. Cure characteristics, dynamic thermal-mechanical analysis and tensile properties were investigated.

5.4.3.1 Cure characteristics

Rheographs of NR/PALF/carbon black with different amounts of NBR and their numerical values are shown in Figure 5.54 and Table 5.17 respectively. The reversion process occurs in all composites containing carbon black whatever the NBR content are superimpose. Torque after M_H of composites with NBR slightly decreases by increasing cure time to equilibrium. Replacing part of NR with NBR significantly increases M_H by about 30%. However, these values do not change by increasing NBR content. t_{s2} and t_{c90} of composites do not changed significantly for NBR content between 5 to 20 phr.

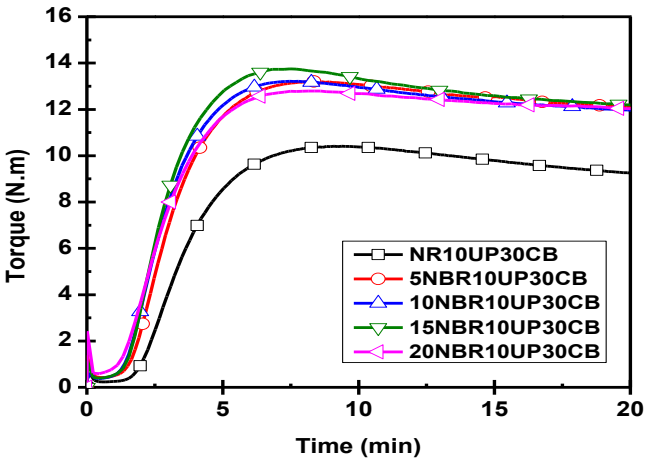

Figure 5.54 Cure curves of NR/PALF/carbon black hybrid composites containing NBR 0, 5, 10, 15 and 20 wt% of total rubber matrix

Table 5.17 Cure characteristics of NR/PALF/carbon black hybrid composites containing NBR 0, 5, 10, 15 and 20 wt% of total rubber matrix

	M_L	M_H	t_{s2} (min)	t_{c90} (min)
NR10UP30CB	0.2	10.4	2.4	5.8
5NBR10UP30CB	0.4	13.2	2.0	5.2
10NBR10UP30CB	0.4	13.2	1.8	5.5
15NBR10UP30CB	0.4	13.7	1.8	5.4
20NBR10UP30CB	0.6	12.8	1.7	5.6

5.4.3.2 Dynamic mechanical thermal analysis

The temperature dependence of E´ and tan delta of the composites is shown in Figure 5.55 and their numerical values are listed in Table 5.18. E´ of hybrid composites largely decreases after the temperature reaches to T_d of NR. The second large decrease of E´ is observed at T_d of NBR in the composites with NBR content at least 10 phr. This T_d of NBR is clearly observed in composite with NBR 20 phr. After this drop, E´ of composites remains roughly constant.

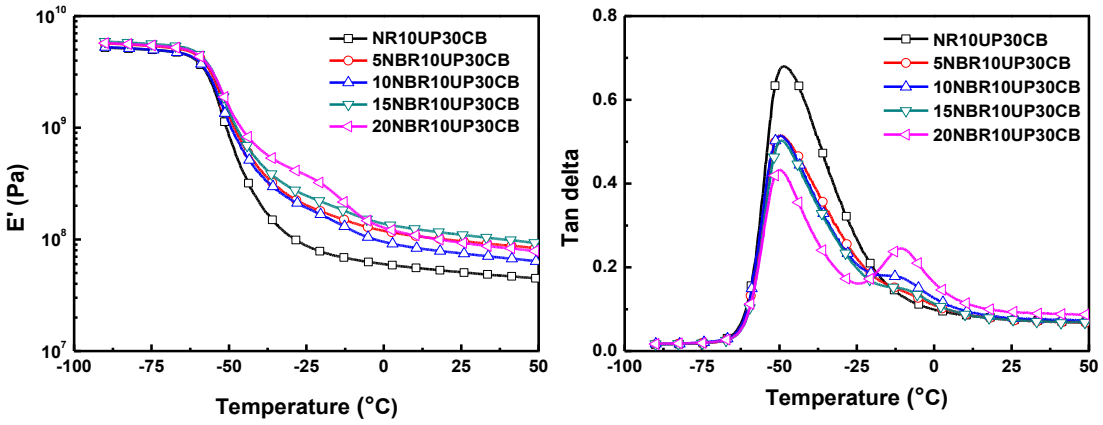

Figure 5.55 Temperature dependences of E´ and tan delta of NR/PALF/carbon black hybrid composites containing NBR 0, 5, 10, 15 and 20 wt% of total rubber matrix

E´ at room temperature increases by the increasing of NBR amount to 20 wt%, as can be seen in Figure 5.56.

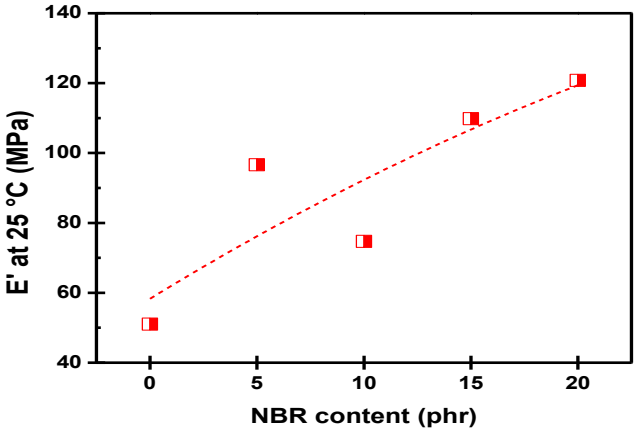

Figure 5.56 The relationship between E´ at room temperature versus NBR content in composites

To gain more insight into the T_d of rubbers, the relation between tan delta and temperature was investigated. Again, the incorporation of NBR does not change T_d of NR, but decreases the magnitude. This magnitude decreases from 0.68 to 0.5, which is not further decreased when NBR content increases up to 15 wt% of total rubber. Replacing part of NR by NBR 20 wt% results in the further decrease of this magnitude. T_d of NBR is observed when the amount of NBR is at least 10 wt%. This peak can be clearly seen when NBR 20 wt% is incorporated into composite.

Table 5.18 Viscoelastic properties of NR/PALF/carbon black hybrid composites containing NBR 0, 5, 10, 15 and 20 wt% of total rubber matrix

		Tan δ_{NR}		**Tan δ_{NBR}**	
		Magnitude	**T (°C)**	**Magnitude**	**T (°C)**
NR	10UP30CB	0.7	-48	-	-
5NBR		0.5	-48	-	-
10NBR		0.5	-49	0.2	-11
15NBR		0.5	-49	0.2	-11
20NBR		0.4	-50	0.2	-10

5.4.3.3 Mechanical properties

The effect of NBR content on tensile properties of NR/carbon black/PALF composites was investigated. The amount of NBR was varied at 0, 5, 10, 15, 20 wt% of total rubber content. Stress-strain curves of composites are displayed in Figure 5.57 and their numerical values i e, E_{10}, σ_y, E_{100}, E_{300}, onset upturn strain, tensile strength and elongation at break are reported in Figure 5.58. Modulus at low deformation increases by incorporation of NBR at least 5 wt% of total rubber. E_{10} improves from 4.3 MPa up to 6.5 MPa, whereas σ_y improves from 5 MPa to 7 MPa. By the way, the increasing of NBR content more than 5 wt% does not further improve these values. The deformation at moderate and high strains exhibits the same trend, in which E_{100} and E_{300} slightly increase by incorporation of NBR at 5 wt% but not further improve by increasing NBR content. Onset upturn strain, tensile strength and elongation at break are not affected by NBR content.

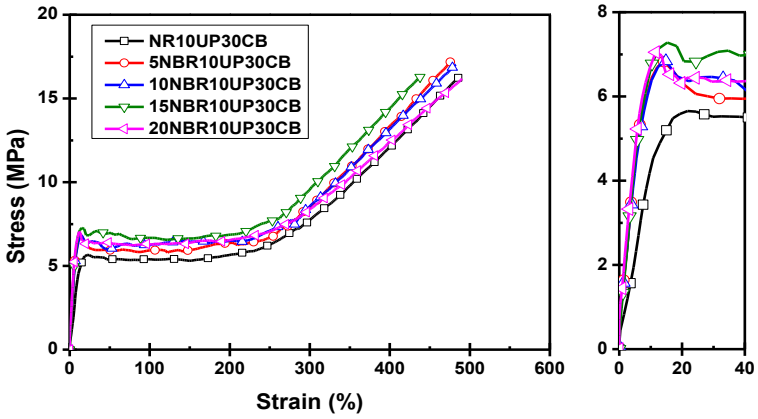

Figure 5.57 Stress-strain curves of NR/PALF/carbon black hybrid composites containing NBR 0, 5, 10, 15 and 20 wt% of total rubber matrix

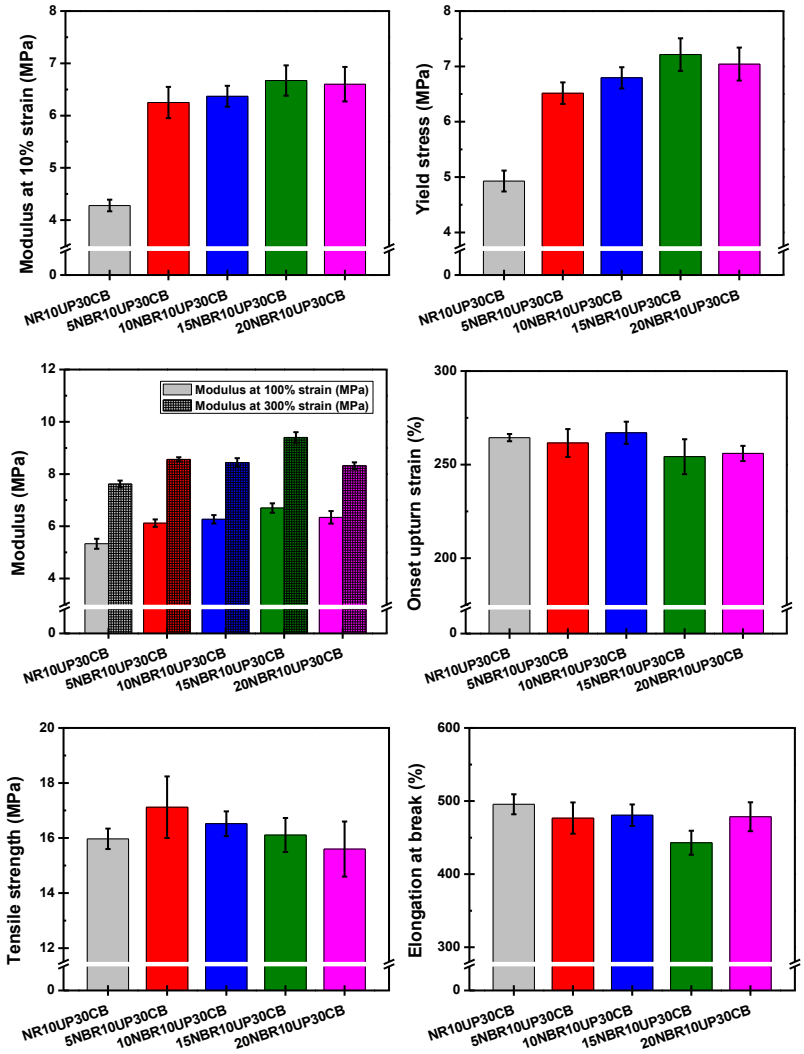

Figure 5.58 Tensile properties of NR/PALF/carbon black hybrid composites containing NBR 0, 5, 10, 15 and 20 wt% of total rubber matrix

To summarize, the incorporation of NBR enhances the tensile properties at low deformation of NR/PALF/carbon black hybrid composites. E_{10} and σ_y increase by incorporation of NBR at least 5 wt% of total rubber. The enhancement of tensile properties at low strain region is consistent with the previous results of the replacing part of NR by NBR in NR/PALF composites, which was studied in section 5.1. Next, the effect of fillers distribution in the blends will be studied by changing the mixing method.

5.4.4 Effect of mixing method

In the studies of rubber blends containing fillers, the mixing method can affect the final properties of composites. The distribution of filler in each rubber is the main parameter to enhance the mechanical properties [43]. In the previous studies of the filler effect in section 5.4.1, PALF has been used to improve the tensile properties at low deformation region, whereas carbon black has been used to improve tensile properties at high deformation region. In this study, three mixing schemes were proposed to control the filler distribution in rubber blends. Three different mixing schemes are listed in Table 4.8.

The conventional mixing scheme that has been used to study the effects of filler, carbon black content and NBR content is mixing scheme A. Masterbatch of NR/carbon black was first prepared and dispersed in NR matrix together with NBR then followed by PALF. NBR was added together with NR at the first step to avoid a phase separation during mixing.

For mixing scheme B, masterbatches of NR/carbon black and NBR/carbon black/PALF were prepared separately. This mixing scheme provides the similar carbon black content in each rubber, whereas only NBR encases PALF.

For scheme C, two masterbatches of NR/carbon black and NBR/PALF were prepared separately. Again, there is only NBR that encases PALF. However, carbon black is only in NR matrix. Composites mixed by scheme A is named as 20NBR10UP30CB in order to have similar name in whole section 5.4. Composites with –B and –C are named corresponding to the mixing scheme.

The models of the distribution of carbon black and PALF in NR and NBR are displayed in Figure 5.59.

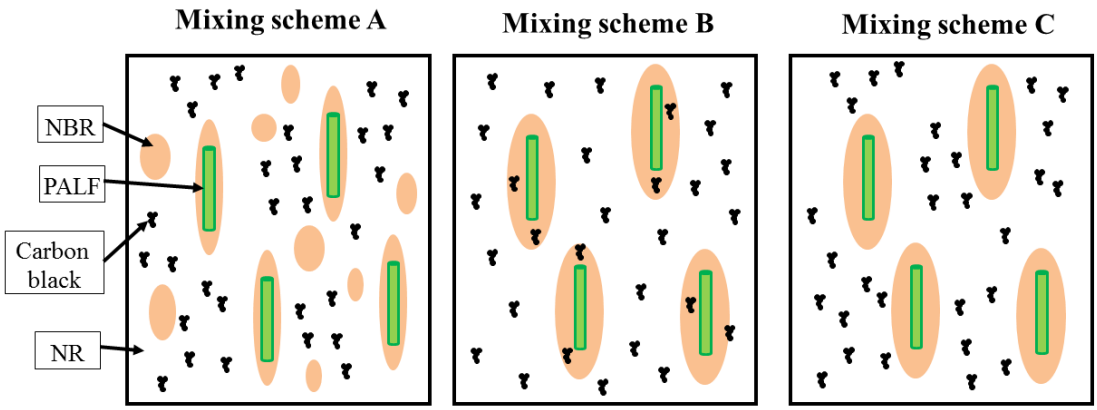

Figure 5.59 Models of 20NBR10UP30CB composites compounding by different mixing schemes

5.4.4.1 Cure characteristics

The rheograms and cure characteristics of 20NBR10UP30CB composites compounding by different mixing schemes are shown in Figure 5.60 and Table 5.19. The three composites exhibit the reversion process. It is observed that the curing rates, which is the slope of the cure curve, of composites compounding by mixing schemes B and C are similar to those composites compounding by mixing scheme A. However, M_H does not rise to the same values. M_H of composite mixed by scheme C is slightly lower than that mixed scheme A, whereas composite mixed by scheme B is even lower than that mixed scheme C. t_{s2} are very close for the three samples whereas t_{c90} is shorten for mixing scheme C and even slightly lower for mixing scheme B.

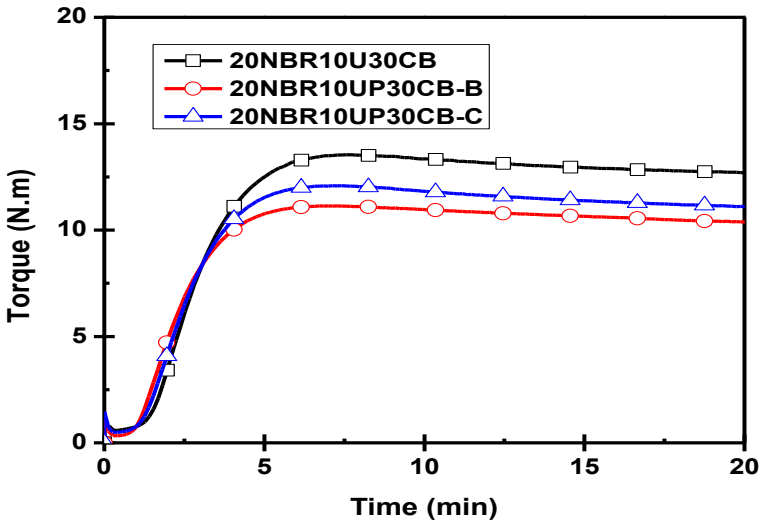

Figure 5.60 Cure curves of NR/NBR/PALF/carbon black hybrid composites compounding with different mixing schemes

Table 5.19 Cure characteristics of NR/NBR/PALF/carbon black hybrid composites compounding with different mixing schemes

	M_L	M_H	t_{s2} (min)	t_{c90} (min)
20NBR10UP30CB	0.6	12.8	1.7	5.4
20NBR10UP30CB-B	0.3	11.1	1.4	4.1
20NBR10UP30CB-C	0.5	12.1	1.6	4.4

5.4.4.2 Dynamic mechanical thermal properties

In order to understand the fillers distribution in the immiscible NR/NBR blend, DMTA of composites was carried out. Graphs of E´ and tan delta against temperatures are illustrated in Figure 5.61 and typical values are shown in Table 5.20. 20NBR10UP30CB and 20NBR10UP30CB-C display similar trace of E´. E´ of 20NBR10UP30CB-B, in which carbon black was equally distributed in both rubbers, is lower than that of the other composites by about 50%. The magnitude of tan delta of NR for 20NBR10UP30CB-B is greater than that of other composites by 24%. T_gs of NR and NBR are not affected by the mixing method. This result can be used to confirm that when carbon black is incorporated into rubber, most of carbon black is still in that

rubber phase. The drop of E´ indicates that carbon black should be dispersed only in rubber matrix in order to optimize the mechanical properties.

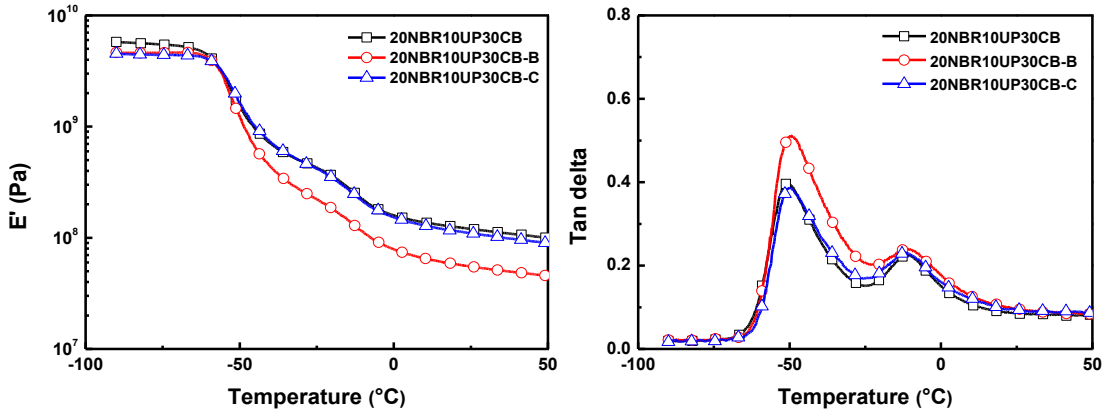

Figure 5.61 Temperature dependences of E´ tan delta of NR/NBR/PALF/carbon black hybrid composites compounding with different mixing schemes

Table 5.20 Viscoelastic properties of NR/NBR/PALF/carbon black hybrid composites compounding with different mixing schemes

	E´ at 25 °C (MPa)	Tan δ_{NR}		Tan δ_{NBR}	
		Magnitude	T (°C)	Magnitude	T (°C)
20NBR10UP30CB	120.8	0.4	-50	0.2	-10
20NBR10UP30CB-B	55.1	0.5	-50	0.2	-10
20NBR10UP30CB-C	109.8	0.4	-50	0.2	-11

5.4.4.3 Mechanical properties

The effect of mixing method on tensile properties of hybrid composites was investigated. Stress-strain curves of 20NBR10UP30CB, -B and –C composites are displayed in Figure 5.62. The mixing method slightly affects tensile properties at both low strain and more at high strain regions, in which the stress upturns until it reaches the maximum stress.

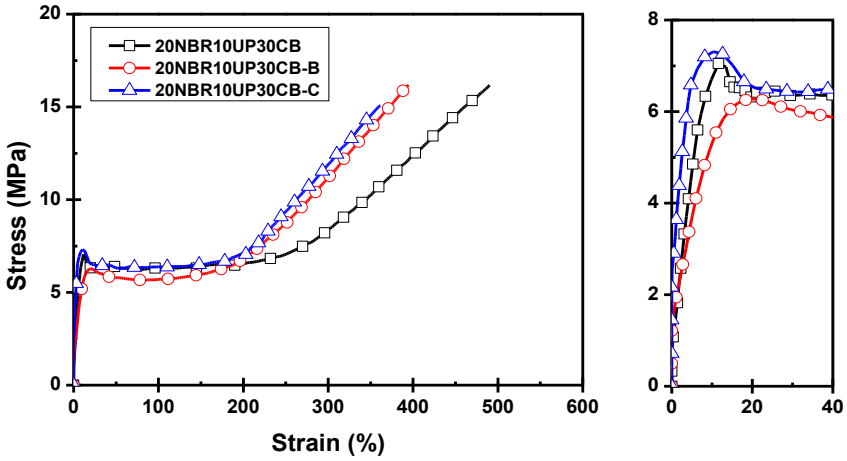

Figure 5.62 Stress-strain curves of NR/NBR/PALF/carbon black hybrid composites compounding with different mixing schemes

E_{10} and σ_y of composites are reported in Figure 5.63. E_{10} and σ_y of 20NBR10UP30CB-B composite, which carbon black was distributed equally in both rubber phases, are about 20% lower than 20NBR10UP30CB. 20NBR10UP30CB-C, in which NR/carbon black and NBR/PALF masterbatches were first prepared before being mixed to yield the final compound, has highest E´, which is 10% higher than 20NBR10UP30CB. σ_y of 20NBR10UP30CB-C is similar to 20NBR10UP30CB.

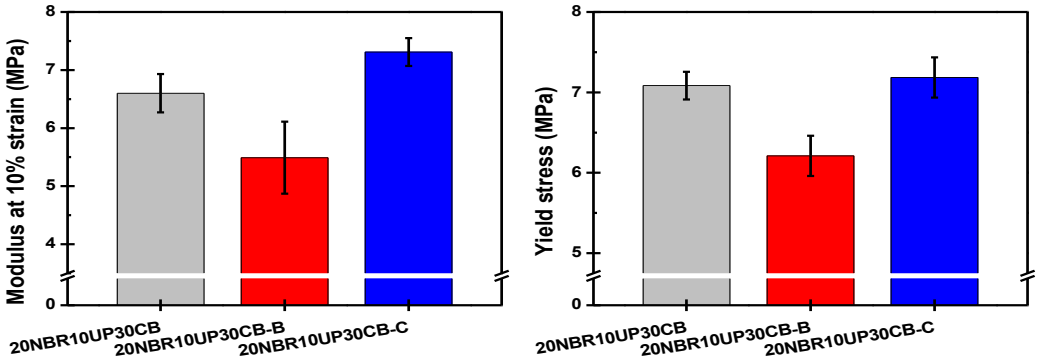

Figure 5.63 E_{10} and σ_y of NR/NBR/PALF/carbon black hybrid composites compounding with different mixing schemes

E_{100}, E_{300} and onset upturn strain of composites are displayed in Figure 5.64 to determine the deformation behavior at moderate and high strain regions. E_{100} of 20NBR10UP30CB and 20NBR10UP30CB-C are similar, whereas 20NBR10UP30CB-B is slightly lower than those composites. Onset upturn strains of

20NBR10UP30CB-B and 20NBR10UP30CB-C, which NBR/PALF was mixed as masterbatch, are earlier obtained from 250% to 195% and E_{300}s are 30% higher than 20NBR10UP30CB.

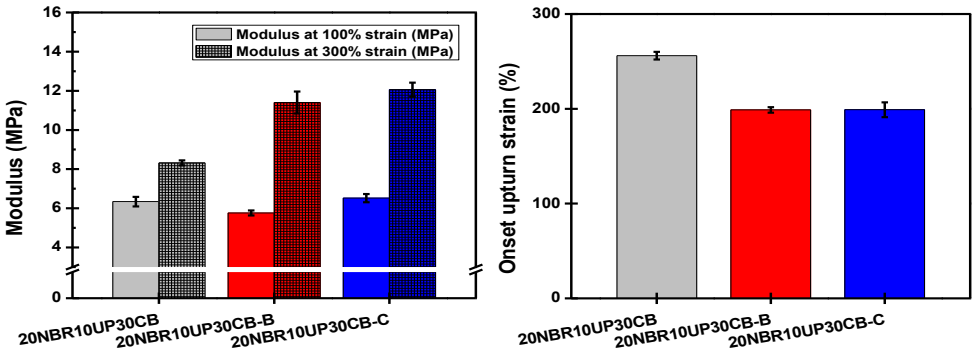

Figure 5.64 E_{100}, E_{300} and onset upturn strain of NR/NBR/PALF/carbon black hybrid composites compounding with different mixing schemes

The ultimate properties are displayed in Figure 5.65. The mixing method does not affect tensile strength of composites. However, as a result of earlier upturn stress, elongation at breaks of 20NBR10UP30CB-B and –C composites are lower than 20NBR10UP30CB.

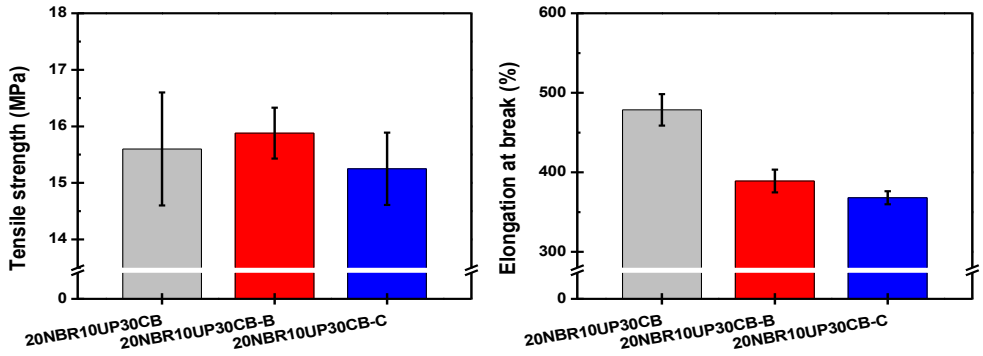

Figure 5.65 Tensile strength and elongation at break of NR/NBR/PALF/carbon black hybrid composites compounding with different mixing schemes

It is clear that mixing scheme C provides the highest modulus at low strain and also earlier upturn stress rather than mixing scheme A and B. Thus, the premixing of two masterbatches of NR/carbon black and NBR/PALF is proposed to control filler distribution in immiscible blends, which results in the optimized mechanical properties of composite.

5.4.5 Discussion

The incorporation of carbon black and NBR into NR/PALF composites result in modification of curing behaviors and significant improvement of mechanical properties. The effect of fillers in NR followed by NR/NBR blends on cure characteristics, dynamic thermal mechanical properties and tensile properties will be first discuss before the effect of mixing method.

Carbon black and PALF can be used to increase M_H of composites. The increase of M_H of carbon black-filled composites is higher than those of PALF-filled composites. Lopattananon and coworkers reported that M_H of cellulose fiber/silica-reinforced NR composites decreased proportionally by increasing the ratio of cellulose/silica [115]. This is due to applied force in dynamic shearing mode. Thus, the level of enhancement of particulated fillers is higher than fiber due to no fiber orientation effect. The combination of PALF and carbon black in composites results in the highest M_H. This indicates that carbon black and PALF can be used to reinforce composites together. This can be confirmed by the sequential increase of M_H by increasing the amount of carbon black from 0 to 30 phr in NR/carbon black/PALF hybrid composites, which is shown in Figure 5.47. The reversion process (MDR measurement) is only obtained when carbon black is incorporated into rubber/PALF composites, while composites containing only PALF and non-reinforced rubber exhibit an equilibrium value. The similar results were reported by Pittayavinai and coworkers who shown that the reversion process was obtained by increasing the amount of carbon black in NR/PALF hybrid composites using CBS as accelerator [118]. In case of carbon black-filled NR, it was reported by Choi and coworkers that the reversion process could be observed by using a sulfenamide as accelerator such as CBS and TBBS [144]. Moreover, Hamed and Boonkerd reported that the reversion process of carbon black-filled NR was obtained in a specific ratio of sulfur and accelerator N,N-dicyclohexyl-2-benzothiazole sulfenamide (DCBS). In their case, using sulfur/DCBS at the ratio of 1.17 caused the highest degree of reversion [145]. Although the mechanism of the reversion process of NR in presence of carbon black is still unclarified, it was reported that this process occurred depending on the type of accelerator and a ratio of sulfur/accelerator.

Type of fillers also affects dynamic thermal mechanical properties of composites [141]. The improvement of E´ will be first discussed, following by the changing of T_d. E´s at room temperature of PALF-reinforced composites are higher than carbon black-filled rubbers. This improvement is not consistent with MDR result, which M_H of carbon black-filled rubber is higher than PALF-filler rubber. This can be explained by the different applied force for the measurement. DMTA is used to measure E´ in dynamic tension mode, thus, the effect of fiber orientation is higher than MDR, which is used to measure torque in a dynamic shear mode. The combination of PALF and carbon black in composites results in the highest E´.

The effect of fillers on tensile properties of NR is first discussed. Unfilled rubber and carbon black-filled rubber exhibited low modulus at low strain region, while rubbers containing PALF exhibit strong resistance to applied strain and the stress required is high. It can be summarized that PALF is incorporated to improve modulus at low deformation, whereas carbon black is incorporated to enhance stress at high deformation. This is due to fiber reinforcement in longitudinal direction [146] and carbon black reinforcement by physical adsorption on rubber [48]. In hybrid composites, the applied stress at all strain region of PALF-filled rubbers increases by incorporation of carbon black. This indicates that carbon black and PALF can be used to reinforce composites together.

By replacing NR by NBR 20 wt%, composites containing different type of fillers improves the cure characteristics in a different order. NBR does not affect on non-reinforced rubber, whereas it slightly increases M_H of PALF-filled composites by 7%. The enhancement of M_H by NBR in presence of carbon black in NR is higher than PALF-filled NR. The level of improvement of M_H by NBR in carbon black-filled NR is similar to hybrid-filled NR, which M_H is increased by 20%. Replacing NR by NBR 20 wt% indicates that the amount of carbon black in NR matrix is higher, thus, the reinforcement effect using dynamic shear force is higher. This can be confirmed by varying the amount of NBR in hybrid composites, which is shown in Figure 5.54. The incorporation of NBR at least 5 wt% in hybrid composite significantly improves M_H. By mixing scheme A, carbon black has been incorporated in NR as the masterbatch, hence, carbon black is mainly in NR, not in NBR. This behavior was confirmed by

using DMTA (Figure 5.49), which will be explained in a later section. By the way, the reversion process does not change by NBR incorporation.

By incorporation of NBR, E´ at room temperature is further increased. As the measurement is in tension mode, the effect of fiber reinforcement with NBR can be obtained. By replacing NR with NBR 20 wt%, E´ of PALF-filled NR is increased by 50% and E´ of PALF/carbon black-filled NR is increased by 140%. The role of NBR, which has been studied in section 5.1, is to encase PALF. This results in the better stress transfer between matrix and fibers. Moreover, the modulus of matrix is enhanced by carbon black. Thus, the reinforcement by fiber and carbon black can be further enhanced by NBR. After the effect of NBR on various type of fillers is discussed, the amount of NBR is further explained. The incorporation of NBR at least 5 wt% in hybrid composite significantly improves E´ and causes no significant difference when NBR content is up to 20 wt%. Hence, only small amount of NBR can be used to improve the modulus of NR/PALF/carbon black hybrid composites.

Since NR and NBR have different polarities, they are not compatible [29]. Thus, the distribution of carbon black in the blends will be explained. Carbon black which was incorporated in NR as masterbatch, is mainly distributed in NR matrix phase. This was confirmed by DMTA measurement by varying carbon black content. The magnitude of Tan δ_{NBR} does not change by increasing carbon black content, which can be seen in Figure 5.49. Massie and coworkers reported that the migration of carbon black from rubber to another rubber after it is incorporated is rarely occurring [42]. As a result of the most favorable distribution of carbon black in NR (less in NBR), the reinforcement is higher than using only NR as matrix. Next, tensile properties of composites will be presented.

Tensile properties at low strain region of hybrid composites are significantly enhanced by incorporation of NBR. E_{10} and σ_y are improved. Thus, the result shows that NBR still encapsulate the fibers and improves the stress transfer from matrix to fiber. Moreover, this improvement in hybrid composites is higher than incorporation of NBR in PALF-reinforced NR composite. The higher rigidity of matrix, which is obtained by incorporation of carbon black into NR, further enhances modulus when stress is transferring from matrix to PALF via NBR. This result can be confirmed by the improvement of modulus at low strain in the presence of carbon black in

NR/NBR/PALF composites, which is shown in Figure 5.51. The enhancement of stress transfer between NR and PALF does not depend on the amount of carbon black, whereas higher modulus at high deformation is achieved when higher amount of carbon black is incorporated into composites. The incorporation of carbon black into NR/NBR/PALF composites also increases of tensile strength, which is displayed in Figure 5.53. For NR/PALF composite without carbon black, the enhancement of the stress transfer by incorporation of NBR reduces tensile strength of composite. By incorporation of carbon black, tensile strength of composites with enhancing stress transfer by NBR is similar to those composites without NBR. Only small amount of NBR is required to improve tensile properties at low strain region in hybrid composites. E_{10} and σ_y are significantly improved by incorporation of NBR at least 5 wt% of total rubber, which are shown Figure 5.58. This result is not similar to those composites without carbon black. The enhancement of modulus depends on NBR content. Thus, in a presence of carbon black, lower amount of NBR is required to improve tensile properties at low deformation.

The sequence of mixing is very important to provide the appropriate structure for maximum reinforcement. The three different mixing sequences provide composites with different structure regarding the distribution of fillers in the blend. The models are previously shown in Figure 5.59. For scheme A, there should be two types of NBR, i e. one part is dispersed in NR matrix and the other part encases PALF. Carbon black is in NR matrix. For scheme B, there is only that NBR encases PALF. Both NR matrix and NBR contain similar content of carbon black. For scheme C, again, there is only NBR that encases PALF. Carbon black is distributed mainly in NR matrix. Consequently, the three composites have different properties. In order to achieve the optimum tensile properties in term of E_{10} and onset upturn strain, carbon black should be distributed in NR matrix and PALF should be encased in NBR, which are obtained by mixing scheme C.

Lastly, NBR is used as a matrix mixing with UPALF and carbon black to compare with NR matrix and the blends of NR and NBR. The stress-strain curves of this composite with the same amount of carbon black and fibers was published by Prukkaewkanjana [117]. Stress-strain curves of their composites are displayed in Figure 5.66. It can be seen that modulus at low strain and σ_y of NBR hybrid composites are the highest due to the polar-polar interactions. By the way, replacing 20 wt% of NR by

NBR increases both modulus at low strain and σ_y close to NBR as matrix. By proper mixing of 20NBR hybrid composite, earlier onset upturn strain and higher modulus at high strain are achieved. This can be used to confirm that NBR-encased PALF provides more friction between NR and PALF *via* NBR, which friction is higher than using only NBR as matrix.

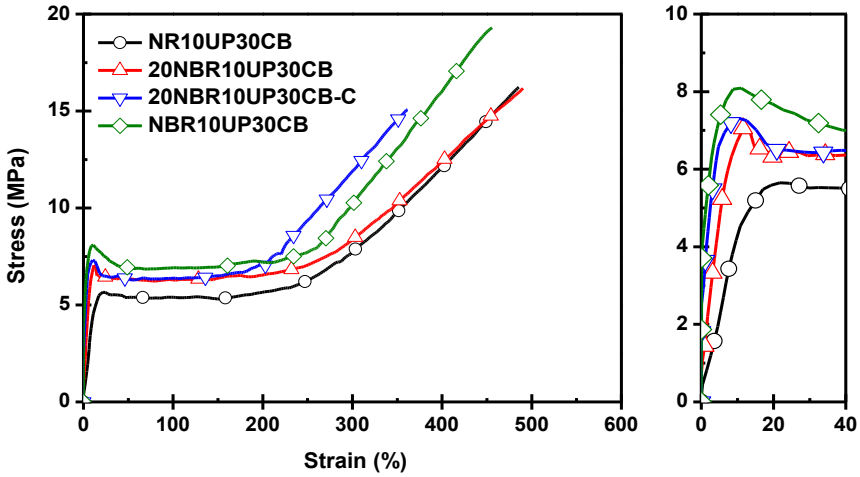

Figure 5.66 Stress-strain curves of NR, NBR and its blends containing the same amount of PALF and carbon black [117]

5.4.6 Summary

Tensile properties of PALF-reinforced NR can be improved by the incorporation of NBR and hybrid filler (carbon black and PALF). NBR improves the stress transfer and thus tensile properties at low deformation, while carbon black improves the tensile properties at high deformation. However, to achieve such improvement, it is important that NBR encases PALF properly while carbon black distributes only in the matrix phase. This structure is obtained by using a proper mixing sequence. Two masterbatches of NR with carbon black and NBR with PALF are prepared first. The two masterbatches are then diluted in NR matrix to get the required contents of each component.

5.5 Effect of fiber surface treatment on NR/PALF/carbon black hybrid composites

From the previous results, alkali and silane treatments of PALF could be used to improve the stress transfer between NR and PALF. Alkali treatment increased the volume fraction of fibers leading to higher surface area. Moreover, the mechanical interlocking between NR and APALF improved the modulus of composites. For silane treatment, the sulfidic bonds between NR and silane-treated PALF were formed during vulcanization, which resulted in higher tensile properties in term of modulus. However, ultimate properties i e. tensile strength and elongation at break were reduced. To improve these ultimate properties, carbon black has been incorporated into NR/PALF composites. The model of NR/PALF/carbon black hybrid composites is shown in Figure 5.67. Hence, tensile properties could be improved at both low and high deformation regions.

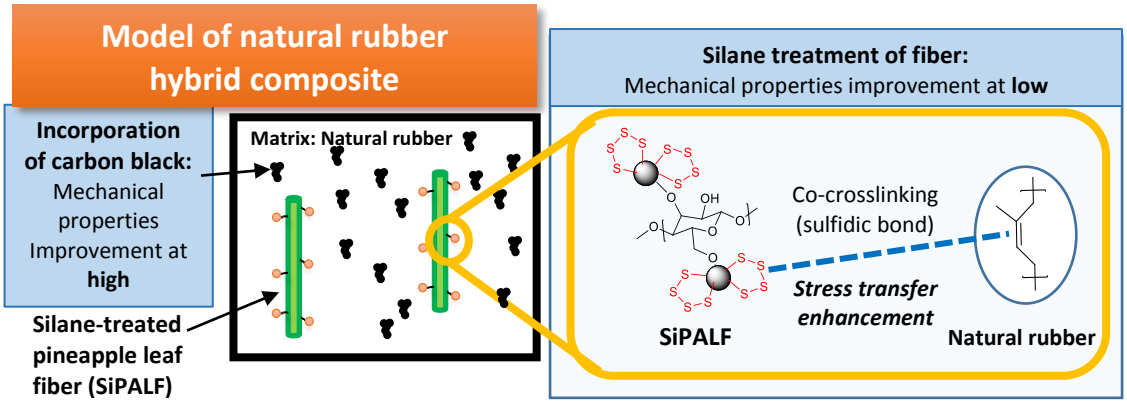

Figure 5.67 Model of NR/silane-treated PALF/carbon black hybrid composite

The effects of alkali treatment and silane treatment of fibers on composites containing various carbon black content at 0, 10, 20 and 30 phr were investigated. PALF content was fixed at 10 phr. Three different types of PALF, which are untreated PALF (UPALF), alkali-treated PALF (APALF) and silane-treated PALF (SiPALF) were incorporated in this study. It should be noted that silane-treated PALF was first pretreated by alkali treatment. The condition of treatment was using silane-69 3 wt% in pure ethanol corresponding up to the best mechanical properties of composite. These tensile properties were previously studied and discussed in section 5.2. Composites were produced using mixing scheme A, which means that a masterbatch of NR/carbon

black was first prepared. NR, NR/carbon black masterbatch were mixed, followed by the incorporation of PALF and in the final step the curatives.. Cure characteristics, dynamic mechanical thermal properties and tensile properties were investigated.

5.5.1 Cure characteristics

The effect of fiber surface treatment on cure behavior of composites containing various amounts of carbon black was first studied. The rheograms of composites are displayed in Figure 5.68 and their cure characteristics are shown in Figure 5.69. Fiber surface treatments do not affect the cure behavior of composites without carbon black, neither M_H , t_{s2} or t_{c90} are changed. By incorporation of carbon black, the reversion process is observed.

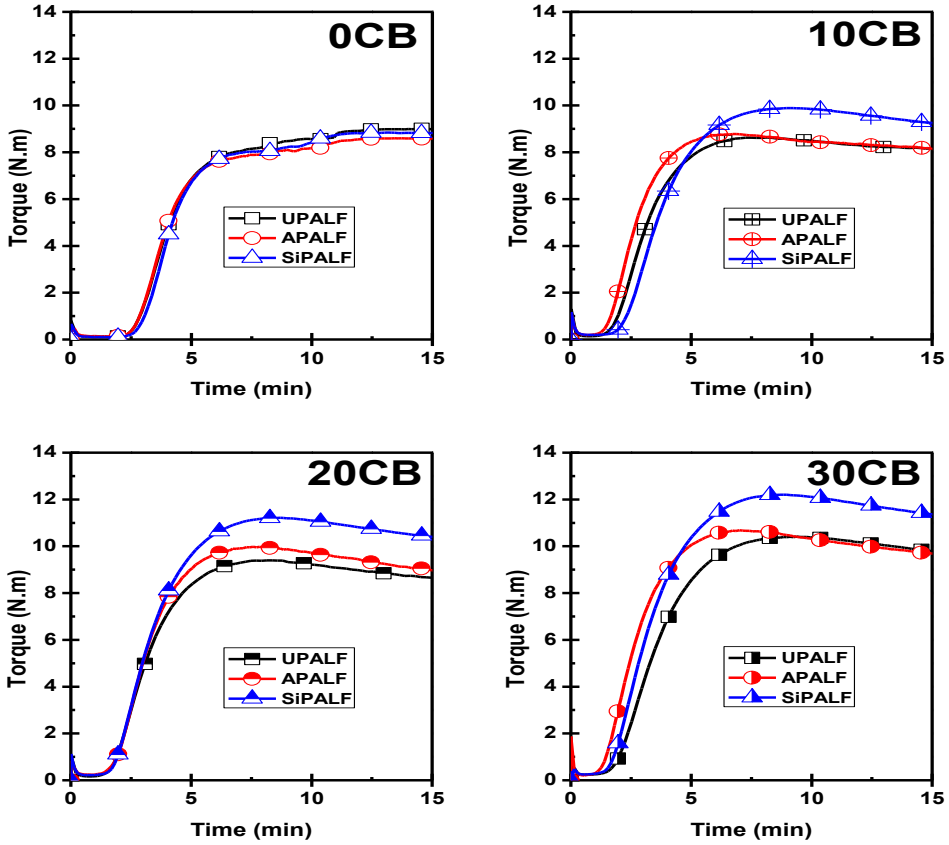

Figure 5.68 Cure curves of NR containing various amounts of carbon black and different surface-treated PALFs

t_{s2} and t_{c90} decreases from 3.5 to 2.5 min and 7 to 5 min respectively by incorporation of carbon black. t_{s2} of carbon black-filled composites does not change by

fiber surface treatments, whereas t_{c90} of carbon black-filled composite containing APALF is slightly lower than those containing Si- and UPALFs. M_Hs of composites increase proportionally with carbon black content. By increasing carbon black to 30 phr, M_L and M_H of composites increases proportionally to carbon black content, however, the fiber surface treatment does not modify M_L. The effect of fiber surface treatments can be seen on cure behaviors can be observed in term of M_H of composites containing carbon black. Carbon black 30 phr causes the increasing of M_H of hybrid composites containing SiPALF by 40%, whereas it causes 30% increase of M_H of those containing APALF. Thus, M_Hs of carbon black-filled composites containing SiPALF are higher than those containing APALF.

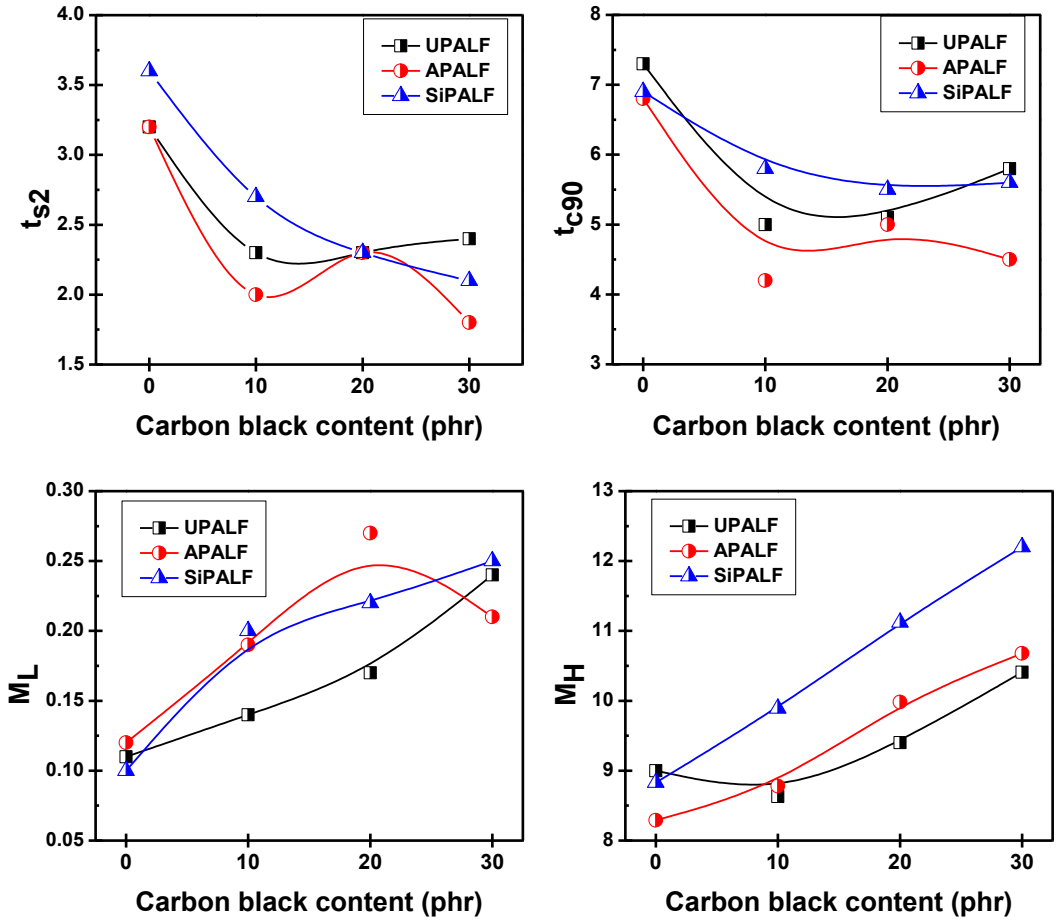

Figure 5.69 Cure characteristics of NR containing various amounts of carbon black and different surface treated PALFs

5.5.2 Dynamic mechanical thermal analysis

The temperature dependences of E´ of the composites are shown in Figure 5.70. The sharp drop of E´, which corresponds to glass transition domain of NR, is observed as previously. Again, the main reinforcing effect is obtained from the incorporation of carbon black. The increase of E´ at 25°C is proportional to carbon black content. The surface treatment of fibers is a secondary effect.

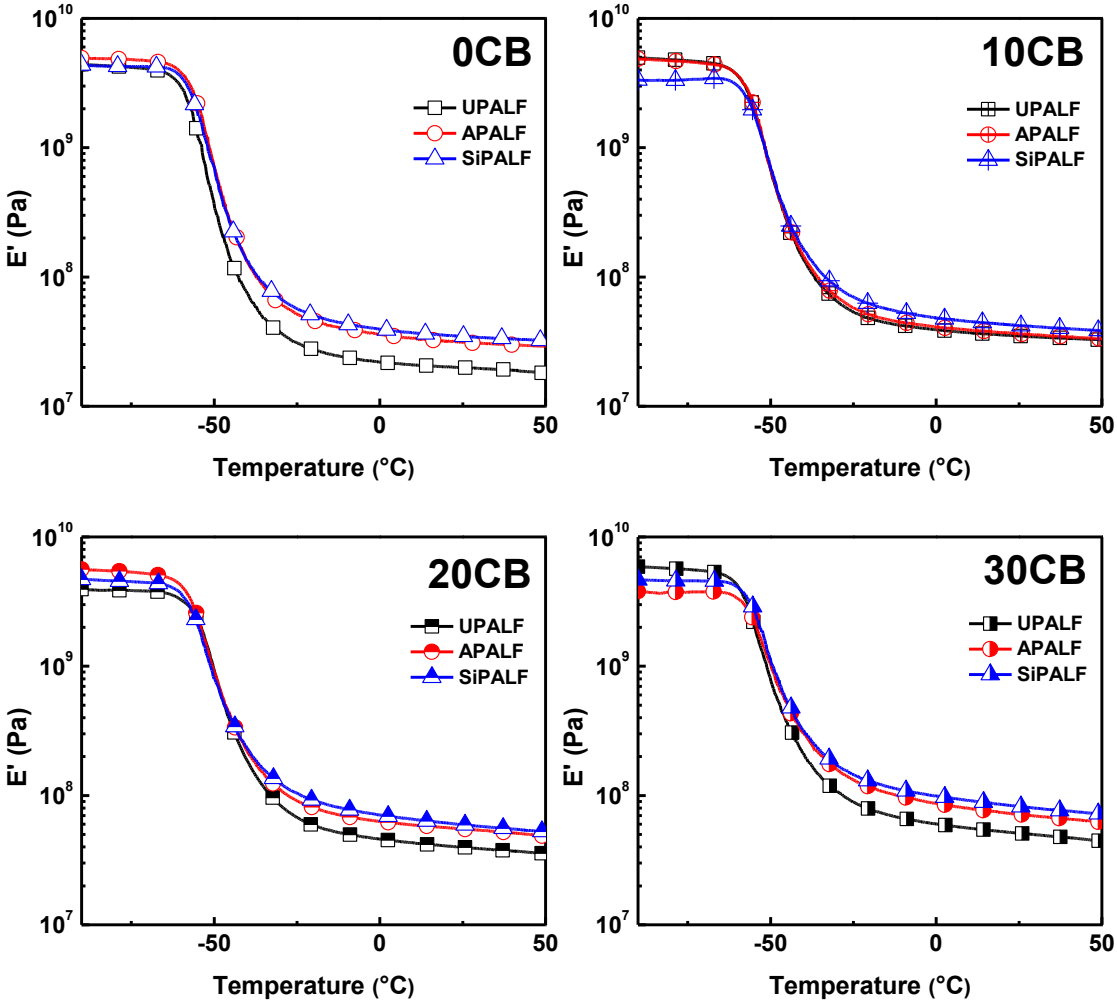

Figure 5.70 Temperature dependences of E´ of NR containing various amounts of carbon black and different surface treated PALFs

The relationship between E´s at 25°C and carbon black content is plotted in Figure 5.71. E´s at 25°C for hybrid-filled NR containing UPALF is multiplied by 2.5 by increasing carbon black content to 30 phr. Carbon black-filled composites reinforcing with UPALF exhibit lowest E´ at 25°C, which is significant lower than those

surface-treated PALF composites. Carbon black/PALF-filled and fiber-filled composites containing SiPALF exhibit the slightly higher of E´ at 25°C than those composites containing APALF.

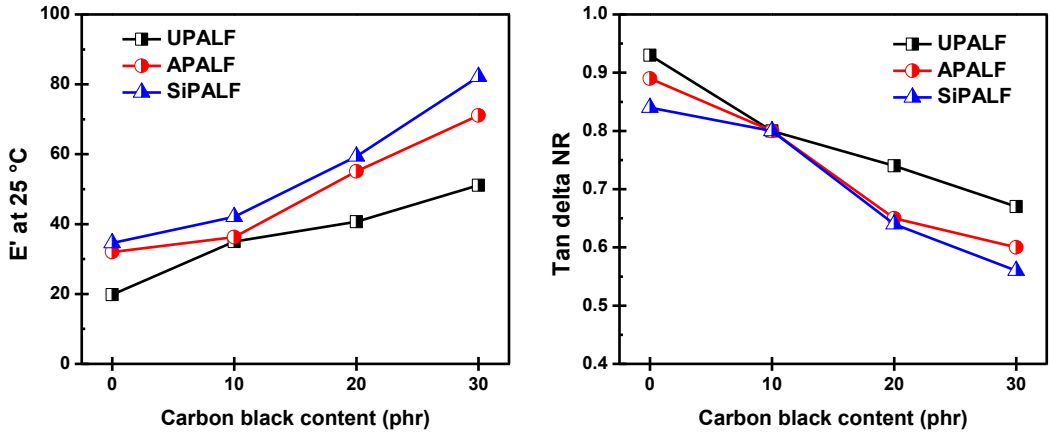

Figure 5.71 Relationship between E´ at 25 °C/tan delta NR and carbon black content

The temperature dependences of tan delta of composites are displayed in Figure 5.72 and their numerical values are reported in Figure 5.71. The peak position of tan delta, which corresponds to the T_d of NR, is not changed by fiber surface treatment or incorporation of carbon black. Magnitude of tan delta of NR decreases proportionally to the increase of carbon black content. This magnitude is decreased by 40% by incorporation of carbon black 30 phr. Alkali and silane treatments of fiber do not change the tan delta magnitude. Thus, carbon black affects to dynamic mechanical thermal properties more than fiber surface treatment does.

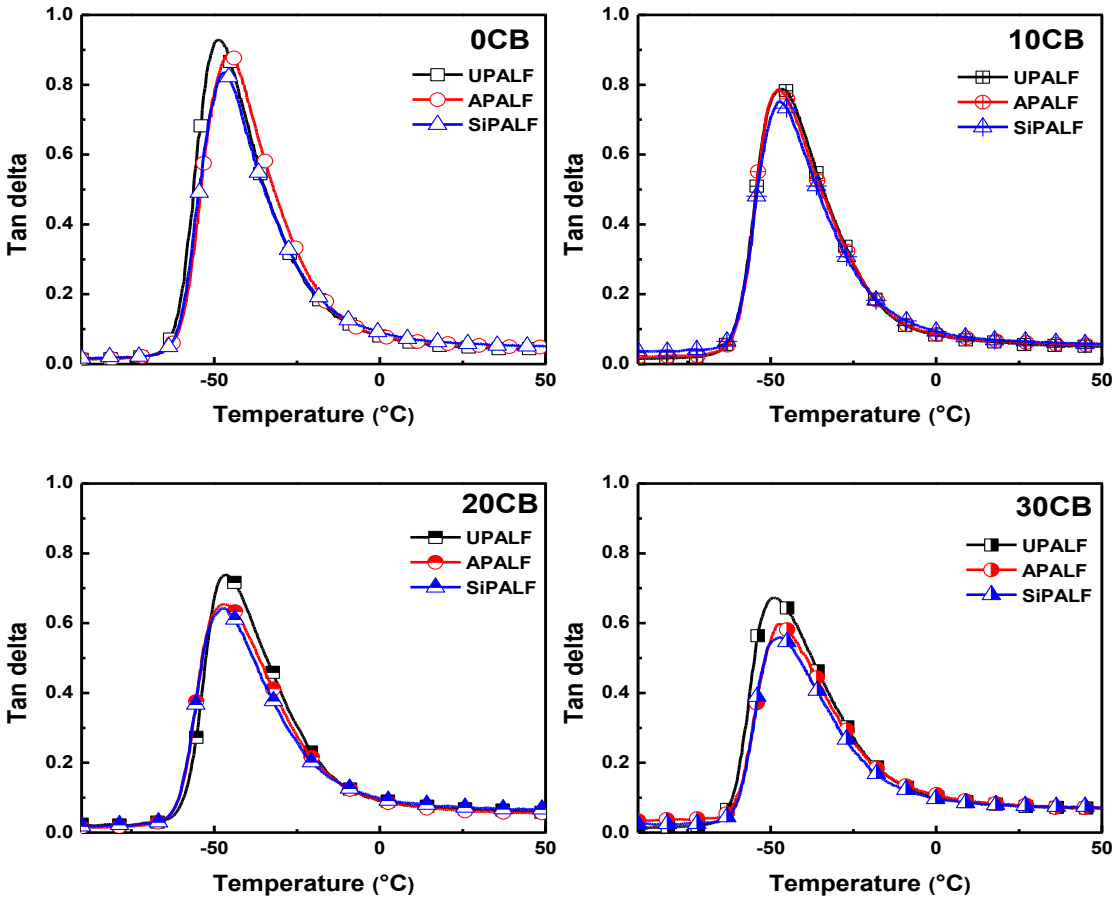

Figure 5.72 Temperature dependences of tan delta of NR containing various amounts of carbon black and different surface treated PALFs

5.5.3 Mechanical properties

Stress-strain curves of composites with various amounts of carbon black and surface treatments are displayed in Figure 5.73. All composites exhibit the yield-like behavior, which are generally obtained for composites containing PALF [68]. By surface treatment of fibers with the incorporation of carbon black, yield stress is observed at lower strain. After yield point, the curves of composites without carbon black and with carbon black 10 phr are rough due to the presence of fiber. The curves are smooth when high amount of carbon black is incorporated. Surface treatments of fibers affect the onset upturn stress, which causes higher stress at high deformation.

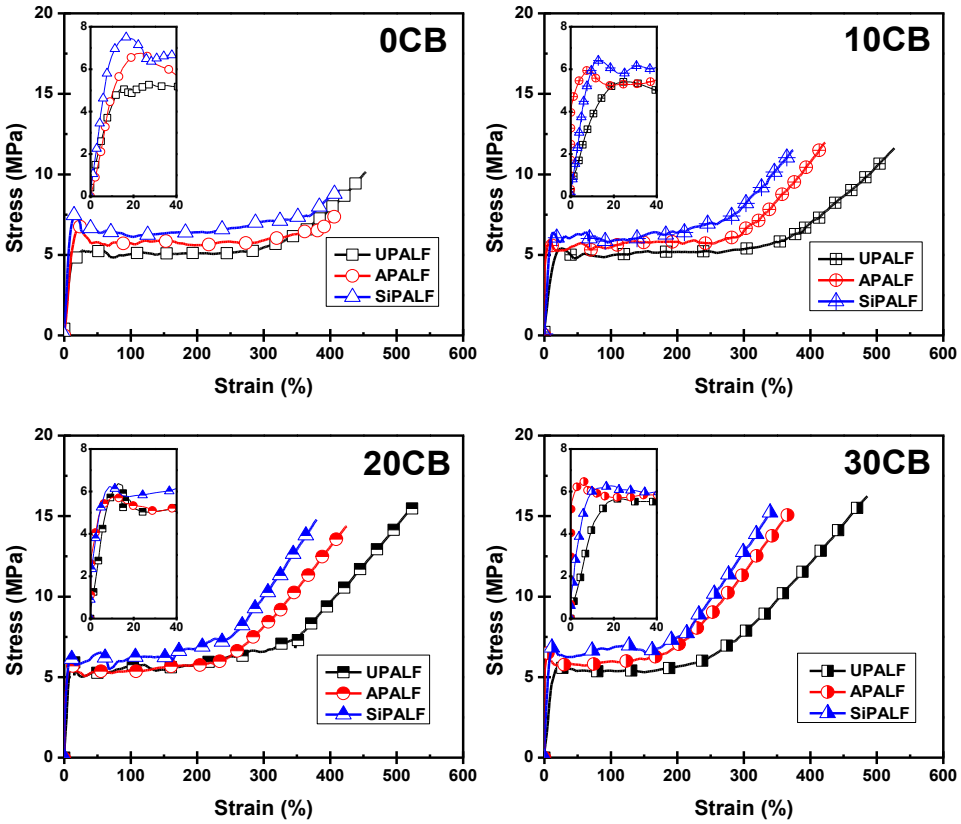

Figure 5.73 Stress-strain curves of NR containing various amounts of carbon black and different surface treated PALFs

In this specific case, the stress reaches a σ_y value less than 10% strain for composites containing carbon black as displayed in Figure 5.73. Thus, modulus at 1% strain (E_1) is reported instead of E_{10}. E_1 and σ_y are used to represent the deformation at very low strain region and show in Figure 5.74 (E_{10} is also displayed as reference). For composites without carbon black, E_1 increase by alkali treatment of fibers, and slightly increase by silane treatment. This trend is changed by incorporation of carbon black into composites. E_1 increases from 0.78 MPa to 5.8 MPa by alkali treatment, however, it decreases back to 1.2 MPa by silane treatment. E_1 is not significantly affected by carbon black content. σ_y of composites increases by alkali treatment and further increases by silane treatment for composites without carbon black and with carbon black 10 phr. Higher content of carbon black causes the similar σ_y of composites containing APALF and SiPALF.

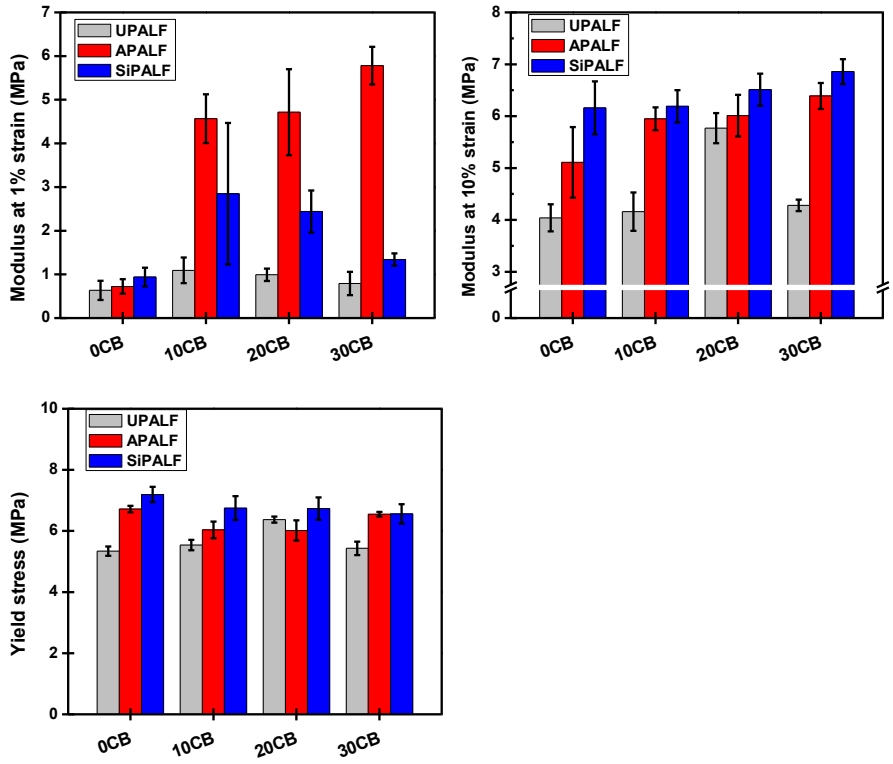

Figure 5.74 E_1, E_{10} and σ_y of NR containing various amounts of carbon black and different surface treated PALFs

E_{100} is used to analyze the deformation at moderate strain region after yield point, which is displayed in Figure 5.75. E_{100} increases by fiber alkali treatment and further increases by silane treatment for composites. E_{100} is not affected by carbon black content due to no upturn stress in this strain region. The reinforcement of carbon black combination with fiber can be clearly seen at high strain region. The values are represented as onset upturn strain and E_{300} and are displayed in Figure 5.75. Onset upturn strain of carbon-black-filled composites containing SiPALF is lowest, whereas those composites containing APALF has slightly higher than SiPALF. It means that composites containing UPALF has slowest upturn stress. The higher amount of carbon black is, the improvement of E_{300} is higher. E_{300} of composites containing carbon black 30 phr and UPALF is increased by APALF from 7.7 MPa to 11.2 MPa, and E_{300} is further increased by SiPALF up to 12.8 MPa. the highest improvement is obtained by silane treatment. Thus, not only carbon black increases the stress at high deformation but the fiber surface treatment also plays the reinforcing effect with carbon black in hybrid composites.

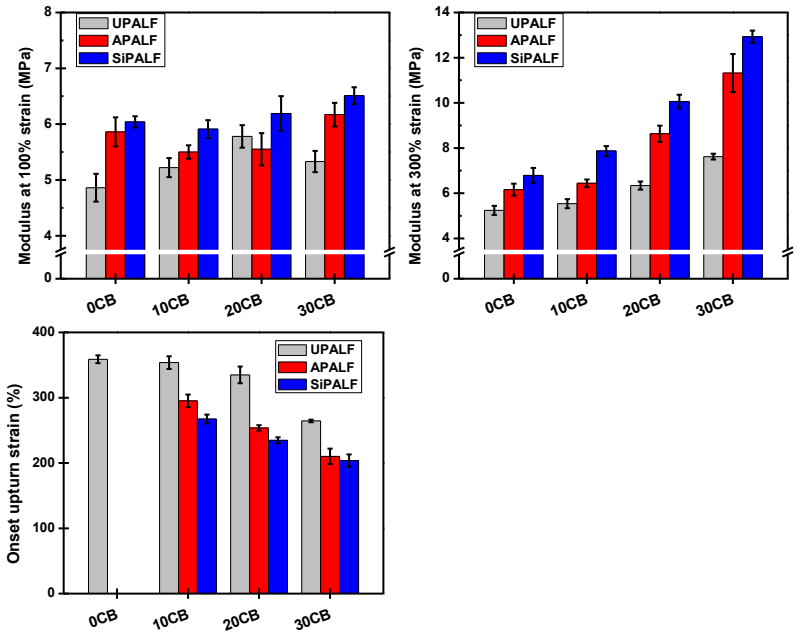

Figure 5.75 E_{100}, E_{300} and onset upturn strain of NR containing various amounts of carbon black and different surface treated PALFs

Ultimate properties are displayed in Figure 5.76. For composites without carbon black, the surface treatment of fiber decreases tensile strength and elongation at break. This decrease of tensile strength can be greatly reduced by incorporation of carbon black at least 10 phr. Thus, tensile strengths of composites with treated fibers are almost similar to those composites with untreated fiber. However, elongation at breaks of hybrid composites with surface-treated fibers remain lower than untreated fibers.

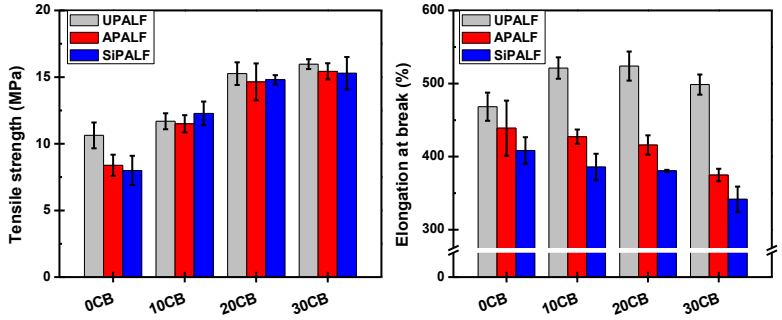

Figure 5.76 Tensile strength and elongation at break of NR containing various amounts of carbon black and different surface treated PALFs

5.5.4 Discussion

The incorporation of carbon black in NR/surface-treated PALF composites modifies curing behavior and mechanical properties. The surface treatment of PALF improved modulus at low deformation of composites. In addition, it can be combined with carbon black to improve stress at high deformation. We will now attempt to explain these improvement effects.

Chen and Yan reported that the effect of short fiber reinforcement can be achieved from high matrix modulus, high fiber strength and high fiber-matrix interactions [146]. Thus, the reinforcement effect will be discussed based on these three factors. From the tensile properties of NR/PALF composites by fiber surface treatments in section 5.2, modulus at low strain region and σ_y were improved. Alkali treatment provides a higher volume fraction of fibers. Moreover, smooth individual surface of fibers is observed, thus, the mechanical interlocking between matrix and fiber leads to enhance the tensile properties of composites [73,95,97-98]. Silane treatment provides the chemical bonds formation between NR and PALF during vulcanization [115]. Silane-69 can be grafted to the rubber *via* sulfidic bonds [108], thus, modulus at low strain region of composites is increased. However, the surface treatment of PALF has also caused the lower ultimate properties i e. tensile strength and elongation at break of composites. Thus, carbon black was incorporated into NR/surface-treated PALF composites to improve these ultimate properties. The effect of carbon black combined with surface-treated fibers on composites will be discussed.

Curing behaviors and dynamic thermal mechanical properties are first discussed. The reversion process on curing behavior is occurring by carbon black incorporation. This process is discussed in previous section (5.4.5), it depends on type of accelerator and ratio of sulfur/accelerator. The incorporation of carbon black increases M_H and E´ of NR/PALF composites in a different order, depending on the type of surface treatment of PALF. For PALF-filled composites without carbon black, curing behavior is not affected by surface treatment of fiber. Carbon black-filled composites containing silane-treated PALF have highest M_H, whereas hybrid composites containing untreated and alkali-treated PALFs have lower M_H. Thus, there is a combination of reinforcements by carbon black and silane treatment of fiber. Dannenberg reported that carbon black has been used to reinforce a rubber through the strong physical adsorption

of rubber on carbon black, which is known as bound rubber [48]. This bound rubber is strongly adsorbed on carbon black and cannot be extracted by solvent extraction. Hence, the rubber matrix containing carbon black has higher reinforcement effect than without carbon black. When the force is applied to the composite, the force goes from carbon black-filled rubber to fiber through the interface between rubber and PALF. Thus, by silane treatment, the interface between carbon black-filled rubber and PALF is high due to covalent bonds formation. The covalent bonds formation between rubber and fiber does not change T_g of composites. This might be hypothesized from a low amount of silane grafting onto the fiber, comparing to the effect of fillers amount (carbon black and fiber). Thus, changing of interface between NR and PALF cannot be detected by DMTA.

Tensile properties at low strain region of hybrid composites were enhanced by alkali treatment and silane treatment of fibers. The incorporation of APALF significantly increases modulus of composites in the presence of carbon black. This can be explained by higher amount of cellulosic content and the partial removal of binding between individual fibers after treatment, which was discussed in section 5.2. Moreover, it was reported by Roy and co-workers that alkali treatment can be used to increase the strength of jute fiber [147]. The combination of reinforcement effects by fiber alkali treatment and carbon black leads to higher modulus at low strain of composites. However, modulus at low strain region of carbon black-filled composites with SiPALF is lower than those composites filled with APALF. This result is not consistent with composites without carbon black, which SiPALF causes the highest modulus at low strain. It is suggested from the reduction of chemical bonding formation between NR and SiPALF by chemical bonding between sulfur at the surface of SiPALF and carbon black. Sterns and Johnson reported that carbon black can react chemically with the polymer through sulfur bonds [148]. However, the mechanism of this reaction is not well understood due various functional groups on the surface of carbon black. This phenomenon was further confirmed by Rivin and coworkers [149]. Ampoule reaction was carried out by incorporation of carbon black with other curing additives then freeze-thaw, followed by curing at high temperature. The results show that carbon black can be chemically bonded with sulfur. However, sulfur bonding is only one tenth when compare with normal physical adsorption with rubber. From these results, it can

be suggested that most of the sulfur on SiPALF can react with rubber, and few of it reacts with carbon black. The evidence of this reaction will be further confirmed indirectly from the results of tensile properties at high deformation.

Nelson and Hancock reported that yield point on the stress-strain curve appears when the interface between rubber and fiber is fully slipped [150]. After yield point, the friction between rubber and fiber has taken place. Composites containing surface-treated fibers without carbon black have no stress upturn and low tensile strength. By incorporation of carbon black, stress at high deformation is improved and upturn is shifted to higher ultimate strength. This is obtained from the strong interaction between rubber and carbon black. Carbon black-filled composites containing APALF have higher E_{300} and the stress upturn occurs earlier than carbon black-filled composites containing UPALF. This is achieved by better mechanical locking between surface of APALF and rubber, leading to higher friction at the interface. Hybrid composites containing SiPALF has highest modulus at E_{300} and stress upturn occurs earlier due to the better frictional force between three phases of NR, carbon black and SiPALF. NR has strong interactions with carbon black via bound rubber and can co-crosslinking with SiPALF via sulfidic bonds. In addition, carbon black is hypothesized to partial co-crosslink with SiPALF. This is confirmed from the tensile results at low deformation that most of sulfur on the fiber can react with NR, whereas few of it reacts with carbon black. Tensile strength of hybrid composites is not changed by surface treatment of PALF, thus, only carbon black plays a role for reinforcing composite at failure.

5.5.5 Summary

Tensile properties of PALF-reinforced NR can be improved by the surface treatment of fiber and incorporation of carbon black. Carbon black improves the tensile properties of composites from the strong physical adsorption of NR on carbon black. The reinforcing effect of fiber surface treatment is changed by incorporation of carbon black. Alkali treatment increases cellulosic content. Hence, these fibers can be used to improve tensile properties at low strain. By incorporation of carbon black with APALF, tensile properties at high deformation are also improved due to the better mechanical interlocking between them. Silane treatment provides co-crosslinking between NR and SiPALF, which results in better stress transfer between them. By incorporation of

carbon black, tensile properties at high deformation are improved due to the co-crosslinking of SiPALF with both NR and carbon black.

5.6 Comparison between effects of NBR and silane treatment of PALF on mechanical properties of NR/PALF/carbon black hybrid composites

The reinforcing effect by the incorporation of NBR or fiber surface treatment of carbon black/PALF filled NR composites are compared. It should be noted that the composites with the highest improvement of tensile properties, which were studied in the sections 5.4 and 5.5, are chosen. To distinguish the difference between composites properly, the ingredients of composites are listed in Table 5.21.

Table 5.21 Comparison of the ingredients between composites

Composites	Rubber		Fiber			Carbon black
	NR	20NBR	UPALF	APALF	SiPALF	
NR10UP30CB[a]	✓	-	✓	-	-	✓
20NBR10UP30CB[a]	-	✓	✓	-	-	✓
NR10AP30CB[a]	✓	-	-	✓	-	✓
NR10SiP30CB[a]	✓	-	-	-	✓	✓
20NBR10UP30CB-C[b]	-	✓	✓	-	-	✓

[a]: composite mixed by scheme A, [b]: composite mixed by scheme C

The stress-strain curves of these composites are displayed in Figure 5.77 and their tensile properties are shown in Figure 5.78. Composites mixed by scheme A will be first compared. The incorporation of NBR and fiber surface treatment can be used to improve the tensile properties at low deformation of NR/PALF/carbon black hybrid composites in term of Young's modulus and σ_y. E_{10}s of composites are improved by about 60% by NBR or fiber surface treatment, whereas σ_ys of composites containing NBR is improved by 30% and those containing surface-treated PALF is improved by 20%. Young's modulus of composites containing APALF is the highest, whereas

composites containing SiPALF and NBR are lower. This modulus of composites containing SiPALF is similar to composites containing NBR. σ_y of composites with NBR is higher than composites with APALF or SiPALF. Onset upturn stress of hybrid composites does not change by the incorporation of NBR. The upturn stress of composites with APALF and SiPALF are earlier than those of composites. Tensile strength of composites are neither changed by incorporation of NBR nor by fiber surface treatment. Thus, for hybrid composites with the same mixing method, the surface treatment of fibers provides higher tensile properties in term of higher Young's modulus and earlier onset upturn stress than the incorporation of NBR.

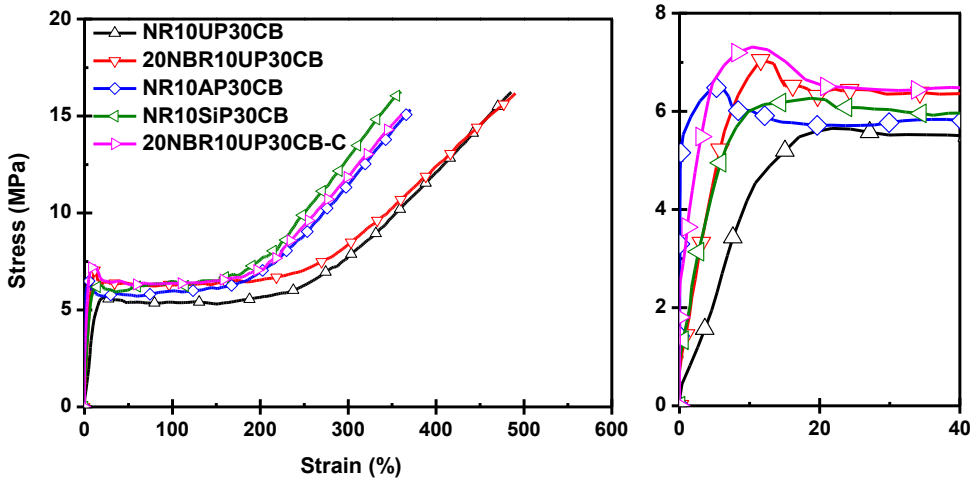

Figure 5.77 Stress-strain curves of NR/PALF composite, NR/PALF/carbon black hybrid composites with the incorporation of NBR and fiber surface treatment

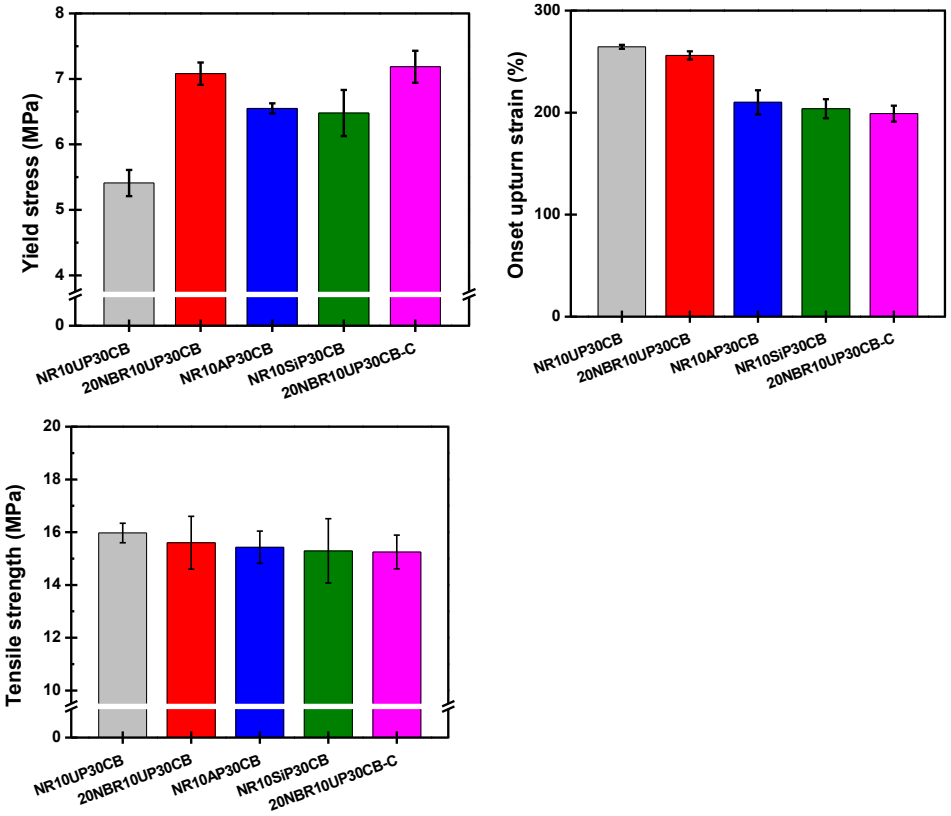

Figure 5.78 E_{10}, σ_y, onset upturn strain and tensile strength of NR/PALF composite, NR/PALF/carbon black hybrid composites with the incorporation of NBR and fiber surface treatment

To improve mechanical performance at high strain and optimize failure at low deformation, the proper mixing is required. By surface treatment of PALF, modulus at low strain and σ_y are improved. However, σ_y of those composites are still lower than that of 20NBR10UP30CB-C. It can be suggested that NBR-encased PALF has higher slippage resistance at the interface than the treated PALFs. Onset upturn strain of 20NBR10UP30CB-C is similar to those of carbon black/surface-treated PALF-filled composites. Thus, the enhancement of friction between NR and PALF by NBR is similar to surface treatment of PALF. It can be concluded that the tensile properties of NR/PALF can be optimized by incorporation of NBR and carbon black with a proper mixing process. Thus, E_{10}, σ_y, upturn stress and tensile strength can be improved.

CHAPTER VI
CONCLUSIONS

Conclusions of the mechanical properties improvement of NR/PALF composites are listed below:

1. Mechanical properties at low deformation can be improved by incorporation of NBR. NBR is proposed to encase PALF leading to the better stress transfer between NR and PALF. Two-step-mixed NR/NBR/PALF composites results in earlier upturn stress, whereas single-step-mixed composites does not provide the same level of improvement.

2. Alkali treatment can be used as a pretreatment on fiber. The cellulosic content of PALF increased leading to the enhancement of mechanical properties of composites. The mechanical properties of NR/PALF are further improved by silane treatment. Silane-69 treatment provides free sulfur for crosslinking with NR during vulcanization, which is used to enhance the interfacial stress between them. The optimum condition is using silane-69 for treatment at concentration of 3 wt% of PALF using washing method. Pure ethanol is used as a solvent.

3. Mechanical properties at high deformation of NR/PALF composites could be improved by incorporation of carbon black. This is due to the strong physical adsorption between them. By combination of PALF and carbon black, the tensile properties at both low and high strains can be improved.

4. The incorporation of NBR into NR/PALF/carbon black hybrid composites improves mechanical properties at low strain. To achieve the optimum improvement, it is important that NBR encases PALF properly while carbon black distributes mainly in NR matrix phase. To control the distribution of fillers in rubber blends, two masterbatches of NR with carbon black and NBR with PALF are prepared first. The two masterbatches are then diluted in NR matrix to get the required contents for each component.

5. Fibers surface treatment also improves the mechanical properties of NR/PALF/carbon black hybrid composites. By incorporation of APALF, mechanical properties are improved by the higher cellulosic content and mechanical interlocking between carbon black-filled NR and fibers. By incorporation of SiPALF, mechanical properties are improved by the co-crosslinking between SiPALF with both NR and carbon black.

Suggestion for the future work

1. To achieve the opportunity in the industrial applications, composites containing Kevlar will be produced in order to compare with composites containing PALF. As we know that Kevlar is a para-aramid synthetic fiber, its mechanical properties are high compared to PALF. Thus, the improvement of stress transfer by incorporation of NBR or fiber surface treatment will be used to reach the optimum properties of NR/PALF composites.

2. In this study, the mixing of NR/PALF composites cannot break all bundle of fibers into elementary fibers. In the future work, bundle of fibers will be broken before mixing. The homogenizer can be used in this method. If the elementary fibers can be achieved, the L/D ratio of fibers will be higher. Thus, the mechanical properties of composites will be improved.

3. To understand more about PALF, the geometry, biological structure, mechanical properties of fibers will be studied. This knowledge will be used to relate with the fibers reinforcement in this work and also in the future work.

REFERENCES

[1] "Vehicle and tyre." [Online]. Available: http://www.therubbereconomist.com/The_Rubber_Economist/Vehicle_and_tyre.html. [Accessed: 02-Nov-2016].

[2] "How tire is made - material, history, used, processing, parts, components, composition, steps, product." [Online]. Available: http://www.madehow.com/Volume-1/Tire.html. [Accessed: 02-Nov-2016].

[3] "Viking - footwear from natural rubber." [Online]. Available: https://www.vikingfootwear.com/natural-rubber-1.aspx. [Accessed: 02-Nov-2016].

[4] "Natural World Eco .:. Vision." [Online]. Available: http://www.naturalworldeco.com/index.php/vision/en [Accessed: 02-Nov-2016].

[5] "Natural Rubber Heat Resistant Rubber Conveyor Belt," *Made-in-China.com*. [Online]. Available: http://nbhyxj.en.made-in-china.com/product/rvixbDzKCYcC/China-Natural-Rubber-Heat-Resistant-Rubber-Conveyor-Belt.html. [Accessed: 02-Nov-2016].

[6] "Conveyor belts and essential accessories," *Muller Beltex*. .

[7] "BTE - Products - Conveyor belts - Natural Rubber." [Online]. Available: http://www.bandtransporteurope.nl/products/conveyor-belts/natural-rubber. [Accessed: 02-Nov-2016].

[8] H.-H. Greve, "Rubber, 2. Natural," in *Ullmann's Encyclopedia of Industrial Chemistry*, Wiley-VCH Verlag GmbH & Co. KGaA, 2000.

[9] S.-N. Gan, "Storage Hardening of Natural Rubber," *J. Macromol. Sci. Part A*, vol. 33, no. 12, pp. 1939–1948, Dec. 1996.

[10] T. Kakubo, A. Matsuura, S. Kawahara, and Y. Tanaka, “Origin of Characteristic Properties of Natural Rubber—Effect of Fatty Acids on Crystallization of cis-1,4-Polyisoprene,” *Rubber Chem. Technol.*, vol. 71, no. 1, pp. 70–75, Mar. 1998.

[11] S. Kawahara, Y. Isono, T. Kakubo, Y. Tanaka, and E. Aik-Hwee, “Crystallization Behavior and Strength of Natural Rubber Isolated from Different Hevea Clone,” *Rubber Chem. Technol.*, vol. 73, no. 1, pp. 39–46, Mar. 2000.

[12] E. A. Hwee, “CHAPTER 3 Non-Rubbers and Abnormal Groups in Natural Rubber,” in *Natural Rubber Materials: Volume 1: Blends and IPNs*, vol. 1, The Royal Society of Chemistry, 2014, pp. 53–72.

[13] B. Westall, “The molecular weight distribution of natural rubber latex,” *Polymer*, vol. 9, pp. 243–248, Jan. 1968.

[14] G. Markovic, M. Marinovic-Cincovic, V. Jovanovic, S. Samarzija-Jovanovic, and J. Budinski-Simendic, “CHAPTER 1 Natural Rubber Based Blends and IPNs: State of the Art, New Challenges and Opportunities,” in *Natural Rubber Materials: Volume 1: Blends and IPNs*, vol. 1, The Royal Society of Chemistry, 2014, pp. 1–27.

[15] A. Y. Coran, “7 - Vulcanization A2 - Mark, James E.,” in *Science and Technology of Rubber (Third Edition)*, B. Erman and F. R. Eirich, Eds. Burlington: Academic Press, 2005, pp. 321–366.

[16] O. Chaikumpollert, Y. Yamamoto, K. Suchiva, and S. Kawahara, “Mechanical properties and cross-linking structure of cross-linked natural rubber,” *Polym J*, vol. 44, no. 8, pp. 772–777, Aug. 2012.

[17] D. C. Grimm, *Method for the production of nitrile rubber*. Google Patents, 1998.

[18] K. Prukkaewkanjana and T. Amornsakchai, “An anomalous reinforcement of ordinarily weak synthetic rubber,” *J. Polym. Res.*, vol. 22, no. 8, pp. 1–6, 2015.

[19] M. H. R. Ghoreishy, M. Rafei, and G. Naderi, “Optimization of the vulcanization process of a thick rubber article using an advanced computer simulation technique,” *Rubber Chem. Technol.*, vol. 85, no. 4, pp. 576–589, Dec. 2012.

[20] Z. Man, L. Deng, M. Yang, Y. Chen, and Z. Jin, “Effect of in situ surface modified nano-zinc oxide on the structure and properties of conventional vulcanization in natural rubber,” *Rubber Chem. Technol.*, vol. 87, no. 1, pp. 21-30, Sep. 2013.

[21] M. Anandhan, N. S. Kaisare, K. Kannan, and B. Varkey, “Population balance model for vulcanization of natural rubber with delayed-action accelerator and prevulcanization inhibitor,” *Rubber Chem. Technol.*, vol. 85, no. 2, pp. 219–243, Jun. 2012.

[22] N. J. Morrison and M. Porter, “Temperature Effects on the Stability of Intermediates and Crosslinks in Sulfur Vulcanization,” *Rubber Chem. Technol.*, vol. 57, no. 1, pp. 63–85, Mar. 1984.

[23] C. G. Moore and M. Porter, “Structural Characterization of Natural Rubber Vulcanizates,” *Rubber Chem. Technol.*, vol. 36, no. 2, pp. 547–557, May 1963.

[24] “Cure measurement as quality tool.” [Online]. Available: https://rubbertech.wordpress.com/2013/08/02/cure-measurement/ [Accessed: 30-Nov-2016].

[25] C. T. Loo, “High temperature vulcanization of elastomers: 2. Network structures in conventional sulphenamide-sulphur natural rubber vulcanizates,” *Polymer*, vol. 15, no. 6, pp. 357–365, Jun. 1974.

[26] R. Mukhopadhyay, S. K. De, and S. N. Chakraborty, “Effect of vulcanization temperature and vulcanization systems on the structure and properties of natural rubber vulcanizates,” *Polymer*, vol. 18, no. 12, pp. 1243–1249, Dec. 1977.

[27] Z. Bei-Long, W. Yong-Zhou, W. Ping-Yue, and H. Hong-Hai, “Study on vulcanization kinetics of constant viscosity natural rubber by using a

rheometer MDR2000," *J. Appl. Polym. Sci.*, vol. 130, no. 1, pp. 47–53, 2013.

[28] L. Bateman, *The Chemistry and Physics of Rubber-Like Substances*. New York: Wiley, 1963.

[29] M. V. Lewan, "NR/NBR blends — basic problems and solutions," in *Blends of Natural Rubber: Novel Techniques for Blending with Speciality Polymers*, A. J. Tinker and K. P. Jones, Eds. Dordrecht: Springer Netherlands, 1998, pp. 53–67.

[30] C. Sirisinha, S. Limcharoen, and J. Thunyarittikorn, "Oil resistance controlled by phase morphology in natural rubber/nitrile rubber blends," *J. Appl. Polym. Sci.*, vol. 87, no. 1, pp. 83–89, 2003.

[31] U. Šebenik, A. Zupančič-Valant, and M. Krajnc, "Investigation of rubber–rubber blends miscibility," *Polym. Eng. Sci.*, vol. 46, no. 11, pp. 1649–1659, 2006.

[32] G. M. Bartenev and G. S. Kongarov, "Dilatometric Determination of Polymer Compatibility," *Rubber Chem. Technol.*, vol. 36, no. 3, pp. 668–674, 1963.

[33] A. J. Tinker, "Crosslink Distribution and Interfacial Adhesion in Vulcanized Blends of NR and NBR," *Rubber Chem. Technol.*, vol. 63, no. 4, pp. 503–515, 1990.

[34] P. Kueseng, P. Sae-oui, and N. Rattanasom, "Mechanical and electrical properties of natural rubber and nitrile rubber blends filled with multi-wall carbon nanotube: Effect of preparation methods," *Polym. Test.*, vol. 32, no. 4, pp. 731–738, Jun. 2013.

[35] C. A. Cruz, D. R. Paul, and J. W. Barlow, "Polyester–Polycarbonate blends. IV. Poly(ε-caprolactone)," *J. Appl. Polym. Sci.*, vol. 23, no. 2, pp. 589–600, 1979.

[36] M. L. Huggins, “The Solubility of Nonelectrolytes. By Joel H. Hildebrand and Robert S. Scott.,” *J. Phys. Chem.*, vol. 55, no. 4, pp. 619–620, Apr. 1951.

[37] M. J. Forrest, *Rubber Analysis: Polymers, Compounds and Products*.

[38] S. Y. Hobbs and V. H. Watkins, “The use of chemical contrast in the SEM analysis of polymer blends,” *J. Polym. Sci. Polym. Phys. Ed.*, vol. 20, no. 4, pp. 651–658, 1982.

[39] T. Shiibashi and Jarunee, “Gel structure characterization of NR and IR and direct observation of individual polymer molecules by electron microscopy,” *Int. Polym. Sci. Technol.*, vol. 14, no. 12, p. T/33-T/39, 1987.

[40] M. J. R. Loadman and A. J. Tinker, “The Application of Swollen-State CW-1H NMR Spectroscopy to the Estimation of the Extent of Crosslinking in Vulcanized Polymer Blends,” *Rubber Chem. Technol.*, vol. 62, no. 2, pp. 234–245, May 1989.

[41] J. Wootthikanokkhan and B. Tongrubbai, “A study on morphology and physical properties of natural–acrylic rubber blends,” *J. Appl. Polym. Sci.*, vol. 86, no. 7, pp. 1532–1539, 2002.

[42] J. M. Massie, R. C. Hirst, and A. F. Halasa, “Carbon Black Distribution in NR/Polybutadiene Blends,” *Rubber Chem. Technol.*, vol. 66, no. 2, pp. 276–285, May 1993.

[43] J. Wootthikanokkhan and N. Rattanathamwat, “Distribution of carbon black in natural rubber/acrylic rubber blends,” *J. Appl. Polym. Sci.*, vol. 102, no. 1, pp. 248–256, 2006.

[44] D. Edirisinghe and P. Freakley, “Effect of varied carbon black distribution on the morphology and properties of blends of natural and nitrile rubber,” *J. Rubber Res. Inst. Sri Lanka*, vol. 86, p. 58, 2003.

[45] B.-L. Lee and C. Singleton, “Experimental study of the relationship of processing to the morphology in blends of SBR and cis-polybutadiene with carbon black,” *J. Appl. Polym. Sci.*, vol. 24, no. 10, pp. 2169–2183, 1979.

[46] B.-L. Lee, “Flow of carbon black loaded styrene-butadiene (SBR)-cis-polybutadiene blends through capillary dies—influence of mixing and the location of carbon black,” *Polym. Eng. Sci.*, vol. 21, no. 5, pp. 294–300, 1981.

[47] A. K. Sircar, T. G. Lamond, and P. E. Pinter, “Effect of Heterogeneous Carbon Black Distribution on the Properties of Polymer Blends,” *Rubber Chem. Technol.*, vol. 47, no. 1, pp. 48–56, Mar. 1974.

[48] E. M. Dannenberg, “Bound Rubber and Carbon Black Reinforcement,” *Rubber Chem. Technol.*, vol. 59, no. 3, pp. 512–524, 1986.

[49] M. Pawlyta, J.-N. Rouzaud, and S. Duber, “Raman microspectroscopy characterization of carbon blacks: Spectral analysis and structural information,” *Carbon*, vol. 84, pp. 479–490, Apr. 2015.

[50] G. Kraus, “Reinforcement of elastomers by carbon black,” *Angew. Makromol. Chem.*, vol. 60, no. 1, pp. 215–248, 1977.

[51] J. L. Leblanc, “A molecular explanation for the origin of bound rubber in carbon black filled rubber compounds,” *J. Appl. Polym. Sci.*, vol. 66, no. 12, pp. 2257–2268, 1997.

[52] S. Kohjiya, A. Katoh, T. Suda, J. Shimanuki, and Y. Ikeda, “Visualisation of carbon black networks in rubbery matrix by skeletonisation of 3D-TEM image,” *Polymer*, vol. 47, no. 10, pp. 3298–3301, May 2006.

[53] S. Kaufman, W. P. Slichter, and D. D. Davis, “Nuclear magnetic resonance study of rubber–carbon black interactions,” *J. Polym. Sci. Part - 2 Polym. Phys.*, vol. 9, no. 5, pp. 829–839, 1971.

[54] Y. Fukahori, “The Mechanics and Mechanism of the Carbon Black Reinforcement of Elastomers,” *Rubber Chem. Technol.*, vol. 76, no. 2, pp. 548–566, May 2003.

[55] S. Wolff, M.-J. Wang, and E.-H. Tan, “Filler-Elastomer Interactions. Part VII. Study on Bound Rubber,” *Rubber Chem. Technol.*, vol. 66, no. 2, pp. 163–177, May 1993.

[56] A. K. Mohanty, M. Misra, and L. T. Drzal, “Sustainable Bio-Composites from Renewable Resources: Opportunities and Challenges in the Green Materials World,” *J. Polym. Environ.*, vol. 10, no. 1, pp. 19–26, 2002.

[57] D. Klemm, B. Heublein, H.-P. Fink, and A. Bohn, “Cellulose: Fascinating Biopolymer and Sustainable Raw Material,” *Angew. Chem. Int. Ed.*, vol. 44, no. 22, pp. 3358–3393, 2005.

[58] A. Bourmaud, C. Morvan, A. Bouali, V. Placet, P. Perré, and C. Baley, “Relationships between micro-fibrillar angle, mechanical properties and biochemical composition of flax fibers,” *Ind. Crops Prod.*, vol. 44, pp. 343–351, Jan. 2013.

[59] A. Lefeuvre, A. Bourmaud, C. Morvan, and C. Baley, “Elementary flax fibre tensile properties: Correlation between stress–strain behaviour and fibre composition,” *Ind. Crops Prod.*, vol. 52, pp. 762–769, Jan. 2014.

[60] “This Gorgeous, Sustainable ‘Leather’ Is Made From Pineapple Waste,” *Co.Exist*, 25-Apr-2016. [Online]. Available: https://www.fastcoexist.com/3059190/this-gorgeous-sustainable-leather-is-made-from-pineapple-waste. [Accessed: 02-Nov-2016].

[61] “Eco-fiber corporate premium gifts from 100% original pineapple leaf fiber Squa,” *imgrum*. [Online]. Available: http://www.imgrum.net/media/1049240176161755761_1904708107. [Accessed: 02-Nov-2016].

[62] “Pinatex - new materials for a new world,” *ananas anam*. [Online]. Available: http://www.ananas-anam.com/pinatex/product-range/. [Accessed: 02-Nov-2016].

[63] N. Kengkhetkit and T. Amornsakchai, “Utilisation of pineapple leaf waste for plastic reinforcement: 1. A novel extraction method for short pineapple leaf fiber,” *Ind. Crops Prod.*, vol. 40, no. 0, pp. 55–61, Nov. 2012.

[64] A. K. Mohanty, M. Misra, and G. Hinrichsen, “Biofibres, biodegradable polymers and biocomposites: An overview,” *Macromol. Mater. Eng.*, vol. 276–277, no. 1, pp. 1–24, 2000.

[65] Q. T. H. Shubhra, “CHAPTER 9 Long and Short Glass Fibre Reinforced Natural Rubber Composites,” in *Natural Rubber Materials: Volume 2: Composites and Nanocomposites*, vol. 2, The Royal Society of Chemistry, 2014, pp. 247–289.

[66] M. Jacob, S. Thomas, and K. T. Varughese, “Mechanical properties of sisal/oil palm hybrid fiber reinforced natural rubber composites,” *Compos. Sci. Technol.*, vol. 64, no. 7–8, pp. 955–965, Jun. 2004.

[67] B. Ellis and G. Welding, *Techniques of polymer science*. London: Society of the Chemical Industry, 1964.

[68] J. E. O’Connor, “Short-Fiber-Reinforced Elastomer Composites,” *Rubber Chem. Technol.*, vol. 50, no. 5, pp. 945–958, Nov. 1977.

[69] C. L. Tucker III and E. Liang, “Stiffness predictions for unidirectional short-fiber composites: Review and evaluation,” *Compos. Sci. Technol.*, vol. 59, no. 5, pp. 655–671, Apr. 1999.

[70] H. L. Cox, “The elasticity and strength of paper and other fibrous materials,” *Br. J. Appl. Phys.*, vol. 3, no. 3, p. 72, 1952.

[71] J. C. H. Affdl and J. L. Kardos, “The Halpin-Tsai equations: A review,” *Polym. Eng. Sci.*, vol. 16, no. 5, pp. 344–352, 1976.

[72] A. G. Facca, M. T. Kortschot, and N. Yan, “Predicting the elastic modulus of natural fibre reinforced thermoplastics,” *Compos. Part Appl. Sci. Manuf.*, vol. 37, no. 10, pp. 1660–1671, Oct. 2006.

[73] V. G. Geethamma, R. Joseph, and S. Thomas, “Short coir fiber-reinforced natural rubber composites: Effects of fiber length, orientation, and alkali treatment,” *J. Appl. Polym. Sci.*, vol. 55, no. 4, pp. 583–594, 1995.

[74] N. Lopattananon, K. Panawarangkul, K. Sahakaro, and B. Ellis, “Performance of pineapple leaf fiber–natural rubber composites: The effect of fiber surface treatments,” *J. Appl. Polym. Sci.*, vol. 102, no. 2, pp. 1974–1984, 2006.

[75] L. Mathew and R. Joseph, “Mechanical properties of short-isora-fiber-reinforced natural rubber composites: Effects of fiber length, orientation, and loading; alkali treatment; and bonding agent,” *J. Appl. Polym. Sci.*, vol. 103, no. 3, pp. 1640–1650, 2007.

[76] U. Wisittanawat, S. Thanawan, and T. Amornsakchai, “Mechanical properties of highly aligned short pineapple leaf fiber reinforced – Nitrile rubber composite: Effect of fiber content and Bonding Agent,” *Polym. Test.*, vol. 35, no. 0, pp. 20–27, May 2014.

[77] H. Dressler, “The Use of Resorcinol in Rubber Compositions,” in *Resorcinol: Its Uses and Derivatives*, Boston, MA: Springer US, 1994, pp. 59–83.

[78] G. C. Derringer, “Short Fiber-Elastomer Composites,” *J. Elastomers Plast.*, vol. 3, no. 4, pp. 230–248, Oct. 1971.

[79] H. Ismail, N. Rosnah, and H. D. Rozman, “Effects of various bonding systems on mechanical properties of oil palm fibre reinforced rubber composites,” *Eur. Polym. J.*, vol. 33, no. 8, pp. 1231–1238, Aug. 1997.

[80] L. Mathew, J. Ulahannan, and R. Joseph, “Effect of curing temperature, fibre loading and bonding agent on the equilibrium swelling of isora-natural rubber composites,” *Compos. Interfaces*, vol. 13, no. 4–6, pp. 391–401, Jan. 2006.

[81] C. S. L. Baker, I. R. Gelling, and R. Newell, “Epoxidized Natural Rubber,” *Rubber Chem. Technol.*, vol. 58, no. 1, pp. 67–85, Mar. 1985.

[82] V. Tanrattanakul, B. Wattanathai, A. Tiangjunya, and P. Muhamud, “In situ epoxidized natural rubber: Improved oil resistance of natural rubber,” *J. Appl. Polym. Sci.*, vol. 90, no. 1, pp. 261–269, 2003.

[83] H. Ismail, A. Rusli, and A. A. Rashid, “The Effect of Filler Loading and Epoxidation on Paper-Sludge-Filled Natural Rubber Composites,” *Polym.-Plast. Technol. Eng.*, vol. 45, no. 4, pp. 519–525, May 2006.

[84] C. Nakason, S. Saiwaree, S. Tatun, and A. Kaesaman, “Rheological, thermal and morphological properties of maleated natural rubber and its reactive blending with poly(methyl methacrylate),” *Polym. Test.*, vol. 25, no. 5, pp. 656–667, Aug. 2006.

[85] Z. Zeng, W. Ren, C. Xu, W. Lu, Y. Zhang, and Y. Zhang, “Maleated natural rubber prepared through mechanochemistry and its coupling effects on natural rubber/cotton fiber composites,” *J. Polym. Res.*, vol. 17, no. 2, pp. 213–219, 2010.

[86] C. Nakason, S. Saiwari, and A. Kaesaman, “Rheological properties of maleated natural rubber/polypropylene blends with phenolic modified polypropylene and polypropylene-g-maleic anhydride compatibilizers,” *Polym. Test.*, vol. 25, no. 3, pp. 413–423, May 2006.

[87] C. Nakason, A. Kaesaman, Z. Samoh, S. Homsin, and S. Kiatkamjornwong, “Rheological properties of maleated natural rubber and natural rubber blends,” *Polym. Test.*, vol. 21, no. 4, pp. 449–455, 2002.

[88] H. Ismail, A. Rusli, and A. A. Rashid, “Maleated natural rubber as a coupling agent for paper sludge filled natural rubber composites,” *Polym. Test.*, vol. 24, no. 7, pp. 856–862, Oct. 2005.

[89] W. Wongsorat, N. Suppakarn, and K. Jarukumjorn, “Effects of compatibilizer type and fiber loading on mechanical properties and cure characteristics of sisal fiber/natural rubber composites,” *J. Compos. Mater.*, vol. 48, no. 19, pp. 2401–2411, 2014.

[90] H. Yan, K. Sun, Y. Zhang, and Y. Zhang, “Effect of nitrile rubber on properties of silica-filled natural rubber compounds,” *Polym. Test.*, vol. 24, no. 1, pp. 32–38, Feb. 2005.

[91] B. Wang, S. Panigrahi, L. Tabil, and W. Crerar, “Pre-treatment of Flax Fibers for use in Rotationally Molded Biocomposites,” *J. Reinf. Plast. Compos.*, vol. 26, no. 5, pp. 447–463, 2007.

[92] X. Li, L. G. Tabil, and S. Panigrahi, “Chemical Treatments of Natural Fiber for Use in Natural Fiber-Reinforced Composites: A Review,” *J. Polym. Environ.*, vol. 15, no. 1, pp. 25–33, 2007.

[93] A. Valadez-Gonzalez, J. M. Cervantes-Uc, R. Olayo, and P. J. Herrera-Franco, “Effect of fiber surface treatment on the fiber–matrix bond strength of natural fiber reinforced composites,” *Compos. Part B Eng.*, vol. 30, no. 3, pp. 309–320, Apr. 1999.

[94] A. Nopparut and T. Amornsakchai, “Influence of pineapple leaf fiber and it’s surface treatment on molecular orientation in, and mechanical properties of, injection molded nylon composites,” *Polym. Test.*, vol. 52, pp. 141–149, Jul. 2016.

[95] M. S. Sreekala, M. G. Kumaran, S. Joseph, M. Jacob, and S. Thomas, “Oil Palm Fibre Reinforced Phenol Formaldehyde Composites: Influence of Fibre Surface Modifications on the Mechanical Performance,” *Appl. Compos. Mater.*, vol. 7, no. 5, pp. 295–329, 2000.

[96] D. Ray, B. K. Sarkar, A. K. Rana, and N. R. Bose, “Effect of alkali treated jute fibres on composite properties,” *Bull. Mater. Sci.*, vol. 24, no. 2, pp. 129–135, 2001.

[97] L. Y. Mwaikambo, N. Tucker, and A. J. Clark, “Mechanical Properties of Hemp-Fibre-Reinforced Euphorbia Composites,” *Macromol. Mater. Eng.*, vol. 292, no. 9, pp. 993–1000, 2007.

[98] V. G. Geethamma, K. Thomas Mathew, R. Lakshminarayanan, and S. Thomas, “Composite of short coir fibres and natural rubber: effect of chemical modification, loading and orientation of fibre,” *Polymer*, vol. 39, no. 6, pp. 1483–1491, Jan. 1998.

[99] W. Wongsorat, N. Suppakarn, and K. Jarukumjorn, “Sisal Fiber/Natural Rubber Composites: Effect of Fiber Content and Interfacial Modification,” *Adv. Mater. Res.*, vol. 410, pp. 63–66, 2012.

[100] H. F. Wu, D. W. Dwight, and N. T. Huff, “Effects of silane coupling agents on the interphase and performance of glass-fiber-reinforced

polymer composites," *6th Int. Conf. Compos. Interfaces*, vol. 57, no. 8, pp. 975–983, 1997.

[101] B. D. Favis, M. Leclerc, and R. E. Prud'Homme, "Coupling of polystyrene to a silane-treated mica," *J. Appl. Polym. Sci.*, vol. 28, no. 11, pp. 3565–3572, 1983.

[102] Y. Xie, C. A. S. Hill, Z. Xiao, H. Militz, and C. Mai, "Silane coupling agents used for natural fiber/polymer composites: A review," *Compos. Part Appl. Sci. Manuf.*, vol. 41, no. 7, pp. 806–819, Jul. 2010.

[103] M. Abdelmouleh, S. Boufi, A. ben Salah, M. N. Belgacem, and A. Gandini, "Interaction of Silane Coupling Agents with Cellulose," *Langmuir*, vol. 18, no. 8, pp. 3203–3208, Apr. 2002.

[104] P. K. Pal and S. K. De, "Studies on peroxide vulcanization of silica-filled EPDM rubber in presence of vinyl silane coupling agent," *Polymer*, vol. 25, no. 6, pp. 855–862, Jun. 1984.

[105] M. Hughes, J. Carpenter, and C. Hill, "Deformation and fracture behaviour of flax fibre reinforced thermosetting polymer matrix composites," *J. Mater. Sci.*, vol. 42, no. 7, pp. 2499–2511, 2007.

[106] C. A. S. Hill and H. P. S. Abdul Khalil, "Effect of fiber treatments on mechanical properties of coir or oil palm fiber reinforced polyester composites," *J. Appl. Polym. Sci.*, vol. 78, no. 9, pp. 1685–1697, 2000.

[107] A. Ansarifar, F. Saeed, S. Ostad Movahed, L. Wang, K. Ansar Yasin, and S. Hameed, "Using a sulfur-bearing silane to improve rubber formulations for potential use in industrial rubber articles," *J. Adhes. Sci. Technol.*, vol. 27, no. 4, pp. 371–384, Feb. 2013.

[108] J. W. te. Brinke, S. C. Debnath, L. A. E. M. Reuvekamp, and J. W. M. Noordermeer, "Mechanistic aspects of the role of coupling agents in silica–rubber composites," *NANO- MICRO-Compos. Proc. Symp. N 2002 E-MRS SPRING Meet. JUNE 18-21*, vol. 63, no. 8, pp. 1165–1174, Jun. 2003.

[109] H. Dohi and S. Horiuchi, “Locating a Silane Coupling Agent in Silica-Filled Rubber Composites by EFTEM,” *Langmuir*, vol. 23, no. 24, pp. 12344–12349, Nov. 2007.

[110] S.-S. Choi, I.-S. Kim, and C.-S. Woo, “Influence of TESPT content on crosslink types and rheological behaviors of natural rubber compounds reinforced with silica,” *J. Appl. Polym. Sci.*, vol. 106, no. 4, pp. 2753–2758, 2007.

[111] Z. Zeng, W. Ren, C. Xu, W. Lu, Y. Zhang, and Y. Zhang, “Effect of bis(3-triethoxysilylpropyl) tetrasulfide on the crosslink structure, interfacial adhesion, and mechanical properties of natural rubber/cotton fiber composites,” *J. Appl. Polym. Sci.*, vol. 111, no. 1, pp. 437–443, 2009.

[112] A. Ashori, A. Nourbakhsh, and A. K. Tabrizi, “Thermoplastic Hybrid Composites using Bagasse, Corn Stalk and E-glass Fibers: Fabrication and Characterization,” *Polym.-Plast. Technol. Eng.*, vol. 53, no. 1, pp. 1–8, Jan. 2014.

[113] S.-Y. Fu and B. Lauke, “Characterization of tensile behaviour of hybrid short glass fibre/calcite particle/ABS composites,” *Compos. Part Appl. Sci. Manuf.*, vol. 29, no. 5–6, pp. 575–583, 1998.

[114] R. Jumaidin, S. M. Sapuan, M. Jawaid, M. R. Ishak, and J. Sahari, “Thermal, mechanical, and physical properties of seaweed/sugar palm fibre reinforced thermoplastic sugar palm Starch/Agar hybrid composites,” *Int. J. Biol. Macromol.*, vol. 97, pp. 606–615, Apr. 2017.

[115] N. Lopattananon, D. Jitkalong, and M. Seadan, “Hybridized reinforcement of natural rubber with silane-modified short cellulose fibers and silica,” *J. Appl. Polym. Sci.*, vol. 120, no. 6, pp. 3242–3254, 2011.

[116] U. Wisittanawat, S. Thanawan, and T. Amornsakchai, “Remarkable improvement of failure strain of preferentially aligned short pineapple leaf fiber reinforced nitrile rubber composites with silica hybridization,” *Polym. Test.*, vol. 38, no. 0, pp. 91–99, Sep. 2014.

[117] K. Prukkaewkanjana, S. Thanawan, and T. Amornsakchai, “High performance hybrid reinforcement of nitrile rubber using short pineapple leaf fiber and carbon black,” *Polym. Test.*, vol. 45, pp. 76–82, Aug. 2015.

[118] P. Pittayavinai, S. Thanawan, and T. Amornsakchai, “Manipulation of mechanical properties of short pineapple leaf fiber reinforced natural rubber composites through variations in cross-link density and carbon black loading,” *Polym. Test.*, vol. 54, pp. 84–89, Sep. 2016.

[119] K. Prukkaewkanjana, S. Thanawan, and T. Amornsakchai, “High performance hybrid reinforcement of nitrile rubber using short pineapple leaf fiber and carbon black,” *Polym. Test.*, vol. 45, no. 0, pp. 76–82, Aug. 2015.

[120] “The Bernasek Lab.” [Online]. Available: http://chemists.princeton.edu/bernasek/. [Accessed: 21-Jul-2016].

[121] H. Yan, K. Sun, Y. Zhang, and Y. Zhang, “Effect of nitrile rubber on properties of silica-filled natural rubber compounds,” *Polym. Test.*, vol. 24, no. 1, pp. 32–38, Feb. 2005.

[122] N. Clythong and J. Wootthikanokkhan, “Effects of Accelerator Type and Curing Temperature on Crosslink Distributions and Tensile Properties of Natural-Acrylic Rubber Blends,” *Rubber Chem. Technol.*, vol. 76, no. 5, pp. 1116–1127, Nov. 2003.

[123] K. Sahakaro, C. Pongpaiboon, and C. Nakason, “Improved mechanical properties of NR/EPDM blends by controlling the migration of curative and filler via reactive processing technique,” *J. Appl. Polym. Sci.*, vol. 111, no. 4, pp. 2035–2043, 2009.

[124] A. V. Chapman and A. J. Tinker, “Vulcanization of blends - Crosslink Distribution and its Effect on Properties,” *Kautsch. Gummi Kunststoffe*, vol. 56, no. 10, pp. 533–544.

[125] M. Kader, W. Kim, S. Kaang, and C. Nah, “Morphology and dynamic mechanical properties of natural rubber/nitrile rubber blends containing

trans-polyoctylene rubber as a compatibilizer," *Polym. Int.*, vol. 54, no. 1, pp. 120–129, 2005.

[126] N. A. M. Nor and N. Othman, "Effect of Filler Loading on Curing Characteristic and Tensile Properties of Palygorskite Natural Rubber Nanocomposites," *5th Int. Conf. Recent Adv. Mater. Miner. Environ. RAMM 2nd Int. Postgrad. Conf. Mater. Miner. Polym. MAMIP*, vol. 19, pp. 351–358, Jan. 2016.

[127] F. M. Helaly, S. H. El Sabbagh, O. S. El Kinawy, and S. M. El Sawy, "Effect of synthesized zinc stearate on the properties of natural rubber vulcanizates in the absence and presence of some fillers," *Mater. Des.*, vol. 32, no. 5, pp. 2835–2843, May 2011.

[128] H. Hantsche, "High resolution XPS of organic polymers, the scienta ESCA300 database," *Adv. Mater.*, vol. 5, no. 10, pp. 778–778, 1993.

[129] L. Q. N. Tran, C. A. Fuentes, C. Dupont-Gillain, A. W. Van Vuure, and I. Verpoest, "Wetting analysis and surface characterisation of coir fibres used as reinforcement for composites," *Colloids Surf. Physicochem. Eng. Asp.*, vol. 377, no. 1–3, pp. 251–260, Mar. 2011.

[130] E. Adler, "Lignin chemistry—past, present and future," *Wood Sci. Technol.*, vol. 11, no. 3, pp. 169–218, 1977.

[131] M. S. Islam, K. L. Pickering, and N. J. Foreman, "Influence of Hygrothermal Ageing on the Physico-Mechanical Properties of Alkali Treated Industrial Hemp Fibre Reinforced Polylactic Acid Composites," *J. Polym. Environ.*, vol. 18, no. 4, pp. 696–704, 2010.

[132] M. de F. V. Marques, R. P. Melo, R. da S. Araujo, J. do N. Lunz, and V. de O. Aguiar, "Improvement of mechanical properties of natural fiber–polypropylene composites using successive alkaline treatments," *J. Appl. Polym. Sci.*, vol. 132, no. 12, p. n/a-n/a, 2015.

[133] M. K. Thakur, R. K. Gupta, and V. K. Thakur, "Surface modification of cellulose using silane coupling agent," *Carbohydr. Polym.*, vol. 111, pp. 849–855, Oct. 2014.

[134] P. Muensri, T. Kunanopparat, P. Menut, and S. Siriwattanayotin, “Effect of lignin removal on the properties of coconut coir fiber/wheat gluten biocomposite,” *Compos. Part Appl. Sci. Manuf.*, vol. 42, no. 2, pp. 173–179, Feb. 2011.

[135] F. Zhou, G. Cheng, and B. Jiang, “Effect of silane treatment on microstructure of sisal fibers,” *Appl. Surf. Sci.*, vol. 292, pp. 806–812, Feb. 2014.

[136] M. S. Huda, W. F. Schmidt, M. Misra, and L. T. Drzal, “Effect of fiber surface treatment of poultry feather fibers on the properties of their polymer matrix composites,” *J. Appl. Polym. Sci.*, vol. 128, no. 2, pp. 1117–1124, 2013.

[137] A. Valadez-Gonzalez, J. M. Cervantes-Uc, R. Olayo, and P. J. Herrera-Franco, “Effect of fiber surface treatment on the fiber–matrix bond strength of natural fiber reinforced composites,” *Compos. Part B Eng.*, vol. 30, no. 3, pp. 309–320, Apr. 1999.

[138] M. Abdelmouleh, S. Boufi, M. N. Belgacem, and A. Dufresne, “Short natural-fibre reinforced polyethylene and natural rubber composites: Effect of silane coupling agents and fibres loading,” *Compos. Sci. Technol.*, vol. 67, no. 7–8, pp. 1627–1639, Jun. 2007.

[139] S.-H. Chough and D.-H. Chang, “Kinetics of sulfur vulcanization of NR, BR, SBR, and their blends using a rheometer and DSC,” *J. Appl. Polym. Sci.*, vol. 61, no. 3, pp. 449–454, 1996.

[140] E. R. Pohl and F. D. Osterholtz, “Kinetics and Mechanism of Aqueous Hydrolysis and Condensation of Alkyltrialkoxysilanes,” in *Molecular Characterization of Composite Interfaces*, H. Ishida and G. Kumar, Eds. Boston, MA: Springer US, 1985, pp. 157–170.

[141] B. Zhong, Z. Jia, Y. Luo, D. Jia, and F. Liu, “Understanding the effect of filler shape induced immobilized rubber on the interfacial and mechanical strength of rubber composites,” *Polym. Test.*, vol. 58, pp. 31–39, Apr. 2017.

[142] G. R. Cotten, “Mixing of Carbon Black with Rubber. II. Mechanism of Carbon Black Incorporation,” *Rubber Chem. Technol.*, vol. 58, no. 4, pp. 774–784, Sep. 1985.

[143] M. L. Studebaker, “The Chemistry of Carbon Black and Reinforcement,” *Rubber Chem. Technol.*, vol. 30, no. 5, pp. 1400–1483, Nov. 1957.

[144] S.-S. Choi, B.-H. Park, S.-G. Lee, and B.-T. Kim, “Binary Cure Systems of 1,6-Bis(N,N’-dibenzylthiocarbamoyldithio)-hexane and Benzothiazole Sulfenamides in Carbon Black-filled Natural Rubber Compounds,” *Bull. Korean Chem. Soc.*, vol. 23, no. 2, pp. 320–324, Nov. 2001.

[145] G. R. Hamed and K. Boonkerd, “Effect of cure efficiency on properties of gum and black filled natural rubber vulcanizates,” *Rubber Chem. Technol.*, vol. 84, no. 2, pp. 229–242, Jun. 2011.

[146] Z. Chen and W. Yan, “A shear-lag model with a cohesive fibre–matrix interface for analysis of fibre pull-out,” *Mech. Mater.*, vol. 91, Part 1, pp. 119–135, Dec. 2015.

[147] A. Roy, S. Chakraborty, S. P. Kundu, R. K. Basak, S. Basu Majumder, and B. Adhikari, “Improvement in mechanical properties of jute fibres through mild alkali treatment as demonstrated by utilisation of the Weibull distribution model,” *Bioresour. Technol.*, vol. 107, pp. 222–228, Mar. 2012.

[148] R. S. Stearns and B. L. Johnson, “Interaction between Carbon Black and Polymer in Cured Elastomers,” *Ind. Eng. Chem.*, vol. 43, no. 1, pp. 146–154, Jan. 1951.

[149] D. Rivin, J. Aron, and A. I. Medalia, “Bonding of Rubber to Carbon Black by Sulfur Vulcanization,” *Rubber Chem. Technol.*, vol. 41, no. 2, pp. 330–343, May 1968.

[150] D. J. Nelson and J. W. Hancock, “Interfacial slip and damping in fibre reinforced composites,” *J. Mater. Sci.*, vol. 13, no. 11, pp. 2429–2440, 1978.

[151] M. Cai *et al.*, “Influence of alkali treatment on internal microstructure and tensile properties of abaca fibers,” *Ind. Crops Prod.*, vol. 65, no. 0, pp. 27–35, Mar. 2015.

[152] P. Garside and P. Wyeth, “Identification of Cellulosic Fibres by FTIR Spectroscopy: Thread and Single Fibre Analysis by Attenuated Total Reflectance,” *Stud. Conserv.*, vol. 48, no. 4, pp. 269–275, 2003.

APPENDIX A
THE DIFFUSION OF CURATIVES BETWEEN NR AND NBR SHEETS

Swelling test was used to study the migration of curing additives of rubber sheet. However, the migration of curing additives should mostly occurs at the interface of rubber sheets. The aim of this study was to try to demonstrate the appearance of a mechanical properties gradient at the interface of two films of NR and NBR vulcanized into contact. Low field ^{1}H-NMR spectroscopy on surface – NMR-MOUSE was used to highlight the migration of curing additives in the view of depth-scanning from side by side.

1.1 Samples Preparation

Pre-sheets of NR and NBR were mixed with curing additives separately and then were attached together and cured. Samples were then detached and analyzed separately. The structure of the interface has been the subject of investigations by surface NMR-MOUSE.

To compare the results, two reference samples have been prepared using the same process but a Mylar film has been introduced at the interface to avoid any migration of additives from one rubber to a second one.

1.2 Technique of characterization:

Samples were characterized by a NMR-Mouse provided by Magritek. The resonant frequency of the system is 27,06 MHz and the used dead time is 9 µs.

1.3 Results

First reference samples of NR and NBR sheet were analysed. After the magnetic field is applied, magnetized spin will relax to the disordered state. $T2_{eff}$ is inversely proportional to crosslink density because polymer chain with lower degree of crosslink density will take more time to be able to move.

The relation of spin density and T_{2eff} versus depth of both separate rubber sheet are shown in Figure A.1. As a reference, the value 0 of the depth corresponds to the contact zone of rubber: interfacial area between both rubbers.

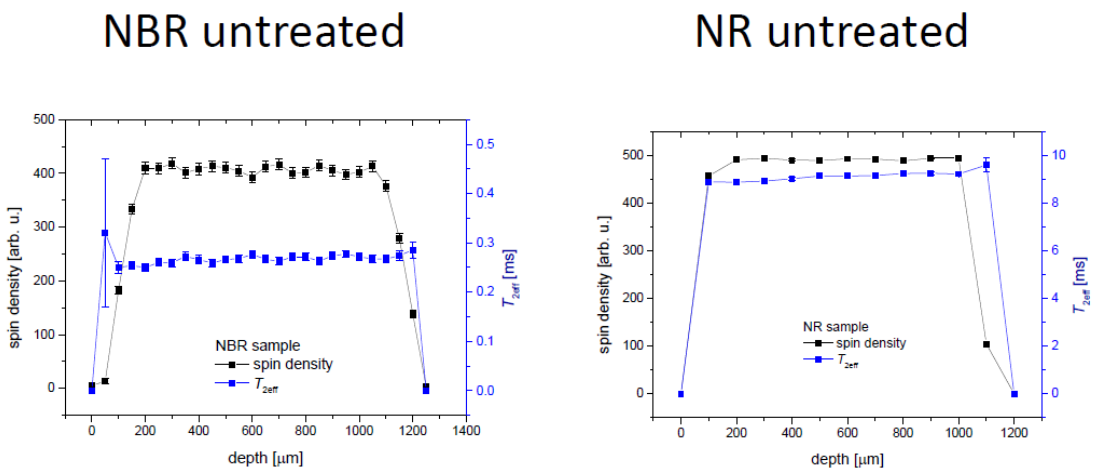

Figure A.1 left) spin density (CPMG sequence) and T_{2eff} graphs corresponding to a single vulcanized NBR sheet; right) spin density (CPMG sequence) and T_{2eff} graphs corresponding to a single NR sheet.

The NR and NBR films, those were vulcanized independently under press, lead to very distinguished results in terms of spin density (CPMG sequence) and T_{2eff} as shown in Figures A.1. T_{2eff} is much lower for NBR than for NR : about 0.27 ms compared to 9 ms indicating a higher rigidity for NBR as expected. In addition, the values are very homogeneous along the profile of the samples.

The spin density gives also homogeneous data all through the samples. No gradient appear along the cross-section of the rubber sheet. To explain this homogeneity of the NMR results, NR and NBR were vulcanized under press and the interface between both elastomers was protected by a Mylar film. Hence, this protecting film has blocked the migration of additives, such as activator, sulfur, and accelerator from one elastomer to the second one.

However, spin density value is slightly lower for NBR than for NR (Figure A.1). This discrepancy can be explained by the presence of the nitrile group on the rubber chain of the NBR that lower the density of proton in NBR compared to NR.

Then, a similar experiment has then been carried out by contacting NR and NBR sheets under press during vulcanization. The NMR profile analysis was displayed in Figure A.2.

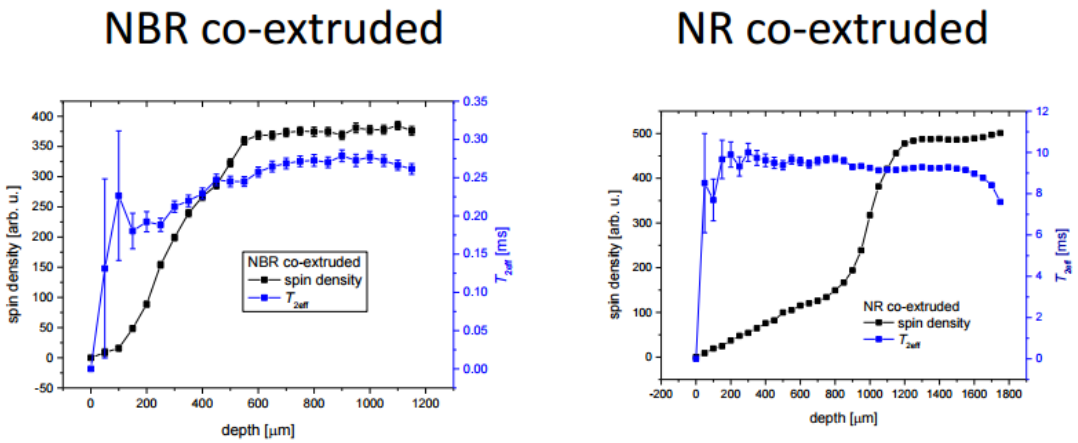

Figure A.2 left) spin density (CPMG sequence) and T_{2eff} graphs corresponding to a vulcanized NBR sheet co-extruded with NR; right) spin density (CPMG sequence) and T_{2eff} graphs corresponding to a NR sheet co-extruded with NBR.

Results of both spin density and T_{2eff} show the presence of a gradient of values along the cross-section of both NR and NBR sheet. However, it seems that the spin density is more affected by the rubber contact during vulcanization.

For NBR, spin density curve increases quite rapidly from the interface to the center of the sheet to reach a plateau value (370)- which is lower than the previous one obtained for non-contacted NBR (420). This low value of spin density at the interface can be due to the presence of additives that have migrated from NR to NBR. Identically, the T_{2eff} curve increases quite slowly from the interface to reach a plateau value of 0.25ms (value slightly lower to the T_{2eff} of non-contacted NBR sheet). This low value of T_{2eff} at the interface indicates a higher rigidity of NBR at the interface compared to the center of the sheet. This phenomenon can then be explained by an accumulation of additives in this zone generating a higher crosslink density compared to the average value at the center of NBR sheet.

For NR, spin density curve increases slowly from the interface to the center of the sheet. The presence of the specific gradient can be attributed to the presence of voids due to the loss of additives in this area. These voids also lead to a decrease of the

number of protons available at the interfacial area. A majority of additives have migrated from NR film to NBR, leading to the presence of nano or macrovoids.

In addition, the T_{2eff} curve of NR indicates a strong increase at the interface down slowly to a slightly lower value in the center of the NR sheet. This high interfacial value indicates the presence of a softer material on the contact zone than in the center of the NR sheet. This decrease of crosslinking density can be explained by a migration of additives to NBR sheet that has reinforced the crosslinking density of NBR at the interface compared to NR one. This migration can be explained by the high affinity of additives with the polar NBR elastomer compared to NR. During the vulcanization process the mobile components, such as accelerator and sulfur will have different diffusion process depending on the local temperature, but also the advancing vulcanization front and the polarities of both rubber. This has nothing to do with the mechanism of chain interdiffusion. As a result, this migration of the additives leads to different ratios of these constituents locally in the thickness of the films. It is well known that these ratios are closely related to the vulcanization state (both in the number of the crosslinking bridges and their length) generating a crosslinking density gradient from the interface of both elastomer o the center.

To conclude, NMR-Mouse test has allowed to highlight the possibility of migration of additives at the interface of NR and NBR sheets. This migration and crosslinking density analysis have been previously carried out and discussed in the chapter by a destructive swelling test. Both destructive test and non-destructive NMR surface characterization have led to the same phenomenon of migration of additives from NBR to NR during vulcanization of rubber sheet in contact. This diffusion process has induced an overcrosslink density of NBR and at the opposite a lower one for NR in the contact interfacial zone of both elastomers.

APPENDIX B
FTIR ANALYSIS OF NR/NBR/PALF COMPOSITES

To study the incorporation of NBR into NR/PALF composites, ATR-FTIR spectroscopy was performed. IR spectra of pure NR (without PALF) and NR/NBR/PALF composites with different NBR content are displayed in Figure B.1. These spectra were first normalized in order to compare with each other spectrum. The intensity of broad signal of hydroxyl and in NR at 3500 to 3100 cm^{-1} increases with the introduction of cellulose, which the signal of O-H stretching overlaps in this region. The appearance of C-O stretching at 1050 cm^{-1} signal is also obtained from the presence of fiber, which contains hydroxyl functional groups as repeating units of cellulose. C≡N stretching signal at 2237 cm^{-1} is characteristic of NBR in the blend. By plotting the relation between NBR content and the intensity of the peak at 2237 cm^{-1}, the linear increase of intensity proportional to NBR content in the composite is observed. Ge crystal diameter is 2 mm, thus, NBR is well-dispersed in NR in this scale.

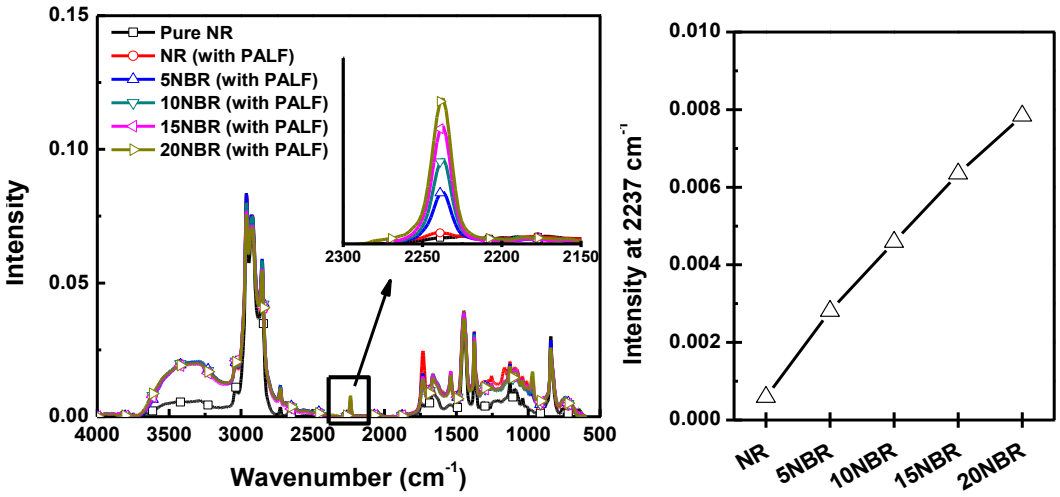

Figure B.1 FTIR spectra of NR without PALF and NR/PALF composites with NBR content 0, 5, 10, 15, 20 wt% of total rubber content. Peak intensity at 2237 cm^{-1} as a function of NBR content

APPENDIX C
FTIR ANALYSIS OF PALF WITH DIFFERENT SURFACE TREATMENTS

Alkali treatment is the conventional and effective method to use as a pretreatment for non-cellulosic substances removal. To investigate the effect of alkali treatment of PALF, ATR-FTIR spectroscopy was utilized. The IR spectra of untreated PALF (UPALF) and alkali-treated PALF (APALF) are shown in Figure C.1. The signal assignment of UPALF is shown in Table C.1. The absence of the signals of C=O vibration at 1740 cm^{-1} and C-O stretching at 1235 cm^{-1} of APALF indicates that hemicellulose is successfully removed by alkali treatment [94,137]. Silane-69 treatments, both washing (sSiPALF) and non-washing (sSiPALF-nw) methods do not cause the difference on the FTIR spectra.

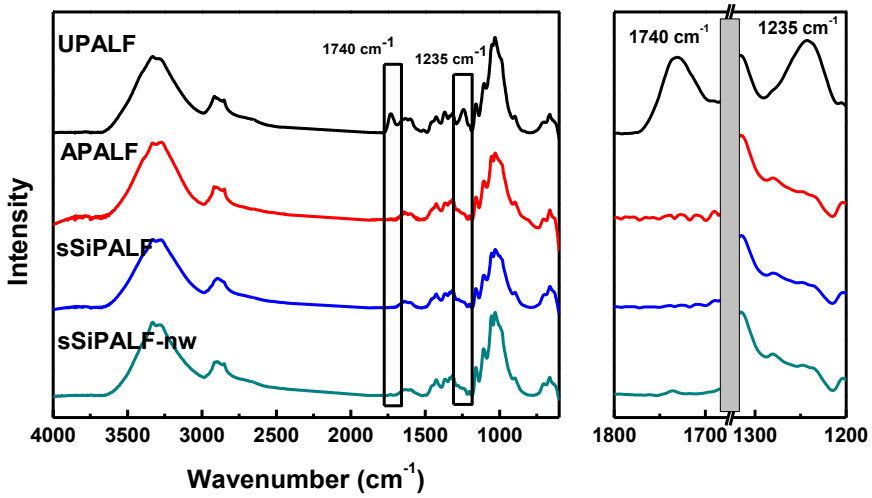

Figure C.1 FTIR spectra of untreated, alkali-treated and silane-treated PALFs including zoom-in spectra between wavenumber 1800 to 1200 cm^{-1}

Table C.1 Assigned signals of untreated PALF [152]

Signal position (cm^{-1})	**Assignment**
3300	O-H stretching
2900	C-H stretching
2850	CH_2 symmetrical stretching
1740	**C=O stretching**
1640	Adsorbed water
1475	CH_2 scissoring
1427	CH_2 asymmetric deformation
1370	CH_3 symmetric deformation
1335	CH_2 wagging
1320	O-H vibration
1280	CH_2 twisting
1235	**C-OH out-of-plane bending**
1200	C-OH and C-CH coupling
1160	C-O-C asymmetric stretching
1105	C-O-C asymmetric stretching
1052	C-OH (2° alcohol)
1035	C-OH (1° alcohol)
900	C-O-C in-plane stretching

APPENDIX D
CALCULATION OF SILANE AMOUNT ON FIBERS

To calculate an amount of silane on the surface of fiber, high-resolution XPS of C1s, O1s, S2p and Si2p were analyzed. The %atomic content of silane-69 as reference was measured and then shows in Table D.1. The atomic content ratio of (C-C)/(S-S) and (C-O)/(S-S) are calculated to use as the reference, which are 4.46 and 3.14 respectively. These values will be multiplied by (S-S), which is obtained by XPS analysis on each fiber to calculate the amount of (C-C) and (C-O) respectively.

The amount of silane on the surface of fiber was calculated in Table D.2 for silane treatment by washing method and in Table D.3 for silane treatment by non-washing method.

Table D.1 Extracted high resolution XPS spectrum of silane-69

Bonding		**%Atomic content**
C1s	C-C, C-H	27.16
	C1 (C-OR)	19.10
	C2 (O-C-O)	-
	C-Si	8.07
O1s	O1 (-OH)	-
	O2 (C-O-C)	-
	Si-O, C-O (Silane)	19.37
S2p	S-S	6.08
	C-S	6.08
Si2p	$Si(-O)_2$	-
	$Si(-O)_3$	8.05
Total		**100%**

Table D.2 Calculation of the amount of silane on silane-treated PALF by washing

Bonding		**%Atomic content**	**%Amount of atoms of silane molecules on the fiber**
C1s	C-C, C-H	25.54	(**4.46** × 0.19) = 0.85 (Only C-C bond from silane)
	C1 (C-OR)	32.56	(**3.14** × 0.19) = 0.60 (Only C-OR bond from silane)
	C2 (O-C-O)	6.64	- (Only fiber has this bond)
	C-Si	0.44	0.44 (Only silane has this bond)
	C-S	0.19	0.19 (Only silane has this bond)
O1s	O1 (-OH)	19.7	- (Only fiber has this bond)
	O2 (C-O-C)	13.2	- (Only fiber has this bond)
	Si-O, C-O (Silane)	0.88	0.88 (Only silane has this bond)
S2p	S-S	0.19	0.19 (Only silane has this bond)
	C-S	0.19	0.19 (Only silane has this bond)
Si2p	$Si(-O)_3$	0.45	0.45 (Only silane has this bond)
Total			**3.8%**

Table D.3 Calculation of the amount of silane on silane-treated PALF by non-washing method

Bonding		**%Atomic content**	**%Amount of atoms of silane molecules on the fiber**
C1s	C-C, C-H	38.03	(**4.46** × 2.82) = 12.57 (Only C-C bond from silane)
	C1 (C-OR)	20.09	(**3.14** × 2.82) = 8.96 (Only C-OR bond from silane)
	C2 (O-C-O)	2.64	- (Only fiber has this bond)
	C-Si	3.89	3.89 (Only silane has this bond)
	C-S	2.82	2.82 (Only silane has this bond)
O1s	O1 (-OH)	7.99	- (Only fiber has this bond)
	O2 (C-O-C)	5.35	- (Only fiber has this bond)
	Si-O, C-O (Silane)	9.64	9.64 (Only silane has this bond)
S2p	S-S	2.82	2.82 (Only silane has this bond)
	C-S	2.82	2.82 (Only silane has this bond)
Si2p	$Si(-O)_3$	3.89	3.89 (Only silane has this bond)
Total			**47.4%**

APPENDIX E
THERMAL DEGRADATION OF PALF

The thermal degradation of fiber was studied using thermogravimetric analysis (TGA). Fibers 5 mg were placed into the pan and were measured the weight loss by increasing temperature from 40 to 600 °C at heating rate 20 °C/min. The relation between temperature and percent weight is plotted in Figure E.1. From the result, the onset degradation temperature of fibers is observed at 210 °C. Thus, fibers are not degraded during vulcanization of composites, which the curing temperature is 150 °C.

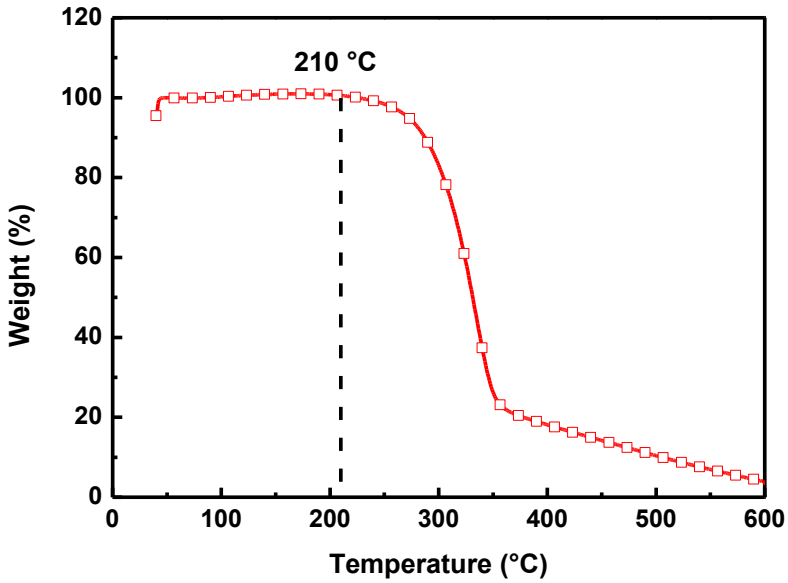

Figure E.1 Thermogravimetric analysis curve of untreated PALF

APPENDIX F
VARIATION OF STRESS-STRAIN CURVES OF COMPOSITES

The mechanical properties of 5 specimens of NR containing PALF 10 phr with and without NBR are displayed in Figure F.1. From the results, the improvement of mechanical properties by the incorporation of NBR can be observed with low variation.

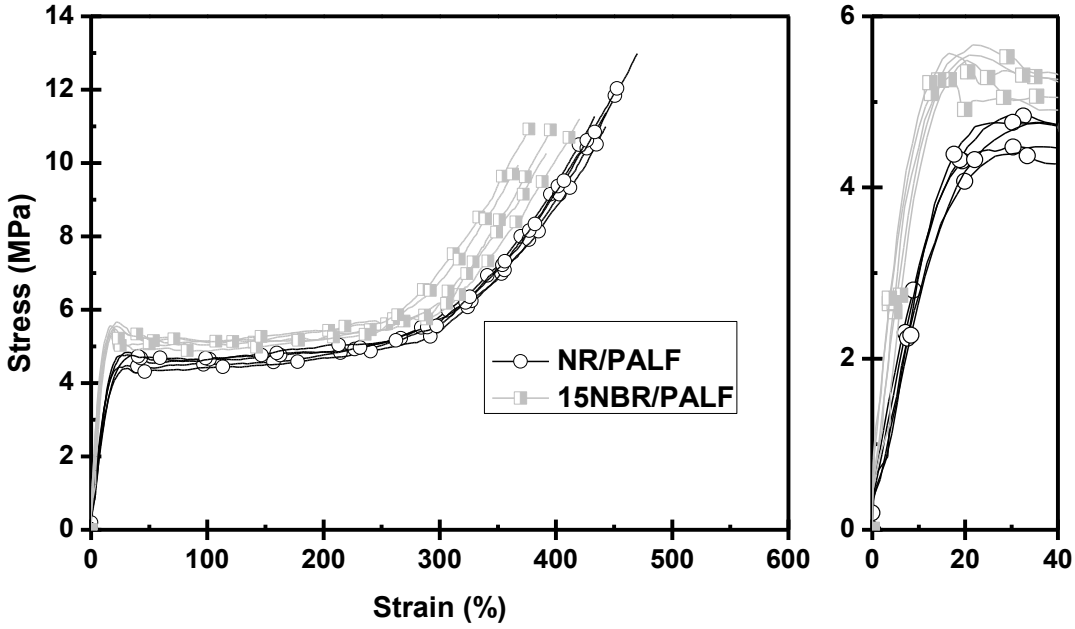

Figure F.1 Stress-strain curves of NR/PALF and 15NBR/PALF composites

APPENDIX G
EFFECT OF FIBER ORIENTATION ON MECHANICAL PROPERTIES OF COMPOSITES

Mechanical properties of NR/PALF composites with fiber orientation in longitudinal direction (LD) and transversal direction (TD) are displayed in Figure G.1. The effect of fiber orientation on tensile properties of composites can be observed at low deformation region. Yield stress can be observed only in composite with fiber orientation in LD and Young's modulus is higher than that of composite with fiber orientation in TD. Thus, this reinforcement effect is originated from the orientation of short fibers. At high deformation, the strain induced crystallization of NR results in the similar stress at high deformation and ultimate properties.

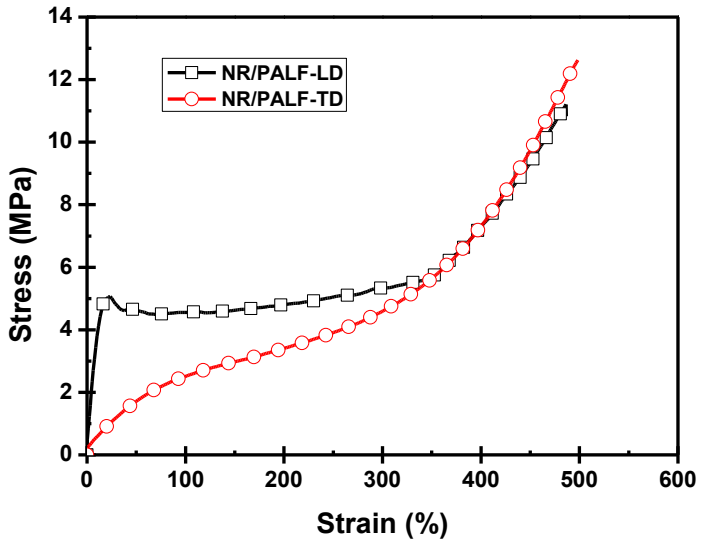

Figure G.1 Stress-strain curves of NR/PALF composites with fiber orientation in longitudinal direction (LD) and transversal direction (TD)